

Design and Synthesis of Molecular Inhibitors of c-FLIP Activity as a Therapeutic Strategy to Target Breast Cancer Cells and Cancer Stem-like Cells

Olivia Hayward

Thesis submitted for the award of PhD,

October 2015

Under the supervision of Dr Richard Clarkson
European Cancer Stem Cell Institute, Cardiff University

Co-supervised by Dr Andrea Brancale and Dr Andrew Westwell
School of Pharmacy and Pharmaceutical Sciences, Cardiff University



Declaration

This work has not been submitted in substance for any other degree or award at this or any other university or place of learning, nor is being submitted concurrently in candidature for any degree or other award.

Signed (candidate) Date

STATEMENT 1

This thesis is being submitted in partial fulfilment of the requirements for the degree of PhD

Signed (candidate) Date

STATEMENT 2

This thesis is the result of my own independent work/investigation, except where otherwise stated. Other sources are acknowledged by explicit references. The views expressed are my own.

Signed (candidate) Date

STATEMENT 3

I hereby give consent for my thesis, if accepted, to be available for photocopying and for inter-library loan, and for the title and summary to be made available to outside organisations.

Signed (candidate) Date

STATEMENT 4: PREVIOUSLY APPROVED BAR ON ACCESS

I hereby give consent for my thesis, if accepted, to be available for photocopying and for inter-library loans **after expiry of a bar on access previously approved by the Academic Standards & Quality Committee.**

Signed (candidate) Date

Acknowledgements

I would firstly like to extend my greatest thanks to my supervisors Dr Richard Clarkson, Dr Andrea Brancale and Dr Andrew Westwell. Richard has provided me with great support and constructive critical analysis of my work, which I believe has been invaluable. The molecular modelling advice provided by Andrea was vital in this study, in addition to Andrew's contributions to the chemistry side of compound evaluation. This study could not have been done without the teaching, enthusiasm and encouragement of them all, who I thank for all of their contributions and help with my work.

I must also thank Pharmacy students Gilda Giacotti and Mahmoud El-Hiti who synthesised many compounds tested in this study. I thank Dr Ladislav Andera, Dr David Stanek and Honza Svadlenka for the support and expertise provided by during my time at the Institute of Molecular Genetics, Prague.

I am very grateful to Cancer Research Wales, and those who support the charity, who funded my PhD.

I would like to thank Dr Rhiannon French for her help, support and friendship, as well as her contribution to this study. I would also like to thank all other past and present members of the Clarkson lab: Dr Jitka Soukupova, Dr Luke Piggott, Dan Turnham, Will Yang, Dr Tim Robinson and Andreia Silva for their help and entertainment during my project. Dr Giusy Tornillo and Howard Kendrick from our neighbouring lab have provided technical advice with aspects of this project for which I am very thankful.

My closest companions Sophie and Huw have supported me greatly, showing interest and giving advice with my work. I must thank all my friends and trainers at BMF, who have allowed me to sprint my stresses away! Finally, I of course must thank my family for their support and for always showing great interest and pride in my work.

Abstract

Tumour Necrosis Factor-Related Apoptosis Inducing Ligand (TRAIL) is a known anti-cancer agent which exhibits cancer cell specificity. Its efficacy in breast cancer is limited, however, as illustrated by the resistance demonstrated in a number of cell lines. Cellular FLICE-Like Inhibitory Protein (c-FLIP) has been demonstrated to play a key role in TRAIL resistance in these cell line models, through its competitive interference with caspase-8 recruitment to the death inducing signalling complex (DISC). Our lab has demonstrated that breast cancer 'stem cells', the cells proposed to be responsible for disease recurrence and metastasis, can be eliminated by combination of c-FLIP suppression, by siRNA, and TRAIL treatment. While it has been proposed that suppression of c-FLIP could improve TRAIL efficacy in breast cancer, there are no pharmacological c-FLIP specific inhibitors available.

The purpose of this study therefore was to design and validate novel pharmacological inhibitors of c-FLIP and to determine their tumour efficacy in models of breast cancer. Using *in silico* modelling, we have modelled the structure of c-FLIP and associated proteins, and, using virtual pharmacophore screening, we have identified 19 potential small molecule c-FLIP inhibitors. *In vitro* cell viability assays demonstrated 3 of these inhibitors to sensitise TRAIL resistant MCF-7 and BT474 breast cancer cell lines to TRAIL ($p < 0.05$) at micromolar concentrations, with several additional compounds showing a partial ability to sensitise to TRAIL. Each of the three lead inhibitors were shown to be acting via caspase-8 and therefore in a TRAIL specific manner. Two of the lead compounds in combination with TRAIL significantly reduced tumoursphere forming potential in an *in vitro* assay which represents breast cancer stem cell like traits. The ability of our primary compound to target cells with breast CSC-like traits was further supported using a colony forming assay, which demonstrated a significant reduction in the potential for clonal expansion of breast cancer cells following treatment with the novel agent in combination with TRAIL.

Acceptor-photobleaching FRET was successfully utilised to show the mechanism of action of our lead inhibitors to indeed be based on interfering with the c-FLIP FADD interaction. TALEN-mediated targeting of c-FLIP is being optimised to allow for further evaluation of these agents in addition to performing mutagenesis studies in a c-FLIP null background to further delineate the role and mechanism of c-FLIP in the sensitization of breast cancer stem cells to TRAIL.

Here we have identified several small molecule c-FLIP inhibitors which are able to specifically sensitise resistant breast cancer cells to TRAIL induced apoptosis via interfering with c-FLIP FADD interaction at the DISC, and thus allowing caspase-8 mediated apoptosis to occur. These early results show promise for our lead compounds as potential therapeutics in breast cancer, via sensitisation to TRAIL.

Table of Contents

Abstract	i
Table of Contents.....	ii
List of Abbreviations	vii
Table of Figures	ix
Table of Tables.....	xi
Chapter 1: General Introduction	2
1.1 Breast Cancer	2
1.1.1 Introduction	2
1.1.2 Risk Factors and Causes of Breast Cancer	3
1.1.3 Tumorigenesis: Breast Cancer Development and Progression	5
1.1.3.1 Mammary Gland Structure	5
1.1.3.2 Tumorigenesis of the Mammary Gland	6
1.1.4 Metastatic Spread	7
1.1.5 Breast Cancer Heterogeneity	7
1.1.6 Subtypes of Breast Cancer	8
1.1.6.1 Histopathology	8
1.1.6.2 Hormone Receptor Status	9
1.1.6.3 Molecular subtypes	10
1.1.6.4 Experimental Models of Breast Cancer	11
1.1.7 Breast Cancer Stem-like Cells	11
1.1.7.1 Epithelial-Mesenchymal Transition	12
1.1.7.2 Breast Cancer Stem Cell Plasticity	12
1.1.7.3 Experimental Models of Breast Cancer Stem Cells.....	13
1.1.8 Breast Cancer Treatment.....	16
1.1.8.1 Treatment Targets in Breast Cancer	16
1.1.8.2 Combination Therapies in Breast Cancer	19
1.1.8.3 Treatment Challenges in Breast Cancer	20
1.2 Apoptosis	22
1.2.1 Introduction	22
1.2.2 TRAIL Induced Apoptosis	23
1.2.2.1 Alternative roles of TRAIL	26
1.2.2.2 Regulation of TRAIL Signalling	26
1.2.2.3 TRAIL and Untransformed Cells	28
1.2.2.4 TRAIL as a Therapeutic Agent in Cancer	28
1.2.2.5 TRAIL in Cancer Clinical Trials	29
1.2.2.6 TRAIL Resistance in Cancer	32
1.2.2.7 TRAIL Sensitisation Agents.....	33
1.2.3 DED Containing Proteins.....	34
1.2.3.1 DED Domain Structure	35
1.3 Cellular FLICE-like Inhibitory Protein (c-FLIP).....	37
1.3.1 Introduction	37
1.3.2 c-FLIP Structure	38

1.3.3 Functions of c-FLIP	39
1.3.3.1 c-FLIP prevents Apoptosis.....	39
1.3.3.2 c-FLIP Activates Cell Survival Pathways	40
1.3.4 Transcriptional and Post-Translational Regulation of c-FLIP.....	41
1.3.5 c-FLIP in Cancer	41
1.3.6 c-FLIP Targeting Agents.....	42
1.3.7 Interactions of c-FLIP in TRAIL Resistance	45
1.3.7.1 FADD DED Mutational Studies	46
1.3.7.2 Procaspase-8 Mutational Studies	47
1.3.7.3 v-FLIP Mutational Studies	49
1.4 Aims of the Study.....	52
Chapter 2: Materials and Methods	56
2.1 Cell Culture	56
2.1.1 Cell Lines	56
2.1.2 Cell Culture Maintenance	57
2.1.3 Cell Storage	58
2.1.4 Activation and Suppression of Apoptosis	58
2.2 <i>In Silico</i> Protein Modelling	58
2.2.1 c-FLIP and Procaspase-8 Homology Models.....	58
2.2.2 Modelling Intermolecular Interactions.....	59
2.2.3 Protein Analysis and Pharmacophore Design.....	60
2.3 Cell Based Assays	61
2.3.1 Cell Subculture: Seeding for Assays	61
2.3.2 Cell Titre Blue Viability Assay	62
2.3.3 Caspase-8 Activity Assay	62
2.3.4 Functional Stem-Like and Progenitor Cell Assays.....	63
2.3.4.1 Tumoursphere Assay - Adherent Treatment.....	63
2.3.4.2 Tumoursphere Assay - Non-adherent Treatment	63
2.3.4.3 Colony Forming Assay	63
2.4 Compound Handling	64
2.4.1 Compound Solubility.....	64
2.5 Co-Immunoprecipitation (Co-IP) and Western Blot Protein Analysis...65	
2.5.1 Solutions Used for Co-IP and Western Blot.....	65
2.5.2 Sample Extraction and Preparation for Co-Immunoprecipitation	66
2.5.3 Sample Preparation for Western Blot	66
2.5.4 Protein Quantification	67
2.5.5 Western Blotting.....	67
2.5.6 SDS-PAGE	67
2.5.6.1 SDS-PAGE: Co-Immunoprecipitation.....	67
2.5.6.2 SDS-PAGE: Western Blot.....	67
2.5.7 Protein Transfer to PVDF Membrane	68
2.5.8 Membrane Probing.....	68
2.5.9 Protein Visualisation	69
2.6 Expression of Recombinant Proteins.....	69
2.6.1 Expression Constructs.....	69
2.6.2 Plasmid Propagation	70
2.6.2.1 Transformation into <i>E.coli</i>	70

2.6.2.2 DNA Extraction.....	70
2.6.2.3 Sequencing Plasmids.....	71
2.6.3 Site Directed Mutagenesis	71
2.6.3.1 Primer Design.....	71
2.6.3.2 PCR Amplification	72
2.6.3.3 Digestion of Template DNA Strand.....	72
2.6.4 FRET Construct DNA Preparation	73
2.6.4.1 Primer Design.....	73
2.6.4.2 Cloning of FRET Constructs	73
2.6.5 Agarose Gel Electrophoresis and DNA Extraction	74
2.6.6 DNA Ligation	75
2.6.7 Transient Transfection	75
2.7 FRET Analysis	76
2.7.1 Confocal Microscopy.....	76
2.7.2 FRET Cell Stimulation	76
2.8 TALEN	77
2.8.1 TALEN Transfection.....	79
2.8.2 FACS Sorting and Clone Culture Conditions	79
2.8.3 TALEN Transfection Analysis.....	80
2.8.3.1 gDNA Isolation	80
2.8.3.2 Confirmation of Expression	81
2.8.4 Second Transfection	82
2.9 RNA Analysis	83
2.9.1 RNA Extraction	83
2.9.2 cDNA Synthesis	83
2.9.3 q-RT-PCR Analysis	83
2.9.3.1 qPCR Data Analysis	84
2.10 Data Analysis.....	85
Chapter 3: Modelling of c-FLIP and Associated Proteins	87
3.1 Introduction	87
3.1.1 Molecular Modelling.....	87
3.1.1.1 Homology Modelling.....	88
3.1.1.2 Molecular Dynamics	88
3.1.1.3 Virtual Screening: Structure Based Design	89
3.1.1.4 Docking Software	90
3.2 Results	91
3.2.1 Constructing Models of c-FLIP Structure and Interactions.....	91
3.2.1.1 <i>In Silico</i> Homology Models of c-FLIP and Procaspase-8 Death Effector Domains	91
3.2.2 Generation of c-FLIP:FADD and Procaspase-8:FADD Complexes.....	94
3.2.3 Generation of a Pharmacophore Model: Structure-Based Virtual Screening.....	97
3.2.4 Virtual selection of inhibitors to c-FLIP:FADD interaction.....	100
3.4 Discussion	104
Chapter 4: Evaluation of c-FLIP Small Molecule Inhibitors	108
4.1 Introduction	108
4.2 Results	110

4.2.1 Solubility of the compounds in cell culture media	110
4.2.2 Inhibitors of c-FLIP demonstrate an ability to sensitise to TRAIL in Breast Cancer cell lines.....	112
4.2.2.1 c-FLIP Inhibitors Sensitise TRAIL-resistant MCF-7 Bulk Cells to TRAIL.....	112
4.2.2.2 c-FLIP Inhibitors Sensitise TRAIL-resistant BT474 Bulk Cells to TRAIL	119
4.2.2.3 c-FLIP Inhibitor Bulk Cell Summary and Lead Compound Selection.....	124
4.2.3 Small Molecule Inhibitors of c-FLIP Increase Sensitivity of Breast CSCs to TRAIL	128
4.2.3.1 OH14 Sensitises Tumoursphere-Forming Cells to TRAIL in a Dose-Dependent Manner.....	132
4.2.4 TRAIL Sensitivity in Clonogenic Colony Forming Assay.....	136
4.2.4.1 Compound OH14 Increases TRAIL Sensitivity of Colony Forming Cells.....	138
4.2.5 Compounds Appear Less effective in Triple Negative and HER2+ve Breast Cancer Cell Lines	140
4.2.6 Repeated Treatment with OH14 Slows Proliferation but does not Significantly Reduce Viability	144
4.2.7 Lead Compound OH14 is Non-Toxic to Non-Tumourgenic Cells.....	147
4.3 Discussion	149
Chapter 5: Exploring the Mechanism of Action of OH14.....	154
5.1 Introduction	154
5.1.1 FRET Acceptor Photobleaching.....	155
5.1.2 TALEN Gene Manipulation.....	157
5.2 Results	158
5.2.1 Procaspase-8 Cleavage Increases Over Time after TRAIL Treatment.....	158
5.2.3 TRAIL Increases Caspase-8 Activity in Sensitive Cell Lines.....	161
5.2.3 c-FLIP Inhibitors Increase Caspase-8 Activity upon TRAIL Treatment.....	163
5.2.2 FRET Acceptor Photobleaching.....	165
5.2.2.1 FRET Optimisation: Plasmid Ratios.....	165
5.2.2.2 FRET Optimisation: Overexpression of FADD and c-FLIP FRET Constructs Induces Caspase-Mediated Apoptosis.....	166
5.2.2.2 CFP-YFP Construct Demonstrates FRET in HeLa Cells.....	168
5.2.2.3 OH14 Reduces the Number of Detectable FADD:c-FLIP Interactions in TRAIL Treated Cells	170
5.2.2.4 OH14 does not act by Reducing Overall c-FLIP Levels.....	174
5.2.3 Generation of a c-FLIP TALEN Cell Line.....	176
5.2.3.1 Evaluation of Second Round of TALEN Transfected Cells.....	180
5.2.4 Selection of Mutations for c-FLIP Mutational Studies.....	183
5.2.5 <i>In Vitro</i> Assay of CSC Plasticity.....	185
5.2.5 OH14 Impacts on MCF-7 Cell Plasticity after siRNA c-FLIP Treatment.....	187
5.3 Discussion	189
Chapter 6: Biological Evaluation of OH14 Analogues	195
6.1 Introduction	195
6.2 Results	196
6.2.1 SPECS Based Analogues	196
6.2.2 OH14 Synthesis and Analogue Design	196
6.2.3 Analogue Modifications and Synthesis.....	198
6.2.3.1 Cardiff School of Pharmacy Synthesised Analogues.....	200

6.3 Analogue Analysis	200
6.3.1 Compound Solubility.....	200
6.3.2 Testing the Efficacy of Novel Compounds	202
6.2.1.1 SPECS Analogues of OH14: Colony Forming Assay	202
6.2.2.2 SPECS Analogues of OH14: Tumoursphere Assay	204
6.2.2 Pharmacy Synthesised Analogues	206
6.2.2.1 Pharmacy Synthesised Analogues N1-17: Colony Forming Assay	206
6.2.2.2 Pharmacy Synthesised Analogues GG1-12: Colony Forming Assay	210
6.3 Discussion	212
Chapter 7	215
Chapter 7: General Discussion	216
7.1 Targeting c-FLIP with Small Molecule Inhibitors	216
7.2 Biological Evaluation of c-FLIP Small Molecule Inhibitors.....	217
7.3 Mechanism of Action: c-FLIP:FADD Interactions	219
7.4 Residues Involved in c-FLIPs Anti-Apoptotic Role.....	220
7.5 Future Directions	222
Bibliography.....	226
Appendices	248
A6.1 OH14 Synthesis.....	248
A6.2: Analogue Synthesis.....	248

List of Abbreviations

5-FU	5-Fluorouracil
ABC	ATP-Binding Cassette
AC	Doxorubicin (Adriamycin) and Cyclophosphamide
AIC	Apoptotic Inhibitory Complex
AP-FRET	Acceptor Photobleach-FRET
BID	Bcl2 homology domain 3 Interacting Domain
BMI	Body Mass Index
BRCA	Breast Cancer
c-FLIP	Cellular FLICE Like Inhibitory Protein
CFU	Colony Forming Unit
clAP	Cellular Inhibitor of Apoptosis
CMF	Cyclophosphamide, Methotrexate and 5-FU
CMH	4-(4-choloro-2-methylphenoxy)-N-hydroxybutamamide
co-IP	Co-Immunoprecipitation
CRD	Cysteine-Rich Domain
CRUK	Cancer Research UK
CSC	Cancer Stem Cell
DcR	Decoy Receptor
DCIS	Ductal Carcinoma <i>In Situ</i>
DD	Death Domain
DED	Death Effector Domain
DEF	Death Effector Filament
DISC	Death Inducing Signalling Complex
DMSO	Dimethyl Sulfoxide
DNA-PK	DNA-Protein Kinase
DR	Death Receptor
EMT	Epithelial-Mesenchymal Transition
ER	Oestrogen Receptor
ErbB2	HER2
FADD	Fas-Associated protein with Death Domain
FEC	5-FU, Epirubicin and Cyclophosphamide
FLICE	FADD-Like Interleukin-1 beta-Converting Enzyme
FLIM-FRET	Fluorescence Lifetime Imaging-FRET
FRET	Fluorescence Resonance Energy Transfer
HER2	Human Epidermal growth factor Receptor 2
HMEC	Human Mammary Epithelial Cell
IDC	Invasive Ductal Carcinoma
IHC	Immunohistochemistry
LCIS	Lobal Carcinoma <i>In Situ</i>
MEBM	Mammary Epithelial Cell Growth Medium
MET	Mesenchymal-Epithelial Transition
NCIN	National Cancer Intelligence Network
NK	Natural Killer
NSCLC	Non-Small Cell Lung Cancer
OPG	Osteoprotegerin
PBS	Phosphate Buffered Saline

PCD	Programmed Cell Death
PCR	Polymerase Chain Reaction
PDB	Protein Data Bank
PEA-15	Phosphoprotein enriched in astrocytes 15-KDa
PPI	Protein Protein Interaction
PR	Progesterone Receptor
pTEN	Phosphatase and tensin homolog
PVDF	Polyvinylidene Fluoride
qRT-PCR	Quantitative Real-Time –PCR
RIP	RPA-Interacting Protein
ROI	Region Of Interest
RPA	Replication Protein A
RVD	Repeat Variable Diresidue
SE-FRET	Sensitized Emission-FRET
SNP	Single Nucleotide Polymorphism
TALEN	Transcription Activator-like Effector Nuclease
TDLU	Terminal Ductal-Lobular Units
TNBC	Triple Negative Breast Cancer
TNF	Tumour Necrosis Factor
TNFR	TNF Receptor
TRADD	TNFR type 1-associated DD
TRAIL	TNF Related Apoptosis Inducing Ligand
WHO	World Health Organisation
WT	Wild type
ZFN	Zinc Finger Nuclease
Z-VAD-FMK	Carbobenzozy-valyl-alanyl-aspartyl-[O-methyl]-fluoromethylketone

Table of Figures

Figure 1.1: Net Breast Cancer Survival rates for Women in Wales and England from 1971-2011.....	3
Figure 1.2: Steps involved in the tumoursphere forming assay.....	15
Figure 1.3: Cancer Stem Cell Targetted Therapies aim to Significantly Reduce the Risk of Relapse.....	21
Figure 1.4: Simplified Schematic of TRAIL induced extrinsic apoptosis.....	25
Figure 1.5: The family of some of the key DED domain containing proteins.....	35
Figure 1.6: NMR structure of DED domain from FADD.....	36
Protein chains are coloured from N- to C-terminal using a rainbow spectral colour gradient.....	36
Figure 1.7: Basic structures of the 3 c-FLIP splice variants which are expressed as proteins and the 2 cleaved products.....	37
Figure 1.8: Simplified Schematic of c-FLIP Inhibitor.....	54
Figure 2.1: Location of c-FLIP TALEN Pairs.....	78
Figure 2.2: Optimizing of PCR conditions and test of BsrI cleavage.....	82
Figure 3.1: Construction of c-FLIP and procaspase-8 homology models.....	93
Figure 3.2: Modelling c-FLIP key protein:protein interactions.....	96
Figure 3.3: Characterisation of the DED1 c-FLIP:FADD binding pocket and Pharmacophore Model on Binding Surface.....	99
Figure 3.4: Visual inspection of one of the 19 compounds within the pocket on c-FLIP DED1.....	101
Figure 4.1: Compound Visual Solubility Assessment.....	111
Figure 4.2: Initial viability dose response of OH1-OH19 inhibitor panel on the bulk population of TRAIL resistant MCF-7 cells.....	118
Figure 4.3: Initial dose response of 'OH' inhibitor compound panel on the bulk population of TRAIL resistant BT474 cells.....	123
Figure 4.4: Summary of 'OH' compounds on the ability to sensitise MCF-7 and BT474 bulk cells to TRAIL.	126
Figure 4.5: 3 Three Initial Inhibitors Demonstrate some Efficacy in Increasing Sensitivity of MCF-7 Tumoursphere Forming Cells to TRAIL.....	131
Figure 4.6: Compound OH14 significantly sensitises MCF-7 tumoursphere forming cells to TRAIL in a dose dependent manner.....	134
Figure 4.7: Compound OH14 sensitises BT474 tumoursphere forming cells to TRAIL in a dose dependent manner.....	135
Figure 4.8: Colony Forming Cells are Sensitive to TRAIL.....	137
Figure 4.9: Colony forming cells are TRAIL sensitive and can be further sensitised by treatment with OH14.	139
Figure 4.10: OH14 has a modest ability to sensitise MDA-MB-231 Tumoursphere Forming Cells to TRAIL only after Passaging.....	141
Figure 4.11: OH14 does not Sensitise SKBR3 Bulk or Tumoursphere Forming Cells to TRAIL.....	143
Figure 4.12: Daily Treatment with OH14 Slows Proliferation but does not Significantly Reduce Viability.....	145
Figure 4.13 Day Daily Treatment with OH14 Partially Reduces Tumoursphere Forming Ability.....	146
Figure 4.14: Lead Compound OH 14 is Non-Toxic to Non-Tumourgenic MCF-10A Cells Alone but partially decrease viability in combination with TRAIL.....	148
Figure 5.1: Representation of the FRET spectral overlap requirement of donor and acceptor.....	156
Figure 5.2: Schematic of FRET Acceptor Photobleaching using CFP Donor and YFP Acceptor.....	156
Figure 5.3: Caspase-8 Cleavage and Interaction with FADD Increases over Time in TRAIL Sensitive Cells.....	160
Figure 5.4: Caspase-8 Activity Increases upon TRAIL addition in TRAIL sensitive Cell Lines.....	162
Figure 5.5: Small Molecule c-FLIP Inhibitors Sensitise to TRAIL via Caspase-mediated Pathway.....	164
Figure 5.6: Pan-caspase Inhibitor Z-VAD-FMK Prevents Cell Death Induced by Overexpression of c-FLIP and FADD FRET Constructs.....	167
Figure 5.7: Fluorescence image of HeLa cells expressing CFP-YFP fusion construct.....	169
Figure 5.8: OH14 Reduces FADD:c-FLIP Interactions in TRAIL Treated TRAIL-resistant HeLa and MCF-7 Cells	173
Figure 5.9: OH14 does not decrease c-FLIP protein levels.....	175
Figure 5.10: Analysis of clones from Initial round of MCF-7 TALEN transfection revealed potential c-FLIP heterozygotes.....	177
Figure 5.11: Western Blotting Confirms Reduced c-FLIP Protein in TALEN Transfected Cells.....	178

Figure 5.12: TRAIL sensitivity is not significantly increased after initial round of TALEN transfection in MCF-7 cells.....	179
Figure 5.13: MCF-7 TALEN Double Transfected Cell Morphology and Growth Assessments.	181
Figure 5.14: qPCR and Cell Viability Analysis of MCF-7 TALEN transfected cells from second round of transfection.	182
Figure 5.15: Interacting Residues in the c-FLIP DED1 Pocket and Generation of SDM Constructs.	184
Figure 5.16: <i>In Vitro</i> Model of breast CSC Plasticity	186
Figure 5.17: Treatment with Lead Compound OH14 Impairs Ability of Cells to reacquire Tumoursphere Forming Ability following FLIPi + TRAIL.....	188
Figure 6.1: Ligand interaction of Compound OH14 in the predicted binding pocket on c-FLIP	197
Figure 6.2: Central Scaffold for Pharmacy Synthesised Analogues of OH14	199
Figure 6.3: Specs Analogues 14.1-14.9 in combination with TRAIL have similar effects on colony growth of MCF-7 and BT474 cells.	203
Figure 6.4: Several SPECS Analogues Sensitise MCF-7 and BT474 Tumoursphere Forming Cells to TRAIL to a similar level as OH14.	205
Figure 6.5: Several Series 1 Analogues Sensitise MCF-7 colonies to TRAIL in a similar manner to OH14..	208
Figure 6.6: Analogues are less toxic to the bulk population of MCF-7 cells than colony forming cells	209
Figure 6.7: Several Series 2 Analogues Sensitise MCF-7 colonies to TRAIL in a similar manner to OH14..	211
Figure 6.8: Structures of Most Efficacious Pharmacy Synthesised Analogues	214

Table of Tables

Table 1.1: Summary of Chemotherapeutic Drugs	18
Table 1.3: Clinical Trials for rhTRAIL.....	31
Table 1.2: Summary of Key Mutational Studies performed on FADD, v-FLIP and Procaspase-8 at the time of Modelling Study (2012/2013).....	50
Table 2.1: Conditions and maintenance of cell lines used within this study	57
Table 2.2: Subculture tissue culture plates	61
Table 2.3: Solutions and Reagents required for Protein Analysis Protocols.....	65
Table 2.4: Primary Antibodies and Respective Secondaries used for Co-IP and Western Blot	66
Table 2.5: Constructs Used within this Study.....	69
Table 2.6: Mutagenic primers.....	72
Table 2.7: PCR conditions for mutagenesis.....	72
Table 2.8: Primers used for FRET	73
Table 2.9: PCR conditions for FRET Constructs	74
Table 2.10: Optimised DNA ratios for FRET Plasmid Transfection	75
Table 2.11: TALEN primer sequence	78
Table 2.12: Reagents required for genomic DNA isolation.	80
Table 2.13: Forward and Reverse Primers for Testing the Efficiency of c-FLIP TALEN Clones	81
Table 3.1 Structure of 19 Compounds Selected from <i>In Silico</i> Screening.....	102
Table 4.1: Solubility of Initial 19 Compounds in Media.	111
Table 4.2: Initial Lead Compound selection.	127
Table 6.1: Aromatic Ring Substitutions for Pharmacy Synthesised Analogues of OH14.....	199
Table 6.2: Solubility of SPECS Analogues of OH14.....	201
Table 6.3: Solubility of Pharmacy Synthesised Compounds N1-17	201
Table 6.4: Solubility of Pharmacy Synthesised Compounds GG1-12.....	201
Table 7.1: Summary of all compounds tested.....	224
Table A6.1: SPECS analogues of Compound OH14 (14 and 14.2 are the same compound).	249
Table A6.2: Pharmacy Synthesised Compounds – GG1-12	250
Table A6.3: Pharmacy Synthesised Analogues N1-17.....	252

Chapter 1

General Introduction

Chapter 1: General Introduction

1.1 Breast Cancer

1.1.1 Introduction

Cancer is one of the leading causes of mortality worldwide, accounting for around 8.2 million deaths in 2012 (WHO Statistics Ferlay *et al.*, 2012). Lung, liver, stomach, colorectal and breast cancer are the five cancers which contribute most to this statistic, although the occurrence of these cancers differs between males and females (WHO Statistics: Bray *et al.*, 2013). Breast cancer, despite almost exclusively affecting women, is the most common cancer in the UK and the second most common cancer worldwide (Hutchinson, 2010). The disease, in fact the most prevalent cancer in women, is diagnosed in around 50,000 people each year in the UK alone (NCIN, 2011) and resulted in over 500,000 deaths worldwide in 2012; 130,000 of these being European cases (CRUK Statistics, Accessed October 2014). Despite these statistics, improved options for therapy over the past 40 years has resulted in an increases of around 15, 35 and 40% in net survival over 1, 5 and 10 years respectively (Figure 1.1) (CRUK Statistics, Accessed October 2014).

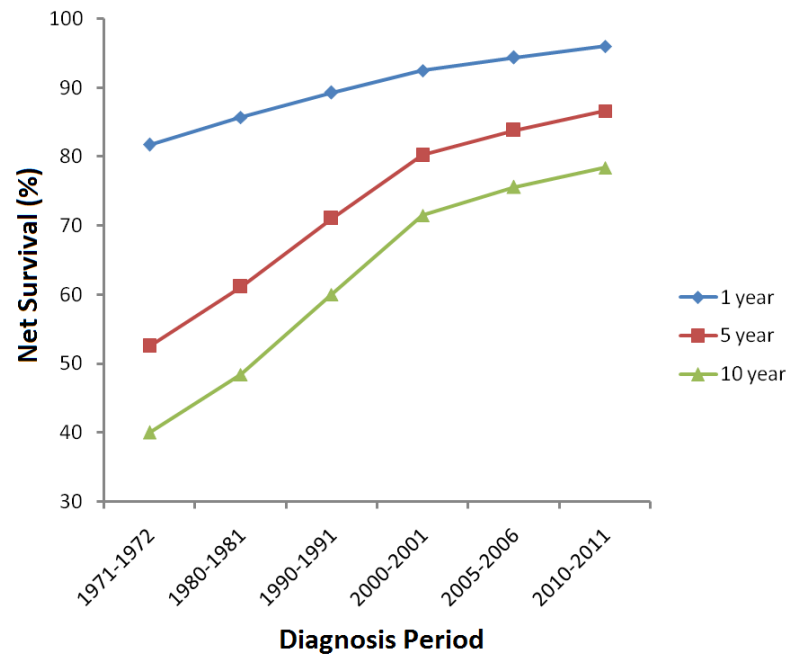


Figure 1.1: Net Breast Cancer Survival rates for Women in Wales and England from 1971-2011.

1, 5 and 10 year survival rates of breast cancer patients in Wales and England over several diagnosis periods spanning 40 years (Figure adapted from CRUK Stats, 2014, Accessed 30 November 2014).

Although statistics for breast cancer survival are improving, with a 10 year survival of approximately 80% (Rachet *et al.*, 2009), drug resistance and disease relapse remain problematic for breast cancer treatment. Further research into breast cancer including focussing on new therapeutics to target cancer cells specifically and to prevent the spread and relapse of the disease, is imperative in order to continue to improve on these statistics.

1.1.2 Risk Factors and Causes of Breast Cancer

The exact initial cause of the cancer is often difficult to identify and one may be able to elucidate several plausible features of a patient's lifestyle or genetics which have had large contributions in the development of breast cancer.

One of the greatest risk factors in breast cancer is increasing age and indeed around 80% of those diagnosed are women over the age of 50 (McPherson *et al.*, 2000). The strong trend seen with increasing age and risk of breast cancer is likely to be due a link with hormonal status as the levels of sex hormones, including oestrogen,

progesterone and testosterone alters with age, with the biggest changes occurring post-menopause. The observed increase around age 50 may also be partly due to the fact that this is the age around which women are invited to attend breast cancer screening clinics, and thus more cases may be detected (McPherson *et al.*, 2000).

As with the vast majority of cancers there are many lifestyle and environmental factors which can increase the risk of developing breast cancer although the correlation is not as strong as, for example, perhaps the most well-known example of lung cancer and smoking. Excessive alcohol consumption, for example, is thought to slightly increase risk through mechanisms such as decreasing the efficiency of DNA repair (Vogel, 2000). A similar, relatively modest link to increase in risk, has been identified with smoking tobacco (Terry and Rohan, 2002). Other environmental factors include a person's weight and height, and thus, their body mass index (BMI): post-menopausal women who are overweight have a higher than average risk of breast cancer (McPherson *et al.*, 2000).

Genetics can play a large part in the risk of developing breast cancer, with susceptibility of an individual significantly increased if a first degree relative has had the disease. Furthermore, genetically inherited cancer genes exist which are well-documented to significantly increase risk of developing breast cancer. Perhaps the most well-known genetically inherited breast cancer genes are the breast cancer 1 and 2 (BRCA) genes. The BRCA genes, BRCA1 and BRCA2, are important for producing tumour suppressor proteins which are involved the repair of in double-stranded DNA breaks, thus, mutations in these genes can cause cells to grow abnormally (O'Donovan and Livingston, 2010). The lifetime risk of breast cancer can be as much as 80% in families with BRCA1 mutations, although slightly lower at 45% for BRCA2 mutations (Milne and Antoniou, 2011). Additional gene mutations which can be inherited and thus increase risk of breast cancer include ATM, TP53, PTEN and CHEK2, amongst several others, although these are much less common than the BRCA mutations (Ripperger *et al.*, 2009).

1.1.3 Tumorigenesis: Breast Cancer Development and Progression

The development of all cancers essentially results from the aberrant, uncontrolled proliferation of cells which have obtained mutations in genes important for cell growth and survival. The acquisition of such mutations gives these cells certain properties, or 'hallmarks' which deem them to be cancerous. Initially, six hallmarks of cancer were defined which are thought to be exhibited by most of all cancers. These properties included: resistance to programmed cell death (PCD); self-sufficiency in growth signals; anti-growth signal evasion, ability to invade tissue and metastasise; unlimited replicative potential; and sustained angiogenesis (Hanahan and Weinberg, 2000). More recently, however, these cancer-common properties have been expanded to include four additional features: dysregulation of cellular energetics; genomic instability and mutation; tumour-promoting inflammation; and evasion of immune destruction (Hanahan and Weinberg, 2011).

Breast cancer, as with other cancers, develops as a result of a multistep process involving the acquisition of mutations in genes representing the key hallmarks of cancer, enabling the implicated cells to evade the body's innate anti-cancer mechanisms. In order to fully understand the process of breast cancer tumorigenesis, it is useful to have basic knowledge of the normal mammary gland structure.

1.1.3.1 Mammary Gland Structure

The mammary gland is a complex secretory organ which is made up of a multitude of cell types all coordinating to facilitate the secretion of milk. Epithelial cells grow out from the nipple into an adipocyte formed fat pad, which is infiltrated by several cell types including vascular endothelial cells, fibroblasts and various immune cells. The mammary epithelium is comprised of basal and luminal cells. Cells of the basal epithelium, *i.e.* the outer layer of the gland, consist primarily of myoepithelial cells and a smaller quantity of stem cells, present to generate the different cell types. Ducts and secretory alveoli are formed from the luminal epithelium which is comprised of cells expressing different hormone receptors. The myoepithelium and luminal epithelium combine to effectively generate a structure able to synthesize, secrete and deliver milk during lactation (Macias and Hinck, 2012).

1.1.3.2 Tumorigenesis of the Mammary Gland

Over 80% of adult cancers originate from the transformation of epithelial cells, which have over-proliferated to form an adenoma, to malignant cancerous cells, deeming them carcinomas (Dimri *et al.*, 2005). Almost all breast cancers also develop as carcinomas, in the mammary gland, with the initial conversion of a normal human mammary epithelial cell (HMEC), which lines the milk-forming ducts of the mammary gland, into a cancerous cell (Dimri *et al.*, 2005; Taylor-Papadimitriou *et al.*, 1993). The process of epithelial transformation to malignancy has multiple steps, is governed by a multitude of environmental, genetic and dietary factors and will involve a number of key mutated genes (Hanahan and Weinberg, 2000).

Cells of the mammary gland are usually under tight control, with a finite life span which prevents their over-proliferation. Mammary cell tumorigenesis involves several steps that cause the loss of the control of cell senescence leading, essentially, to HMEC immortalisation (Dimri *et al.*, 2005). Initial carcinoma-causing transformations in the mammary gland usually occur either in the ducts, specifically in the terminal ductal-lobular units (TDLUs) or in the lobes, leading to the two histologically distinct subtypes of breast cancer; ductal or lobular carcinomas respectively (Bombonati and Sgroi, 2011).

The more common of the two histological subtypes, ductal carcinoma, is described to progress through several stages of epithelial transformation from normal through to flat epithelia, followed by atypical ductal hyperplasia and continuing through to ductal carcinoma *in situ* (DCIS) resulting in the most common form of breast cancer, invasive ductal carcinoma (IDC) (Bombonati and Sgroi, 2011). Essentially, epithelia situated on the basement membrane of a mammary gland start to proliferate abnormally, due, for example, to a mutation in a tumour suppressor gene such as p53. The resulting carcinoma may be altered due to additional epigenetic or genetic changes which deem it a carcinoma *in situ*, *i.e.* one that is still present on the basement membrane (Lopez-Garcia *et al.*, 2010). The development of slower-growing mammary lobular carcinomas is a similar multi-step process of transformation from normal lobular epithelium, to transformed atypical hyperplasia which leads to lobular carcinoma *in situ*, the precursor of invasive lobular carcinoma (Bombonati and Sgroi, 2011; Simpson *et al.*, 2003).

1.1.4 Metastatic Spread

Metastasis is the spread of cancer from one part of the body to another and can occur at some point during tumorigenesis of the original tumour. Metastasis in mammary carcinomas occurs as a result of disruption and fragmentation of the underlying basement membrane allowing the carcinoma cells to metastasise or migrate and become invasive through the acquisition of additional cellular and genetic changes (Siegal *et al.*, 1981). The migration of cells from a primary site, *i.e.* metastasis, is proposed to be driven by the process of epithelial-mesenchymal transition (EMT) a process involving a cellular phenotypic switch between epithelial and mesenchymal morphology via the loss of epithelial cell contact (Thiery, 2003; Moreno-Bueno *et al.*, 2008). Interestingly, it is thought that EMT is reversible through the process of mesenchymal-epithelial transition (MET) whereby cells regain their contact-dependence through the expression of E-cadherin (Liu *et al.*, 2013). Metastasis, potentially driven by EMT, can therefore result in the formation of a secondary tumour site which is said to be driven by the process of MET (Thiery, 2002). EMT will be discussed in further detail in Section 1.1.7.

1.1.5 Breast Cancer Heterogeneity

In both pathology and molecular profile, human breast cancers tend to be heterogeneous. Cell type diversity between and within breast cancer tumours is a relatively novel area of research, facilitated by technological advances, such as whole-genome sequencing, which allow for a more thorough analysis of tumour properties (Burtucci and Birnbaum, 2008). It appears that, similar to blood cancers, breast cancers can initiate in multiple different cell types and that not one sole pathway is responsible for tumour progression (Weigelt *et al.*, 2010; Polyak, 2007), as is the case in colon cancer, for example (Stingl and Caldas, 2007). Breast cancers often have a significant amount of intra- and inter- tumoral genetic variations which are only now being fully explored (Hutchinson, 2010).

Breast cancer is often thought to progress in a non-linear manner through the clonal expansion of initial transformed cells, via multiple acquisitions of genetic and epigenetic alterations, which add to the overall heterogeneity of the resulting tumour

or tumours (Polyak, 2008; Almendro and Fuster, 2011). Additionally, breast cancer heterogeneity may be, in part, due to the presence of cancer 'stem-like' cells (CSCs) (Section 1.1.7) which are thought to be the reason that many tumours relapse after treatment and so are an important yet difficult target in research for more efficient therapies (Lawson *et al.*, 2009). CSCs may have a role in heterogeneity primarily due to their ability to produce all cell types (Stingl and Caldas, 2007). Indeed, some evidence does exist to support this theory where CSCs isolated from multiple cancer types, including breast cancer, have given rise to cancers which are very similar to and contain all the different cell types of the original tumour (Pietras, 2011; Al-Hajj *et al.*, 2003). In contrast, non-stem cancer cells generate either no tumours or tumours which lack many of the original cancer's features (Al-Hajj and Clarke, 2004; Al-Hajj *et al.*, 2003).

1.1.6 Subtypes of Breast Cancer

Given the prevalence, heterogeneity and potential severity of breast cancer, accurate methods of classification which assess various aspects of the cancer are vital in order to help diagnose and treat the disease, as well as helping to progress scientific research.

Although several common genetic mutations can indeed be identified in breast cancer cases, there are a vast number of other, less common, potential mutations in breast cancer giving rise to a large variation in mutational status between individual cases. Awareness of the many subtypes and heterogeneity of this malicious disease is vital in order to tailor patient treatment strategies.

1.1.6.1 Histopathology

The traditional method of classification relies on visual assessment of the morphology of tumour cells and their orientation or organisation within a tumour. An initial differentiation of the cancer is utilised which defines a cancer as *in situ* carcinoma or invasive carcinoma. The former subtype can subsequently be classified as ductal or lobular, via assessment of cell growth and morphology. As mentioned in section 1.3.1.2, DCIS cases are far more common than lobular carcinoma *in situ* (LCIS). DCIS is sub-classified by the spatial organisation of cells into five architectural subtypes: Comedo, Cribriform, Micropapillary, Papillary and Solid (Malhotra *et al.*, 2010).

Modern diagnoses tend not to rely solely on this method due to the potential confounding factors including assessor subjectivity, regions of interest or distinct morphologies within a tumour in addition to the fact that it does not take into account any genetics or molecular markers of the particular case. As a consequence, oncologists and researchers will take into account other features of the cancer to make a final diagnosis.

1.1.6.2 Hormone Receptor Status

Immunohistochemical markers, primarily assessing the cancers' hormone receptor status, may also be used as diagnostic and prognostic tools in breast cancer (Subramaniam and Isaacs, 2005; Walker, 2008).

Immunohistochemistry (IHC) has facilitated the assessment of molecular markers, specifically, of hormone receptor expression levels. The cancer cell's oestrogen receptor (ER), progesterone receptor (PR) and human epidermal growth factor receptor (HER2) status further allows the categorisation of breast cancer (Althius *et al.*, 2004). Cells which overexpress a receptor, and so will proliferate when stimulated by the specific hormone ligand are described as receptor-'positive'. 'Negative' expressers do not respond to the specific hormone since they do not exhibit the appropriate receptor. According to this IHC method of characterisation, cells are described as 'ER-positive', 'ER-negative', 'PR-positive', 'PR-negative', 'HER2-positive' or 'HER2-negative'. Additionally, cancers can be negative for all receptors and are thus deemed 'triple-negative breast cancer' (TNBC). ER/PR-positive cancers tend to be the most common, representing around 60% of all cases (Buzdar, 2009), whereas HER2 and TNBC cases are less common and form approximately 20% of cases each (Anders and Carey, 2009). As a general rule, breast cancers which are positive for hormone receptors have a better prognosis due to the presence of hormone- or hormone-receptor targeting agents as first line treatment options. TNBC is a more difficult target for treatment due to the inefficacy of hormone therapies on cells which lack hormone receptor expression.

Breast cancer cells often have a mixed receptor expression pattern, *e.g.* ER-negative, HER2-positive, or may lack expression of all of these receptors as is the case TNBC (Cleator *et al.*, 2007). In addition to individual cells expressing different

combinations of receptor, the heterogeneity of breast cancer means that an individual patient's cancer may be made up of a collection of cells which have varied hormone expression status between cells, and thus some cells may respond to treatment, whilst others remain unaffected. Although hormone receptor classification does provide a great advantage in selecting the first line therapy, it is often not reflective of this heterogeneity and thus treatments may not be as effective as expected.

1.1.6.3 Molecular subtypes

The molecular subtypes of breast cancer, determined by gene expression profiling and microarray analysis which analyse the levels of mRNA expression of specific genes, can be defined as: luminal A; luminal B; basal; ErbB2 (HER2) overexpressing and normal-like (Sorlie *et al.*, 2001; Brenton *et al.*, 2005), with each subtype exhibiting differing risk factors for incidence, treatment responsiveness, disease progression and potential to metastasise (Polyak, 2011). An additional, sixth molecular subtype was defined as claudin-low, which has facilitated further differentiation between the molecular subtypes (Prat *et al.*, 2010). This method of classification in combination with histological data on morphology has enabled for correlations in certain gene subsets to be identified, further aiding with diagnoses and prognoses (Stingl and Caldas, 2007; Malhotra *et al.*, 2010).

Genetic screening and gene-expression profiling can be utilised in order to establish a prognosis (Sotiriou *et al.*, 2006) and aid in the identification of individuals who are expected to be at a higher initial risk of developing breast cancer, for example, those with a known family history of the disease. Mutations in the autosomal dominant genes BRCA1, BRCA2, phosphatase and tensin homolog (pTEN) and p53 increase the risk of developing certain types of breast cancer by 5-10%. BRCA1 and 2 mutations are the leading cause of hereditary breast cancer (Mincey, 2003).

It is not feasible, however, to perform microarray analysis as a routine measure as the procedures involved are quite costly. There are such benefits from having such in-depth molecular classification, however, that a 50-gene signature, known as PAM50, has been determined. The PAM50 provides a way of way of classifying tumours using varied molecular subtypes by utilising quantitative real time PCR (qRT-PCR) and has

been demonstrated to greatly enhance the ability to predict risk of relapse (Parker *et al.*, 2009).

A combination of the different forms of diagnosis and prognosis methods is the best approach in order to fully establish the characteristics of the individual case, including gaining the best representation of the heterogeneity of the cancer (Kreike *et al.*, 2007).

1.1.6.4 Experimental Models of Breast Cancer

Immortalised breast cancer cell lines are commonly used as an *in vitro* model of breast cancer which provide, in effect, 'unlimited', self-replicating models of breast cancer with no terminal differentiation. The available cell lines, which include both animal and human derived cells, quite accurately represent the many different molecular subtypes of breast cancer (Neve *et al.*, 2006). These cell lines are able to replicate some of the heterogeneity of breast cancer due to gene expression variations that develop in some cells (Neve *et al.*, 2006). The cell lines used, as they have been initially extracted from patients, represent different breast cancer subtypes with varying hormone receptor status', gene expression levels, mutations, cellular compositions and many other features which define particular cancers (Kao *et al.*, 2009) and so provide a valuable resource for research into potential treatment targets and strategies.

1.1.7 Breast Cancer Stem-like Cells

The mammary gland contains a subset of multipotent mammary stem cells which initiate the development of the gland at the early stages of embryogenesis and maintain it throughout life (Williams and Daniel, 1983; Blanpain *et al.*, 2011). It has been shown that a single mammary epithelial cell is capable of producing an entire mammary gland, demonstrating a multipotent phenotype of these cells and elucidating their stem cell-like behaviour (Blanpain *et al.*, 2011). Following on from this knowledge, the most recent models of cancer initiation and progression revolve around the 'CSC hypothesis', which was in fact first proposed around 150 years ago (Wicha *et al.*, 2006), with relatively little mention of it for decades until the mid 1990's. The hypothesis states that cancers originate from progenitor, stem-like cells which have surpassed the

normal self-renewal regulation processes. The resulting tumours, therefore, are said to contain a subsection of cells which retain these stem-like properties, including self-renewal and differentiation (Wicha *et al.*, 2006) and thus contribute to the maintenance and spread of disease. Additionally, it is thought that these tumour-initiating or CSCs are slower growing and more resistant to chemotherapy and thus are often a cause of disease relapse.

The interest in CSCs is growing within cancer research due to the potential for these cells to drive tumour metastasis and contribute largely to drug resistance and disease relapse. Although fairly difficult to prove the existence of CSCs in patients directly, via use of cell surface proteins, recent studies have been able to provide both *in vitro* and *in vivo* evidence in support of the idea of CSCs by utilising techniques which measure properties such as self-renewal (Al-Hajj and Clarke, 2004; Al-Hajj *et al.*, 2003, Pietras, 2011).

1.1.7.1 Epithelial-Mesenchymal Transition

The idea of CSCs goes hand in hand with the concept of EMT (mentioned in section 1.1.4), which is also thought to play a key role in organism development (Thiery *et al.*, 2009). EMT is a type of cell plasticity which involves the loss of adherens junctions between epithelial cells and the gain of properties exhibited by mesenchymal cells, including increased motility and altered gene expression (Kalluri and Neilson, 2003). Multiple signalling pathways have been identified that are shared between EMT or EMT-like processes in normal and tumour development, helping to facilitate an understanding of the process and further implicating its role in tumour development (Thiery, 2002).

1.1.7.2 Breast Cancer Stem Cell Plasticity

Plasticity, in breast cancer, describes the conversion of non-stem breast cancer cells to breast CSCs and is thought to occur via the processes of EMT and MET (Thompson and Haviv, 2011; Liu *et al.*, 2013) (Section 1.1.7.1). The roles of EMT and MET in embryogenesis, wound healing and tumorigenesis in particular give evidence for their likely roles in plasticity (Drasin *et al.*, 2011; Luo *et al.*, 2015). Plasticity may occur within a population of tumour cells that facilitates their adaptation when certain conditions, for example when undergoing therapy, drive their need to change in order

to survive. Essentially, only in a situation where a certain stem-like trait should newly arise in a subset of cells which did not previously have this trait could plasticity be declared as having truly occurred. A study such as this has been performed in human mammary epithelial cells, whereby plasticity was demonstrated to be occurring in both untransformed and cancerous cell subsets (Chaffer *et al.*, 2011).

1.1.7.3 Experimental Models of Breast Cancer Stem Cells

Cell lines have been used as a tool for studying cancer stem cells *in vitro* for many years, due to the observations that, like primary tissue, they contain a small population of cells with stem cell-like properties, as evaluated using stem-cell like markers and further evidenced with *in vivo* tumour initiation experiments. Although not as representative as primary tissue or *in vivo* studies, it is often beneficial to utilise cell lines for studying CSCs, in particular, for relatively high-throughput drug screening studies due to their availability, ease of handling and relatively low cost. Utilising cell lines to study cancer stem cells *in vitro* will reduce the requirement on *in vivo* experiments for studying a very interesting and important aspect of cancer, with particular emphasis on the potential for studying CSC targeted therapeutics. The primary disadvantage of using cell lines *in vitro* in general, and for studying CSCs, is the loss of the inter-relationships between cells and between cells, the heterogeneity of a tumour, and the existence of a tumour microenvironment that would exist *in vivo* (Holliday and Speirs, 2011). Ideally, cell lines would be utilised to perform initial screens to evaluate drug effects on CSCs, which would be followed up with work on primary cells and tumour initiation *in vivo*, when a potential drug candidate or candidates have been identified.

The *in vivo* mouse xenograft tumour initiation assay is considered the 'gold standard' experimental model of CSCs. Essentially, human cancer cells are serially transplanted at different doses into immunocompromised mice and assessed at several time points for tumour formation. Once formed, cells from the tumour are extracted and grafted into a second animal to evaluate their self-renewal ability (Han *et al.*, 2013). Although possibly the closest representation to a human tissue *in situ*, these studies are often difficult to reproduce, require specific strains of mouse and sites of implantation and therefore are often not the most cost effective and accurate way to evaluate therapeutic strategies for targeting CSCs.

Some key *in vitro* models which aim to isolate breast CSCs do also exist, however, and although many were initially developed using primary tissue, they have been also shown effective at isolating CSCs when utilising immortalised breast cancer cell lines as a basis (Iglesias *et al.*, 2013). These *in vitro* models require much less time and resources than animal models and facilitate a more high-throughput screening process for compound testing. Ideally, in order to draw complete conclusions on cell-stemness, *in vitro* assays would ideally need to be backed-up by an *in vivo* experiment. The optimal *in vitro* assay would provide quantitative, specific data and be able to measure low frequency stem cells, whilst also being relatively high-throughput.

Perhaps the most well-known and utilised *in vitro* model is the tumoursphere assay, developed by Dontu *et al.* (Dontu *et al.*, 2003). This protocol was developed by making appropriate modifications to the neurosphere assay which was designed and developed by Reynolds and Weiss to culture cells that exhibit stem cell properties from the adult brain (Reynolds and Weiss, 1992). The tumoursphere assay involves the formation of non-adherent 'tumourspheres' which are enriched in cells which exhibit the functional characteristics of stem cells, specifically, their ability to survive in suspension culture compared to non-stem cells. When established cell lines are plated in single cell suspension in non-adherent conditions, achieved using reduced-serum media and low-attachment cell culture plates, the non-stem cells will die and only the breast cancer 'stem cells' will remain due to their anoikis resistance. After approximately 7 days, the breast CSCs will have formed clusters of cells which are termed 'tumourspheres' (Dontu *et al.*, 2003). Tumourspheres, which contain both stem and non-stem cells, are counted to obtain a quantity of tumoursphere forming units and then broken-up to be re-processed in the same way as initially in order to assay the self-renewal ability of the population, another key property of CSCs (Figure 1.2).

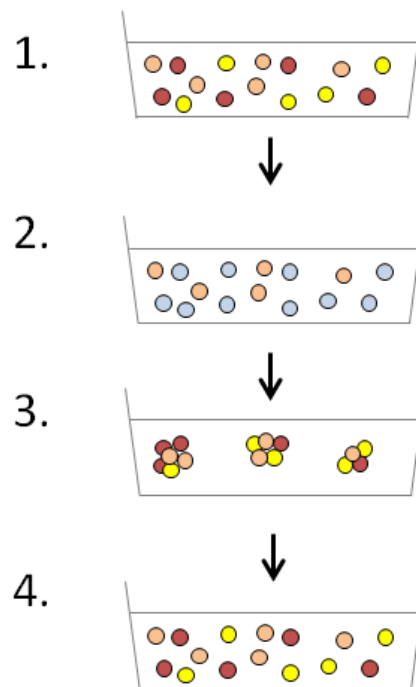


Figure 1.2: Steps involved in the tumoursphere forming assay.

1) Adherent breast cancer cells are plated in non-adherent conditions, using a specific media and cell culture plate. 2) Non-stem cells will be unable to survive, leaving only the breast cancer stem cells to survive. 3) After approximately 7 days, the breast cancer stem cells will have formed clusters of cells, termed 'tumourspheres' which are counted under light microscope. 4) Tumourspheres contain a mixture of stem- and non-stem cells which are broken up and repassaged to assay for self-renewal.

An additional assay for progenitor-like, rather than specifically cancer stem-like cells is the colony forming assay, also known as the clonogenic or CFU assay. The assay is often interpreted as a clonal and proliferation assay (Zhang and Waxman, 2010). The CFU assay has been routinely used to evaluate cell reproductive death after radiation, but has more recently been used to test cytotoxic agents. Some studies suggest that single cells, obtained by plating at low densities, which are capable of forming colonies of over 32 cells are representative of stem cells. The colonies that form in this assay are deemed 'holoclones' and are thought to represent stem cells due to the expression of certain survival and self-renewal genes (Barrandon and Green, 1987), including p63 (Pellegrini *et al.*, 2001) and BMI-1 (Claudinot *et al.*, 2005). Essentially, cells are plated in adherent conditions at a very low density in order to monitor their ability to exhibit these properties under different assay conditions, for example in the presence or absence of a drug, or different treatment regime.

Label-retention assays are also often utilised to measure cancer stem-like cells *in vitro*, although the process does not facilitate high-throughput testing, of, for example, therapeutic agents (Clarke *et al.*, 2006).

1.1.8 Breast Cancer Treatment

Breast cancer screening consists of a combination of patient history, clinical examination, mammography results and ultrasound assessment (Howard and Bland, 2012). Once diagnosed, treatment for breast cancer, like any cancer type, depends primarily on the stage and grade of the case. A review of the molecular, histological and clinical features (Section 1.1.6) of the cancer will be performed in order to select the most suitable treatment strategy (Malhotra *et al.*, 2010).

For a long time, the primary and almost exclusive treatment method for breast cancer involved the use of cytotoxic chemotherapeutics but developments in research have enabled a more targeted approach often using multiple treatment options (Tinoco *et al.*, 2013). In general, treatment will begin using a combination of surgery, to remove the cancerous mass, with radiotherapy to treat the surrounding tissue and prevent recurrence, although individual cases may require a different initial treatment strategy. Treatment tailoring will be most important at this stage whereby hormone or chemotherapy will usually follow surgery in order to attempt to further reduce the cancer whilst also aiming to help prevent relapse (Section 1.1.8.2) (Tinoco *et al.*, 2013).

Ultimately, all cancer treatment aims to reduce or eliminate cancerous cells, either via physical removal or through the induction of cell death, thus preventing their growth and metastasis. The target of the treatment will vary between cancer cases: from targeting the physical mass to specifically hitting particular gene targets.

1.1.8.1 Treatment Targets in Breast Cancer

Many targets exist in breast cancer; from hormones and their receptors, to oncogenes and specific proteins in signalling pathways. Hormone receptor positive tumours, which make up around 60% of all cases (Clarke *et al.*, 1984), will generally be treated using endocrine therapy, *i.e.* hormone targeting agents. TNBC cancers or cases

where a tumour has become resistant to endocrine therapy will be primarily targeted using radiotherapy and cytotoxic chemotherapy.

ER-positive cancers are the earliest example of a successful targeted therapy in breast cancer, through targeting expression of the ER itself (Jordan and Murphy, 1990). Tamoxifen, for example, is a non-steroidal ER blocker, which acts via binding to and inducing conformational changes in the ER-receptor (McDonnell and Wardell, 2010). More recently, however, aromatase inhibitors, which reduce levels of the hormone oestrogen are becoming more widely prescribed for ER positive cancers (Fabian, 2007). The HER2 receptor has also proved a viable target for drug development, with the production of the HER2-targeting agent trastuzumab (brand name Herceptin), a monoclonal antibody which binds to and blocks a portion of HER2. Although these drugs are highly specific to their hormonal targets, they are still commonly used in combination with chemotherapeutic agents in order to produce the greatest anti-cancer effects and attempt to overcome the resistance that can occur due to upregulation of different signalling pathways (Schlotter *et al.*, 2008; Leary *et al.*, 2007) (Section 1.1.8.2).

Chemotherapeutics generally target highly proliferating cells, often impairing such processes as mitosis (Table 1.1). Chemotherapeutic agents such as Paclitaxel and Cisplatin are highly cytotoxic drugs which are associated with multiple side effects from relatively mild, yet unpleasant effects of nausea and vomiting, to more substantial issues including neuropathy, thrombosis and myalgia (Partridge *et al.*, 2001). These drugs are effective at killing some cancer cells, but their non-specific cytotoxicity means these side effects are common and thus research is more focused into generating or improving compounds in order to exhibit more specificity and selectivity for cancer cells (Chari, 2008).

Table 1.1: Summary of Chemotherapeutic Drugs
(Hassan *et al.*, 2010; Cardoso *et al.*, 2014; Senkus *et al.*, 2013)

Type	Mechanism	Cancer Targets	Examples
Alkylating agents	Direct DNA damage – prevent cell reproduction	Leukaemia, lymphoma, Hodgkin disease, multiple myeloma, sarcoma, lung, breast , ovary	Cyclophosphamide
Antimetabolites	Interfere with DNA and RNA production	Leukaemia, breast , ovary, intestinal	5-fluorouracil, gemcitabine, methotrexate
Anti-tumour antibiotics e.g. Anthracyclines	Interfere with enzymes involved in DNA replication	Breast , leukaemia, lymphoma, bladder, Hodgkin disease, lung cancer	Doxorubicin, Epirubicin
Topoisomerase inhibitors	Interfere with topoisomerase enzymes involved in DNA separation in S-phase of cell cycle	Leukaemias, lung, ovarian, gastrointestinal	Topo I inhibitors: Topotecan, Irinotecan Topo II inhibitors: Etoposide
Mitotic Inhibitors	Stop mitosis in M phase of cell cycle and can prevent enzymes producing proteins needed for cell reproduction	Breast , lung, myeloma, lymphoma, leukaemia	Taxanes: Paclitaxel & docetaxel Vincristine
Platinum Agents	Inhibition of DNA, RNA and protein synthesis	Ovarian, lung, breast (TNBC) .	Cisplatin, carboplatin

Some agents which are thought to target CSCs have been evaluated, although many failed at early stages of research, some showing serious side effects which may be due to harming normal stem cells required for normal cell regenerative processes (Hu and Fu, 2012). Some agents have, however, made it on to the market. Vismodegib, for example, a hedgehog-signalling inhibitor has been approved for use in basal cell carcinoma. The specificity for Vismodegib, however, in targeting the stem cell population has not been clearly established; therefore it is not necessarily a true CSC-targeting agent (Sandhiya *et al.*, 2013). Tarextumab is a monoclonal antibody, targeting Notch pathway proteins. Results from a safety study using a combination of Tarextumab and conventional pancreatic cancer drugs were overall very positive, with 83% of 29 patients' pancreatic tumours stabilising or shrinking over 8 weeks to one year. This drug is now in phase II trials for pancreatic and lung cancer (Yen *et al.*, 2015). Verastem is a company set up by Dr Max Wicha which exists to screen already licensed drugs for the ability to block focal adhesion kinase, an enzyme highly implicated in cancer progression and metastases due to its ability to aid cell adhesion and cancer stem cell survival. The first FAK inhibitor candidate did not show promising results in clinical trials, however, another agent, Reparixin, which was initially developed to target transplant rejection, appeared to eliminate cancer cells through blocking a receptor involved in their growth. Reparixin demonstrated early promise in a safety study on triple-negative breast cancer, and is now in a phase II trial of breast cancer (Kaiser, 2015).

1.1.8.2 Combination Therapies in Breast Cancer

The idea of using several different chemotherapeutics in combination as a treatment regime in cancer was first proposed in 1970s (Bonadonna *et al.*, 1976). Combination therapies have been increasingly common in the treatment of breast cancer, especially in advanced, metastatic stages of the disease (Carrick *et al.*, 2009; Overmoyer, 2003). Several commonly used chemotherapeutic combinations include 'FEC' – 5-Fluorouracil (5-FU), Epirubicin and Cyclophosphamide (Zamagini *et al.*, 1991), 'AC' – Doxorubicin (brand name Adriamycin) and Cyclophosphamide (Fisher *et al.*, 1990), and 'CMF' – Cyclophosphamide, Methotrexate and 5-FU (Bonadonna *et al.*, 1976). The drugs used in these combination therapies have varied mechanisms of

action thus allowing them to target different pathways and features of cancerous cells. These wide acting therapies are compiled in order to help facilitate an increased chance of successful treatment, *i.e.*, long-term disease-survival (Buzdar *et al.*, 1982) and attempt to overcome issues of resistance and relapse.

Combination therapies can also include the co-treatment of a patient using chemotherapy and hormonal therapies, as mentioned in section 1.1.8.2, surgery and radiotherapy. Drugs with different mechanisms of action may be utilised as adjuvant therapies after the initial treatment has begun, or occasionally as neoadjuvant therapy, before the primary treatment has begun (Mauri *et al.*, 2004). Ultimately, this will lead to a combination therapy treatment course with drugs administered at different stages, the schedule of administration being particularly important since the effects of these drugs are often schedule-dependent (Fujimoto-Ouchi *et al.*, 2001).

1.1.8.3 Treatment Challenges in Breast Cancer

Despite some treatments being successful in breast cancer, resistance and relapse are a common occurrence. Both resistance and relapse can be explained by the presence of CSCs (Section 1.1.7) which exhibit promoting properties of self-renewal; apoptosis resistance; independent growth abilities; and metastatic potential, thus allowing cancers to survive treatments and reseed at different locations. CSCs share many properties of normal stem cells, *i.e.*, they exhibit properties which facilitate a long lifespan such as: relative quiescence; resistance to drugs and toxins (due to the expression of ATP-binding cassette (ABC) transporters); ability to repair DNA damage; apoptosis resistance (Dean *et al.*, 2005). CSCs are therefore generally resistant to cancer drugs, in addition to radiotherapy, surviving even after a rigorous treatment regime which may successfully eliminate the bulk cells. CSCs therefore provide an important yet challenging target in the search for more efficient therapies which prevent the successful seeding of new tumours and slow the growth of already developed ones by removing their self-renewal potential (Figure 1.3) (Lawson *et al.*, 2009).

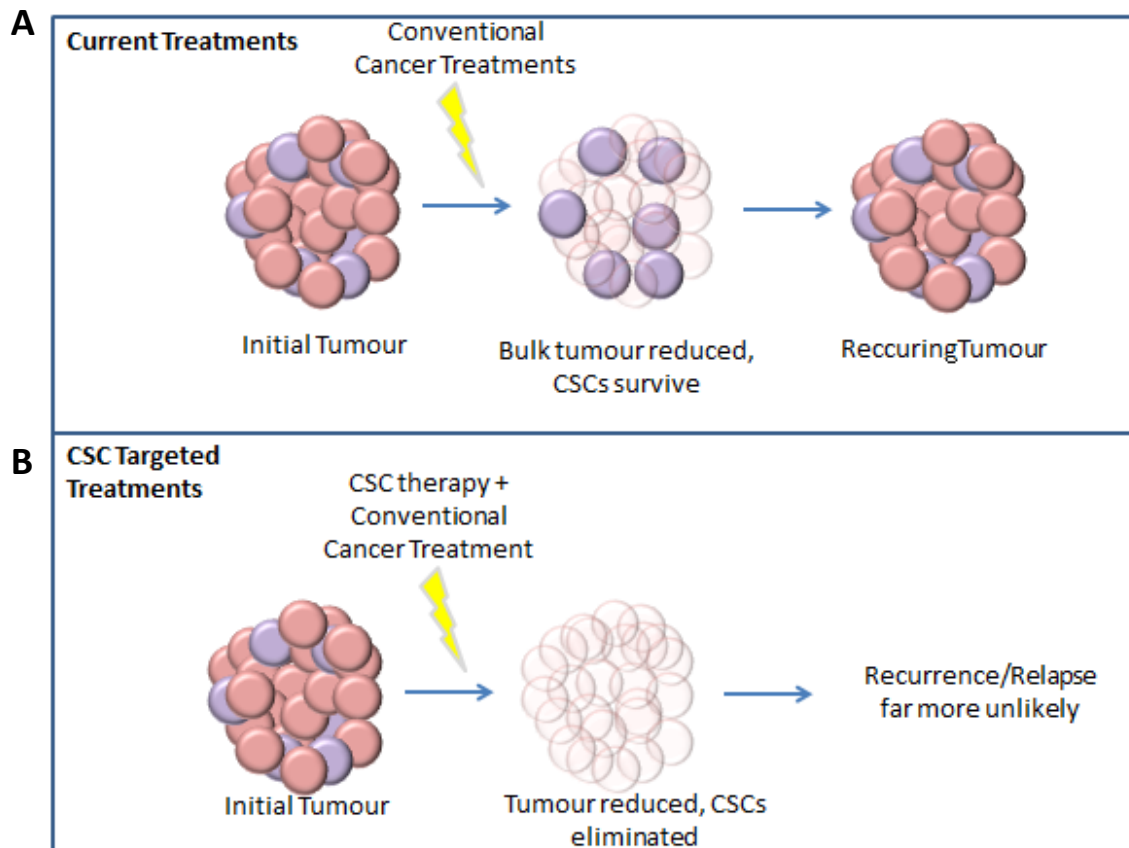


Figure 1.3: Cancer Stem Cell Targetted Therapies aim to Significantly Reduce the Risk of Relapse

A) Most current treatments are able to successfully eliminate a large proportion of the bulk tumour cells, although do not act on the CSC population. B) CSC targetted treatments, in combination with conventional bulk targetting agents, aim to eliminate the CSC population, thus significantly reducing the risk of relapse (Adapted from Verastem, Accessed 2015).

Heterogeneity (Section 1.1.5) is a major consideration for cancer therapeutics, and although combination therapies provide some means to target multiple cell types within a tumour, heterogeneity still remains a challenge as cancers mutate and change throughout the course of disease and often become more difficult to define and therefore treat, as is the case in TNBC (Hutchinson, 2010).

An additional challenge is the fact that most anti-cancer agents or regimes do not target only the cancer cell population, thus, the therapeutic efficacy of these treatments is limited by their additional toxicity to 'normal' healthy cells and so the patient is left weak and immunocompromised, often experiencing highly unpleasant side effects (Chari, 2008).

These challenges mean that treatment and research into treatment is evolving to become more target based in order to achieve a higher specificity and a lower general toxicity of the therapeutics and ultimately provide new and refined treatment strategies (Binkley *et al.*, 2012). Additional treatment strategies in cancer include agents which aim to target one of the hallmarks of cancer, apoptosis evasion, by inducing apoptosis in cancer cells, allowing for a more cancer-cell targeted effect (Discussed in Section 1.2.2).

1.2 Apoptosis

1.2.1 Introduction

Apoptosis, or programmed cell death (PCD) is a crucial process for the maintenance of tissue homeostasis and therefore of normal organism development (Shirley and Micheau, 2010). The process is characterised by a series of precisely regulated mechanisms observed in mammalian cells during the genetically defined cell suicide. Apoptosis initiation may occur due to an immune reaction, response to disease (Norbury and Hickson, 2001), cellular aging, or by chemical agents, hormones and drugs (Elmore, 2007). Broadly, apoptosis is divided into the intrinsic, *i.e.* dependent on intracellular signals and mitochondria-mediated, and the extrinsic pathway, which requires the binding of death ligands to death receptors (DRs) present on the surface of cells.

The intrinsic pathway, sometimes known as the mitochondrial pathway, involves non-receptor mediated signals. A key feature of the intrinsic pathway, sometimes referred to as the p53-mitochondrial pathway, involves mitochondrial membrane permeabilization. This permeabilization is performed in a controlled manner, regulated by proteins of the Bcl-2 family, mitochondrial lipids, metabolic proteins and other key permeability regulating proteins. The result is the release of pro-apoptotic proteins into the cell cytosol, which then mediate caspases further down in the pathway to further activate PCD and induce other cell death processes such as nuclear DNA fragmentation (Green and Kroemer, 2004).

The extrinsic pathway is initiated through ligand binding to DRs which are members of the tumour necrosis factor (TNF) superfamily. These TNF superfamily DRs

all contain a cytoplasmic death domain (DD) of around 80 amino acids in length (Ashkenazi and Dixit, 1998). When an appropriate death ligand, such as TNF-related apoptosis inducing ligand (TRAIL) (Section 1.2.2) binds, which is usually a trimeric structure; an adaptor protein will be recruited on the cytoplasmic portion of the receptor. The initial adaptor protein contains a DD which is able to bind with the DD present on the receptor and thus functions to convey the initial ligand binding signal further along to the intracellular components of the pathway. Apoptosis is then mediated by a series of procaspases which are cleaved to become the activated caspases (Ashkenazi and Dixit, 1998; Elmore, 2007).

Disturbances in the regulation of apoptosis can promote cancer initiation due to prolonging the life of cells beyond their normal lifespan. Consequently, it follows that apoptosis is often reduced in cancer cells, which is likely controlled by anti-apoptotic proteins taking precedence over apoptosis-inducing proteins (Section 1.2.2.6 and 1.3) (Schlotter *et al.*, 2008; Wong, 2011).

In the case of the mammary gland, microarray profiling has been performed on the mouse mammary gland during several key processes: pregnancy; lactation; and involution. Post-lactation, during the remodelling process of involution, a number of changes involving high levels of PCD occur in the mammary gland. The previously important cells required during lactation undergo apoptosis controlled by multiple apoptosis-related proteins, which were identified by the screen as multiple members of the TNF- α superfamily. TRAIL, amongst other TNF ligands, was detected as a possible apoptosis-inducing ligand in the mammary gland (Clarkson *et al.*, 2004).

1.2.2 TRAIL Induced Apoptosis

TRAIL is an endogenous death ligand and a member of the TNF superfamily. The 20 kDa protein is primarily expressed on immune cells due to its significant roles in both T-cell homeostasis and natural killer (NK) or T-cell killing of both virally and oncogenically transformed cells (Wang and El-Deiry, 2003).

TRAIL is a type II transmembrane protein, containing an extracellular domain which is cleaved to form the biologically active soluble form of TRAIL. The protein was initially identified based on a high sequence homology with CD95 ligand (28%

homologous) and TNF α (23% homologous). The fact that TRAIL has a cleavable extracellular carboxy portion, which forms the active soluble form, however, makes it unique from CD95L and TNF- α (Mariani and Krammer, 1998).

TRAIL has two transmembrane surface receptors: DR4 and DR5 which are capable of inducing apoptosis. The two remaining TRAIL receptors are the decoy receptors (DcR), DcR1 or DcR2 (Pan *et al.*, 1997), which lack the functional DD and thus do not facilitate apoptosis due to the lack of signal transduction after TRAIL binding (Ashkenazi, 2002). A fifth TRAIL receptor does exist, osteoprotegerin (OPG) which is a secreted TNF family member that acts to inhibit osteoclastogenesis (Emery *et al.*, 1998).

The two active TRAIL receptors, DR4 and DR5, consist of an extracellular cysteine-rich domain (CRD) and an intracellular DD. Homotrimerisation of TRAIL leads to conformational changes in the receptors, including their oligomerisation which enables the receptors DD to recruit and bind, via a DD:DD interaction, to intracellular Fas-associated death domain (FADD). FADD, in its role as an adaptor protein, then recruits and interacts, via the DED domains, with the zymogen caspases, procaspase-8 or -10, forming the death inducing signalling complex (DISC) and leading to the initiation of the caspase cascade (Ashkenazi and Dixit, 1998; Medema *et al.*, 1997). Cleavage of procaspase-8/-10 to their active caspase subunits, p18 in the case of caspase-8, facilitates the subsequent activation of 'executioner' caspases, primarily involving caspase-3, ultimately leading to apoptosis (Figure 1.4).

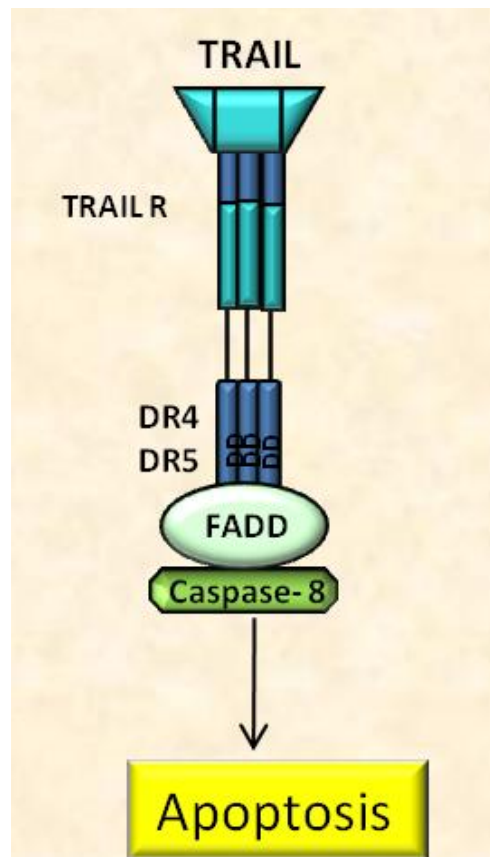


Figure 1.4: Simplified Schematic of TRAIL induced extrinsic apoptosis

TRAIL binds to its surface receptors DR4 or DR5, that trimerise and recruit the adaptor protein FADD via DD interactions. FADD in turn recruits procaspase-8 which is cleaved to the active caspase-8 form which then leads to apoptosis through cleavage of downstream caspases or through the intrinsic pathway of apoptosis, via Bid cleavage.

The active caspase-8 is also able to induce the protein 'Bcl2 homology domain 3 interacting domain' (BID) which in turn initiates activation of the intrinsic, mitochondrial pathway of apoptosis. Bid cleavage to truncated Bid induces activation of Bax and Bak which translocate and form pores in the mitochondrial membrane, facilitating the release of cytochrome C. An interaction between apoptotic protease factor-1 (Apaf-1) with caspase-9 can then occur, thus completing the formation of the apoptosome complex and in turn, activating caspase-9. Caspase-9 leads to further activation of effector caspases and enhances the signal induced via the extrinsic pathway (Chen *et al.*, 2000; Ashkenazi and Dixit, 1998).

1.2.2.1 Alternative roles of TRAIL

Conversely to its role in both the extrinsic and intrinsic forms of apoptosis, TRAIL is able to activate several pathways involved in cell survival, including the NF- κ B, MAPK and JNK pathways, depending on the components that make up the DISC complex (Johnstone *et al.*, 2008). Although not fully established, it is thought that some of the key proteins involved in the alternative functions of TRAIL are FADD, TNFR type 1-associated DD (TRADD), procaspase-8/-10, replication protein A-interacting protein (RIP), c-FLIP and inhibitor of apoptosis proteins 1 and 2 (IAP1/2) (Johnstone *et al.*, 2008). DISC composition, therefore, can regulate TRAIL-susceptibility.

1.2.2.2 Regulation of TRAIL Signalling

The multistep pathway of TRAIL induced apoptosis has many potential areas, from receptor level to intracellular signalling components, which may be altered in order to regulate responses to TRAIL. In particular, expression of the death receptors can impact cell sensitivity or resistance to TRAIL. Lack of surface expression of DR4 or DR5, which has been observed in neuroblastoma tumour cells, for example, is correlated with reduced TRAIL sensitivity (Yang *et al.*, 2003). However, DR4 or DR5 expression levels have not been found to impact on breast cancer cell TRAIL sensitivity (Rahman *et al.*, 2009; Zhang and Zhang, 2008). Localisation of DRs in lipid rafts, due to palmitoylation controlled by O-glycosylation enzymes can alter TRAIL sensitivity. This occurs in DR4 only, impacting on the ability of the receptor to form trimers in lipid rafts when TRAIL is unbound (Wagner *et al.*, 2007; Rossin *et al.*, 2009). Internalisation of DRs can occur by endocytosis, with the absence of DR4 conferring TRAIL resistance in leukaemia cancer cells (Cheng *et al.*, 2006). Of particular interest is that endocytosis of both TRAIL receptors can impact on breast cancer cell sensitivity to TRAIL (Zhang and Zhang, 2008)

Expression of the decoy receptors, DcR1 or DcR2, which compete with DR4 and DR5 for binding with TRAIL and do not induce apoptosis due to lack of a DD have been shown to induce TRAIL resistance when overexpressed (Rahman *et al.*, 2009). Expression of the decoy receptors, however, in breast cancer cell lines (or indeed in other tumours) is not clearly associated with TRAIL resistance, despite appearing to contribute, at least in part, to the TRAIL resistance in normal cells (Rahman *et al.*, 2009;

Le Blanc and Ashkenazi, 2003). Binding of TRAIL to the fifth TRAIL receptor, OPG, does not lead to apoptosis induction due to the fact that OPG is secreted, and, thus the response upon TRAIL-binding is similar to that observed with the DcRs. The TRAIL-inhibiting effect of OPG has been observed in Jurkat cells, using overexpression of OPG to prevent TRAIL-induced apoptosis (Emery *et al.*, 1998). Contradictory information surrounds OPG, however, since, although expression levels have been correlated with poor prostate cancer prognosis (Brown *et al.*, 2001), it has also been demonstrated to reduce bone metastases in a model of breast cancer (Morony *et al.*, 2001).

Mutation, rather than overall expression levels, of the TRAIL receptors, however, may have at least a partial role in TRAIL sensitivity. In a study of 57 clinical breast cancer samples, three samples were found to have mutations in the DD of DR4, and four in the DD of DR5 which impinged their ability to induce apoptosis. These mutations were only observed in the metastatic set of 34 samples, whereas no mutations were observed in the 23 non-metastasised samples (Shin *et al.*, 2001).

As mentioned in Section 1.2.2, the additional roles of TRAIL, *i.e.* its ability to induce cell survival rather than apoptosis, depending upon the DISC components, is an area in which resistance mechanisms can be explored. The regulation of procaspase-8/-10 activation can be controlled by several anti-apoptotic proteins, such as Bcl-2 and, in particular, cellular FLICE-Like Inhibitory Protein (c-FLIP), which acts via directly preventing the ability of FADD to recruit procaspase-8/-10 (Scaffidi *et al.*, 1999; Safa, 2012). We and others have demonstrated that c-FLIP contributes to TRAIL resistance in breast cancer and that targeted inhibition of c-FLIP by siRNA is able to partially sensitise adherent breast cancer cells to TRAIL whilst also eliminating the breast CSC population (Piggott *et al.*, 2011). c-FLIP and its role in TRAIL resistance will be discussed in Section 1.3.

The Myc oncogenic pathway can enhance TRAIL sensitivity by transcriptional repression of c-FLIP (Ricci *et al.*, 2004). Furthermore, Myc has been shown to increase DR5 expression and thus, caspase-8 activation (Wang *et al.*, 2004). Myc has been demonstrated to regulate TRAIL-dependent transcription of several genes, including NF- κ B and cellular inhibitor of apoptosis protein 2 (CIAP2), which impact on TRAIL sensitivity (Ricci *et al.*, 2007).

1.2.2.3 TRAIL and Untransformed Cells

The ability of untransformed cells to resist TRAIL, whilst apoptosis is induced in cancer cells, is one of the major factors that makes TRAIL such a desirable cancer therapy (Ashkenazi *et al.*, 1999; Walczak *et al.*, 1999; Gura, 1997). Although the exact mechanism of this TRAIL resistance has not been fully elucidated, evidence for many potential mechanisms does exist. It is thought that TRAIL resistance in normal cells is partly controlled by an elevated expression of the decoy receptors (Zhang *et al.*, 2000; LeBlanc and Ashkenazi, 2003; Daniels *et al.*, 2005). Several normal adult tissues have been shown to express one or more decoy TRAIL receptors which may be contributing to the resistance to TRAIL induced apoptosis (Sheridan *et al.*, 1997). In addition, studies have shown that normal stem cells are resistant to TRAIL induced apoptosis (Szegezdi *et al.*, 2009; Kim *et al.*, 2000).

Additionally, the anti-apoptotic proteins XIAP, Bcl-2 and c-FLIP are thought to contribute in part to the lack of TRAIL sensitivity in non-transformed cells. However, it is likely that a combination of these proteins is required in order to elicit TRAIL resistance in non-transformed cells, rather than just one required in cancerous cells (van Dijk *et al.*, 2013).

Being a naturally secreted ligand, it is unsurprising that TRAIL is well tolerated by animals, including mice, monkeys and chimpanzees (Rahman *et al.*, 2009). Thus, there is clearly much evidence to demonstrate the cancer specific properties of TRAIL and provide reason for its use as a therapeutic in the clinical setting. Furthermore, the initial *in vitro* observations of TRAIL-resistance in normal cells has been confirmed in phase I trials using TRAIL which showed no systemic toxicity, even when administered at high doses (Section 1.2.2.5) (van Dijk *et al.*, 2013).

1.2.2.4 TRAIL as a Therapeutic Agent in Cancer

Many anti-cancer agents function via a non-specific cytotoxicity, by targeting processes such as DNA replication, which, although often altered in cancer cells, are also key functions in non-cancerous cells thus leading to the side effects that are associated with many chemotherapeutics. An ability to cause cancer cells to undergo apoptosis (PCD), either by methods of direct activation of apoptotic pathways, or re-sensitisation to previously redundant pathways, is a desirable property of a cancer

therapeutic since it targets one of the key hallmarks of cancer: apoptosis evasion (Hanahan and Weinberg, 2000) and leaves the untransformed cells unharmed. Many *in vitro* studies have demonstrated that TRAIL is indeed able to preferentially induce apoptosis in a wide range of human tumour cells, whilst sparing the non-transformed cells (Ashkenazi *et al.*, 1999; Gura, 1997; Takeda *et al.*, 2001; Kim *et al.*, 2000; Wiezorek *et al.*, 2010).

In addition to the direct ability of TRAIL to induce apoptosis in cancer cells when administered in recombinant form, there is much interest in the antitumour effects of endogenous TRAIL. Secreted mainly by cells involved in immune regulation, including NK cells, T cells, monocytes and neutrophils, TRAIL has been shown to have a role in the natural immune defence system by virtue of its specific toxicity to transformed cells (Takeda *et al.*, 2001). TRAIL was first observed to have a role as a tumour suppressor in 2001, in an *in vivo* study which demonstrated NK cell-mediated cytotoxicity on tumour xenografts to be at least in part dependant on TRAIL expression from mouse NK cells in the liver. The study was able to demonstrate, using a neutralizing monoclonal antibody against TRAIL, a significant increase in liver metastases of several TRAIL sensitive tumour cell lines (Takeda *et al.*, 2001). Similarly, an *in vivo* study in 2005, using mice which are deficient in TRAIL, demonstrated an increase in spontaneous lymphoid tumour formation compared with those with normal levels of TRAIL (Zerafa *et al.*, 2005).

There is clearly much evidence to support the potential of TRAIL as an anti-cancer therapy, and, as such, several TRAIL receptor agonists have entered clinical trials.

1.2.2.5 TRAIL in Cancer Clinical Trials

There are currently two categories of TRAIL receptor agonists being tested clinically: recombinant forms of TRAIL and agonistic antibodies specific for DR4 or DR5. Early stage clinical trials have demonstrated TRAIL-pathway agonists to be safe and well tolerated, and to show some anticancer activity with partial or complete responses in both non-small-cell lung cancer and non-Hodgkin's lymphoma patients when treated with Dulanermin, a recombinant form of TRAIL, in combination with other anti-cancer agents (Soria *et al.*, 2010; Belada *et al.*, 2010). Several TRAIL receptor agonistic antibodies have demonstrated anticancer activity in combination with chemotherapy in

multiple cancer types, although the effects were modest and non-significant (Lempke *et al.*, 2014).

Recombinant TRAIL was first tested in phase I clinical trials in two prevalent cancers; lung cancer and lymphoma to establish overall safety and tolerability, and was shown to be well-tolerated at serum levels above the therapeutic concentrations used in preclinical studies, demonstrating no overall toxicity (Herbst *et al.*, 2010). In addition, several monoclonal antibodies against DR4 and DR5 have also been well tolerated (Stuckey and Shah, 2013). One such monoclonal antibody, mapatumumab, which acts on DR4, entered Phase II testing for non-Hodgkin lymphoma and generated a promising response in around a third of the trial patients, with one showing a complete recovery (Younes *et al.*, 2010).

Most recently, Tigatuzumab, an agonistic anti-DR5 antibody has been tested, in combination with Paclitaxel, in a clinical trial of patients with triple-negative breast cancer (Forero-Torres *et al.*, 2015). Tigatuzumab functions to trigger apoptosis in DR5 expressing human tumour cells and has demonstrated *in vitro* and *in vivo* activity when tested on basal-like breast cancer cells, when administered in combination with chemotherapeutic agents. Although the responses were relatively modest, the Tigatuzumab-Paclitaxel combination prolonged progression free survival in several patients, thus supporting further studies and trials into anti-DR5 agents as a means of activating the TRAIL pathway in cancer. Indeed, this trial was performed in triple-negative breast cancer, which has been demonstrated *in vitro* to be TRAIL sensitive (Rahman *et al.*, 2009) including in studies performed both *in vitro* and *in vivo* using anti-DR5 antibodies.

There are some clinical trials, however, which have been less successful for TRAIL, primarily when tested as a combination therapy with chemotherapeutic agents, despite *in vitro* studies showing promise for such regimes (Lempke *et al.*, 2014; Shrader *et al.*, 2007). Although further demonstrating a high systemic tolerance to TRAIL, minimal anticancer activity has been observed in many studies (Lemke *et al.*, 2014) (Table 1.3). Therefore, there are needs to improve the clinical performance of TRAIL, and identify those patient subsets which will benefit from TRAIL treatment.

Table 1.2: Clinical Trials for rhTRAIL.

All clinical trials presented here demonstrated safety for the drug tested.

Phase	Agent	Cancer	Combination	n	Efficacy	Ref
I	rhTRAIL	Advanced cancers	-	71	2 patients with metastatic chondrosarcoma had partial responses. 33 patients had stable disease for longer than 6 months.	Herbst 2010
IA	rhTRAIL	Advanced Cancer and Lymphoma	-	39	None reported	Ling 2006
IA	rhTRAIL	CRC, sarcoma, NSCLC	-	31	1 partial response, 5 stable disease	Pan 2007
I	rhTRAIL	Colorectal	+ Chemotherapy + Bevacizumab	23	13 partial responses	Wainberg 2013
I	rhTRAIL	Colorectal		27	6 partial responses	Kasubhai 2012
I	rhTRAIL	Lung		24	1 complete response, 13 partial responses	Soria 2010
II	rhTRAIL	Lung		213	No responses	Soria 2011
I	rhTRAIL	Colorectal	+ Chemotherapy + Cetuximab	30	Evidence of activity - ongoing	Yee 2009
I	rhTRAIL	Lymphoma	+ Rituximab	7	2 complete responses, 1 partial response	Yee 2007
II	rhTRAIL	Lymphoma		48	No responses	Belada 2010
Ib/II	Monoclonal Ab	Non-Hodgkin's Lymphoma	-	40	3 patients with follicular lymphoma responded: 2 complete, 1 partial	Younes 2010
II	Monoclonal Ab	TNBC	+ Chemotherapy	64	3 complete remissions, 8 partial, 11 stable	Forero-Torres 2015

1.2.2.6 TRAIL Resistance in Cancer

One of the most prevalent issues with any anti-cancer agent is the issue of resistance. Cells often adapt and change in order to overcome treatment by certain drugs; however, resistance to TRAIL appears to be a more cell-type specific phenomenon (Rahman *et al.*, 2009). Studies have shown that approximately 60% of tumour cell lines are TRAIL resistant, which significantly limits the clinical potential of TRAIL as a monotherapy (van Dijk *et al.*, 2013). It is possible that TRAIL-resistance can be overcome if used in combination with other clinical agents. An understanding of TRAIL-resistance and regulation mechanisms is therefore vital in order to attempt to establish a viable treatment regime (Section 1.2.2.2).

The efficacy of TRAIL as a therapeutic in breast cancer is severely hampered by the existence of several subtypes of the disease, which make up a large proportion of breast cancer cases, that are resistant to TRAIL (Rahman *et al.*, 2009). Several *in vitro* studies of TRAIL mediated apoptosis in breast cancer cell lines showed that whilst the triple-negative MDA-MB-231 cell line sensitive to TRAIL mediated apoptosis, a large proportion of cell lines were highly TRAIL resistant (Ashkenazi *et al.*, 1999). Further studies have shown that TRAIL sensitivity of breast cancer cells can be categorised by the disease subtype, with triple-negative breast cancers of a mesenchymal phenotype demonstrating the greatest sensitivity to TRAIL. In contrast, the more prevalent ER-positive cancers, of a more luminal phenotype, were highly TRAIL resistant, more so than the HER2 lines which had a modest response to TRAIL (Rahman *et al.*, 2009).

Resistance in these cancers involves several previously mentioned pathways of TRAIL regulation (Section 1.2.2.2). Dysfunctions in the death receptors DR4 and DR5, the adaptor protein FADD, or the initial caspase caspase-8, due to mutations, can lead to TRAIL resistance in cancer (Zhang and Fang, 2005). Primarily, however, anti-apoptotic proteins such as c-FLIP are thought to be the key drivers of TRAIL-resistance in cancers (Section 1.3) (van Dijk *et al.*, 2013; Safa and Pollok, 2011).

1.2.2.7 TRAIL Sensitisation Agents

The majority of current therapeutic strategies in cancer aim to overcome two of the key hallmarks of cancer: excessive proliferation and apoptosis resistance (Hanahan and Weinberg, 2011). Therapeutics which slow or prevent cancer cell proliferation are likely to achieve a stable disease state, through limiting the growth of tumour cells, whereas therapeutics which are able to induce apoptosis may have the potential to eliminate cancer cells, thus potentially forging a route to cure (Lemke *et al.*, 2014). The observation that the endogenous death ligand TRAIL can preferentially target cancer cells through the cancer-cell specific induction of apoptosis (Ashkenazi *et al.*, 1999; Walczak *et al.*, 1999) makes it a highly desirable anti-cancer therapy. Indeed, there are now a multitude of *in vitro* studies which provide evidence of this cancer cell-specific effect (Section 1.2.2). Although initial *in vitro* studies demonstrated great promise for TRAIL as a cancer-cell specific therapy, these clinical trials, at phases I, II and III, performed in multiple cancer types have demonstrated positive, although much less significant results for TRAIL as a potential therapeutic. In addition, many *in vitro* studies have confirmed the existence of multiple TRAIL-resistant cell lines in both breast and other cancer types (Rahman *et al.*, 2009), which may partially explain the reason for the modest *in vivo* effects. These observations have evidentially decreased the initially apparently broad therapeutic range of TRAIL as a monotherapy. Ways of overcoming TRAIL resistance and increasing the therapeutic efficacy of TRAIL are becoming an important research target.

Agents which enhance TRAIL-mediated apoptosis do exist, acting in a variety of different *in vitro* cancer cell lines and via several mechanisms of action. Mechanisms of these agents include increasing expression of TRAIL receptors, particularly DR5, increasing expression or activation of caspases, including caspase-8, and downregulating c-FLIP (Section 1.3.6) amongst several other mechanisms (Trivedi and Mishra, 2015).

GGTI-298, for example, is a geranylgeranyltransferase I (GGTase I) small molecule inhibitor which was shown to augment TRAIL-induced apoptosis in a panel of lung cancer cell lines. Reduced c-FLIP levels were also observed, which may have been due to the inhibition of Akt phosphorylation, although the primary mechanism of action was suggested to be via induction of DR4 and DR5 expression (Chen *et al.*, 2010). The

actions and effects of GGTI-298 are similar to that of farnesyltransferase (FTase) inhibitors, that is, reducing Akt phosphorylation in some cell lines and enhancing the apoptosis-inducing ability of TRAIL (Qiu *et al.*, 2007).

In the last year, a novel caspase-8 selective small molecule has been developed using *in silico* modelling which potentiates TRAIL-induced death in prostate cancer cells by directly binding to and promoting caspase-8 activation (Bucur *et al.*, 2015).

There are many additional TRAIL sensitising agents that exist, although the majority act via a relatively non-specific targeting of several involved proteins. Agents which regulate c-FLIP, and thus, TRAIL sensitivity are further explored in Section 1.3.6.

1.2.3 DED Containing Proteins

Many of the key proteins involved in the extrinsic pathway of apoptosis, introduced in Section 1.2, are death effector domain (DED) containing proteins. The key proteins involved include FADD, procaspase-8/-10 and c-FLIP. The reason that the TRAIL pathway can have such opposing effects of inducing apoptosis or cell survival is based on which DED-containing proteins make up the DISC complex Section 1.2.2.1 (Johnstone *et al.*, 2008).

The DED domain is a site of protein interaction which, as the name suggests, is mostly associated with the induction or processing of apoptosis, although the domain itself has no enzymatic activity. DED domains facilitate predominantly hydrophobic interactions (Eberstadt *et al.*, 1998) between TNF receptor (TNFR) family members followed by recruitment of the DED containing linker protein, FADD, and the induction of a caspase cascade usually involving procaspase-8/-10 (Valmiki and Ramos, 2009).

In addition to the key TRAIL signalling proteins, additional DED containing proteins include: death effector domain containing DNA binding (DEDD), DEDD2 and phosphoprotein enriched in astrocytes 15-KDa (PEA-15), which are more commonly involved in TNF- α receptor family processes (Figure 1.3). These additional proteins demonstrate further that not only are DED proteins required for apoptosis induction, as is the case with procaspase-8/-10 but, conversely, they also have roles in processes such as transcription, migration and proliferation (Valmiki and Ramos, 2009).

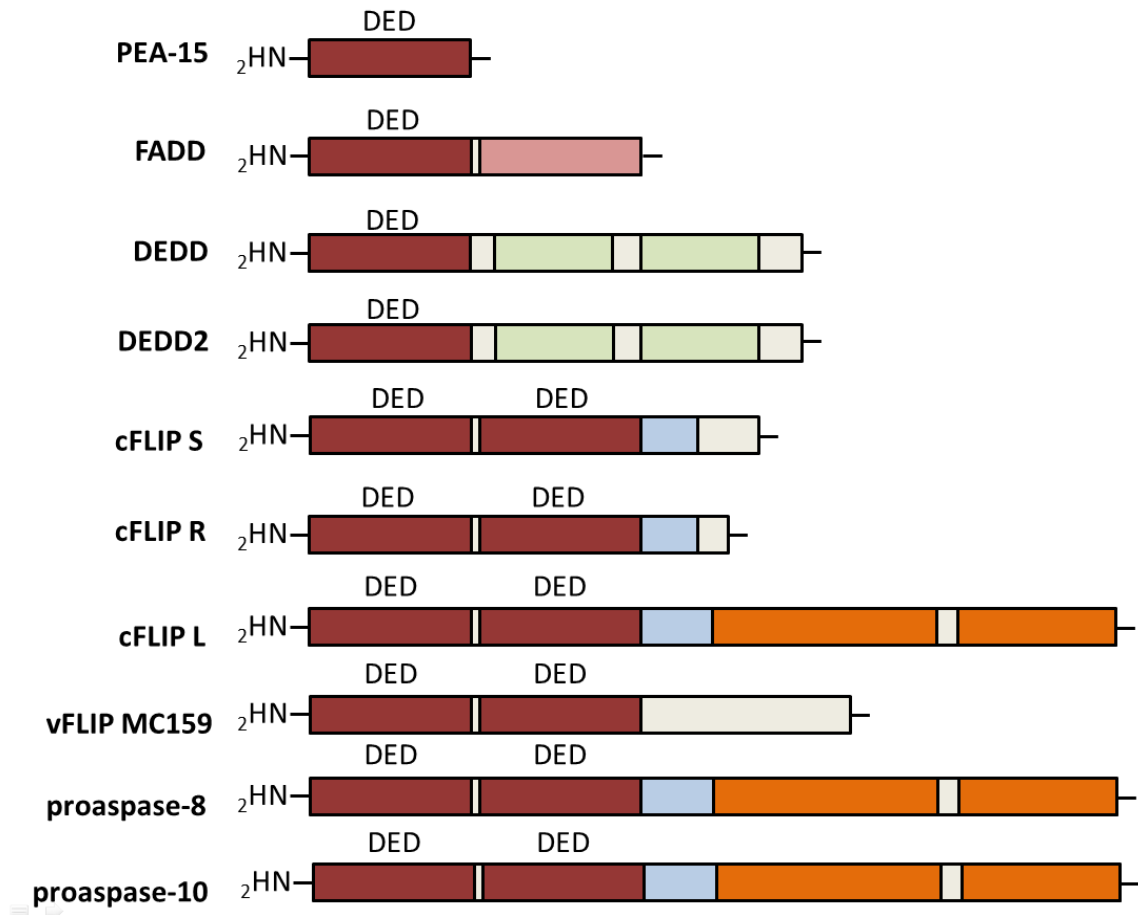


Figure 1.5: The family of some of the key DED domain containing proteins

Summary of the key DED (shown in red) containing proteins. Displayed sizes are relative to protein base pair length (Adapted from Valmiki and Ramos, 2009).

1.2.3.1 DED Domain Structure

The structure of the DED domain is generally very highly conserved between proteins and was first defined in 1995, in a transient transfection assay using FADD (Chinnaiyan *et al.*, 1995). Basic computer modelling was used to predict the folding of the DED initially, before full NMR characterisation was performed in 1996, enabling the elucidation of the structure of FADDs DED (Eberstadt *et al.* 1998). FADD is a member of the death domain (DD) superfamily and thus has the features of an amphipathic, antiparallel bundle of six α -helices (Figure 1.6), shared between members of the DD superfamily, despite the family having an overall low sequence homology (Weber and Vincenz, 2001).

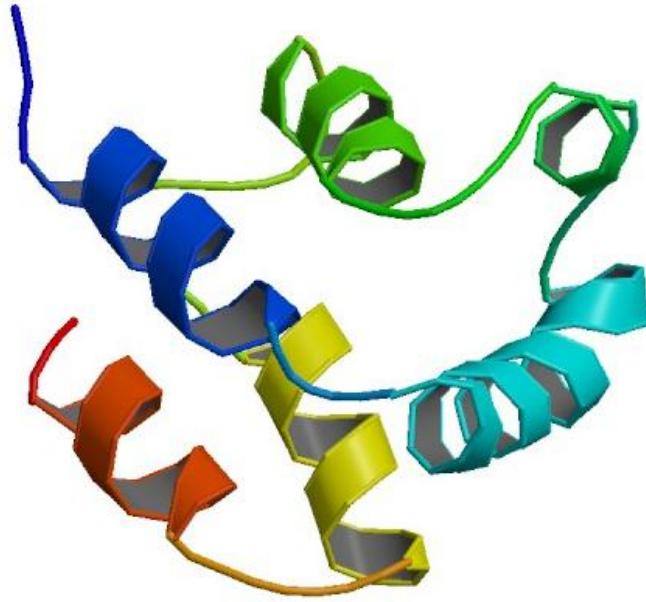


Figure 1.6: NMR structure of DED domain from FADD.

Protein chains are coloured from N- to C-terminal using a rainbow spectral colour gradient (Image from PDB-1A1W).

Many DED proteins have an 'FL motif' which, in tandem DED proteins, will be present on DED1 and thus occupy a pocket in the surface of DED2 (Dickens *et al.*, 2012). FADD, containing one DED only, has an FL motif at F25/L26 which is not buried within another domain and is therefore available to form interactions with other DED proteins, including procaspase-8/-10 or c-FLIP (Eberstadt *et al.*, 1998). Further detail into DED structure and interactions is provided in Section 1.3.7.

1.3 Cellular FLICE-like Inhibitory Protein (c-FLIP)

1.3.1 Introduction

c-FLIP, otherwise known as Casper, FLAME-1, iFLICE, CASJ, CLARP, CFLAR or MRIT (Schuchmann *et al.*, 2006; Safa and Pollok, 2011), has been demonstrated to be a key regulator of apoptosis. The identification of c-FLIP, as a cell expressed homolog of viral FLIPs (v-FLIPs), in 1997, sparked an interest in research to divulge the function of this novel cellular expressed protein (Irmeler *et al.*, 1997). Although 13 splice variants of c-FLIP have been identified, only 3 isoforms appear to be expressed as proteins: 55 kDa c-FLIP long (L), 26 kDa c-FLIP short (S) and 24 kDa c-FLIP Raji (R) (Figure 1.7). The two shorter forms of c-FLIP, c-FLIP S and R still contain two functional DED domains but lack the caspase-like domain. All three forms of c-FLIP have been demonstrated to have a role in the regulation of signalling pathways including both survival and apoptosis, although the least is known about the role of c-FLIP R (Safa *et al.*, 2008; Safa, 2012).

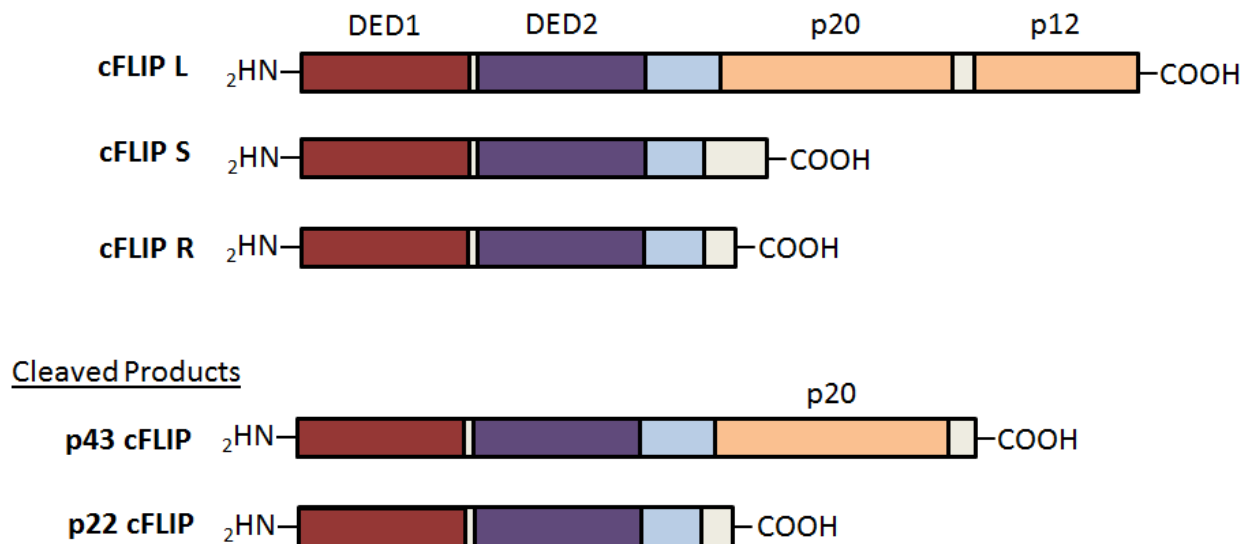


Figure 1.7: Basic structures of the 3 c-FLIP splice variants which are expressed as proteins and the 2 cleaved products.

c-FLIP-L, the longest form of c-FLIP is made up of two DEDs; DED1 and DED2. The carboxyl tail is made up of two subunits, p20 and p12 which are not present on c-FLIP-S or -R. Upon homodimerisation or heterodimerisation with procaspase-8 (or-10), c-FLIP may be cleaved to one or both of the cleaved products shown. Sizes are relative to protein length (Adapted from Safa, 2012).

In addition to the cellular forms of c-FLIP, v-FLIPs also exist, initially identified in molluscum contagiosum virus (MCV) and in forms of γ -herpesviruses with one of the most studied v-FLIPs being the MCV, MC159 (Garvey *et al.*, 2002). These FLIP variants have been demonstrated to block the activation of DRs at the point of DISC assembly in the same manner as c-FLIP (Thome and Tschopp, 2001) and are thought to have evolved to inhibit apoptosis of infected host cells in MCV (Garvey *et al.*, 2002). Like c-FLIPs, v-FLIPs also contain 2 tandem DED domains which have been demonstrated to be able to interact with the DED domains of both FADD and procaspase-8 (Yang *et al.*, 2005; Li *et al.*, 2006).

1.3.2 c-FLIP Structure

c-FLIP L is 55 kDa protein, highly homologous to procaspase-8 (Scaffidi *et al.*, 1999; Naito *et al.*, 2004), containing two N terminal DEDs, DED1 and DED2, which, like procaspase-8, allow binding to the DED of FADD when in complex with TRAIL receptors DR4 or DR5. Unlike procaspase-8, c-FLIP does not have an active caspase domain, due the substitution of tyrosine for a conserved cysteine residue in its C-terminal caspase-like domain, and is therefore caspase-inactive (Irmeler *et al.*, 1997; Peter, 2004). The DED domains, DED1 and DED2 of c-FLIP and procaspase-8 are able to interact with the one DED present on FADD, when in complex with the membrane bound death receptors DR4, DR5, DcR1 or DcR1. The complex of these proteins results in the formation of a DISC. Since c-FLIP is catalytically inactive, binding to FADD competitively inhibits the induction of apoptosis by procaspase-8/10 (Grunert *et al.*, 2012; Safa and Pollok, 2011). Furthermore, in addition to preventing apoptosis competing with procaspase-8 for FADD binding, c-FLIP is also able to bind to procaspase-8 itself, thus preventing the formation of a complete DISC, which has recently been proposed to consist of 'chains' of processed caspase-8 homodimers, bound initially to FADD via a DED:DED interaction (Dickens *et al.*, 2012).

The caspase-like C-terminal domain of c-FLIP has been resolved by crystallography, however, the full protein, including its DED domains has not been yet been resolved. The crystal structure of v-FLIP, MC159's DED domains have, however, been resolved, which is useful for aiding *in silico* studies of c-FLIP (Dickens *et al.*, 2012)

(Chapter 3) and indeed other DED domain containing proteins (Li *et al.*, 2006). c-FLIP S, in particular, is similar in structure to the v-FLIPs; the main difference being the presence of 20 additional amino acids on c-FLIP S which are important for its ubiquitination and proteosomal degradation. c-FLIP R, similarly to v-FLIPs, contains the two DED domains but lacks the additional C-terminal amino acids. c-FLIP L has a much extended C terminus to c-FLIP S and R which is similar to the C-terminals of procaspase-8/10, although the substitution of a cysteine residue in this domain deems c-FLIP catalytically inactive and thus does not act as a caspase (Safa *et al.*, 2008).

1.3.3 Functions of c-FLIP

Many roles for c-FLIP in cellular processes have been elucidated since its discovery, with regulation of apoptosis being the primary of its functions. At a cellular level, it has been shown to have a dual-role in both cell death, *i.e.* apoptosis and necroptosis, and cell survival processes. On a larger scale, *in vivo* studies have shown c-FLIP to have an important role in T-cell proliferation (Zhang *et al.*, 2008) and the development of heart tissue in early embryonic development (Yeh *et al.*, 2000).

1.3.3.1 c-FLIP prevents Apoptosis

Exploring the reasons for TRAIL resistance indicates that c-FLIP expression plays a key role in this mechanism, and indeed with the mechanism of resistance to Fas-L and TNF- α induced apoptosis (Section 1.2.2.6) (Safa and Pollok, 2011). Indeed, c-FLIP (both long and short) expression levels have been correlated with TRAIL-responsiveness, with elevated expression of c-FLIP shown to correlate with resistance to both TRAIL and chemotherapy-induced apoptosis (Safa and Pollok, 2011; Safa, 2013).

c-FLIP is described as a regulator of death-receptor induced apoptosis, and amongst its other functions, a key focus of research is on its ability to compete with procaspase-8 (or procaspase-10) at the DISC and thus inhibit TRAIL induced apoptosis (Section 1.2.2.6) (Griffith *et al.*, 1998; Safa *et al.*, 2008; Cheung *et al.*, 2009; Grunert *et al.*, 2012). In addition to causing TRAIL resistance, c-FLIP has been shown to have anti-apoptotic roles in Fas and TNF- α -mediated signalling and has been demonstrated to induce chemotherapeutic drug resistance in several diseases (Safa *et al.*, 2008; Micheau, 2003).

Both c-FLIP L and S have been shown to have anti- and pro- apoptotic roles in additional signalling pathways, including an ability to activate or upregulate pro-survival signalling proteins such as Akt, ERK and NF- κ B (Safa, 2012). c-FLIP expression is demonstrated to enhance tumorigenicity and result in a poor clinical outcome for many cancer types due to its effects on enhancing resistance to chemotherapeutics and TRAIL (Day and Safa, 2009). Akt, serine-threonine kinase involved in cell survival regulation, is a key protein with which c-FLIP interacts. This interaction enhances the anti-apoptotic functions of Akt through modulation of Gsk3 β and is mediated by regulation of p27 and caspase-3 expression as assessed by Yeast-2-hybrid in several cancer cell lines (Quintaville *et al.*, 2010). An increased response to TRAIL has been observed when the Akt pathway is downregulated, for example, by suppressing DNA-protein kinase (DNA-PK) in the human chronic myelogenous leukemia cell line, K562 (Kim *et al.*, 2009). The anti-apoptotic role of c-FLIP has also been demonstrated in primary pancreatic tumour cells (Haag *et al.*, 2011), in primary T-cells (Lens *et al.*, 2002) in addition to other primary cells.

Not only has c-FLIP been demonstrated to compete with procaspase-8/-10 for binding with FADD, it has also been shown to interact directly with DR5, FADD and caspase-8 in order to form an apoptotic inhibitory complex (AIC) in the MCF-7 breast cancer cell line (Day *et al.*, 2008). The anti-apoptotic interactions of c-FLIP will be explored further in Section 1.3.7.

1.3.3.2 c-FLIP Activates Cell Survival Pathways

c-FLIP is able to directly activate cytoprotective pathways which involve cell survival, proliferation and carcinogenesis (Safa, 2012). In fact, even its interaction with procaspase-8 can be pro-apoptotic as opposed to anti-, in that in certain conditions it can actually directly activate caspase-8 (Micheau *et al.* 2002; Dohrman *et al.*, 2005). c-FLIP overexpression is able to activate NF- κ B and ERK pathways through binding to proteins involved in these pathways (Safa, 2012; Ueffing *et al.*, 2008). The key proteins with which c-FLIP binds in these pathways are TRAF2 and RIP1, although more efficient binding and robust activation is achieved with the processed p43 N-terminal fragment of c-FLIP L (Dohrman, *et al.*, 2005; Safa, 2012).

c-FLIP L appears to have a role in the modulation of Wnt signalling through the inhibition of β -catenin ubiquitylation (Naito *et al.*, 2004). The nuclear

translocation of c-FLIP and promotion of β -catenin-mediated gene transcription is able to enhance Wnt signalling. This nuclear localisation, controlled through the functional bipartite nuclear localization signal (NLS) present at the C-terminus, could allow c-FLIP to accumulate and thus allow cells to re-acquire stem cell properties via Wnt-mediated transcription (Katayama *et al.*, 2010).

1.3.4 Transcriptional and Post-Translational Regulation of c-FLIP

c-FLIP is the target of many different transcription factors, which can induce or suppress its expression. These factors are generally involved in survival and apoptosis signalling pathways and are activated by a multitude of cytokines, growth factors and ligands involved in DR signalling. c-FLIP levels are primarily regulated by ubiquitin or proteosomal directed degradation (Safa *et al.*, 2008) although other methods of can regulation control c-FLIP.

The protein, Akt is thought to positively regulate the expression of c-FLIP since suppression or activation of Akt was shown to decrease or increase c-FLIP levels respectively (Panka *et al.*, 2001). The two proteins are able to interact, within the C-terminus of c-FLIP, via Akt's binding to and phosphorylation at S273, resulting in the subsequent stabilisation of c-FLIP L (Shi *et al.*, 2009). Conversely to Akt, JNK activation, induced by the E3 ubiquitin ligase, Itch causes the polyubiquitination of c-FLIP and thus targets it for degradation at the proteasome (Chang *et al.*, 2006).

1.3.5 c-FLIP in Cancer

Abnormal expression levels of c-FLIP have been observed in a range of disease states including multiple sclerosis, Alzheimer's disease, diabetes mellitus, rheumatoid arthritis and cancer (Micheau, 2003). Elevated levels of c-FLIP have been demonstrated in multiple cancer cell lines *in vitro*, and are generally associated with resistance to apoptosis induced by death ligands such as TRAIL. Increased c-FLIP expression has been observed in prostate (Gao *et al.*, 2005), colorectal (Ryu *et al.*, 2001), gastric (Nam *et al.*, 2003), pancreatic (Elnemr *et al.*, 2001), ovarian (Xiao *et al.*, 2003) and breast (Wang *et al.*, 2005) cancers, and also in melanoma (Griffith *et al.*, 1998). Additionally, analysis of primary tissues and cells has shown increased c-FLIP in B-cell chronic lymphocytic leukaemia (Olsson *et al.*, 2001), gallbladder (Zong *et al.*, 2009), non-small cell lung and in several other cancer types (Shirley and Micheau, 2010). These observations are

primarily on c-FLIP L, although upregulation of c-FLIP S has been observed in some gastric and pancreatic cancer cell lines, and in lung adenocarcinoma primary samples (Shirley and Micheau, 2010).

Several groups have demonstrated that suppression of c-FLIP sensitises cancer cells to TRAIL killing (Cheung *et al.*, 2009; Li *et al.*, 2012; Murtaza *et al.*, 2009; Geserick *et al.*, 2008). In addition, our lab have demonstrated that suppression of c-FLIP using siRNA, in combination with TRAIL treatment, can selectively eliminate cancer stem cell activity in all breast cancer cell lines tested, in the *in vitro* model of cancer stem cells (Section 1.1.7.3) (Piggott *et al.*, 2011).

Despite expression levels of c-FLIP appearing to correlate with TRAIL sensitivity, we have recently published data demonstrating that localisation of c-FLIP may be more of an important determinant in TRAIL-sensitivity of several breast cancer cell lines. TRAIL-sensitivity appeared to be associated with breast cancer cells which expressed c-FLIP in the nucleus, whereas cells which expressed the protein in the cytoplasm were TRAIL-resistant (French *et al.*, 2015 in press). Inhibition of c-FLIP, whether sensitivity is controlled by localisation or expression levels, however, is clearly a potential method for TRAIL sensitization.

1.3.6 c-FLIP Targeting Agents

We have previously demonstrated that a combination of c-FLIP elimination, by siRNA, and TRAIL causes a significant reduction in viability of the bulk population of several usually resistant breast cancer cell lines (Piggott *et al.*, 2011). More interestingly, perhaps, is the fact c-FLIP siRNA combined with TRAIL is able to entirely eliminate the tumoursphere forming cells present in several TRAIL-resistant, and one TRAIL-sensitive, breast cancer cell line *in vitro* (Piggott *et al.*, 2011). Cancer stem cells are a very important target for new therapies (Section 1.1.7), and, thus, this observation in particular highlights the potential impact of a c-FLIP inhibitor in combination with TRAIL. Furthermore, the demonstrated correlation between c-FLIP overexpression and resistance to death ligand, *i.e.* FasL or TRAIL induced apoptosis, further highlights that c-FLIP may be a suitable target for cancer therapy (Safa and Pollok, 2011; Safa, 2012).

Many approaches to enhancing the degradation or inhibiting c-FLIP *in vitro* have been studied, including the use of transcriptional regulators, si/shRNA and degradation or ubiquitination inducing agents. Although targeted suppression of c-FLIP using such methods as si/shRNA do sensitise cancer cells to TRAIL *in vitro*, this cannot currently be translated to a clinically viable therapy, thus, the use of pharmacological inhibitors of c-FLIP is being considered. However, the development of such inhibitors is made complex by the homology between the DEDs of c-FLIP and procaspase-8 (Goltsev *et al.*, 1997; Safa, 2012), *i.e.* inhibiting the DED of c-FLIP would potentially also inhibit procaspase-8. Currently, agents which result in inhibition or degradation of c-FLIP are non-specific.

Histone Deacetylase Inhibitors (HDACi), which are able to significantly downregulate c-FLIP expression have been proposed to be inhibitors of c-FLIP, although their action is relatively non-specific (Safa *et al.*, 2008). These inhibitors, alone, have been demonstrated to induce re-differentiation in tumour cells and thus re-establish sensitivity toward apoptosis-inducing agents. Vorinostat (suberoylanilide hydroxamic acid (SAHA), for example, has been shown to down-regulate levels of c-FLIP in various *in vitro* cell models of cancer, thus increasing their sensitivity to apoptosis, particularly that induced by TRAIL. Pre-treatment of breast tumour cells with SAHA has been demonstrated to cause increased sensitivity to TRAIL (Yerbes and Lopez-Rivas, 2012).

A novel small molecule HDAC inhibitor, 4-(4-chloro-2-methylphenoxy)-N-hydroxybutanamide (CMH) or Droxinostat has been identified through use of a high-throughput chemical library screen in which downregulated c-FLIP mRNA expression was identified (Schimmer *et al.*, 2006; Mawji, *et al.*, 2007). Although able to partially sensitise MCF-7 cells to TRAIL, this molecule was significantly toxic to cells alone, which is not a desirable property of a c-FLIP inhibitor. In addition, CMH-induced additional off-target effects of degradation of poly(ADP-ribose) polymerase (PARP) thus demonstrating its lack of specificity (Bijangi-Vishehsaraei *et al.*, 2010).

Several Akt inhibitors have been analysed as inhibitors to c-FLIP and therefore TRAIL-sensitising agents, due to the known ability of the two proteins to interact. API-1, for example, is a small molecule Akt inhibitor, which binds to, and blocks the membrane translocation of Akt (Kim *et al.*, 2010). Synergy was demonstrated in non-small cell lung cancer (NSCLC) cell lines, using the combination of API-1 and TRAIL, although the precise mechanism was not elucidated. Additionally, a cell line tested which was described to

be 'relatively resistant' to TRAIL and showed high levels of c-FLIP expression, was not sensitised to TRAIL by API-1. Furthermore, the overexpression of c-FLIP L or S did not fully abrogate the ability of API-1 to sensitise to TRAIL, thus suggesting the effects not to be primarily c-FLIP-mediated (Li *et al.*, 2012).

Another agent which acts to inhibit Akt, Celecoxib, has been explored in models of colon cancer, for an ability to reduce c-FLIP levels (Chen *et al.*, 2011). This agent is a marketed COX-2 inhibitor which is used as an anti-inflammatory and analgesic drug; however, it has also been demonstrated to exhibit chemopreventive effects and is known to reduce the risk of colon cancer, although little is known about the mechanism behind this. In general, the antitumor effects of celecoxib are considered to be linked with its ability to induce apoptosis (Thun *et al.*, 2002) via inactivation of PDK1/Akt, upregulation of CHOP/GADD153 and calcium ion increase in several cancer cell types (Schonthal, 2006). Apoptosis induced by celecoxib is able to downregulate c-FLIP via a proteasome mediated pathway, through the inhibition of GSK3. The study thus assessed the effects of a GSK3 inhibitor on TRAIL induced apoptosis, which was indeed enhanced (Chen *et al.*, 2011). Celecoxib, and subsequently GSK3 inhibitors have therefore been shown to enhance the effects of TRAIL, with an ability to downregulate c-FLIP, however, like API-1, these effects are relatively non-specific.

There are several other Akt inhibitors, such as Perifosine, which have been demonstrated to have similar effects to API-1 and Celecoxib, *i.e.* they can enhance TRAIL which appears to be mediated through the downregulation of several proteins involved in DR signalling, including c-FLIP (Tazzari *et al.*, 2008).

As with all cancer therapies, the ideal candidate is one that is highly specific and targeted to the desired protein. Although many non-specific c-FLIP inhibitors or down regulators are available, at the time of this study, no specific ways of targeting c-FLIP clinically, or c-FLIP specific agents and small molecule inhibitors existed of which were aware.

1.3.7 Interactions of c-FLIP in TRAIL Resistance

In depth knowledge of the anti-apoptotic interactions that c-FLIP is involved in is imperative in order to be able to attempt to alter or prevent these, as a c-FLIP specific therapeutic strategy. No mutational studies had been performed on the DEDs of c-FLIP L at the time of this study, however, which would elucidate any information about the importance of either DED or specific residues within the DED.

Many studies have shown that the DEDs of c-FLIP, and of procaspase-8/-10 and not the caspase-like domain are important for the interaction with FADD (Irmeler *et al.*, 1997). Furthermore, studies have demonstrated that the DEDs of procaspase-8/-10 can interact with FADD and with each other to form intracellular filaments or fibers known as death effector filaments (DEFs) (Dickens *et al.*, 2012; Ueffing *et al.*, 2008). The formation of complete DEFs can be blocked by v-FLIP proteins (Siegel *et al.*, 1998).

One study on a form of c-FLIP, murine c-FLIP R did look into several DED mutations and the impact of these on interactions with FADD. Mutations were only performed on the FL motif present on DED2 at F119G/L120G which did demonstrate an increase in sensitivity to CD95-mediated apoptosis, with increased caspase-8 processing. Results suggested that only one DED domain of murine c-FLIP R was required for its anti-apoptotic role. In addition, in contrast to c-FLIP L, murine c-FLIP R, did not prevent FADD self-association, and thus is not directly comparable (Ueffing *et al.*, 2008).

There are several mutational studies which have been performed on the single DED domain containing protein, FADD, which have various effects on the proteins functions and interactions. Additionally, unlike c-FLIP or procaspases-8, the NMR structure of the DED of FADD has been resolved, which has helped to provide insight on DED proteins. Furthermore, some groups have looked into the importance of residues present on procaspase-8 and v-FLIP with regards to the important TRAIL mediated interactions. A review of the literature surrounding the importance of these DED mutations is required in order to attempt to comprehend the anti-apoptotic interactions of c-FLIP and therefore to target it therapeutically in order to sensitise to TRAIL.

There are other protein interactions which c-FLIP is involved in (mentioned in Section 1.3.3.1), however, in this study we focus on the DED interactions of c-FLIP, although future work could involve targeting other domains on the protein.

1.3.7.1 FADD DED Mutational Studies

The NMR structure of FADD revealed the existence of two hydrophobic patches (Eberstadt *et al.*, 1998) and enabled a more specific selection of residues which have been analysed in several mutagenesis studies.

Mutation of residues F25 (part of the FL motif) and K33-R38, present in alpha helix 3 of the DED of FADD are able to alter DED interactions between FADD and c-FLIP as demonstrated by co-immunoprecipitation, in addition to interactions between FADD and procaspase-8 (Kaufmann *et al.*, 2002). Interestingly, the F25Y FADD mutant was shown to bind procaspase-8 as well as wild-type FADD (Eberstadt *et al.*, 1998), although the interaction with c-FLIP was significantly reduced, which suggests the two proteins have slightly different binding affinities to FADD and thus show some promise for the development of inhibitors (Kaufmann *et al.*, 2002).

It is known that FADD, like c-FLIP and procaspase-8, can self-associate, although it is unlikely that this self-association occurs in the same way as between FADD and different proteins. Muppidi *et al.*, used CFP and YFP FRET constructs to demonstrate the existence of FADD:FADD interactions in living cells. When the DED was removed from one or both of these constructs, no FRET was observed, thus suggesting the DED of FADD is also required not only for interaction with other proteins, but for its own self-association also. This study used the NMR structures from the previous work by Eberstadt *et al.* to further understand FADD self-association. The first hydrophobic patch, mentioned by Eberstadt *et al.*, contains residues F25, L26 (making up the FL motif), L28, L66 and L70 and is important for the interaction between FADD and procaspase-8. The slightly less conserved second hydrophobic patch contains residues M1, P3, L5, V6, L43, L50, P57 and F82. Mutations of the residues in this second patch did not disrupt the self-association of FADD or Fas signalling, suggesting that the first hydrophobic patch is key to its interactions with the DISC proteins (Muppidi *et al.*, 2006).

In addition to the FL motif, the RXDLL motif is conserved between many DED containing proteins, and indeed, the DED of FADD contains the sequence 'RHDLL' between amino acids 72 and 76. Studies performed on v-FLIP demonstrated that specific point mutations within this domain were important for its antiapoptotic activity (Garvey *et al.*, 2002) thus, Muippidi *et al.*, performed mutagenesis on the RXDLL motif of FADD. Several point mutations were introduced and a combination of co-immunoprecipitation and FRET showed these residues do have a key role in FADD self-association but that they were not important for its interaction with procaspase-8. The study did demonstrate, however, that the mutant forms of FADD were unable to initiate TRAIL-induced apoptosis, despite retaining their ability to bind procaspase-8 and thus conclude that FADD self-association is required for induction of apoptosis but not for proper folding of the FADD DED (Muippidi *et al.*, 2006).

Carrington *et al.*, however, have shown slightly different work to Muippidi *et al.*, regarding the site of FADD self-association. This study suggested that the site of self-association is around F25 of the FL motif in FADDs DED domain but agrees that FADD self-association is at a site distinct to that of procaspase-8 binding. They suggest that FADD interacts with only one of the DED domains of procaspase-8, and that the residues S12, R38, D44 and E51 were potentially involved in the interaction with procaspase-8. Additionally, two residues F25 and K33, previously mentioned for their ability to bind procaspase-8 (Eberstadt *et al.*, 1998) or c-FLIP (Kaufmann *et al.*, 2002) were also analysed. A mutation at F25 of the FL motif was indeed shown to disrupt the ability of FADD to induce apoptosis in addition to being required for FADD self-association (Carrington *et al.*, 2006)

1.3.7.2 Procaspase-8 Mutational Studies

In addition to the studies performed on the DED of FADD, several groups have looked specifically at mutations on the DEDs of procaspase-8 for their impact on interactions with FADD in the DISC. Information elucidated about procaspase-8 interactions could provide vital information surrounding the interactions of c-FLIP since c-FLIP and procaspase-8 bind to FADD in the same manner, and thus areas of importance on the structure of procaspase-8 may also feature on c-FLIP.

A naturally occurring caspase-8 mutant with a deletion of leucine 62, located in DED1 of procaspase-8 was identified in human vulvar squamous carcinoma cells, which are a TRAIL resistant cell line. This procaspase-8 mutant was shown to have no apoptotic activity when overexpressed in several cell lines, suggesting the presence of leucine 62 is vital for caspase-8 to induce apoptosis. Analysis into the interactions of this procaspase-8 mutant showed that it was unable to interact with FADD, unlike overexpressed wildtype- procaspase-8 in addition to being unable to oligomerise with itself, or wildtype- procaspase-8. In addition, it was shown that this mutant retained its enzymatic activity, governed by the N-terminus of the protein, thus, the lack of apoptosis was not due to a mutation in the caspase-domain of the protein (Liu *et al.*, 2002).

Another study has identified a short form of procaspase-8 which encodes DED1 and only a small section of DED2 and has shown it to be present in multiple cell lines, using RT-PCR. This short form of caspase-8 was demonstrated, by co-immunoprecipitation, to still bind to FADD. However, the procaspase-8-mutant was unable to induce apoptosis and therefore this suggests that DED1 alone of caspase-8 is sufficient to induce apoptosis (Xu *et al.*, 2009).

A recent paper by Dickens *et al.* provides further insight into the structure of the DISC, with particular reference to the interactions between FADD and procaspase-8. This study observed FADD to be substoichiometric relative to TRAIL-Rs or DED-only proteins, conversely to the previously accepted triplet expression. Approximately nine times more procaspase-8 than FADD was observed to be present at the DISC, upon stimulation with TRAIL. A model was proposed which suggests that procaspase-8 molecules interact sequentially via their DED domains to form a caspase-activating chain, which fits in with previously observed DISC 'filaments', and that both DED domains of procaspase-8 are required for this for full induction of apoptosis. Mutating key interacting residues in procaspase-8 DED2 was shown to abrogate chain formation and disrupt, but not fully prevent, DISC mediated procaspase-8 activation and thus apoptosis induction which suggests that DED1 may be the important domain for initial FADD binding (Dickens *et al.*, 2012).

In silico modelling was used to study the interactions involved in the Dickens caspase-8 chain model. Caspase-8 DED1/2 were modelled by constructing a homology

model using the crystal structure of v-FLIP MC159 (Carrington *et al.*, 2006; Li *et al.*, 2006; Yang *et al.*, 2005). DED interactions between different procaspase-8 proteins were modelled based on the interaction interface that exists between DED1 and DED2 (FL motif of DED1) in the tandem DEDs of caspase-8 (Dickens *et al.*, 2012). Mutation of F122G/L123G of procaspase-8 DED2 was able to disrupt death effector filament formation, reduced procaspase-8 recruitment to the DISC and prevented procaspase-8 activation. Procaspase-8 recruitment, however, was not totally prevented, thus, they propose that it is unlikely that procaspase-8 is recruited to FADD only by interaction with DED2. The group suggested that it is more likely that either procaspase-8 is recruited to FADD by DED1 or by DED1 and DED2 simultaneously, rather than by DED2 alone (Dickens *et al.*, 2012).

The findings of Dickens *et al.* do not fully agree with research by Yang *et al.*, who suggested that procaspase-8 DED2 does indeed mediate recruitment to FADD. Yang *et al.* proposed this due to the fact that their mutant of F122 reduced interactions with FADD, whilst the double FL mutant, F122G/L123G completely abolished co-IP detectable interactions (Yang *et al.*, 2005).

1.3.7.3 v-FLIP Mutational Studies

Although no studies had been performed on c-FLIP at the time of this study, and in particular, when constructing our models, there are studies which have looked into mutations on the viral form of the protein, v-FLIP, which may elucidate information into the residues or domains of importance in c-FLIP.

The DED domains of v-FLIP, MC159, exhibit intramolecular interactions: DED1 interacts with DED2 via an 'FL' hydrophobic motif conserved in nearly all DEDs, which was used by the previously mentioned study performed by Dickens *et al.* to assist in the construction of a procaspase-8 homology and interaction model. In tandem DED proteins (including c-FLIP and procaspase-8), the FL motif present on DED1 appears to occupy a pocket in the surface of DED2. FADD only has 1 DED and so its own FL motif, F25/L26, is not buried at an intramolecular interface and thus is free to be able to recruit procaspase-8, or c-FLIP. Mutation of this FL motif in FADD has been shown to prevent caspase-8 binding (Eberstadt *et al.*, 1998).

The highly DED-conserved RXDLL motif is present in v-FLIP. In v-FLIP studies performed by Garvey *et al.*, double mutants of the RHDLL to AHALL or RHDA A, but not point mutations, were sufficient to reduce anti-apoptotic activity. 12 mutants of v-FLIP were produced in this study, seven of which had mutations within DED1 and protected against Fas-mediated apoptosis in HeLa cells. Two of the mutants, with residues altered within DED1 showed a loss of protection from Fas- and TRAIL-mediated apoptosis in Jurkat cells. In comparison, two mutants which had mutations in DED2 retained TRAIL-resistance. Garvey and team also explored mutations of the RXDL motif of both DED1 and 2, which demonstrated the motifs in both domains to have a role in death effector filament formation and the anti-apoptotic role of v-FLIP, but not in binding to procaspase-8 or FADD. Furthermore, they showed that two mutations which led to a loss of caspase-8 binding were present within DED1. Mutations performed on the FL-motif present on DED1, F30A, resulted in a reduced binding to caspase-8 and altered the ability of v-FLIP to prevent apoptosis. This group suggest, therefore, that DED1 is required for the anti-apoptotic role of v-FLIP in TRAIL-mediated apoptosis (Garvey *et al.*, 2002).

Summarising the relevant mutational studies demonstrates some key residues involved in the DED interactions (required for Chapter 3) (Table 1.2).

Table 1.3: Summary of Key Mutational Studies performed on FADD, v-FLIP and Procaspase-8 at the time of Modelling Study (2012/2013).

Although at the time of the modelling component of this project (November 2012 - March 2013), no mutational studies had been performed on the DEDs of c-FLIP, several studies involving FADD, v-FLIP or procaspase-8 had been carried out, which provided us with information regarding the importance of DEDs and specific residues within them.

Protein	Residues Mutated	Functional Consequence	Reference
FADD	F25 K33-R38 (FL motif)	Altered DED interactions with c-FLIP	Kaufmann <i>et al.</i> , 2002
FADD	F25Y (FL motif)	Bound with procaspase-8 as well as wt FADD	Eberstadt <i>et al.</i> , 1998
FADD	F25G or F25V (FL motif)	No loss in apoptotic activity Weaker binding with c-FLIP	Eberstadt <i>et al.</i> , 1998
FADD	DED removal	No FADD self-association	Muppidi <i>et al.</i> , 2006
FADD	RXDLL motif	Altered FADD self-association	Muppidi <i>et al.</i> , 2006

		No impact on procaspase-8 interaction Unable to induce TRAIL mediated apoptosis	
FADD	F25 (FL motif)	Alters self-association	Carrington <i>et al.</i> , 2006
FADD	S12, R38, D44, E51	Alter procaspase-8 interaction	Carrington <i>et al.</i> , 2006
FADD	F25	Disrupted apoptosis induction Reduced self-association	Carrington <i>et al.</i> , 2006
Procaspase-8	L62 (DED1)	Deletion associated with TRAIL resistance No apoptotic activity Unable to interact with FADD Unable to self-associate Retained enzymatic activity	Liu <i>et al.</i> , 2002
Procaspase-8	DED2 (protein containing DED1 and short section of DED2)	Retained FADD binding Unable to induce apoptosis	Xu <i>et al.</i> , 2009
Procaspase-8	F122G, L123G (FL motif), DED2	Mutations of residues in DED2 abrogated DISC chain formation but did not completely prevent apoptosis	MacFarlane <i>et al.</i> , 2012
Procaspase-8	F122/L123G	Abolished detectable interactions with FADD	Yang <i>et al.</i> , 2005
v-FLIP	RHDLL (RXDLL motif)	Point mutations altered anti-apoptotic activity but not interaction with FADD or caspase-8	Garvey <i>et al.</i> , 2002
v-FLIP	F30 (FL motif), DED1	Mutations in DED1 reduced anti-apoptotic abilities and binding to caspase-8	Garvey <i>et al.</i> , 2002

1.4 Aims of the Study

Agonists of the endogenous death ligand TRAIL clearly show promise as therapeutics, despite the somewhat mixed responses from early phase clinical trials. Its ability to induce apoptosis preferentially in cancer cells is a highly desirable property and one that should be exploited. Although triple-negative forms of breast cancer are TRAIL sensitive *in vitro*, a large subset of breast cancer types are resistant to treatment with the death ligand. Overcoming this resistance is clearly an important objective in order to widen the therapeutic potential of TRAIL.

Many studies have proven the role of c-FLIP in TRAIL resistance (Safa and Pollok, 2011; Safa, 2012). While we and others have demonstrated that targeted suppression of c-FLIP by si/shRNA sensitise both cancer cells and CSCs to TRAIL (Piggott *et al.*, 2011; Safa, 2012; Day *et al.*, 2009), this method of suppression cannot currently be translated to a clinically viable therapy. It is known that the ability of c-FLIP to prevent TRAIL induced apoptosis is due to its competition with procaspase-8 at the DISC, however, the specific residues which are required for this interaction are not known. In addition, although there are some compounds including histone deacetylase (HDAC), Akt inhibitors and the compound CMH, which exhibit non-specific inhibition of c-FLIP and therefore show general toxicity (Shanakar *et al.*, 2005; Chen *et al.*, 2011) (Section 1.3.6), there are currently no c-FLIP specific inhibitors available.

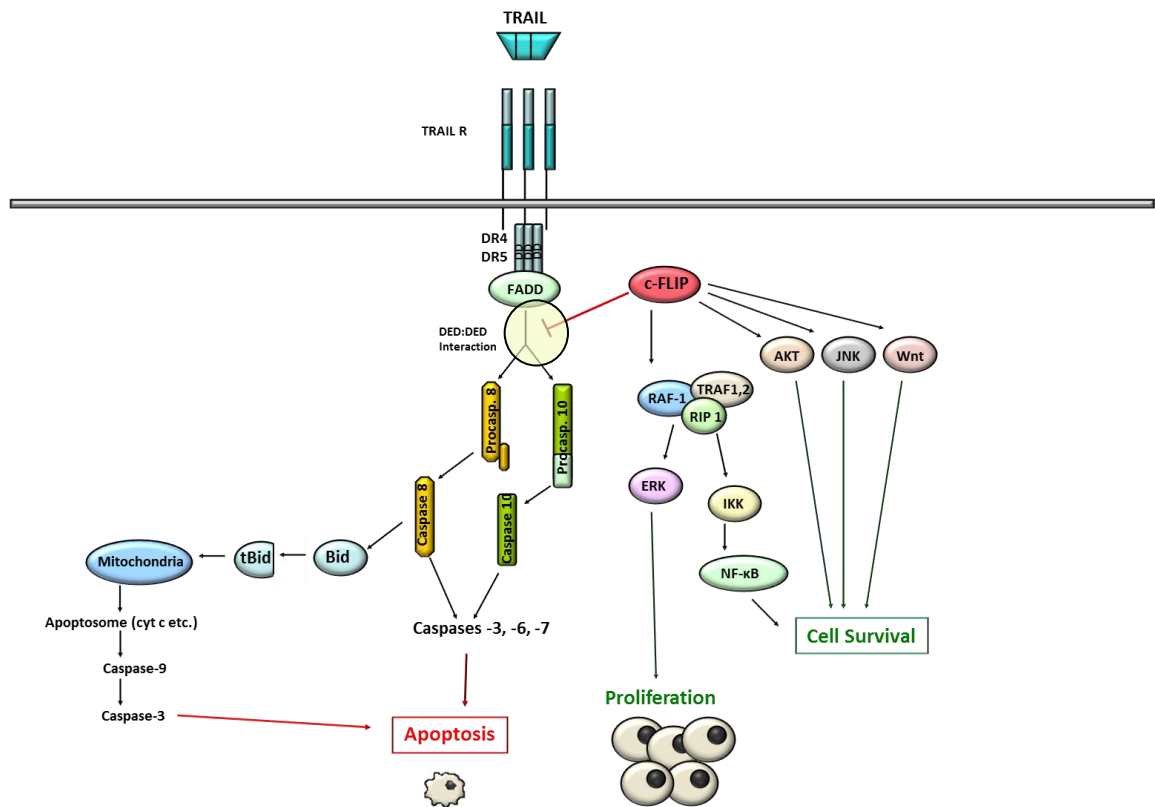
Drug development is constantly changing and adapting to new technologies. One of the more recent developments is the ability to design drugs that are specific to particular features present on protein surfaces, by using the latest *in silico* modelling technologies. In addition, *in silico* protein modelling can help to elucidate information about certain amino acid residues which may be vital for certain cellular processes.

In this study we set out to use a form of *in silico* modelling to design novel small-molecule inhibitors of c-FLIP and then to verify these inhibitors using cell-based *in vitro* assays. More specifically, our objectives were to:

- Model the structures of c-FLIP and procaspase-8 DEDs in order to subsequently model relevant interactions between c-FLIP, FADD and procaspase-8
- Use pharmacophore screening to select and develop specific small molecule pharmacological inhibitors to c-FLIP
- Use *in vitro* assays of cell viability and cancer stem-like cells to test the ability of inhibitors to sensitise to TRAIL
- Validate the mechanism of action of identified inhibitors
- Identify residues which may be involved in the anti-apoptotic role of c-FLIP and could be used to perform mutational studies

The desired action of a small molecule c-FLIP inhibitor was to sensitise breast cancer cells and CSCs to TRAIL induced apoptosis, through interference with the c-FLIP:FADD interaction (Figure 1.8), whilst having low toxicity on 'normal' non-cancerous cells. The development of such inhibitors, however, might be complicated by the homology between the DEDs of c-FLIP and procaspase-8 which could lead to off-target binding of the compounds to caspase-8. Thus, the potential inhibitors should be analysed for their ability to inhibit c-FLIP whilst allowing procaspase-8 to bind FADD and activate apoptosis. In addition, exploring the potential important residues involved in the interaction would provide alternative ways of targeting c-FLIP, should it not be possible to generate active inhibitors.

A



B

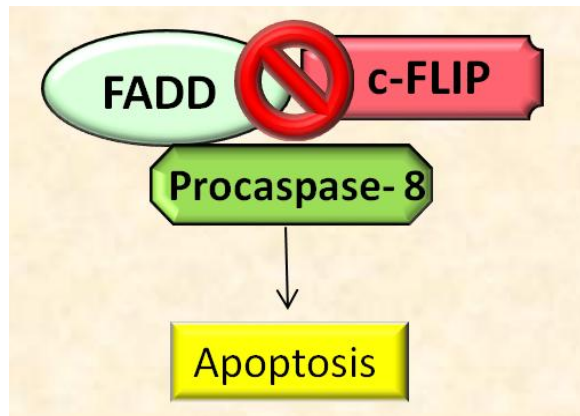


Figure 1.8: TRAIL Pathway and Simplified Schematic of c-FLIP Inhibitor

A) TRAIL induced apoptotic pathway, inhibited by the interaction of c-FLIP with FADD via a DED:DED protein domain interaction (highlighted in yellow circle). B) c-FLIP inhibitors will be designed to inhibit the c-FLIP FADD DED interaction (yellow circle in A), whilst sparing the FADD:Procaspase-8 DED interaction, thus allowing apoptosis to progress.

Chapter 2

Materials and Methods

Chapter 2: Materials and Methods

2.1 Cell Culture

2.1.1 Cell Lines

In this study, we utilised multiple established human breast cancer cell lines which represent the main receptor-defined subtypes of breast cancer: ER-positive; HER2-positive; and TNBC. The principal breast cancer cell lines used were MCF-7, BT474 and MDA-MB-231 respectively. MCF-7 cells are human luminal-like cells derived from a patient with metastatic breast cancer in 1970 (Brooks *et al.*, 1973), which are epithelial-like and represent ER-positive cancer cells. An additional epithelial-like, ER-positive cell line, BT474, was derived from a solid invasive ductal breast carcinoma (Lasfargues *et al.*, 1978). The mesenchymal-like MDA-MB-231 cell line, derived from the pleural effusion of 51 year old patient with long term metastatic breast cancer, represents TNBC. SKBR3 cells were also used, in order to analyse a HER2+ve, ER-ve breast cancer type. MCF-10A cells were used to represent 'normal' non-tumorigenic mammary epithelial cells, although it was recognised that these cells were both transformed and of ductal origin.

Human breast cancer cell lines MDA-MB-231 and MCF-7 cells were kindly supplied by Dr Julia Gee, Cardiff School of Pharmacy, BT474 and SKBR3 cells were purchased from ATCC and MCF-10A cells were obtained from Dr Steven Hiscox, Cardiff School of Pharmacy. HeLa human cervical cancer cells were a gift from Dr Ladislav Andera, Institute Molecular Genetics, Prague. MDA-MB-231, MCF-7, BT474, SKBR3 and HeLa cells were cultured in RPMI-1640 medium (Invitrogen) supplemented with 10% foetal bovine serum (FBS), 2 mM L-glutamine (Invitrogen) and 50 units/ml penicillin-streptomycin. MCF-10A cells were cultured in 1:1 DMEM/F12 (Invitrogen) medium with 5% horse serum (Sigma), 50 units/ml penicillin-streptomycin, 100 ng/ml cholera toxin (Sigma), 20 ng/ml epidermal growth factor (EGF) (Sigma), 0.5 mg/ml hydrocortisone and 10 µg/ml insulin.

2.1.2 Cell Culture Maintenance

Cells were kept in a logarithmic growth phase in 25 cm² cell culture flasks (T25) (Nunc, Thermo) at 37°C in a sterile incubator with a humidified atmosphere of 5% CO₂ and 95% air by passaging or refreshing media when required. Cells were passaged when they had reached 80-100% confluency. Passaging was performed by removing culture medium, before adding an appropriate amount of 0.05% Trypsin-EDTA (Invitrogen) for the size of the flask. Cells were incubated in trypsin for around 5 minutes at 37°C before all cells could be seen to have lifted off the vessel surface and rounded up, at which point, a volume at least 10 times that of trypsin of serum containing media was added to inactivate the trypsin. Cells were passaged at appropriate ratios for the cell line (Table 2.1) and remaining cells were discarded or used as required. Cell lines were kept to a passage number of around 40, after which, a fresh aliquot of low-passage cells would be revived from liquid nitrogen.

Table 2.1: Conditions and maintenance of cell lines used within this study
(Adapted from Holliday and Speirs, 2011)

Cell Line	Media (before supplementation)	Passage Ratio	Breast Cancer Subtype	Classification
MCF-7	RPMI	1:8	ER +ve, PR +/-, HER2-	Luminal A
BT474	RPMI	1:8	ER +ve, PR +/-, Her-2 +	Luminal B
SKBR3	RPMI	1:8	ER -, PR-, Her-2 +	HER2 +ve
MDA-MB-231	RPMI	1:10	TNBC	Claudin-low
MCF10-A	DMEM-F12	1:6	Non-tumorigenic	NA
HeLa	RPMI	1:10	N/A (Cervical Cancer)	NA

2.1.3 Cell Storage

Cells were frozen at low passage number and cryo-stored in liquid nitrogen. To prepare cells for storage, cells were trypsinised and pelleted by centrifugation for 5 minutes at 234 g after which pellets were resuspended in 1 ml complete media with 10% DMSO (Sigma) in 1.5 ml cryo-tubes (Nunc). Around 2×10^6 cells were frozen per aliquot. Cryo-tubes were left overnight at -80°C in an isopropanol cell freezing container after which tubes were transferred to long term storage in liquid nitrogen. To revive cells, tubes were defrosted rapidly in a 37°C waterbath before being spun for 5 minutes at 234 g to obtain a cell pellet. The cell pellet was resuspended in 5 ml of the appropriate growth medium and cultured in a T25 flask, or other appropriately size vessel, depending on cell pellet size.

2.1.4 Activation and Suppression of Apoptosis

Activation of caspase-8 mediated cell death was initiated in cell culture with recombinant soluble human TRAIL (super-killer TRAIL, Enzo Life Sciences) at 20 ng/ml (unless otherwise stated) for 18 h. Inhibition of caspase activity was performed with Pan-caspase-inhibitor Z-VAD-FMK (R and D Systems), 10 μM (unless otherwise stated).

2.2 *In Silico* Protein Modelling

All molecular modelling was performed on a MacPro dual 2.66 GHz Xeon running Ubuntu 9. Crystal structures for FADD and v-FLIP were downloaded from the Protein Data Bank (PDB) (www.pdb.org).

2.2.1 c-FLIP and Procaspase-8 Homology Models

Crystal structures for the DED domains of c-FLIP and procaspase-8 had not been resolved and thus these were constructed based on a homology model. Amino acid sequences for c-FLIP and procaspase-8 were obtained from Genbank. The structures of the two DEDs of c-FLIP and procaspase-8 were generated using MOE (Molecular Operative Environment, 2010) based on sequence alignment homology models with the published 3D structure of MC159 (PDB ID: 2BBR). MC159 was imported to MOE where hydrogen atoms were added to the protein and residue ionisation was set to pH 7.4.

The structure was minimised to keep all heavy atoms fixed until the root mean square deviation (RMSD) gradient of $0.05 \text{ kcal mol}^{-1} \text{ \AA}^{-1}$ was obtained.

MOE-Search PDB was used to identify a suitable template for performing c-FLIP and procaspase-8 model construction. The sequence of target protein, the 'query' is entered and a search is performed of PDB entries in order to find one with a high level of homology for constructing the model. In this case, MC159 was identified as the best template for performing our homology models.

MOE-Align was the first step in building our homology models, whereby the sequence of our target proteins (c-FLIP and procaspase-8) was entered and compared with the sequence of our template protein, MC159. MOE-Align was used to align the sequences which appropriately aligned amino acids, entering gaps where required, in order to obtain a likely sequence to secondary structure of the template protein order.

MOE-Homology was subsequently used to generate a complete, energy-minimized (*i.e.* 'relaxed' protein conformation) 3D model of our target proteins, based on the template structure MC159. This application creates a number of potential models, constructed using a series of Boltzmann-weighted choices of sidechain rotamers and loop conformations using the selection of protein fragment components present in the built-in library of crystallised, high-resolution protein structures. An average model of the target proteins were then constructed and a level of energy minimization was selected, in this case, AMBER99 (Assisted Model Building with Energy Refinement). AMBER99 essentially simulates energy force fields to minimise excessive bond stretching within the protein.

2.2.2 Modelling Intermolecular Interactions

The intramolecular interface (a known interaction (Dickens *et al.*, 2012) between the FL-motif of DED1 and DED2 of c-FLIP and procaspase-8 was used to model the intermolecular interactions between DED2 of procaspase-8 and DED1 of c-FLIP. This interaction was then used to analyse the c-FLIP DED1:FADD and procaspase-8 DED1:FADD interactions (FADD crystal structure from PDB, ID: 1A1W). In brief, c-FLIP or procaspase-8 DED1 was aligned and superimposed to the DED of FADD in MOE in order to simulate the intramolecular interactions that occur within the protein. FADD was

then manually moved into position so that it mimicked this interaction, but on the outer surface of DED1 of c-FLIP or procaspase-8.

Protein complexes were subjected to *in silico* minimisation processes to create the optimum energy-minimised models. Hydrogen atoms were added to the protein and ionization of residues was performed at a pH of 7.4 in MOE. The system was kept minimized by fixing the heavy atoms to obtain an RMSD gradient of $0.05 \text{ kcal mol}^{-1} \text{ \AA}^{-1}$. An average model of the target proteins is then constructed and a level of energy minimization was selected, in this case, AMBER99 (Assisted Model Building with Energy Refinement). AMBER99 essentially simulates energy force fields to minimise excessive bond stretching within the protein, in this case, we ensured the gradient of $0.05 \text{ kcal mol}^{-1} \text{ \AA}^{-1}$ was maintained.

Following this, GROMACS software 4.5 (Hess *et al.*, 2008) was used to perform molecular dynamics on the protein complexes using Gromos 96 forcefield and NPT working environment. Interaction simulations were performed at 300 K, 1 atmosphere and a time step of 0.002 ps. Next, the whole system was equilibrated for 100 ps after which the structure was solvated in a dodecahedron simulation box using spc216 water molecules, to generate a minimum of 9 Å water between the protein and the edge of the box, thus setting boundary constraints to the system. Finalised models were visualised in VMD (Visual Molecular Dynamics).

2.2.3 Protein Analysis and Pharmacophore Design

A pharmacophore query was run on c-FLIP using MOE to identify features on the protein surface which could be targeted by small molecule inhibitors to block the interaction with the FL motif on FADD. The FL motif of FADD was used as if it were a compound-like ligand to set up the query on the surface of DED1 on c-FLIP. After user defined refinement of these features a library of over 350,000 compounds (Specs Database) was virtually screened to identify potential inhibitors to these sites. 14000 positive hits were docked on our modelled interactive surfaces of c-FLIP and procaspase-8 using MAESTRO (Schrodinger) software. 2000 compounds were obtained as a result, which were re-docked on the structures of c-FLIP and procaspase-8. The Glide feature was used to 'score' these compounds based on their ability to bind the proteins. Several docking steps were utilised to obtain a final, refined, 200 compounds

which had high scores for c-FLIP and low scores for procaspase-8. These were analysed visually using MOE, comparing compound binding on the pocket of c-FLIP to the pocket on procaspase-8; those which scored highly for c-FLIP binding and low for procaspase-8 binding, and visually appeared to fit those criteria were selected (19 compounds initially) (further detail in Chapter 3).

2.3 Cell Based Assays

2.3.1 Cell Subculture: Seeding for Assays

Culture medium was removed and trypsin added as in Section 2.1.2. Once detached, cells were passaged as required and the remaining cells were moved to a 15 ml falcon tube (Nunc). Cells were fully resuspended to ensure a single cell suspension before being counted using a Fastread 10-chamber counting grid (Immune Systems).

10 μ l of cell suspension was added to the counting chamber and cells were counted according to manufacturer's instructions in order to calculate the required volumes for cell seeding. The average of four counting squares was obtained and multiplied by the required factor to obtain the number of cells per millilitre. The appropriate dilution for the assay was made before seeding cells into the assay plate required. Cell numbers and media required for sub-culturing varied between assays and plates (Table 2.2).

Table 2.2: Subculture tissue culture plates

Plate Type (No. of wells)	Relative Surface Area	Media Required (μ l)
96	0.2	100
48	0.4	200
24	1	500
12	2.5	1000
6	5	3000

2.3.2 Cell Titre Blue Viability Assay

Cell Titre Blue (Promega) gives a measure of cell viability using metabolism as a marker; it measures the ability of cells to convert resazurin into resorufin, a fluorescent product. Cells which are not viable will not be able to do this and thus will not result in a fluorescent signal.

Adherent cells were removed from culture plates using 0.05% Trypsin/EDTA and were plated in 96 well plates in 100 μ l media at a concentration of 100000 cells/ml in order to achieve an appropriate confluency for assay the next day. After 24 h incubation, media was refreshed with control or test containing medium and left overnight after which CellTiter blue viability assay was performed according to manufacturer's instructions; 20 μ l reagent was added to 100 μ l media in the 96 wp and left for 1-4 h at 37°C at 5% CO₂ in the dark. Fluorescence was measured using excitation/emission wavelengths of 560/590 nm using FluoStar Optima plate reader (BMG Labtech).

2.3.3 Caspase-8 Activity Assay

Caspase-Glo 8 assay (Promega) is an assay that uses luminescence as a measure of caspase-8 activity. Caspase-Glo reagent results in cell lysis followed by caspase cleavage of the substrate and a resulting luminescent signal which gives a measure of caspase-8 activity within the sample. In brief, adherent cells were plated and treated as in Section 2.3.1 using black walled 96 well plates. After 24 h incubation, caspase-Glo 8 assay was performed according to manufacturer's instructions. Luminescence of samples and media control was measured using FluoStar Optima plate reader (BMG Labtech).

2.3.4 Functional Stem-Like and Progenitor Cell Assays

2.3.4.1 Tumoursphere Assay - Adherent Treatment

The tumoursphere assay aims to enrich for cancer stem cells either from cell lines or primary cultures by testing their ability to resist anoikis growth conditions and, upon passaging, self-renewal. Adherent cells were plated as described in section 2.3.1 and treated after 24 h. After 18 h, cells were trypsinised, disaggregated to achieve single cell suspension and transferred to the tumoursphere medium, Mammary Epithelial Cell Growth Medium (MEBM) (Lonza) serum-free epithelial growth medium supplemented with B27 (Invitrogen), 20 ng/ml EGF (Sigma), 5 mg/ml insulin (sigma), 0.0008% v/v β -mercaptoethanol (Sigma), and 1 mg/ml hydrocortisone (Sigma). Cells were seeded in 200 μ l of supplemented MEBM into ultra-low attachment plates (Costar, Corning) at a density of 5000 cells/ml and incubated for 7 days at 37°C and 5% CO₂ after which, tumourspheres were counted. After counting, tumourspheres were then collected by centrifugation at 278 g and dissociated by trypsinising in 0.05% trypsin, 0.25% EDTA (Invitrogen) and reprocessed as before, seeding at a density of 5000 cells/ml and left for a further 7 days to obtain a second passage count.

2.3.4.2 Tumoursphere Assay - Non-adherent Treatment

Adherent cells were trypsinised and plated in ultra-low attachment plates in 200 μ l supplemented MEBM (Section 2.3.4.1) at a density of 5000 cells/ml. Immediately after plating into anoikis conditions, appropriate wells were treated with control or test compound. Cells were left for 7 days at 37°C and 5% CO₂ after which, tumourspheres were counted. After counting, tumourspheres were then disaggregated and reprocessed as described in 2.3.4.1 and left for a further 7 days to obtain a second passage count.

2.3.4.3 Colony Forming Assay

The clonogenic assay is an *in vitro* assay which tests one of the functional characteristics of stem cells: the ability to propagate colonies from single cells through enhanced proliferative potential (Harrison *et al.*, 2010; Locke *et al.*, 2005). The assay is

not as selective for CSCs as the tumoursphere assay since between 10% and 70% of any given cell line population can form colonies.

Cells were plated in 6 or 12wp in order to obtain 50 cells per cm² (Harrison *et al.*, 2010; Locke *et al.*, 2005), and left to attach. After attachment, media was refreshed with appropriate control or test medium. Colonies were left to form for 10 days. After 10 days, colonies were stained by first removing media and washing gently with two 5 minute washes in 1 X PBS. Crystal violet in ethanol solution (Sigma) was then added for 15 minutes to stain the colonies, followed by three 1 x PBS washes for 5 minutes each. Colonies were then visualised and photographed under white light. Colonies of at least 32 cells in size (*i.e.* those that had undergone 5 or more cell divisions) were counted using GelCount plate reader and computer software (Oxford Optronix) by setting a minimum and maximum size threshold for colonies of 100-1000 µm.

2.4 Compound Handling

All compounds obtained from SPECS or synthesised at Cardiff School of Pharmacy were stored in solid form at 4°C. Substances were dissolved in an appropriate volume of DMSO (based on molecular weight and mass), using vortexing/heating as required, to achieve stock solutions of 100 mM (unless otherwise stated), and stored in 10 µl aliquots at -20°C.

2.4.1 Compound Solubility

Compounds were prepared in antibiotic free media at concentrations of 10 nM, 100 nM, 1 µM, 10 µM and 100 µM. In a 96 well plate, 100 µl of each concentration of each inhibitor was left in an incubator overnight 37°C and 5% CO₂. Wells were visually inspected the following day to observe and record the solubility of each compound in media at increasing concentrations.

2.5 Co-Immunoprecipitation (Co-IP) and Western Blot Protein Analysis

2.5.1 Solutions Used for Co-IP and Western Blot

Solutions were prepared for use at different steps during Co-IP and Western blot (Table 2.3).

Table 2.3: Solutions and Reagents required for Protein Analysis Protocols

Solution	Composition
RIPA Buffer	5 ml 1 M Tris pH 7.4, 10 ml 10% Nonidet-P40 (Roche 17545999), 0.25 g Sodium Deoxycholate, 3 ml 5 M NaCl, 0.4 ml 0.25 M EGTA, up to 100 ml with dH ₂ O, pH to 7.4
5 X Laemmli Buffer	60 mM Tris-Cl pH 6.8, 2% SDS, 10% glycerol, 5% β-mercaptoethanol, 0.01% bromophenol blue
PBST	1 X PBS solution (Fisher): 5 tables in 500 ml dH ₂ O plus 0.5 ml Tween (Sigma)
TBST	1 X TBST solution - dissolve 1 TBST tablet (Merck Millipore) in 500 ml ddH ₂ O
Co-IP Resolving Gel Buffer	2.5 ml ddH ₂ O, 3 ml bis-acrylamide (Sigma) 1.88 ml 1.5 M Tris-HCl pH 8.8 and 75 μl 10% SDS
Co-IP Stacking Gel	75 μl APS and 7.5 μl TEMED in 2.5 ml ddH ₂ O, 500 μl bis-acrylamide, 625 μl 0.5 M Tris HCl pH 6.8 and 37.5 μl SDS 10%
Western blot Resolving Gel Buffer	1.5 M Tris-HCl, pH 8.8
Western blot Stacking Gel Buffer	0.5 M Tris-HCl, pH 6.8
10 X Electrophoresis Buffer	30 g Trizma (Sigma), 144.4 g Glycine (Sigma) pH 6.8, dH ₂ O up to 1 l
1 X SDS-PAGE Running Buffer	895 ml dH ₂ O, 100 ml 10X Electrophoresis running buffer, 5 ml SDS (Sigma)
1 X Western Transfer Buffer	700 ml dH ₂ O, 200 ml Methanol, 100 ml 10 X Eletrophoresis running buffer
Blocking Buffer	5 % w/v non-fat milk powder (Marvel): 0.75 g in 15 ml PBST/TBST per transfer membrane
Antibody Dilution Buffer	5 % w/v BSA (Sigma): 0.1 g in 2 ml PBST per antibody

Several antibodies and their respective secondary antibodies were utilised for protein detection (Table 2.4).

Table 2.4: Primary Antibodies and Respective Secondaries used for Co-IP and Western Blot

Antibody	Species	Dilution	Source	Target Size
c-FLIP 5D8 (mAb)	Mouse	1:750	Santa Cruz Biotech	55 kDa
GAPDH	Mouse	1:1000	Santa Cruz Biotech	35 kDa
FADD (IP)	Mouse	1:1000	BD 610400	25 kDa
FADD (IB)	Rabbit	1:500	Santa Cruz Biotech sc5559	25 kDa
Caspase-8	Mouse	1:1000	Cell Signalling 4927	55 kDa

2.5.2 Sample Extraction and Preparation for Co-Immunoprecipitation

Following experimental treatment, MDA-MB-231 and MCF-7 cells were washed twice with cold PBS and harvested using 700 μ l lysis buffer (20 mM Tris HCl pH 7.5, 150 mM NaCl, 10% fresh glycerol, 1% Triton X-100, 2 mM EDTA with protease and phosphatase inhibitors) left on a rocker at 4°C for 20 minutes. Cells were scraped and collected followed by centrifugation at 13793 g for 15 minutes at 4°C. Supernatant was collected and an extra 30 μ l was set aside for quantification. 20 μ l Protein A beads were added to 5 μ l sample and left on spinner at 4°C for 45 minutes. Samples were spun at 735 g for 1 minute and quantified using BCA protein assay kit (Pierce) and following manufacturer's instructions (Section 2.5.4). After this, an equal amount of FADD antibody (BD, 610400) 1:1000 was added to each tube. Samples were left spinning at 4°C overnight.

2.5.3 Sample Preparation for Western Blot

Cells from culture plates were trypsinised and centrifuged for 5 minutes at 234 g. Cell pellets were washed with 1 X PBS, twice, to remove remaining serum containing media. Cell pellets were resuspended in 100 μ l RIPA buffer with complete protease inhibitors (25 X solution, Roche), 200 nM NaVO₃, 1 M NaF and 100 nM Na₄P₂O₇. 23-gauge needles on 1 ml syringes were used to break the samples up by passing them through 8-10 times. Samples were transferred to 1.5 ml microcentrifuge tubes and left

on ice for 30 minutes. Tubes were then centrifuged at 13793 g for 15 minutes at 4°C, after which, the supernatant was collected in 100 µl aliquots and stored at -20°C.

2.5.4 Protein Quantification

The BCA assay was used to quantify levels of protein prepared for Co-IP or Western blot. In brief, 5 µl of sample or BSA standard was mixed with 25 µl BCA reagent and left at 37°C for 30 minutes, before being put on ice. A standard curve for determining protein concentration was produced using a Nanodrop with standards of 2.5, 5 and 10 mg BSA per ml protein buffer.

2.5.5 Western Blotting

Protein samples were prepared at equal concentrations in Laemmli buffer after protein extraction in appropriate lysis buffer (Section 2.5.2 for co-IP extraction). Samples were heated to 95°C for 2 minutes and used immediately after or stored at -20°C.

2.5.6 SDS-PAGE

2.5.6.1 SDS-PAGE: Co-Immunoprecipitation

12% resolving gel was prepared using 50 µl APS (Sigma) plus 10 µl TEMED (Sigma) added to resolving gel buffer (Table 2.3), mixed and immediately poured. dH₂O was quickly pipetted over the top of the gel to ensure the gel remained level. Once set, dH₂O was poured off and stacking gel was mixed and immediately poured, after which, combs were inserted and the gel allowed to set. Gels were placed into the gel running tank (BioRad), in an electrophoresis gasket, and the central gasket was filled with running buffer. Samples were loaded at equal quantities, of 20-30 µl in addition to a molecular weight marker (Pageruler Plus, Fermentas, Fisher). Gels were run at 125 V for approximately 1.5 hours.

2.5.6.2 SDS-PAGE: Western Blot

10% resolving gel was prepared using 100 µl APS (Sigma) with 15 µl TEMED (Sigma), added to the resolving gel buffer before immediately mixing and pouring.

dH₂O was quickly pipetted over the top of the gel to ensure the gel remained level. After 15 minutes, dH₂O was poured off before addition of the stacking gel, prepared by the addition of 100 µl APS to 4% stacking gel buffer. After pouring stacking gel, a comb was immediately inserted into the gel and left to set for approximately 15 minutes. Once set, gels were inserted into the electrophoresis gasket and placed in a gel running tank (BioRad). Running buffer was used to fill the centre of the gasket, ensuring the buffer overflowed so that a depth of around 3 cm was achieved. 20-30 µl of prepared protein samples were loaded, alongside a molecular weight marker (Pageruler, Fermentas, Fisher). Gels were run at 180 V for approximately 1 hour.

2.5.7 Protein Transfer to PVDF Membrane

Western transfer sandwich was prepared by layering sponge, 2x filter paper, protein gel, Polyvinylidene Fluoride (PVDF) membrane, 2x filter paper and sponge onto the transfer cassette. Each layer was soaked in transfer buffer beforehand. PVDF membrane was activated in methanol prior to soaking in transfer buffer for 5 minutes. A stripette was rolled over each layer to ensure no air bubbles were present. The cassette was shut and entered into the transfer tank, along with an ice block. Transfer buffer was added to fill the tank and the transfer was run in the cold room, at 4°C. Transfer was run at 80 V for 45 minutes.

2.5.8 Membrane Probing

After transfer, membranes were washed 3 times in PBST/TBST (1 x 15 min, 2 x 5 min) before immersion in blocking buffer (5% w/v non-fat milk in PBST/TBST) with rocking for 1 h. Membranes were transferred to tubes containing 4 ml of appropriate primary antibody made up in 5% BSA and left rotating overnight at 4°C. Following this, membranes were washed 3 times in PBST/TBST as before and transferred to a tube containing 4 ml of appropriate secondary antibody (Table 2.4) and left to rotate at room temperature for 1 h. Membranes were washed 3 times in PBST/TBST, as before, before protein detection and film development using ECL prime (Amersham) (Section 2.5.7).

2.5.9 Protein Visualisation

Immobilised proteins were detected using ECL or ECL Prime according to manufacturer's instructions. Solutions of ECL were mixed well and left to activate for 1 minute, before adding directly to the membrane. Approximately 1 ml was added to each membrane, depending on its size. X-Ray film (Amersham) was used to detect proteins, using an automatic X-Ray film processor (Xograph).

2.6 Expression of Recombinant Proteins

2.6.1 Expression Constructs

The eCFP-C1 and eYFP-C1 vector plasmids were kindly provided by Dr David Stanek, Institute of Molecular Genetics, Prague. Full-length c-FLIP, FADD and procaspase-8 were kindly provided by Dr Ladislav Andera, Institute of Molecular Genetics, Prague. CFP-YFP fusion protein was obtained from Liusheng He and Jehonathan Pinthus (Addgene plasmid # 24520).

Table 2.5: Constructs Used within this Study

Construct	Expression System	Antibiotic Selection 1	Antibiotic Selection 2	Reference
eCFP-C1	Fluorescent plasmid	Kanamycin	Neomycin	Clontech
eYFP-C1	Fluorescent plasmid	Kanamycin	Neomycin	Clontech
CFP:YFP	Fluorescent plasmid	Kanamycin	-	He <i>et al.</i> , 2003

2.6.2 Plasmid Propagation

2.6.2.1 Transformation into *E.coli*

E.coli OneShotStbl3 cells (Invitrogen), for FRET constructs, or *E.coli* XL-blue cells (Stratagene), for SDM were stored at -80°C were thawed on ice in 50 µl aliquots. 1 µl of DNA to be transformed was added to one 50 µl bacterial cell aliquot and incubated on ice for 30 minutes. Heat-shock was then performed for 45 seconds at 42°C followed by a 2 minute incubation to allow the bacterial cells to recover. 250 µl pre-warmed (to 37°C) SOCS media (Invitrogen) was added to the transformations and left for shaking at 225 rpm for 1 hour at 37°C. The culture was then spread on an agar plate made up with the appropriate antibiotic, and left to incubate overnight (for approximately 12 hours) at 37°C.

Colonies were selected by inoculation of a pipette tip, which was placed into 2 ml (for mini-culture) of LB broth containing the appropriate antibiotic, and incubated with shaking at 225 rpm for approximately 16 h at 37°C before DNA extraction.

When preparing DNA from maxi- culture, the pipette tip was placed into 80 ml of LB broth, unless a starter culture was required, in which case this initial 2 ml culture was added to 80 ml LB-broth with appropriate antibiotic and left at 37°C for 16 hours, with shaking at 225 rpm before DNA extraction.

2.6.2.2 DNA Extraction

DNA extraction from culture was performed using a mini- or maxi- endotoxin-free DNA extraction kit (Qiagen) according to the manufacturer's instructions. In brief, cultures were pelleted after the 16 h incubation, by centrifugation at 8161.4 g for 3 minutes, for a mini-prep or 1741 g for 15 minutes for a 50 ml preparation. Re-suspension of the cell pellet was performed in buffer P1, after which, buffers P2 and N3 were added in order to lyse the cells for extraction. Centrifugation was performed at 13793 g for 10 minutes, before the supernatant was transferred to a DNA-binding column. An additional centrifugation at 13793 g was performed for 1 minute, with all subsequent centrifugations being performed in these conditions. Washing of the DNA-binding column with buffers PB and PE was performed, before a final centrifugation to remove any remaining ethanol before eluting the DNA. 30 µl (or 1 ml in the case of a

maxi-prep) of buffer TE was added to the column and incubated for at least 1 minute at room temperature before centrifugation of the column was performed to collect DNA in a fresh endotoxin-free micro-centrifuge tube. DNA concentration was measured using a Nanodrop (GE healthcare, UK).

2.6.2.3 Sequencing Plasmids

DNA extracted from colonies was diluted to between 50 and 100 ng/ μ l in 15 μ l and primers were diluted to 2 μ M. Sequencing was carried out by BIOSI sequencing core, Cardiff University.

2.6.3 Site Directed Mutagenesis

Site directed mutagenesis was performed on the pcDNA3.1c-FLIP construct, using the QuickChange Kit (Stratagene) according to manufacturer's instructions. Plasmids were custom-designed in order to target specific residues on c-FLIP (I6G, H7A, R38A and D42A).

2.6.3.1 Primer Design

Primers were designed by following the Stratagene guidelines. Essentially, primers were designed in order to achieve the desired mutation within the middle of the primer sequence, including up to 15 bases of correct sequence flanking it. The specific conditions to adhere to were as follows:

- Primers to be between 25-45 bp
- Melting temperature of $\geq 78^{\circ}\text{C}$
- GC content of $\geq 40\%$
- Primer to end with one or more G or C bases

The primers were designed to mutate regions of interest within DED1 of c-FLIP. All primers were purchased from Sigma (Table 2.6).

Table 2.6: Mutagenic primers

Target Mutation	Primer
H7A	3'-CAGACGACTTCAGTAG <u>CGAG</u> TCCAACCTTCTTCGTG- 5' 5'-GTCTGCTGAAGTCAT <u>CGCT</u> CAGGTTGAAGAAGCAC- 3'
R38A	3' -CACCAAGGTGGATTACAG <u>CGC</u> CTGGAAGACCTATAAAATG- 5' 5' -GTGGTCCACCTAATGT <u>CGCG</u> GACCTTCTGGATATTTTAC- 3'
D42A	3' -TTACAGTCCCTGGAAGAC <u>CGA</u> TAAAATGCCCTTCTCCATTC- 5' 5' -AATGTCAGGGACCTTCTGG <u>CT</u> ATTTTACGGGAAAGAGGTAAG- 3'
I6G	3' -CAGACGACTTCAG <u>CCG</u> GTAGTCCAACCTTCTTCG- 5' 5' -GTCTGCTGAAGTC <u>CGCC</u> ATCAGGTTGAAGAAGCA- 3'

2.6.3.2 PCR Amplification

Each mutagenesis used 50 ng of double-stranded DNA template (pcDNA3.1c-FLIPL) made up in 5 µl reaction buffer. 125 ng of each mutagenic (forward and reverse) primer was added, in addition to 1 µl of 10 mM dNTP mix and 1 µl of *Pfu DNA polymerase* (NEB). dH₂O was added to 50 µl before running the PCR on a Biorad T100 Thermal Cycler machine using the manufacturers guidelines (Table 2.7)

Table 2.7: PCR conditions for mutagenesis

Cycle	Temperature	Time	Step
1	95°C	30 s	Denaturation
12	95°C	30 s	Denaturation
	55°C	1 min	Annealing
	68°C	6.5 min (2 min/kb of plasmid)	Extension
1	68°C	10 min	Final Extension
-	4°C	-	Incubation

2.6.3.3 Digestion of Template DNA Strand

After completing the PCR cycle, 1 µl of Dpn1 restriction enzyme was added to the 50 µl reactions and incubated at 37°C for 1 h. Following this, E.coli XL1-blue cells (Stratagene) were transformed (using the protocol defined in Section 2.6.2.1) with prepared DNA, with the remainder being stored at -20°C. DNA was extracted as per

Section 2.5.2.2 and sequencing was carried out at BIOSI sequencing core, Cardiff University performed using primer T4 to check for successful mutations.

2.6.4 FRET Construct DNA Preparation

Plasmids were designed in order to facilitate the cloning of either FADD, c-FLIP or procaspase-8 into the FRET plasmids e-CFP-C1 or e-YFP-C1. A positive control plasmid of CFP fused to YFP was also purchased (He *et al.*, 2003) (Table 2.5).

2.6.4.1 Primer Design

FRET constructs were designed via use of EditSeq and DNASTar software in order to facilitate the cloning of FADD, c-FLIP or procaspase-8 into either e-CFP-C1 or e-YFP-C1 FRET plasmids. FADD tagged to CFP, c-FLIP(L) tagged to YFP and caspase-8 tagged to CFP. Oligonucleotides were custom-designed and purchased from Sigma.

Table 2.8: Primers used for FRET

Primer Name	Primer Sequence
c-FLIP_BglII_fwd	GTACTGGAAGATCTaggatgtctgctgaagtc
c-FLIP_BglII_rev	GTACTGGAAGATCTtgttaggagaggataagtt
Casp8_HindIII_fwd	GTACTGGAAGCTTgggagatggacttcagcagaaa
Casp8_BamHI_rev	G TTCAGCAGGATCCatcagaagggaagacaagtt
FADD_HindIII_fwd	GTACTGCAAAGCTTgggccatggacccgttcctggt
FADD_BamHI_rev	G TTCAGCAGGATCCggacgcttcggaggtagatg

2.6.4.2 Cloning of FRET Constructs

c-FLIP and FADD were subcloned into the vectors eCFP-C1 and eYFP-C1. PCR for the oligos was performed using Phusion High-Fidelity DNA Polymerase (M0530 NEB) and was used to amplify inserts (DNA ratios used according to manufacturer's instructions) (Table 2.9).

Table 2.9: PCR conditions for FRET Constructs

Cycle	Temperature	Time	Step
1	98°C	30 s	Denaturation
12	98°C	10 s	Denaturation
	56°C	1 min	Annealing
	72°C	1.5 min (30 sec/kb of plasmid)	Extension
1	72°C	10 min	Final Extension
-	4°C	-	Incubation

A Qiagen PCR purification kit was used to purify the insert DNA. Restriction digestion of purified vector and insert was performed using restriction enzymes *BamHI* (NEB) and *HindIII* (NEB) for FADD (and caspase-8), *BglII* (NEB) was used for c-FLIP using optimised digestion times: overnight for vectors and 1h for inserts (Table 2.9).

Antarctic phosphatase (NEB) was used to dephosphorylate the vectors post digestion, according to manufacturer's instructions. Digested insert and vector were run on a 1% agarose electrophoresis gel (Section 2.5.3) to check successful digestion before purification of vector and insert was performed using Qiagen gel purification kit.

2.6.5 Agarose Gel Electrophoresis and DNA Extraction

Agarose gel electrophoresis was utilised to analyse DNA digests. 5 µl of Nucleic Acid Stain (Safe View, NBS Biologicals, Cambridgeshire) was added to 50 ml of prepared 1% w/v agarose gel and immediately poured into a gel cast, with a comb inserted. Gels were allowed to set for around 20 minutes. 8 µl of DNA for analysis was mixed with 2 µl of loading dye (GelPilot DNA Loading Dye, 5X, Qiagen) and this 10 µl was loaded on the gel, along with 5-10µl of DNA molecular weight marker (Easy Ladder I, Bioline, London). Gels were run at 80 V for around 1 hour. UV light was used to identify DNA bands for extraction and purification using the Qiagen gel purification kit, following manufacturer's instructions. DNA concentrations were measured using a Nanodrop.

2.6.6 DNA Ligation

After DNA extraction and purification, vector (e-CFP-C1, e-YFP, C1) and insert (c-FLIP, FADD and procaspase-8) DNA was ligated. Protocol optimisation was required in order to obtain successfully cloned plasmids. The optimum ratio of vector to insert in the ligation reaction for all sets of cloning was 1:3 vector:insert. Cloning was optimised for use with T4 DNA Ligase (NEB) and transformation in Stbl3 *E. coli* cells (Section 2.6.2.1) according to manufacturer's instructions. Colonies were selected and grown overnight in kanamycin LB media. The following day, Qiagen mini prep kit was used to purify plasmids and DNA concentration was read on a nanodrop. DNA was then sent for sequencing (Section 2.6.2.3), or run on a gel, to observe ligation success.

2.6.7 Transient Transfection

The TRAIL resistant MCF-7 or HeLa cells were transiently transfected with constructs using the transfection reagent Lipofectamine 3000 (Life Technologies). Transfection conditions were optimised in order to obtain viable, successfully transfected cells (Table 2.10). We observed a significant amount of cell death upon transfection with our c-FLIP and FADD FRET constructs which was rescued by pre-treatment with a pan-caspase inhibitor, Z-VAD-FMK (R and D Systems) for 1 h before transfection, thus, this pre-treatment was used for all FRET transfection experiments.

Table 2.10: Optimised DNA ratios for FRET Plasmid Transfection

Amounts are for transfection of 3 wells of a 96 well plate, in 100 μ l media.

Transfection Condition (with Z-VAD-FMK pretreatment)	DNA (μ l)	OptiMEM (μ l)	P3000 (μ l)	Lipofectamine 3000 (μ l)
Control	0	24	1	1.2
CFP alone (FADD) (433.5 ng/ μ l)	0.5	23.5	1	1.2
YFP alone (c-FLIP) (130.5 ng/ μ l)	1	23	1	1.2
CFP:YFP +ve control (608 ng/ μ l)	0.5	23.5	1	1.2
CFP + YFP Control	0.5 + 1	22.5	1	1.2
CFP + YFP TRAIL	0.5 + 1	22.5	1	1.2
CFP + YFP OH14	0.5 + 1	22.5	1	1.2
CFP + YFP OH14 + TRAIL	0.5 + 1	22.5	1	1.2

2.7 FRET Analysis

In our experiments, eCFP and eYFP served as the donor-acceptor pair for AP-FRET. If donor (eCFP) and acceptor (eYFP) FRET constructs are within < 10 nm of each other and in the correct orientation to each other, upon donor excitation, energy transfer to the acceptor will occur. A subsequent slight decrease in donor emission will occur, in parallel to an increase in acceptor emission. When the acceptor is bleached, by using the YFP appropriate laser at high power, energy transfer will not occur, and thus an increase in donor emission will be observed.

2.7.1 Confocal Microscopy

Measurements were performed on a Zeiss LSM 710 confocal microscope (Zeiss, Germany). For intensity measurements, a HXP120V 150W metal halide mercury lamp (Zeiss, Germany) was used, the output intensity of which could be controlled remotely. The lamp was turned on at least 30 minutes before starting experiments so as to avoid artefacts due to warming up of the lamp. Images were recorded on the Zeiss LSM 710 capture camera and LASOS Argon Laser with 458/488/514 nm band excitation filters was used for CFP imaging and YFP imaging and photobleaching. All FRET measurements were performed at 37°C and 5% CO₂.

2.7.2 FRET Cell Stimulation

A viable cell with similar intensity CFP and YFP expression, standardised by first analysing CFP:YFP fusion protein transfected cells, was selected for analysis, keeping laser exposure times to a minimum. At least 10 cells were recorded per experimental condition. Typically, exposure times were kept between 100-500 ms when locating cells with an appropriate expression of CFP and YFP for evaluation of FRET. 20X magnification was selected for imaging. Multi-track line imaging was selected (for sequential imaging of the CFP and YFP channels). Spectra were recorded using a 458/514 nm double dichroic excitation to facilitate excitation of CFP with the 458 nm laser and YFP with the 514 laser line.

For experiments, a pinhole of 1 Airy disk unit in the CFP channel was selected, with the YFP channel Airy unit selected to ensure the optical section thickness was the same as CFP. Laser power of the CFP laser was set to 9%, and 4% for YFP. Digital gain did not exceed 750. Bleaching with the 514 nm laser line was set to 100%. A region of interest (ROI) was defined on the cell of interest, large enough to enable intensity measurements containing at least 900 pixels, in order to minimise image data noise. 10 bleaches, with 1 second between each was chosen to ensure sufficient YFP bleaching occurred. Image acquisition was set to obtain 5 intensity recordings prebleach and 60 seconds postbleach (approximately 40 recordings).

LSM 710 software measured average intensity in the ROI which was plotted on a curve for each time point.

2.8 TALEN

TALENs contain a *FokI* nuclease domain at their carboxyl termini, similar to zinc finger nucleases (ZFNs), which allows them to create the targeted DNA double-strand breaks required by such genome modification techniques. TALEN DNA-binding domains utilise TALEs - naturally occurring proteins derived from *Xanthomonas* spp. plant pathogenic bacterium. These DNA-binding domains are made up of a tandem array of 33-35 amino acid repeats, which are both able to recognise a single-base pair present within the major targeted groove. Specificity and thus, the ability to design TALEN pairs, is achieved by the two amino acids present at positions 12 and 13, the hypervariable 'repeat variable diresidues' (RVDs) (Kim and Kim, 2014). Two TALEN proteins are required to make a functional genome-editing endonuclease, allowing for the recognition of 34 bases, and, with the incorporation of a FokI DNA-cleaving domain, modifications can take place. When designing TALEN pairs, a target downstream of the translation start codon is chosen for the creation of double-strand breaks, which will be repaired by the process of nonhomologous end joining, thus creating out of frame deletions or insertions into the genetic code (Cermak *et al.*, 2011; Christian *et al.*, 2010). The process of clonal selection involved with TALEN, and indeed other genetic modifying processes such as with the use of zinc finger nucleases, results in a 1.6 - 34% fraction of successfully modified cells (Ding *et al.*, 2013).

TALEN binding pairs were constructed targeting exon 4 of c-FLIP(L) (Figure 2.2) and purchased from the TALEN Library Resource (Seoul National University).

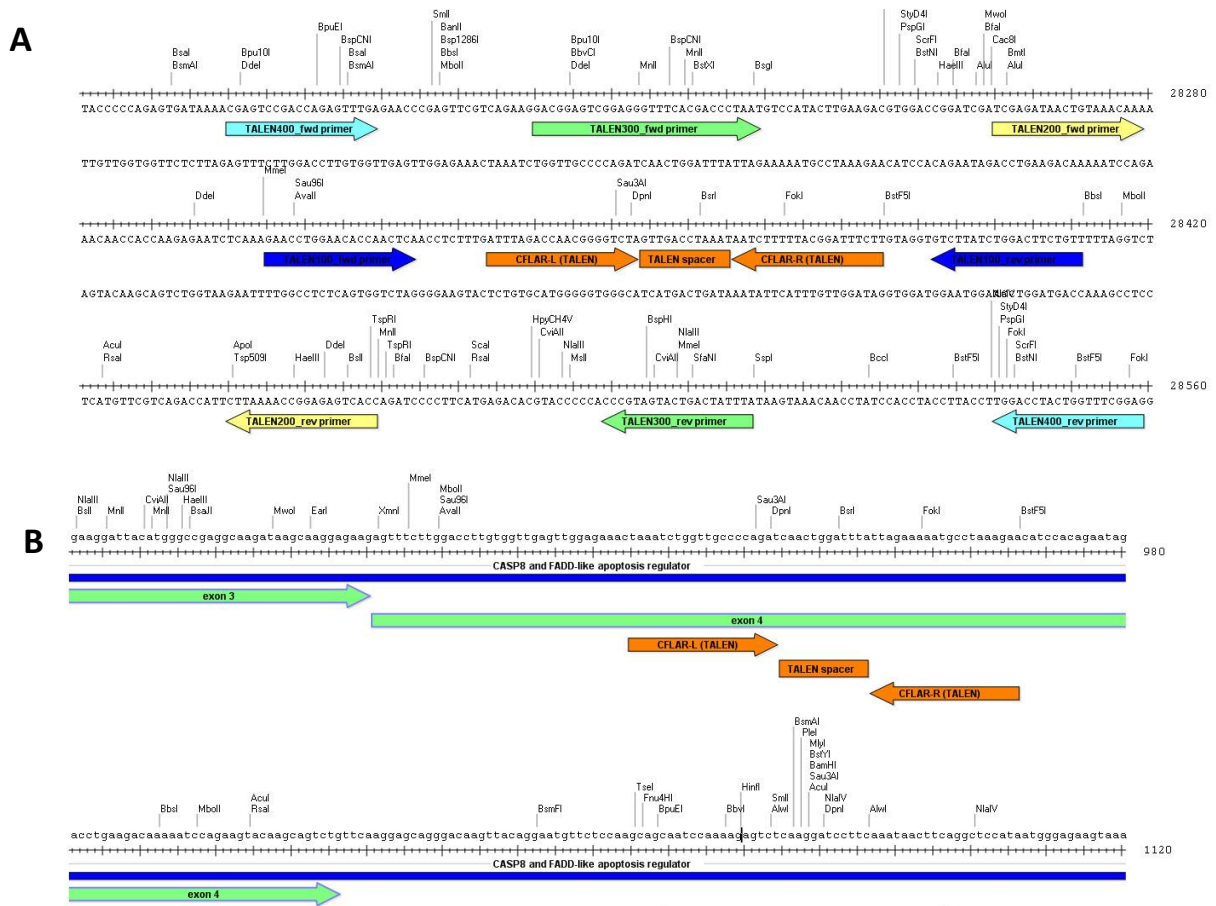


Figure 2.1: Location of c-FLIP TALEN Pairs.

A) Genomic loci and TALEN positions for c-FLIP left (upstream) and right (downstream) TALEN constructs. B) TALEN mRNA constructs for c-FLIP.

The sequences for our c-FLIP TALEN construct primers (Table 2.11) target a site 29.18% into the coding DNA sequence of c-FLIP:

Table 2.11: TALEN primer sequence

Name	Target	Primer
TALEN-c-FLIP-L	Left target sequence	TAAATCTGGTTGCCCCAGAT
Spacer	Spacer	CAACTGGATTTA
TALEN-c-FLIP-R	Right target sequence	TTAGAAAAATGCCTAAGAA

2.8.1 TALEN Transfection

Transfection efficiency was optimised by testing 3 different transfection reagents: Lipofectamine2000, jetPEI or GeneCellen on MCF-7 cells with GFP or m-RFP co-transfected to observe cells effectively transfected and to allow for cell sorting. Lipofectamine2000 and mRFP were chosen as the optimum transfection conditions, as assessed by fluorescence microscopy, and the optimum cell confluence at transfection of 60% was used. After optimisation, MCF-7 cells were transfected, using Lipofectamine2000, with equal amounts (2 µg) of TALEN-L and -R constructs (Table 2.1) as well as mRFP (donated by Dr David Stanek, Institute of Molecular Genetics, Prague).

2.8.2 FACS Sorting and Clone Culture Conditions

Transfected MCF-7 cells were sorted using FACS, selecting around 80% mRFP expressing cells (not 100%) and subcloned into 96 well plates, plated to achieve one cell per well. Cells were plated in MCF-7 conditioned medium in order to obtain optimal cell growth and media was changed after 5 days.

Wells were checked for the presence of single colonies. After around 2 weeks, 80 single colonies were observed and allowed to grow until a relatively high confluence was achieved, after which they were split and re-plated into two replicates, one for further propagation, the second for gDNA isolation, which was used to confirm the knock-down (Section 2.8.3.1).

2.8.3 TALEN Transfection Analysis

Several reagents were utilised in order to extract, isolate genomic DNA from MCF-7 TALEN transfected cells, before analysis could be performed (Table 2.12).

Table 2.12: Reagents required for genomic DNA isolation.

Reagent	Composition
Lysis Buffer	10 mM Tris pH 7.5, 10 mM NaCl, 10 mM EDTA pH 8.0. 0.5% sarcosyl + proteinase K added just before cell lysis, 10 mg/ml was diluted 1:100
NaCl:Ethanol	150 µl of 5 M NaCl was mixed with 10 ml of 96% ethanol
Phusion Reaction Mixture	4 µl buffer, 0.4 µl of 10 mM dNTPs, 2 µl of primer mix (5 + 5 µM), 1 µl of template, 0.2 µl of Phusion, 12.4 µl of H ₂ O
DreamTaq Reaction Mixture	2 µl of primer mix (5 + 5 µM), 1 µl of template, 10 µl of 2x master mix, 7 µl of H ₂ O

2.8.3.1 gDNA Isolation

Isolation of genomic DNA was performed in order to PCR-analyse the first round of TALEN transfected MCF-7 cells. TALEN transfected MCF-7 TALEN clones in 96 well plates, were washed 2 times with PBS and lysed in 50 µl of lysis buffer. The plates were incubated overnight in 55°C to degrade all contaminating proteins, then 100 µl of NaCl:ethanol was added and the plate was incubated for 1 hour. Precipitated DNA was washed by very careful removal of the supernatant and two additions of 150 µl of 70% ethanol. DNA was dried at 55°C and finally diluted in 50 µl of Tris/EDTA, with resuspension to ensure full DNA dilution.

2.8.3.2 Confirmation of Expression

Following gDNA extraction of TALEN clones, Phusion and DreamTaq DNA-polymerases were used according to the manufacturer's protocol (*Thermo Scientific*) (Table 2.6.3) and compared, using normal MCF-7 genomic DNA extract, in order to decide which would be best for analysis of all clones. In addition, multiple primer pairs were designed and tested in various combinations in order to achieve the most clear result for amplifying c-FLIP and checking the transfection of TALEN constructs (Table 2.13).

Table 2.13: Forward and Reverse Primers for Testing the Efficiency of c-FLIP TALEN Clones

Oligos for c-FLIPL TALEN	Primer Sequence
c-FLIP_TALEN200_fwd	AGCTCTATTGACATTTGTTT
c-FLIP_TALEN200_rev	CCACTGAGAGGCCAAAATTC
c-FLIP_TALEN300_fwd	CTGCCTCAGCCTCCCAAAGTGCTGGGATTA
c-FLIP_TALEN300_rev	ATTTATCAGTCATGATGCCC
c-FLIP_TALEN400_fwd	GCTCAGGCTGGTCTCAAAC
c-FLIP_TALEN400_rev	GAGGCTTTGGTCATCCAGGT
c-FLIP_TALEN100_fwd	CTTGGACCTTGTGGTTGAGT
c-FLIP_TALEN100_rev	TTGTCTTCAGGTCTATTCTG

The program for PCR was as follows: initial denaturation (98°C 1 min), 40 cycles (98°C 30 s, 56°C 30 s, 72°C 30 s), final extension (72°C 10 min). The PCR program for DreamTaq was as follows: initial denaturation (95°C 1 min), 40 cycles (95°C 30 s, 56°C 30 s, 68°C 1 min), final extension (68°C 10 min). DreamTaq master-mix provided the best result and was subsequently used for the MCF-7 clones analysis together with 200F + 400R combination of primers (Figure 2.2A and B). Restriction digestion with *EcoRI* enzyme was used to check whether the plasmids contain the correct TALEN. The expected size of the bands was 4260 bp and 2500 bp.

The restriction enzyme used to cleave the DNA was *BsrI*, an enzyme present around 50% into the sequence of c-FLIP (Figure 2.1), and, thus, one which would be expected to generate products around 200 bp in size. Reaction mixture containing 2 µl of PCR mixture, 1.5 µl of B-buffer, 0.2 µl of *BsrI* (*BseNI* by *Thermo Scientific*), 11.3 µl dH₂O was incubated for 3 hours in 65°C. For the subsequent gel electrophoresis in 2%

agarose gel diluted in TAE buffer and ethidium bromide the whole digestion mixture or 2 μ l of PCR mixture were used (Figure 2.2C).

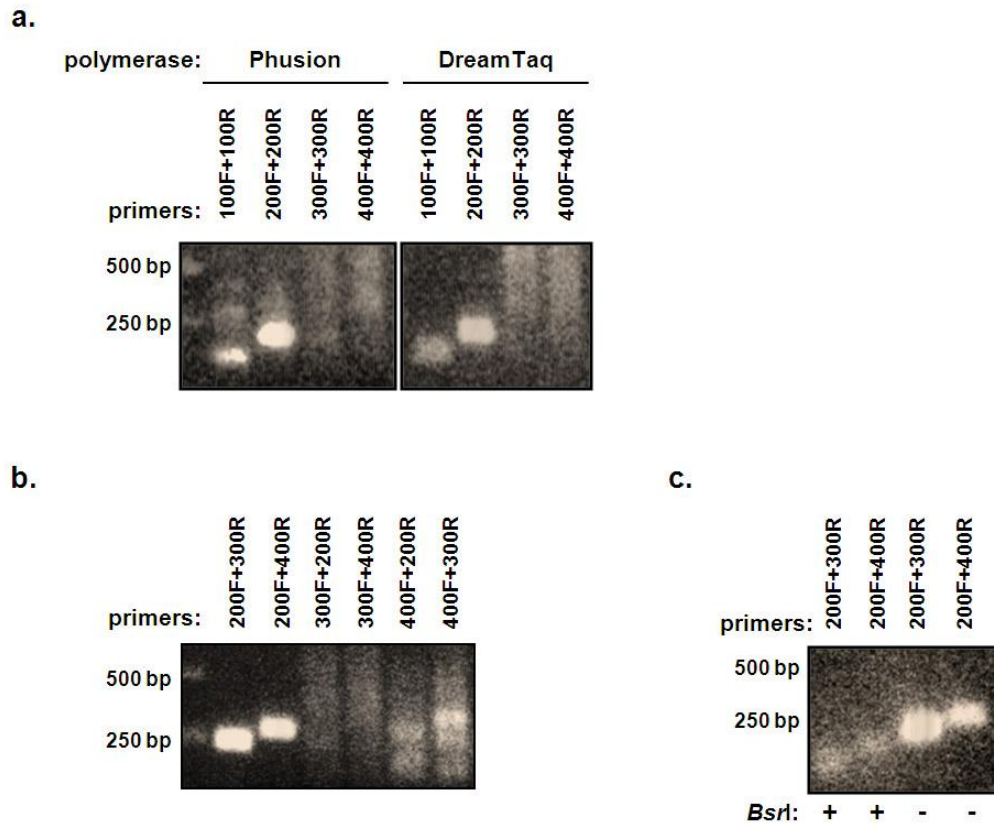


Figure 2.2: Optimizing of PCR conditions and test of *Bsr*I cleavage.

a) Two polymerases, Phusion and DreamTaq were tested using our different primer pairs. The best result was obtained using DreamTaq as it provided the cleanest bands. b) Different primer pairs were tested, with the combination of 200F:300R and 200F:400R providing the best combinations. c) When cleaving the primer pairs using *Bsr*I, the combination of 200F:400R was the optimal combination.

2.8.4 Second Transfection

Second transfection was performed in the same way as Section 2.8.1, and FACS sorting was performed as in Section 2.8.2. RNA was extracted as in Section 2.9.1 and potential clones were analysed using qPCR (Section 2.9.3).

2.9 RNA Analysis

Before extracting and handling RNA, all surfaces and pipettes were cleaned thoroughly with RNase Zap (Ambion).

2.9.1 RNA Extraction

Cultured cells were pelleted by centrifugation at 234 g and subsequently resuspended in 1 ml PBS to wash off media. After re-pelleting, PBS was removed and replaced with 350 μ l Buffer RLT (Qiagen). RNA was extracted using the Qiagen RNEasy kit following the manufacturer's instructions. Following this, RNA was incubated with DNase (Amplicon) for 15 minutes before inactivation in the appropriate inactivation solution. Concentration was measured using a Nanodrop.

2.9.2 cDNA Synthesis

cDNA was synthesised from RNA using M-MLV reverse transcriptase (Promega), following the manufacturer's instructions. Essentially, 50 ng of RNA was mixed with 1 μ l of 500 μ g/ml random of primers, diluted up to 15 μ l with dH₂O and heated to 70°C for 5 minutes, before rapid cooling on ice, to melt secondary structure and prevent it from reforming. Tubes were spun to collect solution at the bottom, after which, 1 μ l of 10 mM dNTPs (Promega), 5 μ l M-MLV 5X Reaction Buffer, 200 units (1 μ l) M-MLV RT, 1 unit/ μ l (0.6 μ l) RNasin (Promega) and dH₂O to 25 μ l was added to the original 15 μ l solution. Samples were incubated at 37°C for 1 h. The resulting DNA was stored at -20°C.

2.9.3 q-RT-PCR Analysis

All qPCR experiments were designed to include primers to target c-FLIP in addition to beta-actin, as the internal control gene. Primers for q-PCR were custom designed using Primer3 web-based program (primer3.ut.ee) (Table 2.14).

Table 2.14: qPCR Primers

Target	Forward Primer Sequence	Reverse Primer Sequence
Beta Actin	CCCAGCACAATGAAGAtCAA	CAGGTGGAAGGTCGTCTACA
c-FLIP	TGATGGCAGAGATTGGTGAG	GATTTAGACCAACGGGGTCT

Levels of beta-actin should be consistent through all cells and thus reflective of the total amount of cDNA present in each sample. A control of no template was also included, with the replacement of cDNA with dH₂O so as to control for the presence of contaminating DNA.

A qPCR reaction mix was prepared to include (per reaction): 0.2 µl Sybrgreen (Invitrogen), 13.7 µl dH₂O (Sigma), 0.1 µl Taq polymerase (GoTaq, Promega), 5 µl GoTaq buffer (Promega), 2.5 µl MgCl₂ (Promega), 0.5 µl 10mM dNTPs (Promega) and 0.25 µl of each 10 mM forward and reverse primers. 22.5 µl of the master-mix was added to 2.5 µl cDNA in a 96-well plate (Applied Biosystems). Wells were mixed by careful pipetting. The plate was sealed and the experiment run on a RealTime PCR machine running StepOne software (Applied Biosystems) using the following protocol: Initial denaturation - 95°C 10 minutes, Denaturation - 45 cycles at 95°C for 15 s and Annealing - 60°C for 1 minute. The software generated a melt curve which was analysed to confirm single peaks - indicating single product, and no peak, in empty controls, to confirm the lack of contamination.

2.9.3.1 qPCR Data Analysis

Data generated by qPCR was analysed by relative quantitation, *i.e.* target gene expression is compared with internal control gene expression in order to normalise for input and efficiency variations, and a reference sample. Expression levels of target gene, c-FLIP, were normalised to the endogenous control in order to obtain data displaying the change in expression. Expression change was expressed relative to 1, thus, a value above 1 indicated an increase in expression, 0 indicated no change and below 1 showed a decrease in expression.

2.10 Data Analysis

Graphs are displayed with error bars (where applicable) representing standard error of the mean values. Statistical significance was determined using the Student's t-test. Box plots were constructed in Graph Pad Prism 6. T-tests were performed between samples and were performed on sample sizes of $n \geq 3$. Statistically significant differences were set at p-value < 0.05 . The tests were performed using Excel 2010 software.

Chapter 3

Modelling of c-FLIP and Associated Proteins

Chapter 3: Modelling of c-FLIP and Associated Proteins

3.1 Introduction

c-FLIP plays a key role in the resistance of several breast cancer cell lines to TRAIL induced apoptosis due to its homology, and therefore competition with, procaspase-8 for binding to FADD via its DED. Many studies exist which evidence the contribution of c-FLIP to TRAIL resistance in both breast and other cancer types (Section 1.2.2.6 and 1.3.3.1). We have previously demonstrated an ability to sensitise resistant breast cancer cell lines to TRAIL using siRNA to knock-out c-FLIP, as well as demonstrating the elimination of tumourspheres in the same conditions (Piggott *et al.*, 2011). To our knowledge, however, there are no reported direct inhibitors of c-FLIP, therefore, in this chapter we aimed to design small molecule inhibitors to c-FLIP in order to prevent its anti-apoptotic function by using *in silico* protein modelling and screening.

3.1.1 Molecular Modelling

In silico modelling has become more common for understanding protein:protein interactions and is increasingly utilised in chemical research to study compounds and their potential interactions with proteins. The ability to visualise protein interactions in 3D, in simulated conditions of a cell or solute is an extremely useful tool for drug design. In particular, the use of protein:ligand docking has greatly enhanced and increased the efficiency of the process of target identification and lead optimisation, allowing researchers to virtually screen vast databases of compounds in a cost-efficient and high-throughput manner.

With increasing computer processing power available even to non-specialists, medicinal chemists are able to design and screen potential drug candidates with increasing confidence and accuracy *in silico*, even taking into account protein-ligand dynamic simulations. The growth in structure-based drug design is also greatly aided by the vast array of protein structures available through the Protein Data Bank (PDB). The PDB, a database of protein structures resolved by X-ray crystallography and nuclear magnetic resonance (NMR), has enabled a vast number of proteins to be studied in such a way, even if their own structure has not yet been resolved, by using homology modelling (Waszkowycz *et al.*, 2011).

3.1.1.1 Homology Modelling

Homology modelling provides a vital tool for analysing proteins *in silico* when the X-ray or NMR structure has not yet been resolved (Nayeem *et al.*, 2006). The process of homology modelling relies on the fact that 3D, structural conformations of proteins are more highly conserved than basic amino acid sequence, and that alterations in this sequence usually result in relatively small alterations to the 3D structure (Lesk and Chothia, 1986). A comparison, therefore, between the sequence of a resolved protein and an unresolved protein, provided they are at least 30% homologous can allow a model of the unresolved protein to be developed (Xiang, 2006). Essentially, a model is developed using several steps: identification of a template 3D protein structure; alignment of this resolved protein with the unresolved target protein; model development of the target based on the 3D template and sequence alignment; and validation or refining of the model until a final model is constructed (Cavasotto and Phatak, 2009). This process is used widely in protein modelling, since initial discussions for the use of structural biology in drug discovery began over 35 years ago, and is now fully recognised and used as a drug development system (Congreve *et al.*, 2005). Many successful small molecules have been selected as a result of homology modelling, as with the case of serine and cysteine protease inhibitors used as anti-parasitic agents, in addition to many other successful examples (Ring *et al.*, 1993).

This study utilises the homology modelling algorithm in the drug discovery software Molecular Operating Environment (MOE) (Chemcorp) which involves several key steps: the copying of any coordinates where residue identity between the two sequences is conserved; Boltzmann-weighted randomized sampling whereby the system runs different sections of the protein backbone with alternative side-chains; finally, model construction involves the creation of several independent models which are scored using a contact energy function. The finalised model is usually the best intermediate model and is subjected to molecular dynamics to further optimise the system (Nayeem *et al.*, 2006).

3.1.1.2 Molecular Dynamics

Molecular dynamics usually follows molecular modelling and involves the computerised simulation of molecular interactions under set parameters following the

basic laws of physics. The purpose of molecular dynamics is to simulate the movement of atoms over time and study the forces acting on these atoms in different conditions. A trajectory for the motion of each atom is calculated in addition to the overall force acting on each atom, as measured by a change in potential energy between two positions in order to best predict their behaviour in a solvent (Kitchen *et al.*, 2004).

In this study we have used GROMACS (GROningen Machine for Chemical Simulations) software which is commonly used to perform molecular dynamics simulations using the concept of periodic boundary conditions. It performs molecular dynamics essentially by putting atoms in virtual boxes, surrounded by solvents such as water, to solvate the protein in the model. Energy minimisation and molecular dynamics are used to attempt to prevent or eliminate any clashes or breaks in hydrogen bonds. Analysis is run alongside in order to monitor energy of the system and calculate the root mean square deviation (RMSD), *i.e.* the average distance between the atoms making up the backbone of the protein. These processes require a high level of computer processing power, *i.e.* a computer which is equipped with multiple central processing units (CPU) or graphics processing units (GPU) and can take several days to run to completion even in the most advanced systems.

3.1.1.3 Virtual Screening: Structure Based Design

Virtual screening is a computational approach utilised to find chemical structures which exhibit certain properties, relevant to the specific system, *i.e.* in a drug discovery process, this entails searching a large database of chemical structures in order to detect compounds which would be suitable for binding to the target.

Two key approaches to virtual screening may be applied: ligand-based and structure based. Ligand-based screening is utilised when the target 3D structure is unknown and thus compounds are selected based on their similarity to the known ligand or compound which is known to bind the target. Conversely, structure-based design requires the 3D structure of the target and involves screening and scoring, or ranking, multiple compounds for their ability to fit to a specific binding pocket on the target. The 'scores' are calculated based on specific algorithms which take into account forces acting on the compound and the target, essentially predicting the affinity of the compound to the target (Hoelder *et al.*, 2012).

In this study we have used the docking function in MOE to perform virtual screening, which uses the 'London dG' scoring function to estimate binding affinity by estimating the free energy of binding of a ligand in a certain pose (Dal Ben *et al.*, 2013).

As opposed to using multiple docking programmes to screen compounds, we screened compounds based on the 3D structures of both c-FLIP and procaspase-8. Essentially, compounds were selected which bound with best affinity, *i.e.* highest docking score in MOE on c-FLIP and, in parallel, had a relatively low score for binding to procaspase-8. Visual evaluation and comparison of these compounds on the DED1 pockets of c-FLIP and procaspase-8 was also performed in order to select which bound with best affinity to c-FLIP but were less able to bind to procaspase-8.

3.1.1.4 Docking Software

In silico docking of small molecules to specific protein sites was established over 30 years ago and has become a vital feature of computerised drug screening (Kitchen *et al.*, 2004). The process allows a prediction of the ligand conformation and orientation within the binding site of the target molecule by running algorithms which test multiple different 'poses' of the ligand within the site.

In this chapter we have successfully utilised *in silico* protein modelling and pharmacophore design to model the previously unmodelled structure of the DEDs of c-FLIP, and the recently modelled DEDs of procaspase-8. By constructing models of interaction with FADD, and pharmacophore design and virtual screening of a library of 350,000 compounds, we have been able to identify 19 small molecules which are potential inhibitors to the c-FLIP DED1:FADD DED interaction.

3.2 Results

3.2.1 Constructing Models of c-FLIP Structure and Interactions

In order to fully comprehend and model the interaction between c-FLIP and FADD, we performed a comprehensive review of literature on studies into relevant mutations available at the time (Section 1.3.7). There is much contradicting information as to which DED on c-FLIP, DED1 or DED2, is most important for binding to FADD and thus inhibiting procaspase-8 binding and apoptosis induction. At the time of this study, no mutational studies on the DED domain of mammalian c-FLIP long (or short) were available, thus a full review of procaspase-8 and FADD mutational studies was required in order to set up *in silico* interaction models. In addition, once basic c-FLIP and procaspase-8 *in silico* models were constructed, analysis of the known intramolecular interactions that exist between DED1 and DED2 of c-FLIP and also of procaspase-8 was used in order to attempt to identify the important residues involved in the interactive surface between c-FLIP:FADD and procaspase-8:FADD.

Overall, the key FADD mutational studies suggested residues F25, K33, R34 and K35 of the FADD-DED are important for apoptosis induction and highlight the relevance of electrostatic forces in DED interactions. It was with a full analysis of all of these studies that we chose to model our proteins based on the intramolecular interaction between DED1 and DED2 and, following this, between FADDs FL motif and the DED1 of c-FLIP or caspase-8, even though other potential sites of interaction are still feasible, and indeed, there may be multiple sites of interaction.

3.2.1.1 *In Silico* Homology Models of c-FLIP and Procaspase-8 Death Effector Domains

At the time of this project, the crystal structures for the DEDs of c-FLIP and procaspase-8 had not been resolved and were therefore constructed based a comparative homology model in MOE. We wished to model both c-FLIP and procaspase-8 in order to compare the structures of the two proteins, so that compounds could be selected based on their ability to bind preferentially to c-FLIP.

The protein MC159 (PDB ID: 2BBR), which has previously been analysed for modelling DED interactions (Carrington *et al.*, 2006; Yang *et al.*, 2005; Dickens *et al.*, 2012) was identified as the best protein for basing the construction of c-FLIP and

procaspases-8 homology models on, via running a sequence comparison search on MOE (Figure 3.1 A summarises the sequence comparison), and was thus used to build the DED structures of c-FLIP (Figure 1.2A) and caspase-8 (Figure 3.1B).

Our homology models demonstrated that the DEDs of highly homologous procaspase-8, which shares 71% sequence homology with c-FLIP (Goltsev *et al.*, 1997), did indeed have a very similar 3D structure to c-FLIP, with approximately 22% structural homology. The DEDs of c-FLIP and procaspase-8 both consist of 6 α helices and 5 anti-parallel β -sheets, although some variations could be identified in the order of residues and orientations of the alpha-helices and beta-sheets which can be more clearly observed when later assessing the interaction models (Section 3.2.2). According to our models, there was approximately 10% and 12% structural homology between DED1 and DED2 of c-FLIP and procaspase-8, respectively as per our model.

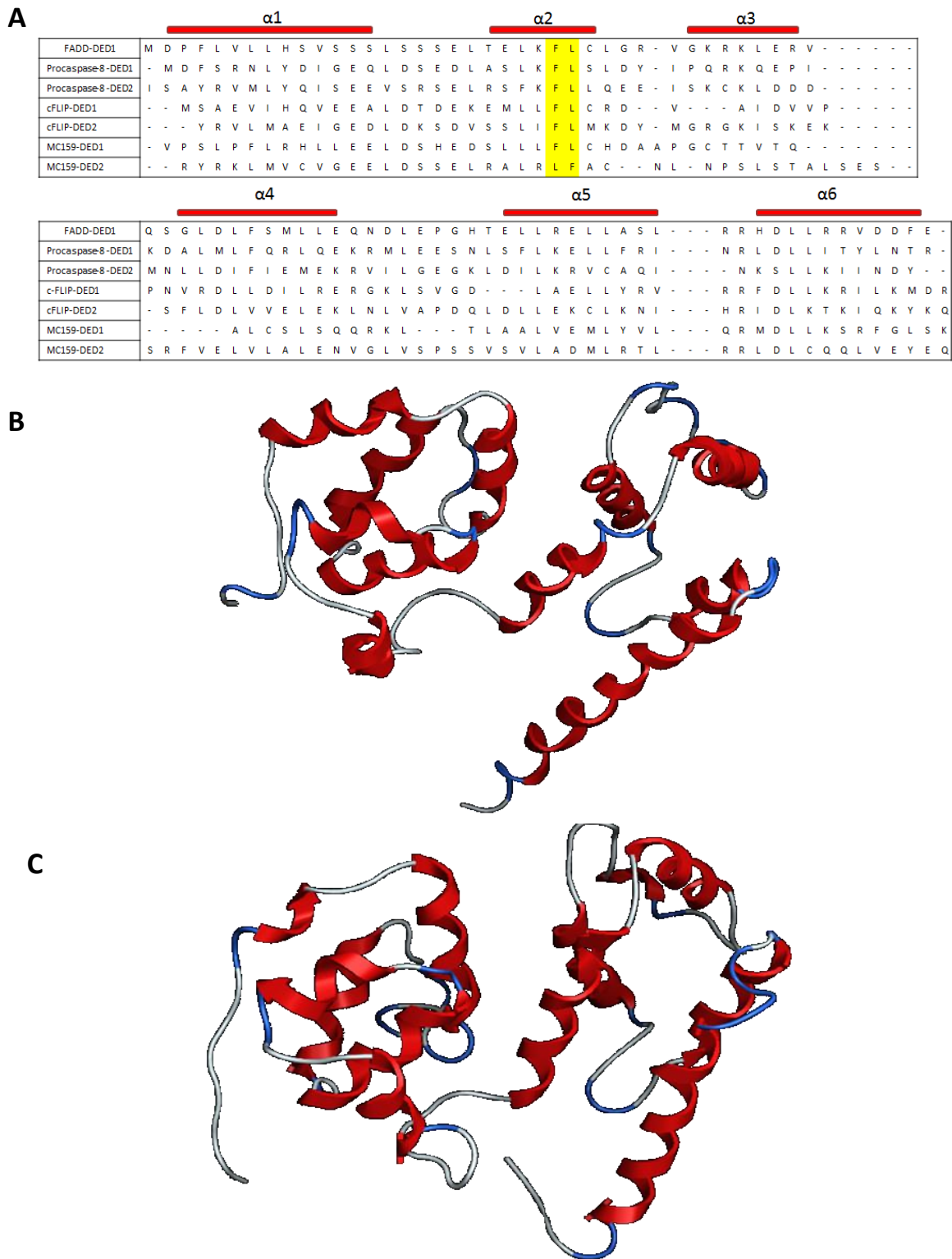


Figure 3.1: Construction of c-FLIP and procaspase-8 homology models

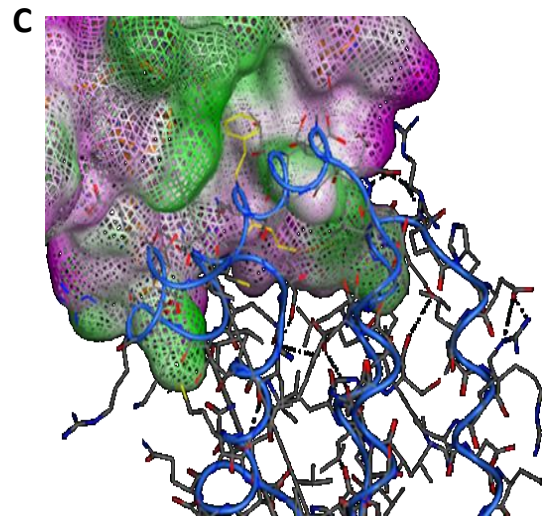
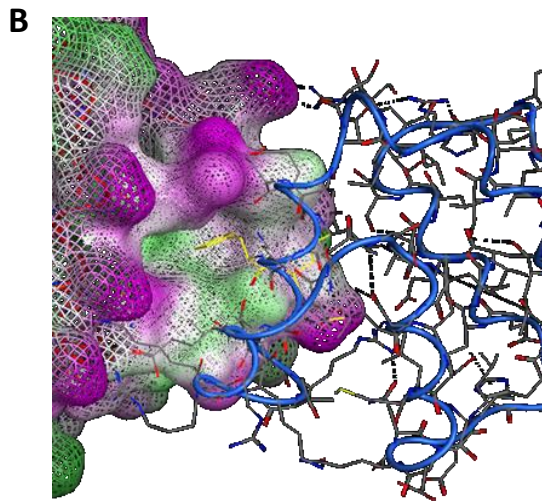
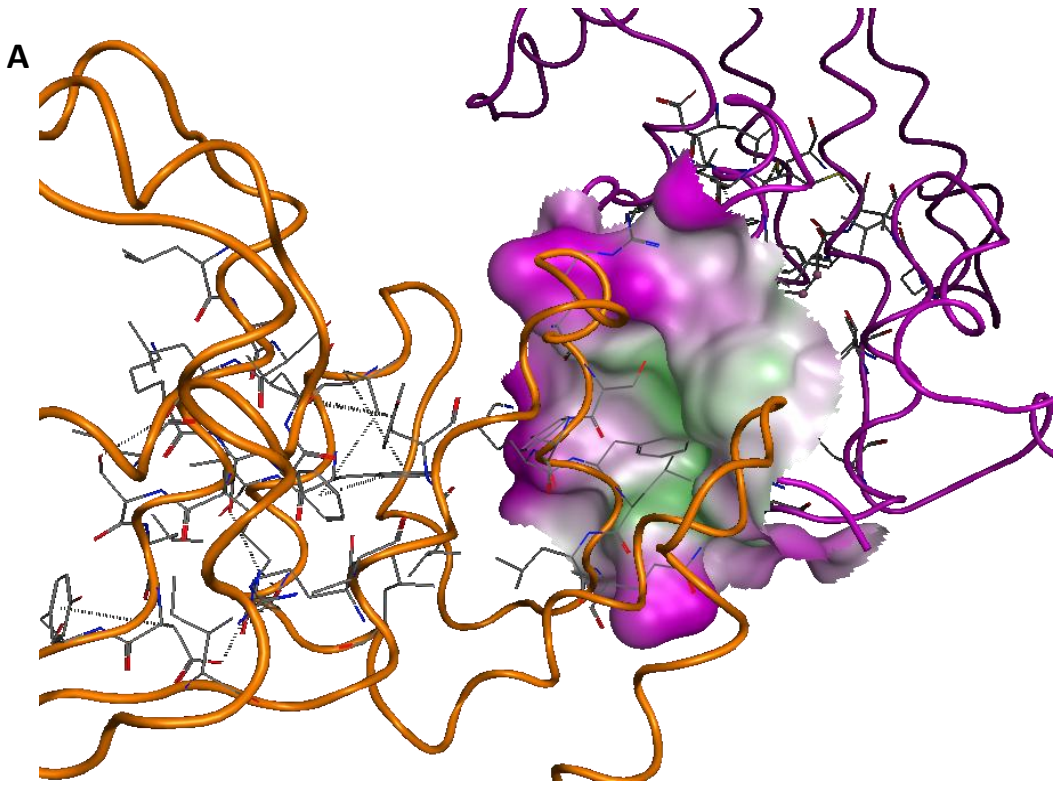
A) DED Amino acid sequence comparison with FADD, procaspase-8, c-FLIP and MC159. Sequences have been aligned based on DEDs. Shared 'FL' sequence highlighted in yellow. Amino-acid sequences were obtained from Eberstadt, *et al.*, 1998. Table adapted from Eberstadt *et al.*, 1998. B-C) DED structures of B) c-FLIP and C) procaspase-8. 3D structures of the two DEDs (DED1 and DED2 from left to right) of A) c-FLIP and B) procaspase-8 modelled *in silico* using a sequence homology model with MC159.

3.2.2 Generation of c-FLIP:FADD and Procaspase-8:FADD Complexes

The known strong, hydrophobic, intramolecular interactions between the internal 'FL motif' on DED1 and a pocket on the internal surface of DED2 of c-FLIP/procaspase-8 (Dickens *et al.*, 2012) were used to model the intermolecular interactions between these proteins, with the FL motif of DED2 binding to pocket on DED1. This intermolecular interaction between procaspase-8 and c-FLIP (Figure 3.2A) was then used to analyse the c-FLIP:FADD and procaspase-8:FADD interactions.

Although there are many potential conformations of interaction, the FL (F25/L26) motif of FADD has been previously demonstrated to be important for procaspase-8 binding (Eberstadt *et al.*, 1998; Kaufmann *et al.*, 2002) and the recent model of DISC formation, which provides evidence that strongly suggests that the DISC consists of a 'chain' of procaspase-8 molecules binding each other via their DED1 pocket and exposed DED2 FL motif (F122/L123) (Dickens *et al.*, 2012), amongst other FADD mutation studies mentioned in Section 1.3.7 meant the first important interaction we chose to model was that of c-FLIP/procaspase-8 DED1 with FADD, which involved the binding of FADDs external FL motif to a pocket on the surface of DED1 on c-FLIP (Figure 3.2B) or procaspase-8 (Figure 3.2C). All constructed models were fully energy minimised after molecular dynamics, as assessed using the RMSD energy plots in MOE.

Comparison of these surface models and of the ribbon models of c-FLIP and procaspase-8 interacting with FADD (Figure 3.2 D and E respectively) demonstrated the pocket on DED1 of c-FLIP to appear to form a more tightly fitting interaction with the FL-motif of FADD than the pocket of DED1 present on the surface of procaspase-8.



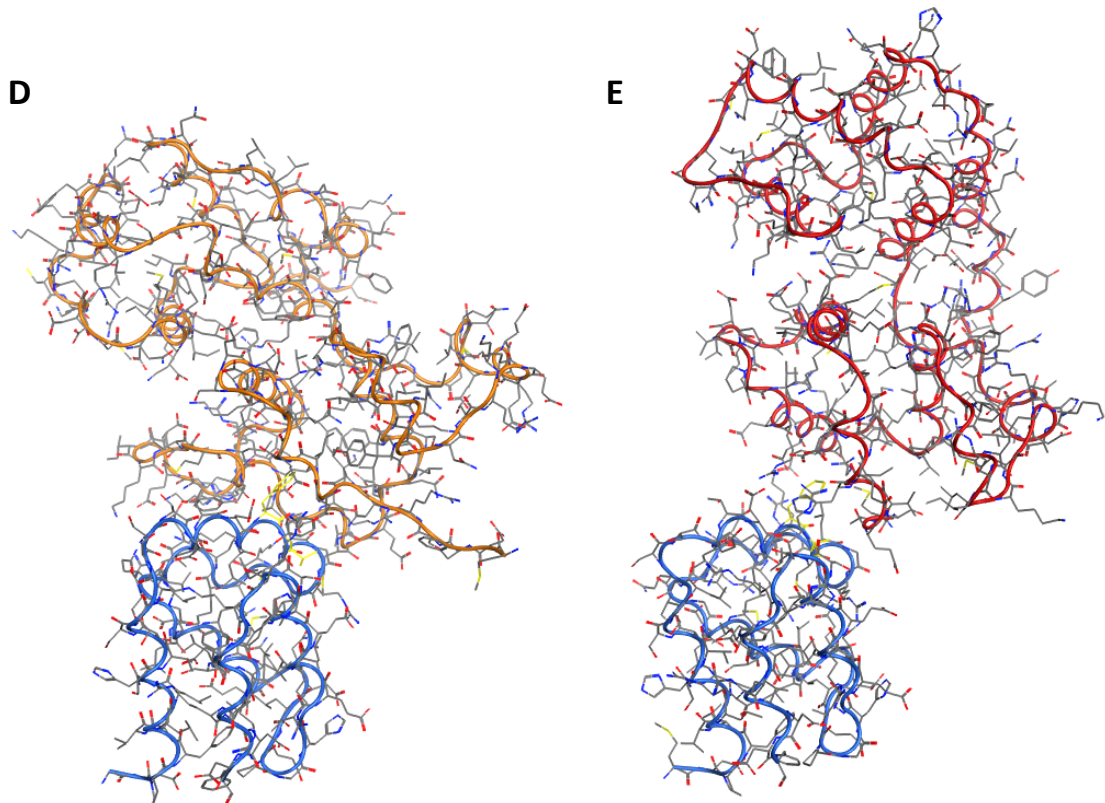
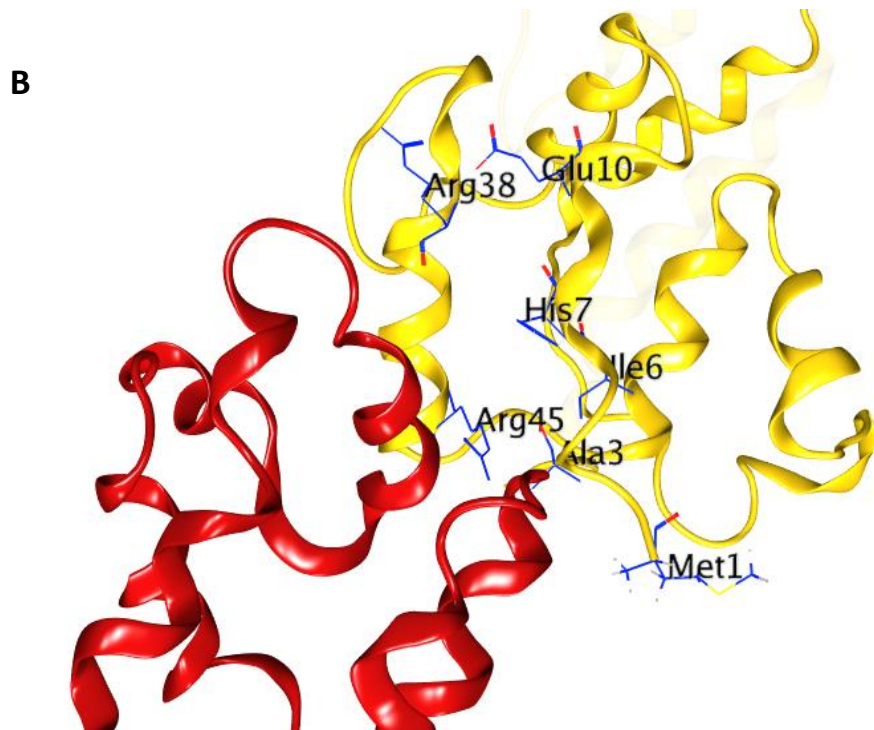
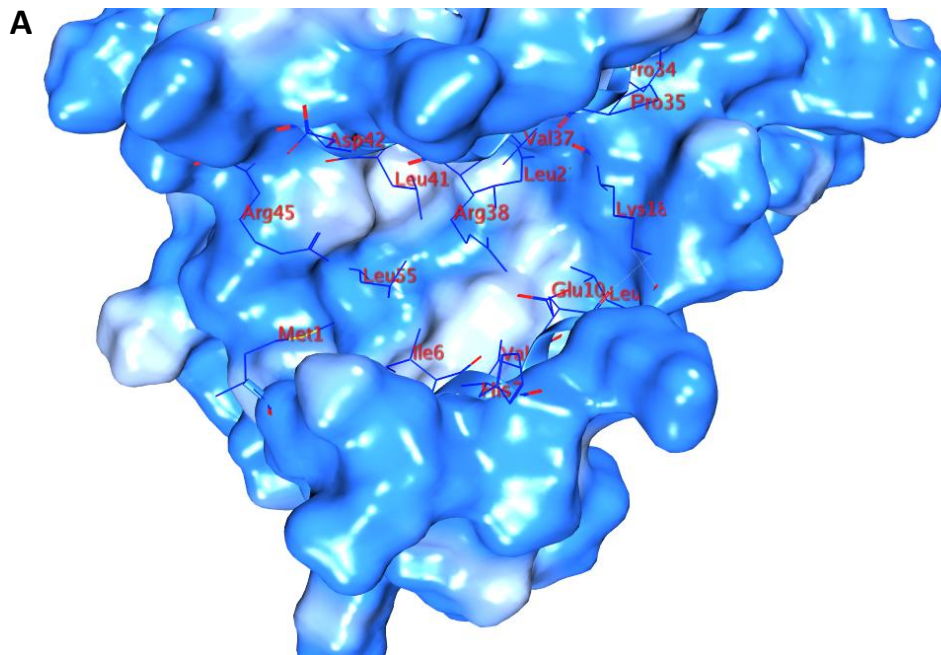


Figure 3.2: Modelling c-FLIP key protein:protein interactions.

Models were constructed based on the chain DISC model (Dickens *et al.*, 2012). A) Interaction between FL motif on procaspase-8 DED2 (orange) and c-FLIP DED1 pocket. B) Interaction between c-FLIP DED1 pocket and FL motif on DED of FADD (blue). C) Interaction between procaspase-8 DED1 pocket and FL motif on DED of FADD (blue). Surfaces shown represent electrostatic surface charge, negative in green, positive in pink. D) Ribbon model of c-FLIP (orange) DED1:FADD (blue) interaction. E) Ribbon model of procaspase-8 (red) DED:FADD (blue) interaction.

3.2.3 Generation of a Pharmacophore Model: Structure-Based Virtual Screening

The interactive surface and apparent pocket on c-FLIP when interacting with FADD was our target for inhibitors when setting up a pharmacophore model in MOE. We utilised a structure-based approach to perform virtual screening on the surface of c-FLIP and by generating a pharmacophore model, the screening of compounds was made specific, as, only those which fit the pharmacophore model would gain high binding affinity scores, and therefore be identified as hits. We set up the pharmacophore query using a collection of three-dimensional chemical features to represent the ligand's, *i.e.* the FL motif of FADD, interacting residues and set volume restrictions to limit the surface area of the compound binding site. Compounds were then selected based on their ability to interact with c-FLIP in a similar manner to the FL-motif in the areas represented by these features, and therefore to compete with the FADD ligand for interaction with the residues in and around the designated area on the surface of c-FLIP DED1 (Figure 3.3A and B). Four features were identified, and, of particular interest, residues around the 'pocket' on c-FLIP were identified to be important for the binding of FADD via the FL-motif (Figure 3.3C).



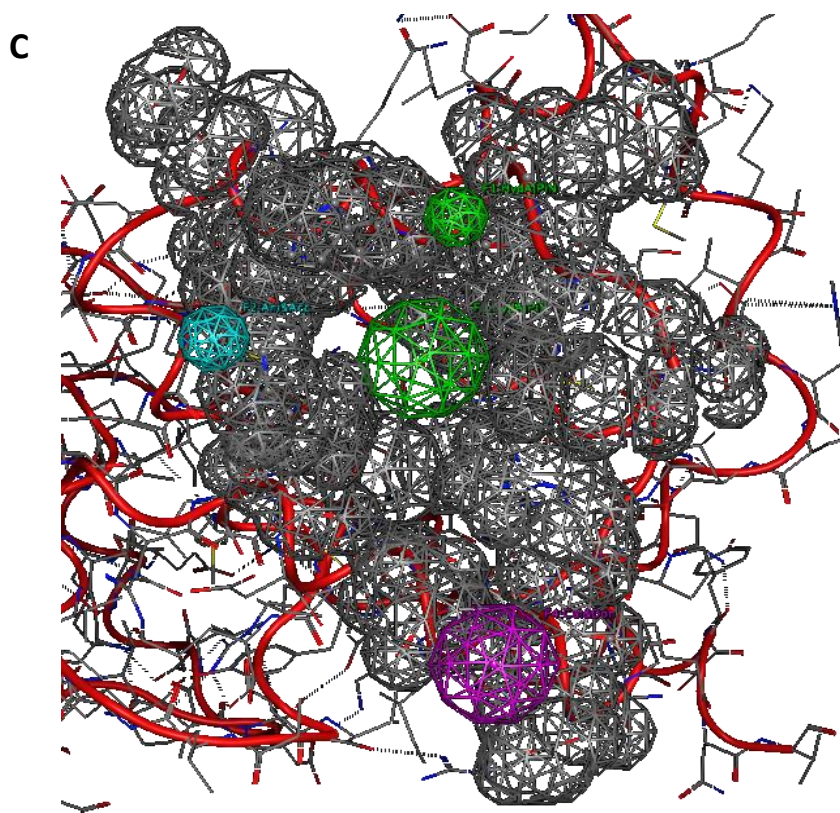


Figure 3.3: Characterisation of the DED1 c-FLIP:FADD binding pocket and Pharmacophore Model on Binding Surface.

A) Pocket on surface of c-FLIP DED1 with residues displayed which were key in the FADD interaction. B) Zoomed view of c-FLIP:FADD interaction showing residues of importance on c-FLIP DED1 (yellow) (FADD shown in red). C) Pharmacophore model used to filter the database of over 350000 small molecules for the virtual screening studies on the interactive surface of c-FLIP (red ribbon). The model consists of 'features' (4 coloured spheres), *i.e.* areas of interaction of the FL-motif of FADD with c-FLIP DED1 which could be targeted by inhibitors. Features are coloured based on their hydrogen acceptor/donor status (blue = aromatic acceptor, green = acceptor, purple = donor). Grey spheres represent carbon atoms on surface of c-FLIP.

3.2.4 Virtual selection of inhibitors to c-FLIP:FADD interaction

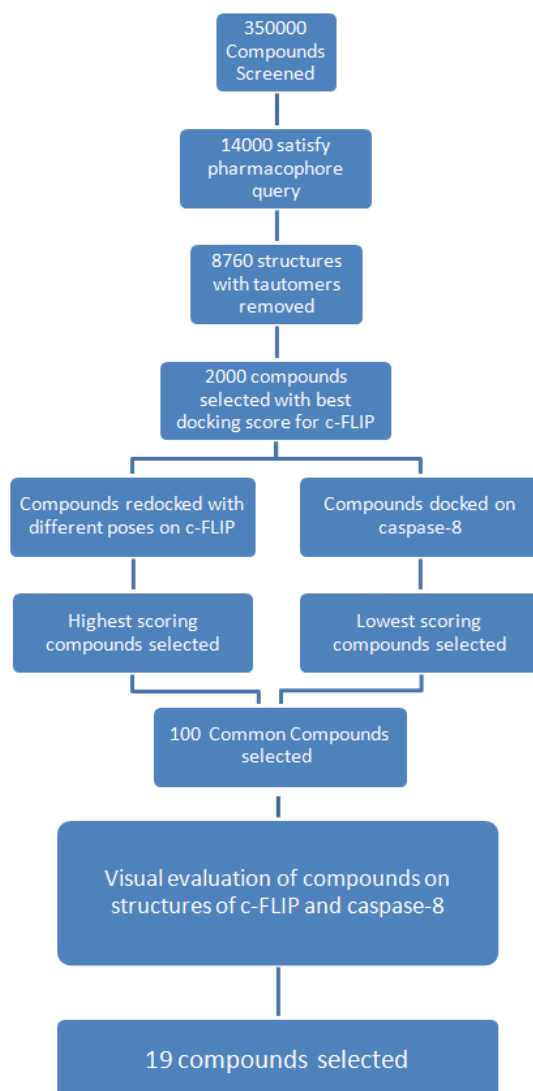
Our finalised pharmacophore model was used to screen a library of over 350,000 commercially available compounds (Specs Database, Delft) in order to identify potential inhibitors to these sites. Approximately 14000 'hits' were identified which were able to satisfy the pharmacophore query by their ability to bind to at least 3 out of 4 of the features, which were then virtually 'docked' on c-FLIP. Compounds were scored based on their ability to bind to the specific features on c-FLIP and after a further two docking refinement steps, we selected 2000 compounds with the highest score, *i.e.* ability to bind to the selected features, to analyse and re-run against caspase-8. The compounds which had the lowest score for caspase-8 were of interest, since they would not bind to this protein with such affinity (Figure 3.4A).

We visually inspected the 'top' 100 scored compounds from c-FLIP and 'bottom' 100 from caspase-8 for their ability to bind to the protein and thus to block the interaction with FADD (Figure 3.4 B and C). For a compound to be selected, they needed to adhere to the criteria we had put in place:

1. Compound must fill the pocket on c-FLIP
2. Compound must not lie outside of the pocket on c-FLIP
3. Compound must not clash within the protein structure
4. Compound should not fill pocket on procaspase-8
5. Compounds selected should be relatively varied in structure

Using these criteria, we selected a final 19 compounds using the combination of MOE docking scores and visual inspection of the compounds within pockets of c-FLIP and procaspase-8. These compounds were chosen to include a range of chemical structures, with varying molecular weights and chemical properties, which were then purchased from Specs database (Table 3.1). All compounds selected adhered to the Lipinski rule of 5 (Molecular weight <500, LogP <5 (lipophilicity), H donors <5, H acceptors <10 (Leeson, 2012)).

A



B

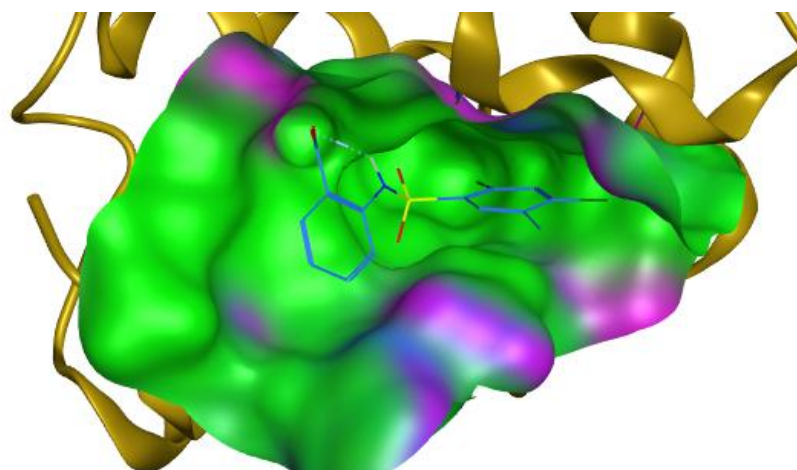


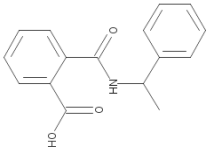
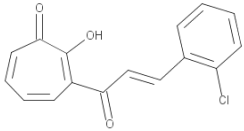
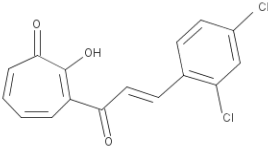
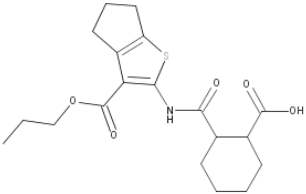
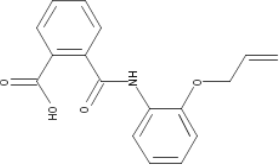
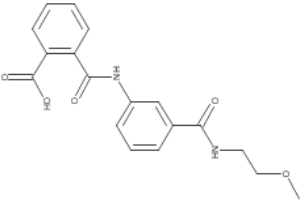
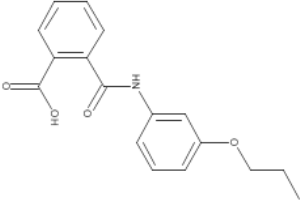
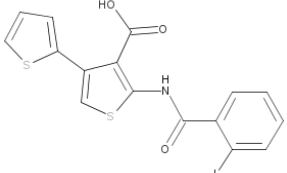
Figure 3.4: Visual inspection of one of the 19 compounds within the pocket on c-FLIP DED1

A) Summary of *in silico* user defined compound selection steps. B) Visual evaluation of around 200 compounds on the FADD-interactive pocket on both c-FLIP and procaspase-8 was performed to select inhibitors which would be specific for the c-FLIP pocket. Compound displayed is OH14.

Table 3.1 Structure of 19 Compounds Selected from *In Silico* Screening

19 Selected compounds all adhered to the Lipinski rules and thus were all valid drug candidates.

MW = molecular weight to 1 d.p.

Cpd	MW	Formula	Displayed
OH1	269.3	C ₁₆ H ₁₅ NO ₃	
OH2	286.7	C ₁₆ H ₁₁ ClO ₃	
OH3	321.2	C ₁₆ H ₁₀ Cl ₂ O ₃	
OH4	397.5	C ₁₉ H ₂₅ NO ₅ S	
OH5	297.3	C ₁₇ H ₁₅ NO ₄	
OH6	342.4	C ₁₈ H ₁₈ N ₂ O ₅	
OH7	299.3	C ₁₇ H ₁₇ NO ₄	
OH8	455.3	C ₁₆ H ₁₀ INO ₃ S ₂	

OH9	347.37	$C_{21}H_{17}NO_4$	
OH10	278.31	$C_{17}H_{14}N_2O_2$	
OH11	354.38	$C_{20}H_{19}FN_2O_3$	
OH12	350.42	$C_{21}H_{22}N_2O_3$	
OH13	360.2	$C_{18}H_{11}Cl_2NO_3$	
OH14	360.22	$C_{14}H_{11}Cl_2NO_4S$	
OH15	382.43	$C_{22}H_{23}FN_2O_3$	Structure unavailable
OH16	358.4	$C_{17}H_{18}N_4O_3S$	
OH17	416.3	$C_{19}H_{14}BrNO_3S$	
OH18	317.4	$C_{17}H_{19}NO_3S$	Structure unavailable
OH19	309.3	$C_{18}H_{15}NO_4$	Structure unavailable

3.4 Discussion

Previously we have demonstrated that genetic knock-out of c-FLIP using siRNA is an effective way to partially sensitise previously resistant bulk breast cancer cells to TRAIL and significantly enhance the sensitivity of breast CSCs, represented by tumourspheres (Piggott *et al.*, 2011). TRAIL itself is a highly cancer cell specific drug, as it is able to induce apoptosis in cancer cells whilst sparing the untransformed cells (Section 1.2.2.3), however, the fact that many breast cancer cell lines are resistant to TRAIL limits its potential as a therapeutic. Our discovery that c-FLIP suppression is able to sensitise to TRAIL suggested that the combination of a small molecule c-FLIP inhibitor, in combination with TRAIL, could be a potentially very beneficial therapeutic. Currently there are no c-FLIP specific inhibitors available (Section 1.3.6), and, at the time of the project, no c-FLIP mutational studies published were able to elucidate any key residues which could be targeted by small inhibitors, thus, the aim of this project, and particularly of this chapter, was to identify potential small molecule inhibitors that are specific to c-FLIP, by the use of *in silico* protein modelling techniques. The main potential hurdle in selecting a c-FLIP specific inhibitor is the reason it is a potent inhibitor of TRAIL induced apoptosis: its homology to procaspase-8, thus, modelling and inhibitor screening was performed on procaspase-8 in parallel with c-FLIP to try to avoid the unwanted and opposite effect of procaspase-8 inhibition.

At the time of this study, the crystal structure of c-FLIP or procaspase-8 had not been resolved. In addition, no *in silico* models of the DED domains of c-FLIP had been generated, thus, this chapter aimed to generate, initially, an *in silico* model of the structure of the DED domains of c-FLIP. Here, we first constructed these models in MOE based on a homology model using v-FLIP, MC159 as the template. In addition, we constructed a model of the DEDs of procaspase-8, again based on a homology model using MC159 as the template. Our models revealed that c-FLIP and procaspase-8 are indeed highly homologous proteins in both structure and sequence, showing 71% sequence homology in their DEDs, which is in accordance with an initial report also demonstrating 71% homology between the DEDs of c-FLIP and procaspase-8 (Goltsev *et al.*, 1997).

Subsequently, the c-FLIP:FADD interaction, which had not yet been modelled, and procaspase-8:FADD interaction, which had recently been studied *in silico* (Dickens

et al., 2012), were modelled. We constructed our initial model based around the intramolecular interactions that exist between DED1 and DED2 on both c-FLIP and procaspase-8 (Dickens *et al.*, 2012). Both models were constructed in MOE, with molecular dynamics being performed in order to further optimise the complex and validate the stability of the interaction models. More recently, Majkut and team have used *in silico* modelling to analyse the c-FLIP:FADD DED interaction, also using MC159 to construct a homology model. Their modelling looked at two potential orientations of the c-FLIP:FADD interaction (Majkut *et al.*, 2014). Although we did recognise that there may be other potential conformations of the interaction, due to time constraints and the fact we were attempting to identify an inhibitor, we were only able to model and screen one interaction. One of the models generated by Majkut *et al.*, was, however, very similar to our model, with c-FLIP DED1 interacting with the FL-motif of FADD (Majkut *et al.*, 2014). Another recent study, by Hwang and colleagues has also modelled the c-FLIP:FADD interaction, although they based their model on DED2 of c-FLIP interacting with FADD and did not explore the DED1 interaction (Hwang *et al.*, 2014).

We decided to target the interactive surface on DED1 of c-FLIP or procaspase-8 for the generation of our pharmacophore model and structure based virtual screening, based on a thorough analysis of previous studies (Section 1.3.7). Although both DED1 and DED2 do appear to have an ability to interact with FADD, time constraints of the project restricted our focus to only one of the potential interactive conformations. Our interaction model between c-FLIP and FADD was the basis of our virtual inhibitor screens, whereby we used the FL motif on the DED of FADD to generate a pharmacophore model and identify a panel of potential small molecule inhibitors against this interaction. The models we constructed here revealed that there are some structural differences in the interactive surfaces on DED1 of c-FLIP and procaspase-8. The 'pocket' present on c-FLIP appeared smaller, thus giving rise to a closer interaction with FADD, when compared with procaspase-8. This suggested that an inhibitor targeted to this pocket would likely be specific for c-FLIP, due to its size and shape, thus sparing procaspase-8, allowing it to bind with FADD and induce apoptosis.

We then performed virtual compound screening on this model, using a library of over 350,000 commercially available compounds (Specs database, Delft, The Netherlands). Only compounds that satisfied the pharmacophore query were then

docked on the surface of c-FLIP and scored based on their ability to bind to at least 3 identified 'features', *i.e.* charged residue pockets, on the FADD interactive surface on DED1 of c-FLIP. After several score-refining and compound-eliminating docking screens in MOE, 200 inhibitors were visually assessed for their ability to bind c-FLIP specifically. We hypothesised that, since c-FLIP and procaspase-8 are similar in structure, screening the same library of compounds on the procaspase-8, and then visually analysing those which did not score well for procaspase-8 would enable us to select more c-FLIP specific inhibitors. Indeed, several compounds which gained high MOE docking scores, appeared to fit well into the pocket on procaspase-8 and so were eliminated as potential compounds. Of the 200 compounds visually screened on both proteins, 19 structurally diverse small molecule compounds were selected from the initial virtual library of over 350,000 compounds for their ability to bind to c-FLIP, preferentially over procaspase-8.

Using pharmacophore generation and virtual compound screening, a classical *in silico* pharmacological approach, here we have successfully identified a panel of 19 potential commercially small molecule inhibitors which aim to target specific residues on DED1 of c-FLIP protein. These inhibitors were tested in *in vitro* assays on breast cancer cells for their ability to sensitise previously resistant cells to TRAIL induced apoptosis (Chapter 4) and thus to block the c-FLIP:FADD interaction, whilst sparing the procaspase-8:FADD interaction (evaluated in Chapter 5).

Chapter 4

Evaluation of c-FLIP Small Molecule Inhibitors

Chapter 4: Evaluation of c-FLIP Small Molecule Inhibitors

4.1 Introduction

Tumour heterogeneity, drug resistance and the existence of cancer stem cells each present distinct challenges to successful treatment of breast cancer and other types of cancer. Indeed, cancer stem cells, themselves, are resistant to many types of cancer therapy, including chemo- and radiotherapy. Agonists of the TRAIL receptor pathway have demonstrated an ability to induce apoptosis in cancerous cells, whilst sparing untransformed cells, making them highly desirable as cancer therapeutics (Gura, 1997; Ashkenazi *et al.*, 1999; Lemke *et al.*, 2014). We and others have previously demonstrated an ability to sensitise previously TRAIL-resistant breast cancer cells to TRAIL induced apoptosis via c-FLIP knockdown using siRNA (Piggott *et al.*, 2011).

Our previous data, in addition to multiple other studies regarding the anti-apoptotic role of c-FLIP, clearly highlight that a c-FLIP inhibitor could be an effective TRAIL sensitising agent and thus a viable combination therapy with TRAIL for treating TRAIL-resistant cancers, in particular, breast cancer, particularly due to the ability to target cancer stem-like cells (Lempke *et al.*, 2014; Safa and Pollok., 2011; Piggott *et al.*, 2011). Currently, however, although agents do exist which alter expression of c-FLIP these do not specifically target the protein, and, as such have off-target effects affecting other important pathways (Section 1.3.6), there are no c-FLIP specific inhibitors available. The aim of this project, and in particular this chapter, was to evaluate the panel of small molecule inhibitors selected in Chapter 3, using a variety of relevant assays, for their ability to block c-FLIP and therefore sensitise to TRAIL. The high degree of homology between procaspase-8 and c-FLIP is likely to be one of the key reasons a c-FLIP small-molecule inhibitor has not yet been developed (Goltsev *et al.*, 1997; Safa and Pollok, 2011). In chapter 3 we selected several potential inhibitors using *in silico* protein modelling and compound screening, including the issue of cross-reactivity in the experimental design.

Previous use of siRNA results in a 20% decrease in overall cell viability and a 100% decrease in tumoursphere formation potential following TRAIL treatment (Piggott *et al.*, 2011). These cell viability data would be adopted as a benchmark for the efficacy

of the putative pharmacological c-FLIP inhibitors identified in Chapter 3. Furthermore, the ideal inhibitor, when tested *in vitro* would be: effective in many cell lines; specific; non-toxic to untransformed cells; active at low concentrations; exert metabolic stability; and be soluble in multiple solvents.

Here we compare the relative ability of the 19 selected compounds identified from the *in silico* screen to sensitize breast cancer cells, and breast cancer stem cells, to TRAIL. These experiments lead to the identification of a single lead compound, OH14, which exhibited the best efficacy while also satisfactorily fulfilling the additional parameters described above.

4.2 Results

4.2.1 Solubility of the compounds in cell culture media

Solubility is one of the most important parameters involved in achieving the desired concentration of drug in systemic circulation when in a clinical setting. It therefore follows that initial drug evaluation must pay attention to the ability of the compounds to dissolve in solutions, as this may otherwise be a barrier to treatment further along the timeline of drug development. In fact, over 40% of new chemical entities developed in the pharmaceutical industry are almost completely insoluble in water (Savjani *et al.*, 2012).

The solubility of the compounds was determined in the culture media used in the cell viability assays. Dimethyl sulphoxide (DMSO) was selected as the solvent to prepare our stock solutions due to the fact that it is a commonly utilised agent, which is able to dissolve both polar and nonpolar compounds, whilst remaining miscible in organic solvents, such as water. Whilst many of the compounds were soluble in DMSO at 100 mM stock solution and remained in solution when further diluted in cell culture media, some were only soluble when made up to 50 mM, and others were seen to come out of solution once diluted in aqueous solution after overnight incubation in cell assay conditions (Figure 4.1 and Table 4.1).

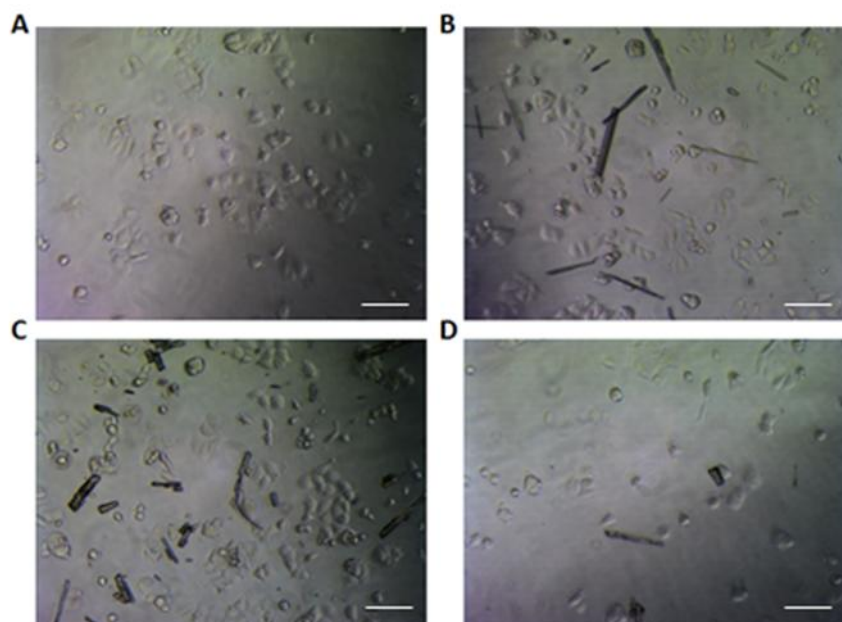


Figure 4.1: Compound Visual Solubility Assessment.

Representative images of compounds which did not remain in solution in media after overnight solubility assessment. A) 0.1% DMSO (highest concentration) alone. B) Compound OH12 in media at 100 μM C) Compound OH15 in media at 100 μM D) Compound OH15 in media at 10 μM . Scale bar = 100 μm .

Table 4.1: Solubility of Initial 19 Compounds in Media.

Visual assessment of compound solubility in DMSO (initial stock made at 100 mM) or after overnight incubation in media at a range of concentrations (100 μM , 10 μM , 1 μM , 0.1 μM , 0.01 μM). Concentration at which compound was observed to be soluble is shown.

Compound	Stock: DMSO (mM)	Working: Aqueous Media (μM)
OH1	50	0.1
OH2	100	1
OH3	50	0.1
OH4	50	10
OH5	100	100
OH6	100	100
OH7	100	10
OH8	100	100
OH9	100	100
OH10	50	100
OH11	50	1
OH12	100	1
OH13	100	100
OH14	100	100
OH15	100	1
OH16	50	100
OH17	100	100
OH18	100	1
OH19	100	100

4.2.2 Inhibitors of c-FLIP demonstrate an ability to sensitise to TRAIL in Breast Cancer cell lines

Initially, compounds were tested on their ability to sensitise the bulk population of the cell lines MCF-7 and BT474 to TRAIL using the Cell Titre Blue viability assay. These cell lines were chosen due to their TRAIL-resistance, previously confirmed sensitivity to c-FLIP siRNA and TRAIL in multiple assays (Piggott *et al.*, 2011), and for the equal expression of c-FLIP between these cell lines (French *et al.*, 2015 in press). The Cell Titre Blue assay was chosen since it had been previously successful in demonstrating the ability of c-FLIP siRNA to sensitise to TRAIL (Piggott *et al.*, 2011), in combination with the fact that it is a high-throughput assay which is beneficial for testing multiple compounds at a range of concentrations.

4.2.2.1 c-FLIP Inhibitors Sensitise TRAIL-resistant MCF-7 Bulk Cells to TRAIL

The adherent bulk population of MCF-7 cells are TRAIL-resistant (Rahman *et al.*, 2009; Piggott *et al.*, 2011). Knocking-down c-FLIP with siRNA in these cells caused 10% reduction in viability and, when treated with TRAIL, this increased to 30% (Piggott *et al.*, 2011). We hypothesised that similar relative levels of cell death would be obtained with an efficient c-FLIP specific small molecule inhibitor. Compounds which demonstrated this synergistic effect with TRAIL, at several concentrations, with no solubility issues were of most interest for further investigation.

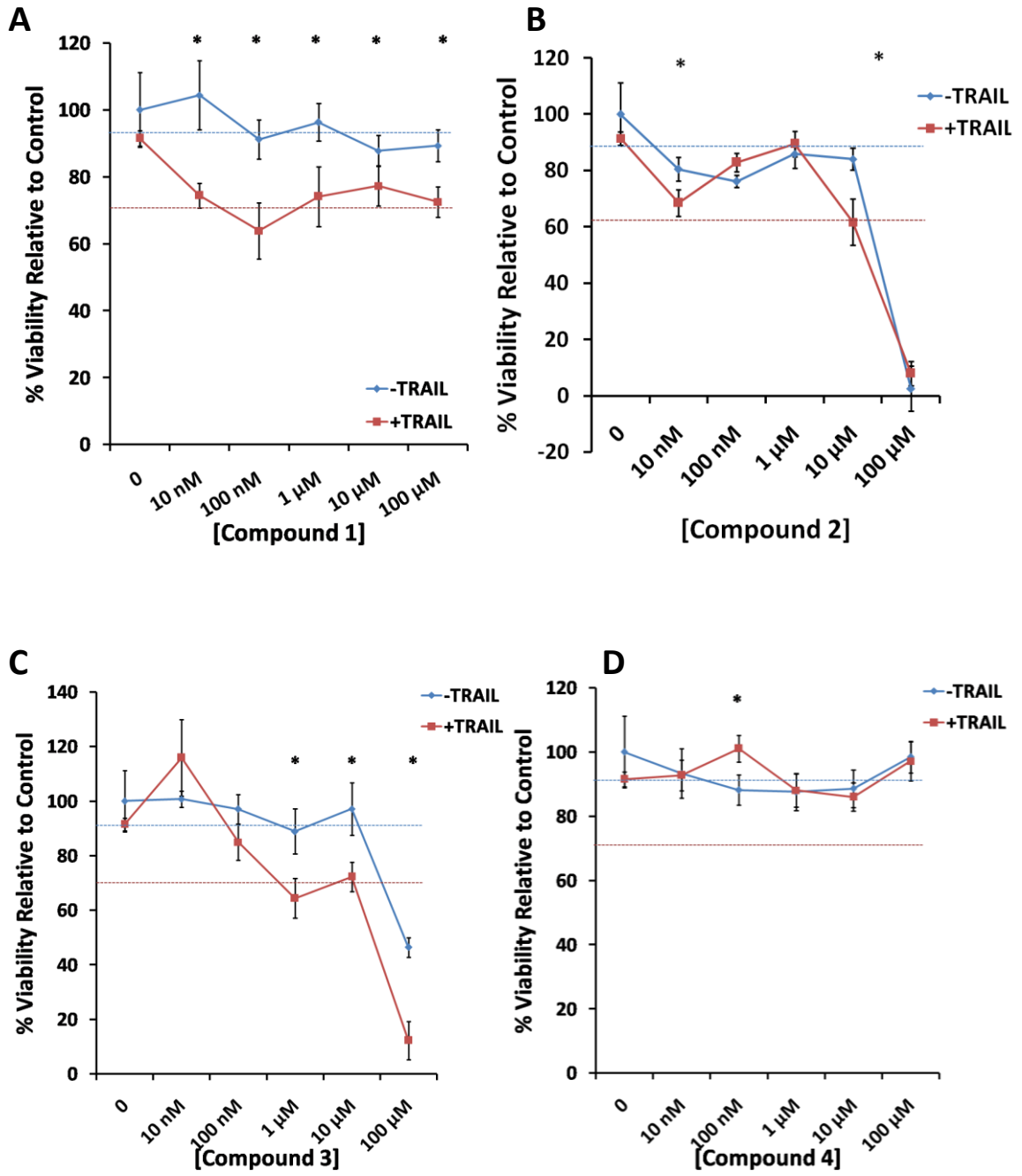
For viability evaluation, compounds (or vehicle control) were added to bulk cells at 70% confluence and left for one hour before the addition of 20 ng/ml TRAIL. After 18 hours, viability was measured using the Cell Titre Blue assay.

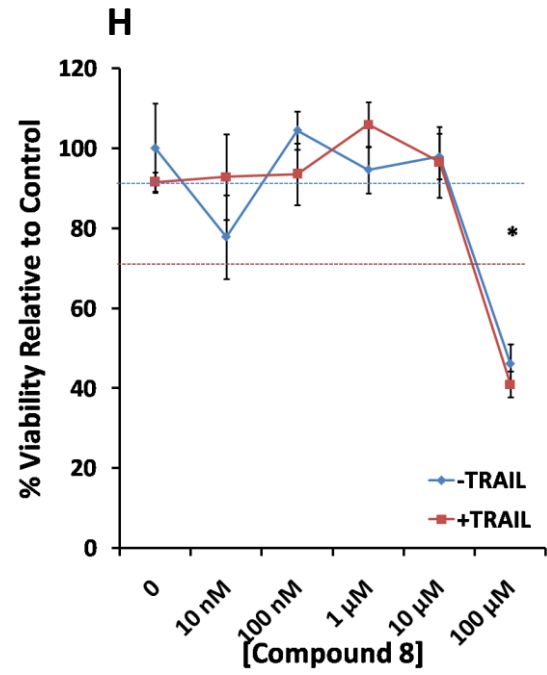
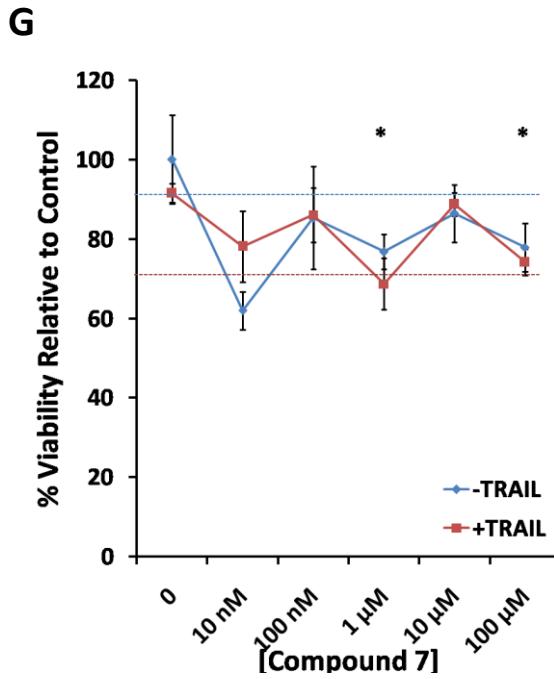
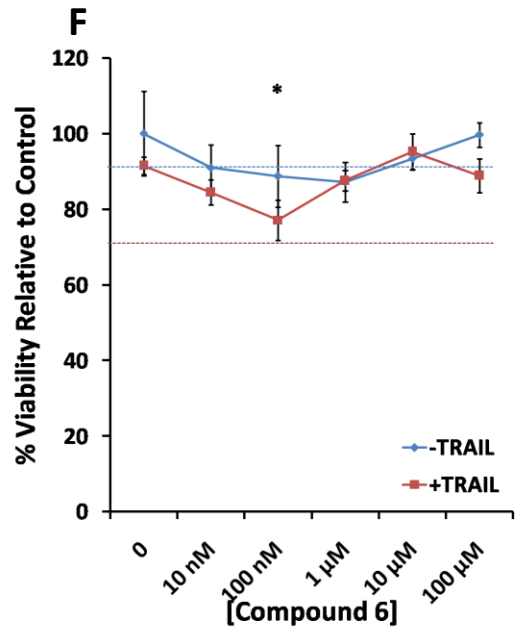
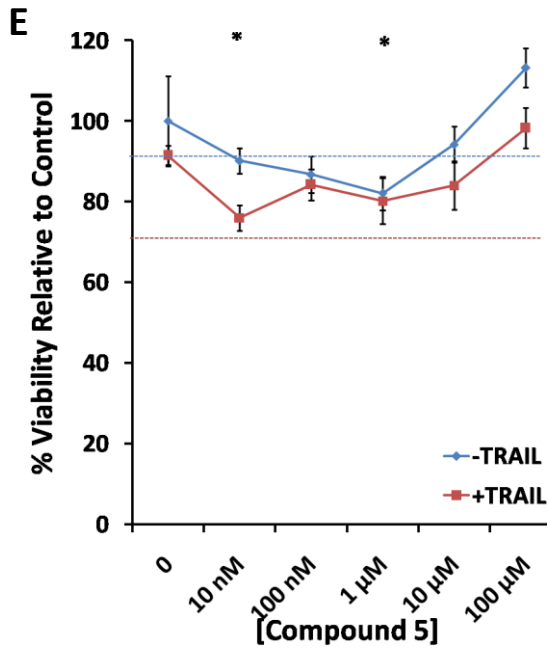
Eight of the 19 inhibitors selected demonstrated an ability to significantly sensitise MCF-7 cells to TRAIL (p -value <0.05) at more than 2 concentrations of compound, whilst causing no change in viability when administered alone, in at least two of these concentrations (Figure 4.2 A, C, L, N, O, P, R, S). The TRAIL-sensitisation of these compounds was at a similar level, approximately 20%, to that previously observed using siRNA c-FLIP (Piggott *et al.*, 2011). These compounds were therefore of most interest due to their efficacy at multiple concentrations, in combination with their lack of significant cytotoxicity, thus demonstrating a seemingly synergistic effect. Although

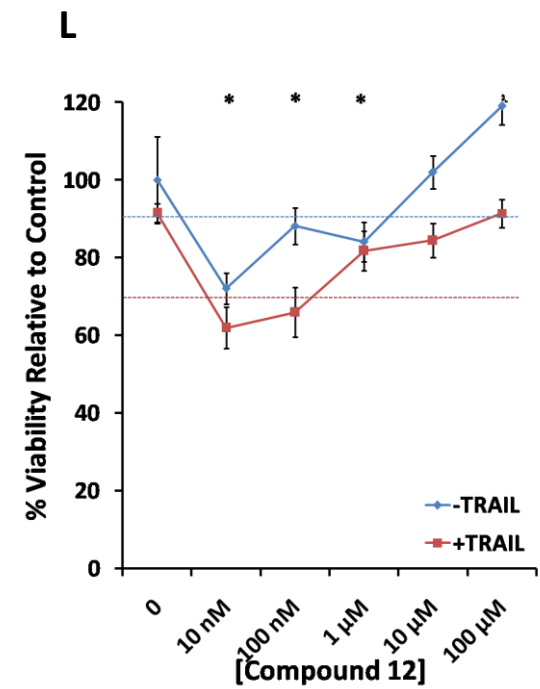
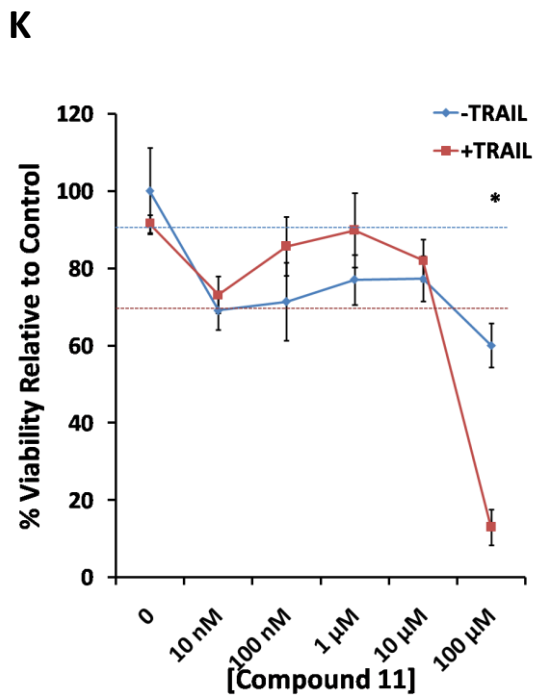
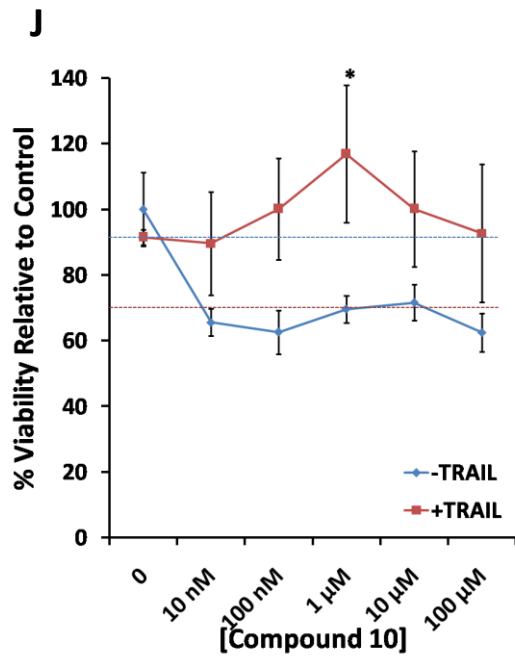
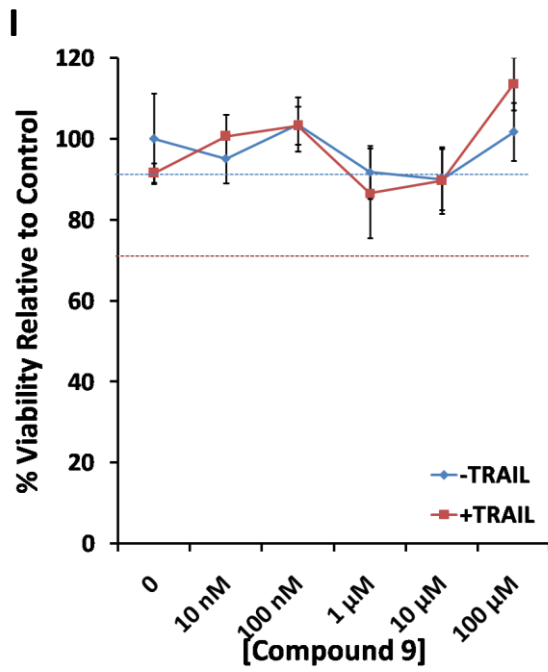
an additional compound increased TRAIL sensitivity at more than 2 concentrations, it also exhibited general cytotoxicity at several molarities (Figure 4.2Q)

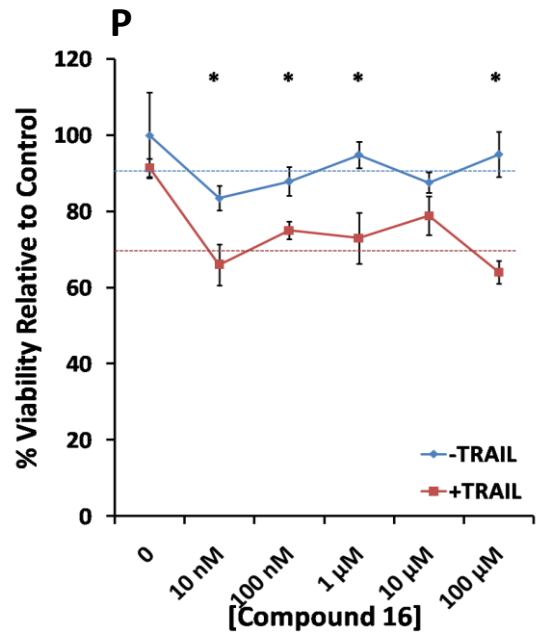
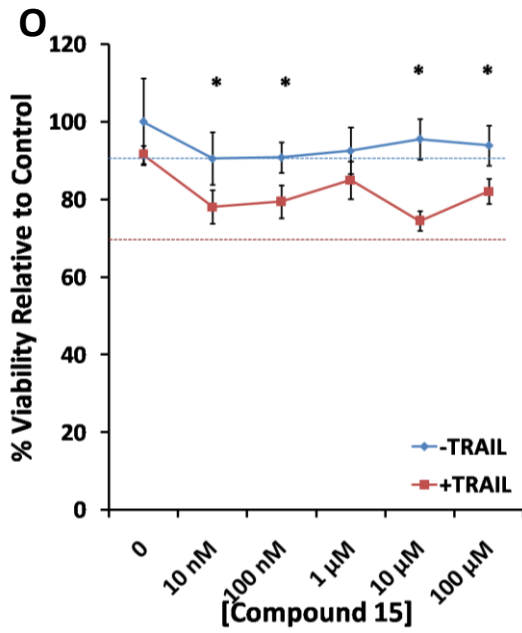
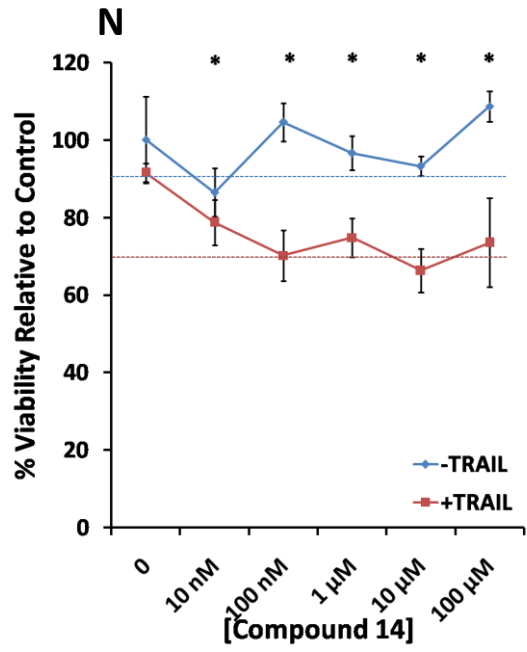
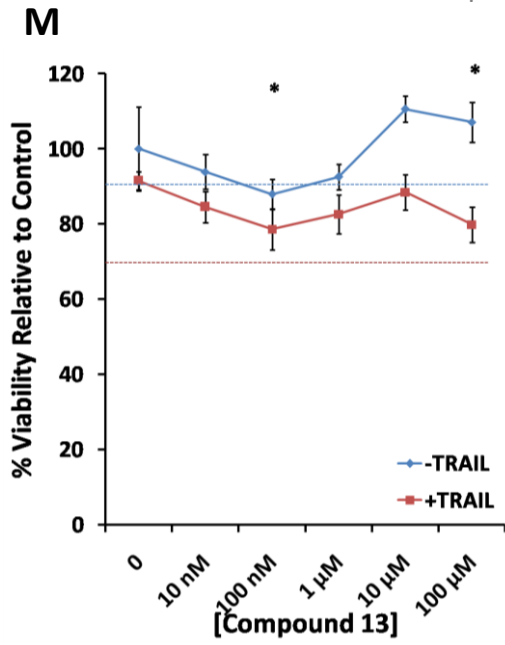
Four of the compounds were able to significantly sensitise to TRAIL at two of the five concentrations evaluated yet there was no correlation with dose of agent as they exhibited a low therapeutic index (Figure 4.2 B, E, M, G) and thus were of less interest. Four compounds evaluated showed no significant ability to sensitise to TRAIL in this cell line (Figure 4.2 D, F, H, I). Furthermore, two compounds, OH10 and OH11, exhibited the opposite effect to our hypothesis and in fact increased viability when treated in combination with TRAIL (Figure 4.2 J and K). Compounds OH10 and OH11 were therefore discounted for any further evaluation studies.

Three compounds increased cell number at several concentrations tested (Figure 4.2 I, J, L), whereas others (Figure 4.2 B, C, H, K) were cytotoxic at several concentrations, and caused reductions in viability to below 50%, thus, any TRAIL sensitisation obtained in these cases was additive, rather than synergistic. It is possible on the basis of molecular homology that one or more of these cytotoxic agents could represent specific inhibitors of caspase-8.









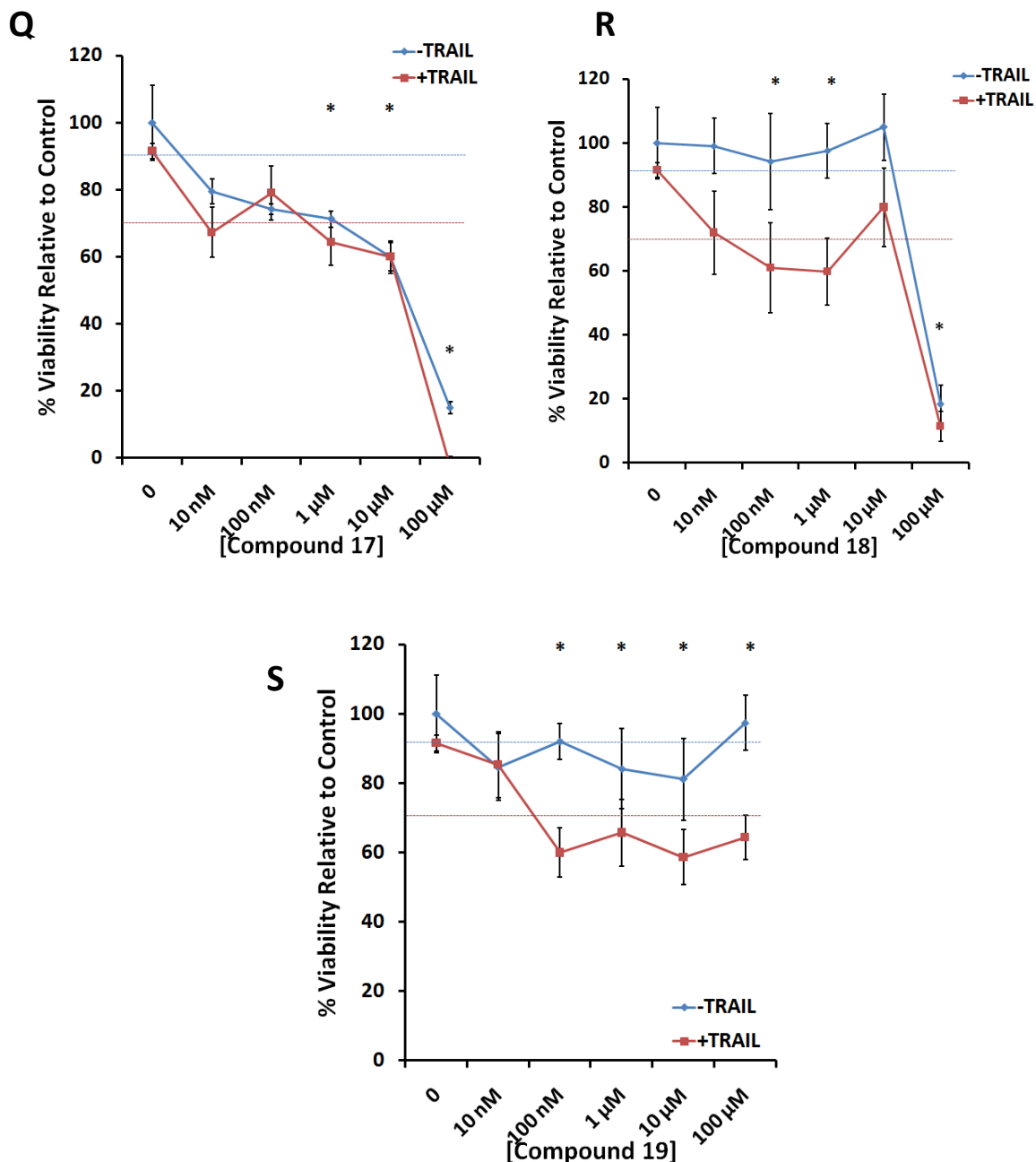


Figure 4.2: Initial viability dose response of OH1-OH19 inhibitor panel on the bulk population of TRAIL resistant MCF-7 cells.

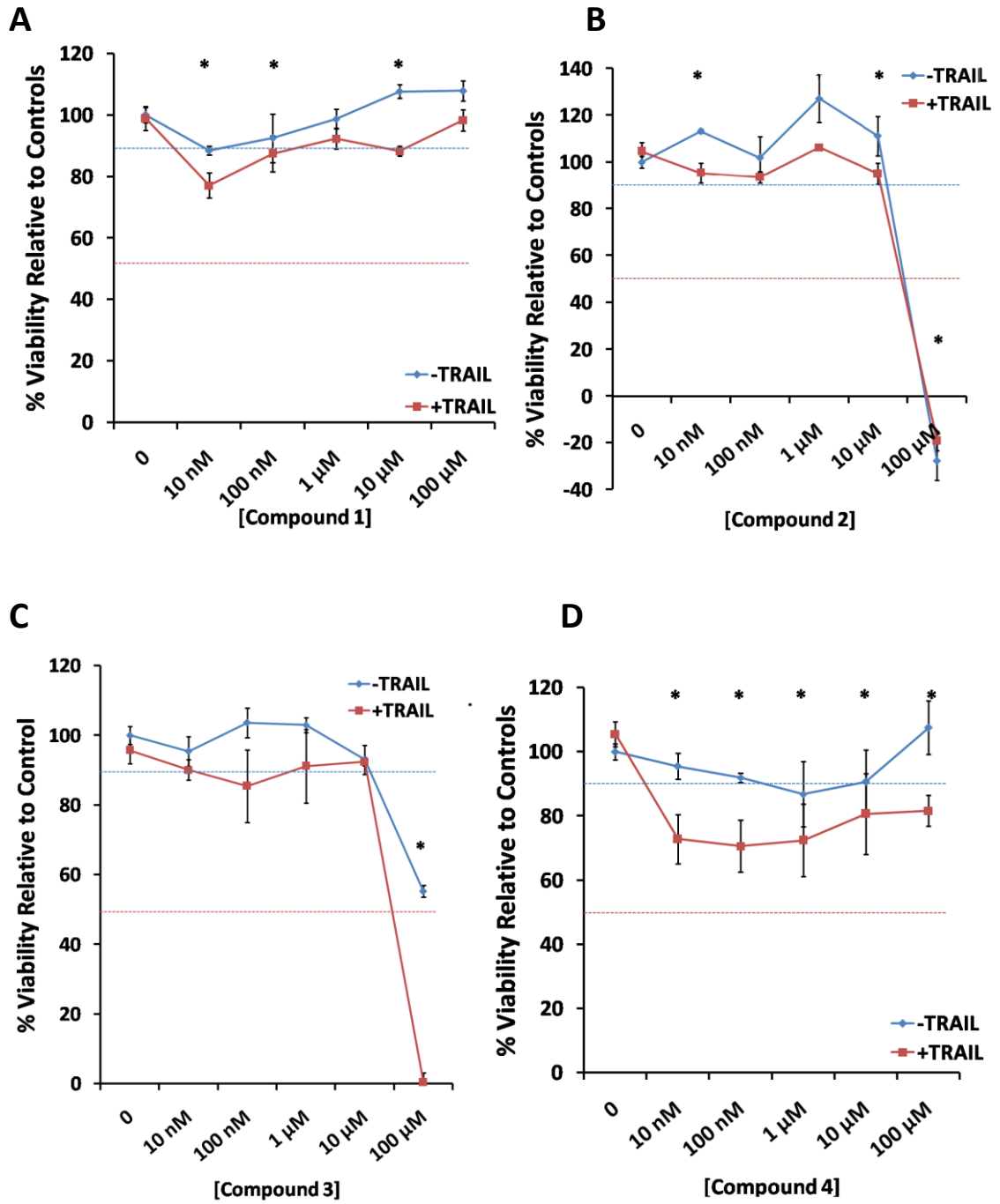
MCF-7 cells were treated in adherent conditions at 70% confluence with a dose range of inhibitor or vehicle control for one hour, before the addition of 20 ng/ml TRAIL (or vehicle control) for 18 hours. Cell Titre blue was then performed to assay for cell viability. Results represent 3 experiments with 4 wells per condition per experiment. Blue and red dashed lines (~90 and 70% respectively) represent the effect of c-FLIP knock out by siRNA and the combination of c-FLIP siRNA with TRAIL treatment respectively (Piggott *et al.*, 2011). *= p -value <0.05 , t-test TRAIL vs compound plus TRAIL. Control of media alone and compound within media were included.

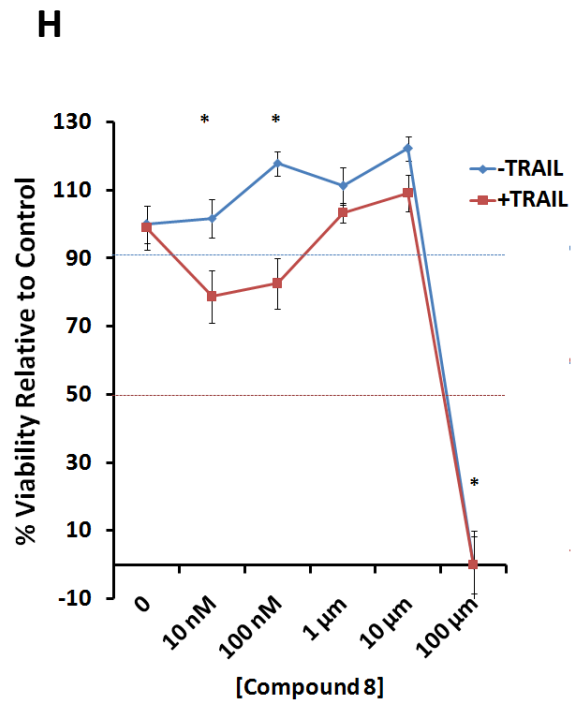
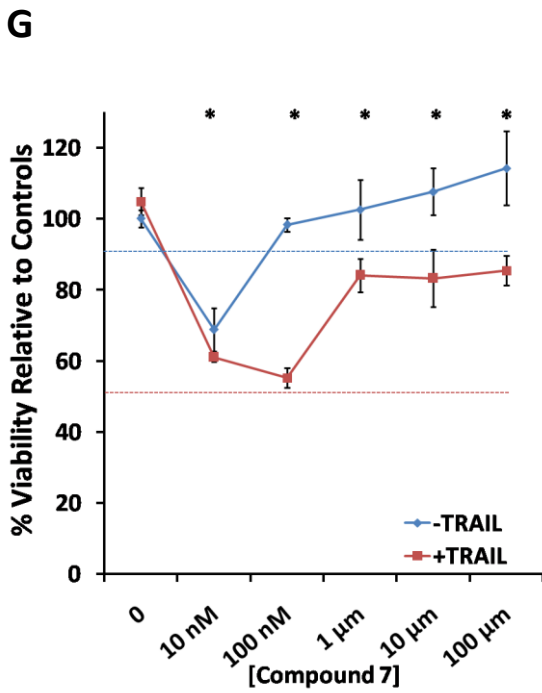
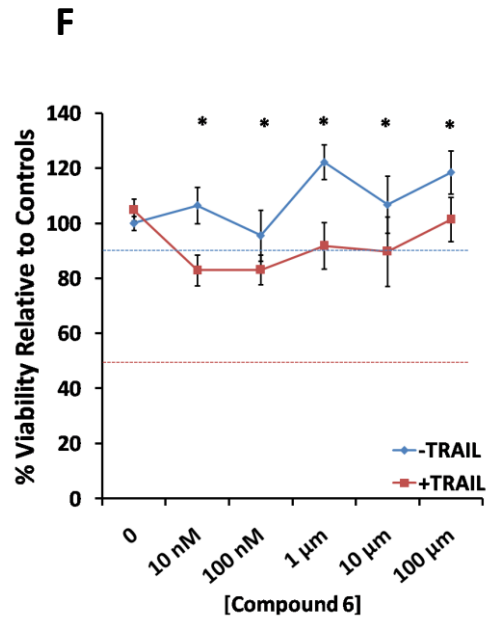
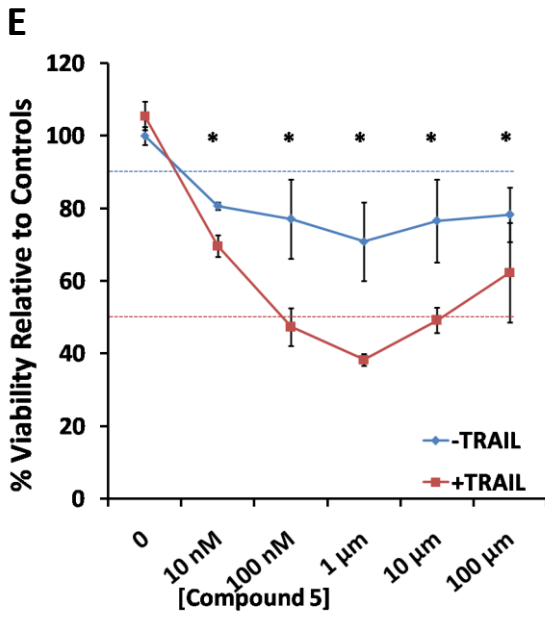
4.2.2.2 c-FLIP Inhibitors Sensitise TRAIL-resistant BT474 Bulk Cells to TRAIL

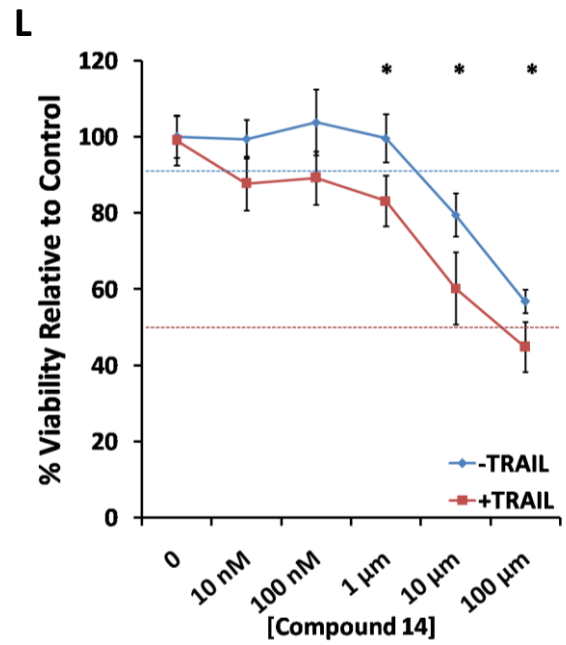
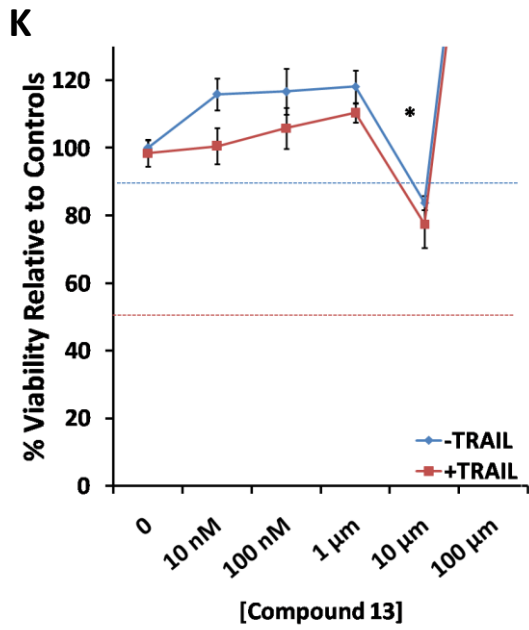
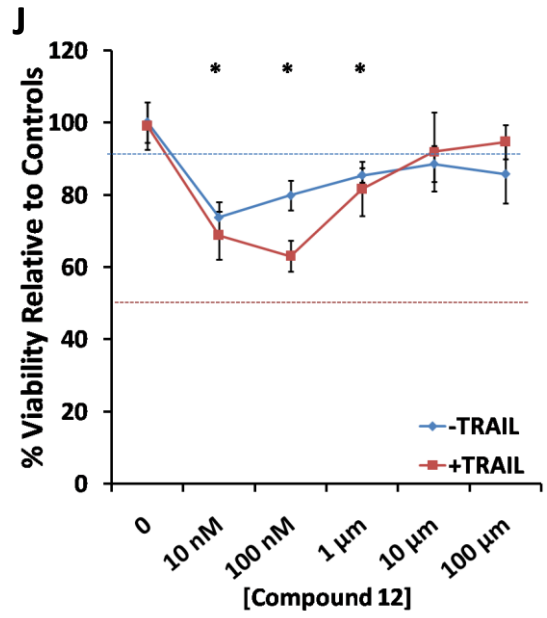
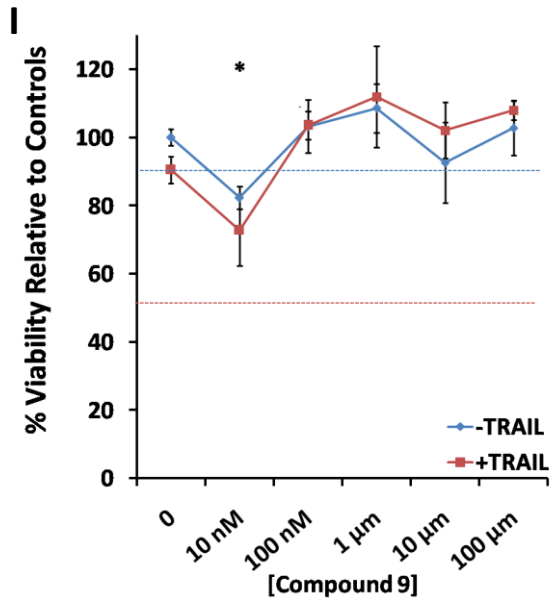
BT474 cells, which are a TRAIL-resistant HER2+ve, ER+ve, PR-ve cell line were treated with 14 of the 19 initial inhibitors. Compounds 10, 11, 15, 17 and 18 were not included for analysis on this cell line due to their lack of efficacy and large fluctuations in response, or alterations to cell viability when administered alone on MCF-7 cells (Figure 4.2), in addition to their lack of solubility in DMSO (Table 4.1).

As before, compounds (or vehicle control) were added to bulk cells at 70% confluence and left for one hour before the addition of 20 ng/ml TRAIL. After 18 hours, viability was measured using the Cell Titre Blue assay. The compounds performed in a similar manner on the bulk population of BT474 cells compared with the MCF-7 cell line (Figure 4.3), with some showing a synergistic ability to sensitise to TRAIL, and others demonstrating no effect. Overall, the effect of the combination therapy was reduced in BT474 cells compared to MCF-7 cells.

Six compounds significantly sensitised to TRAIL at more than two concentrations tested, with little or no effects on viability alone at at least two of these concentrations (Figure 4.3 A, B, D, F, M, L). One additional compound exhibited a modest ability to sensitise to TRAIL, with efficacy only demonstrated at two concentrations (Figure 4.3N). Two compounds showed significant ability to sensitise to TRAIL, yet also had alterations to cell viability when administered alone, thus likely demonstrating a potential lack of specificity and therefore, off-target effects (Figure 4.3 E, G). Three compounds were cytotoxic at 100 μ M (Figure 4.3 B, C, H), whilst one compound demonstrated no effects alone or in combination with TRAIL (Figure 4.3 I). Two compounds increased viability in combination with TRAIL at several concentrations tested and had little ability to increase TRAIL sensitivity (Figure 4.3 J, K).







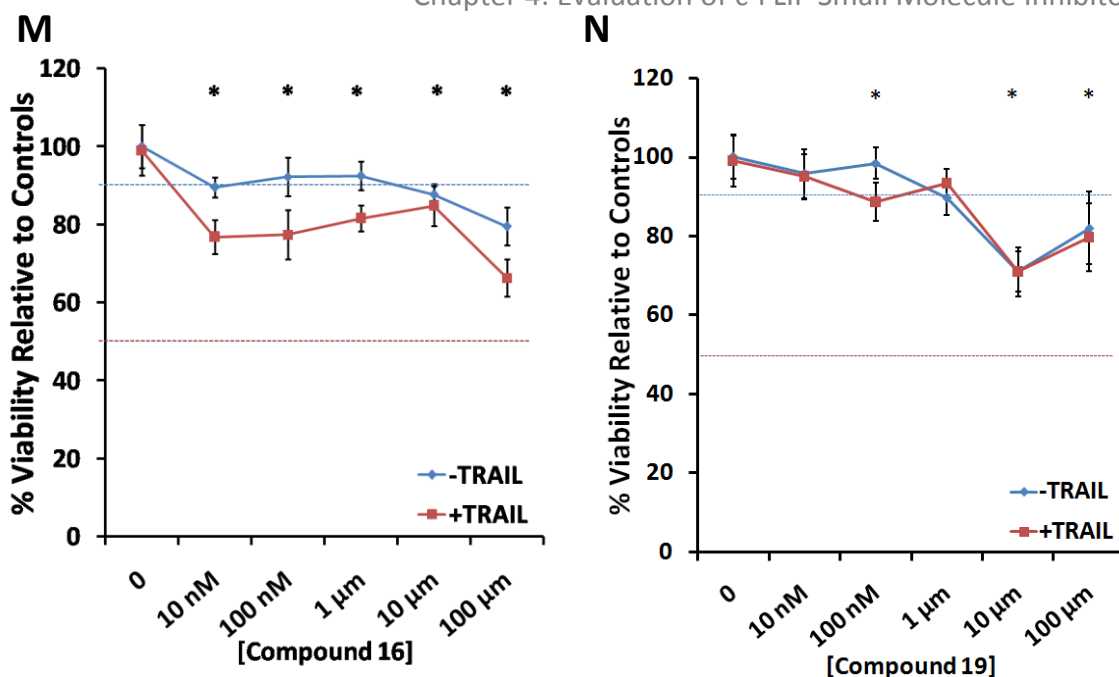


Figure 4.3: Initial dose response of 'OH' inhibitor compound panel on the bulk population of TRAIL resistant BT474 cells.

BT474 cells were treated in adherent conditions at 70% confluence with a dose range of inhibitor or vehicle control for one hour, before the addition of 20 ng/ml TRAIL (or vehicle control) for 18 hours. Cell Titre blue was then performed to assay for cell viability. Results represent 2 experiments with 4 wells per condition. Blue and red dashed lines (~90 and 50% respectively) represent the effect of c-FLIP knock out by siRNA and the combination of c-FLIP siRNA with TRAIL treatment respectively (Piggott *et al.*, 2011). *=p-value<0.05, t-test TRAIL vs compound plus TRAIL. Control of media alone and compound within media were included.

4.2.2.3 c-FLIP Inhibitor Bulk Cell Summary and Lead Compound Selection

To confirm the compounds which had the greatest ability to sensitise to TRAIL and thus select several potential lead compounds for analysis in additional assays, we organised the data by selecting the lowest concentration at which a significant TRAIL-sensitising effect was observed and plotted these on one graph. By this means of analysis, we can see more clearly that, in the MCF-7 bulk population, OH14 decreased viability by the greatest amount, at a low concentration (Figure 4.4A) and as such, in addition to the fact that there were no solubility issues and the effect appeared synergistic rather than additive, is the lead compound from this assay in MCF-7 cells. Although the effect of OH14 is reduced in BT474 cells, it still remained active at a low concentration (Figure 4.4B). These results, with the lack of observed toxicity and solubility issues deemed OH14 as our first lead compound to be analysed in further assays.

Compound OH19 also showed activity at a low concentration in MCF-7 cells, significantly sensitising to TRAIL in a seemingly synergistic manner by 30%. The activity of OH19 was diminished in BT474 cells by comparison, with only a modest sensitisation observed at 100 nM. However, since no solubility or toxicity issues were seen with this compound, and due to its effect in MCF-7 cells, which represent around 60% of clinical patients, we decided to include OH19 as a secondary lead compound for further analysis.

OH16 showed TRAIL-sensitisation efficacy in both the MCF-7 and BT474 cell lines which appeared partially synergistic, as a modest reduction in viability was seen with compound alone at some concentrations. Although OH16 performed best at 100 μ M in MCF-7 cells, its effect, although modest, was in fact best at the lowest concentration, of 10 nM in BT474 cells. The ability of the compound to sensitise to TRAIL at a range of concentrations in both cell lines, in addition to the lack of toxicity and solubility issues led OH16 to be selected as our third lead compound for the next assay.

Other compounds which appeared nearest to the top left of the summary efficacy plots, such as OH8 on BT474 cells and OH1 on MCF-7 cells, were discounted as lead compounds at this stage based on their large alterations to cell viability when administered alone, low efficacy over several concentrations (*i.e.* only affective at two or

less concentrations), or the solubility issues observed at several concentrations previously (Table 4.2).

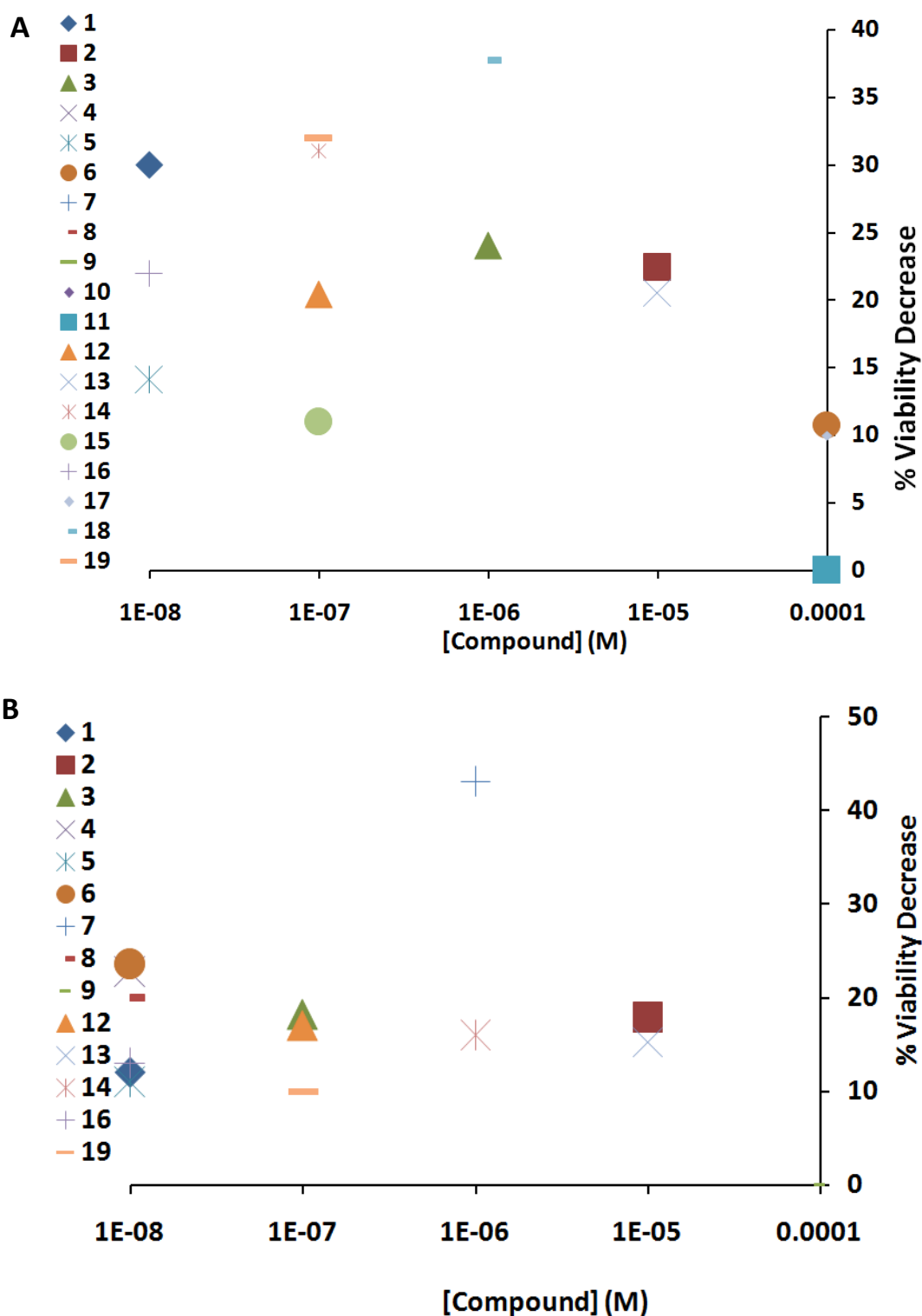


Figure 4.4: Summary of 'OH' compounds on the ability to sensitise MCF-7 and BT474 bulk cells to TRAIL.

The data from A) Figures 4.2 (MCF-7) and B) 4.3 (BT474) is re-presented to compare the lowest concentration at which a significant TRAIL-sensitisation was observed. The concentration of each c-FLIP inhibitor that gave a significant (p -value <0.05) decrease in cell viability, compared with TRAIL, is plotted as a percentage compared to experimental agent alone. On this graph, compounds that appear nearest to the top left of the plot exhibit greatest efficacy.

Table 4.2: Initial Lead Compound selection.

Soluble: ✕ = Insoluble at more than two concentrations in aqueous media or initial DMSO.

Viability: ✓ = no deviation below c-FLIP siRNA (blue line ~90%) or above 100%.

Efficacy: ✓ = significant TRAIL sensitisation at more than two concentrations, with at least one of these concentrations altering viability alone. NA indicates untested compound

Compound	Soluble	Viability MCF-7	Viability BT474	Efficacy MCF-7	Efficacy BT474
1	✕	✓	✓	✓	✓
2	✕	✕	✕	✕	✕
3	✕	✓	✕	✓	✕
4	✕	✓	✓	✕	✓
5	✓	✕	✕	✕	✕
6	✓	✓	✕	✕	✓
7	✓	✕	✕	✕	✓
8	✓	✕	✕	✕	✕
9	✓	✓	✓	✕	✕
10	✓	✕	NA	✕	NA
11	✕	✕	NA	✕	NA
12	✕	✕	✕	✕	✕
13	✓	✓	✕	✕	✕
14	✓	✓	✓	✓	✓
15	✕	✓	NA	✓	NA
16	✓	✓	✓	✓	✓
17	✓	✕	NA	✕	NA
18	✕	✓	NA	✓	NA
19	✓	✓	✓	✓	✓

4.2.3 Small Molecule Inhibitors of c-FLIP Increase Sensitivity of Breast CSCs to TRAIL

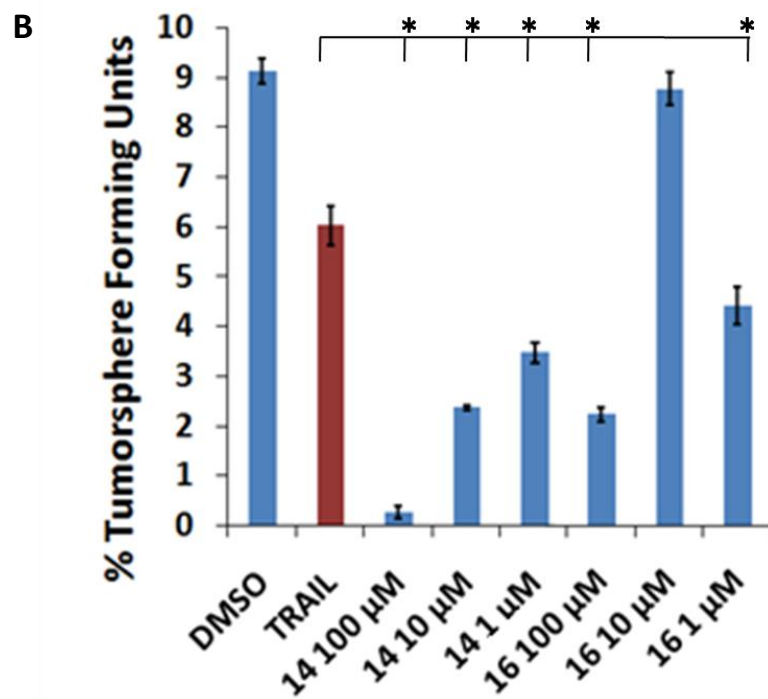
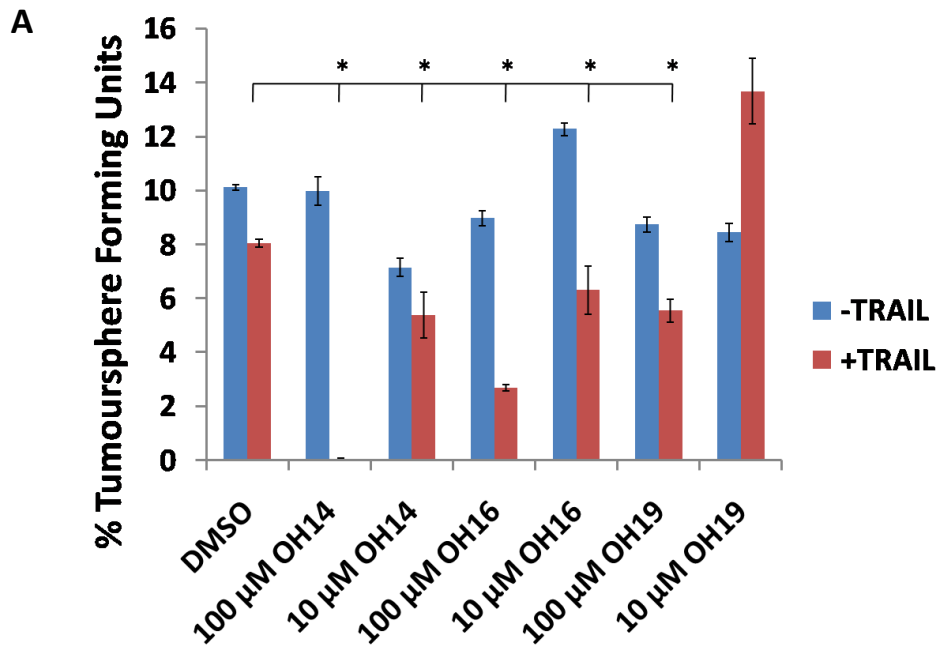
Our observations that some of the initial 19 inhibitors did indeed show an ability to at least partially sensitise the bulk cell population of two previously resistant cell lines to TRAIL, in effect, representing a phenocopy of the results obtained using siRNA c-FLIP, led to the desire to explore their effect on assays representing different aspects of breast cancer development and progression. The most profound *in vitro* effect of c-FLIP siRNA in combination with TRAIL treatment was observed when cells were analysed in the tumoursphere assay, which assesses properties of CSCs (Section 1.1.7.3). We observed that knocking down c-FLIP using siRNA, in adherent conditions, and treating with TRAIL prevented several breast cancer cell lines from being able to form tumourspheres (Piggott *et al.*, 2011). In the same study, it was shown that suppression of c-FLIP alone had little effect on tumoursphere size, formation, or number whilst TRAIL treatment alone exhibited a modest effect on the morphology and number of spheres in MDA-MB-231 and MCF-7. We therefore hypothesised that a similar effect on tumoursphere size and number would be obtained using small molecule inhibitors of c-FLIP in combination with TRAIL. Due to the complexity of the assay, only the three lead compounds, OH14, OH16 and OH19, selected previously based on MCF-7 and BT474 cell viability assays (Section 4.2.2.3), were chosen to be assessed. MCF-7 cells were pre-treated in adherent conditions, with one of the three lead inhibitors (or appropriate DMSO control), for one hour, after which TRAIL was added at 20 ng/ml and left for 18h, as previously described (Piggott *et al.*, 2011). After 18 h, the remaining viable cells were subjected to the tumoursphere assay.

Two of the three lead compounds, OH14 and OH16, resulted in an increase in the sensitivity of MCF-7 tumoursphere forming cells to TRAIL (Figure 4.5A). One of these, OH14, had no significant effect on tumoursphere formation when administered alone, but had a profound effect in increasing TRAIL sensitivity when administered in combination, within 90% of the level of c-FLIP siRNA when administered at 100 μ M (Figure 4.5A). Compound OH16 in combination with TRAIL demonstrated a significant decrease in tumoursphere number, compared with TRAIL alone, at both concentrations tested. An overall increase in tumoursphere number was observed with OH16 alone, however, at 10 μ M. Similarly, OH19 demonstrated a significant increase in

tumourspheres at 10 μM , although this was only observed when administered to the cells in combination with TRAIL. Only when cells were treated at 100 μM , did OH19 demonstrate a significant ability to increase tumoursphere sensitivity to TRAIL.

When treating cells with a larger dose-range of OH14 or OH16 in combination with TRAIL, before plating into tumoursphere conditions, we observed OH14 to retain a significant ability to sensitise to TRAIL at all 3 concentrations tested. OH16, however, gave inconsistent results at the 3 molarities tested. At 100 and 1 μM , a significant TRAIL-sensitisation was observed, however, at 10 μM , no significant sensitisation was observed.

OH14 had no significant impact on tumoursphere morphology or number when administered alone, when compared with untreated or TRAIL treated cells (Figure 4.5C, D and E), only when treated in combination with TRAIL was there a significant impact of OH14 on tumourspheres (Figure 4.5F).



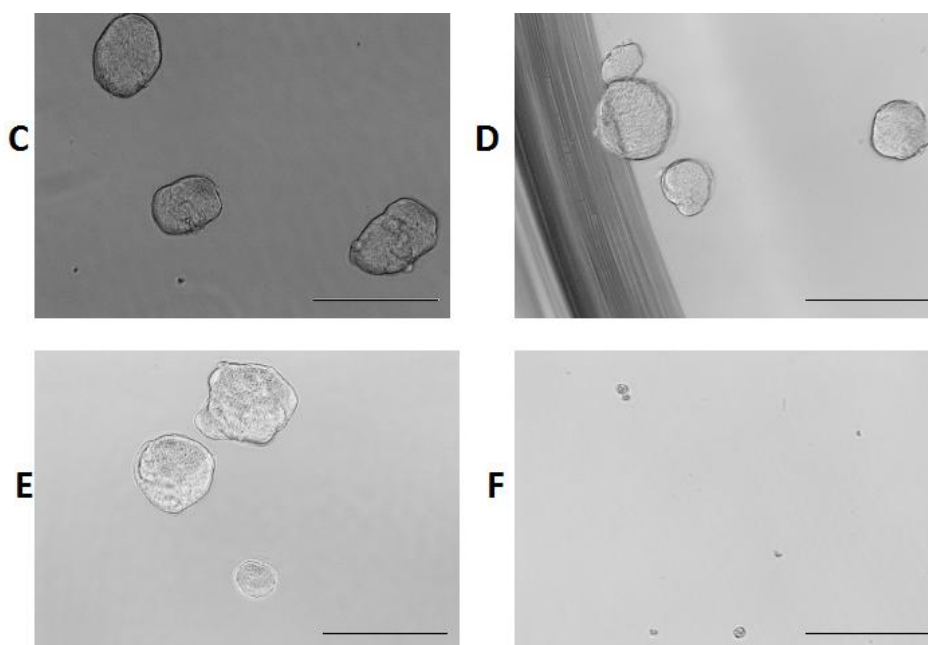


Figure 4.5: 3 Three Initial Inhibitors Demonstrate some Efficacy in Increasing Sensitivity of MCF-7 Tumoursphere Forming Cells to TRAIL.

MCF-7 cells were cultured for 24 h in a 96 well plate, before being treated with vehicle control or compound for 1 h. 20 ng/ml TRAIL (or control) was added after 1 h and the cells were left for 18 h. The following day, cells were subjected to the tumoursphere assay, with no additional drug added. A) One of 3 lead inhibitors (14, 16 and 19) at two concentrations alone and in combination with TRAIL. B) OH14 or OH16 at a range of concentrations in combination with 20 ng/ml TRAIL (no compound alone). Results represent passage 1 of 3 replicates, with error bars displaying standard error of the mean. * = $p < 0.05$, t-test. Representative images of tumourspheres from C) Vehicle control D) 100 μ M OH14 E) 20 ng/ml TRAIL and F) 100 μ M OH14 plus 20 ng/ml TRAIL. Scale bar = 100 μ m.

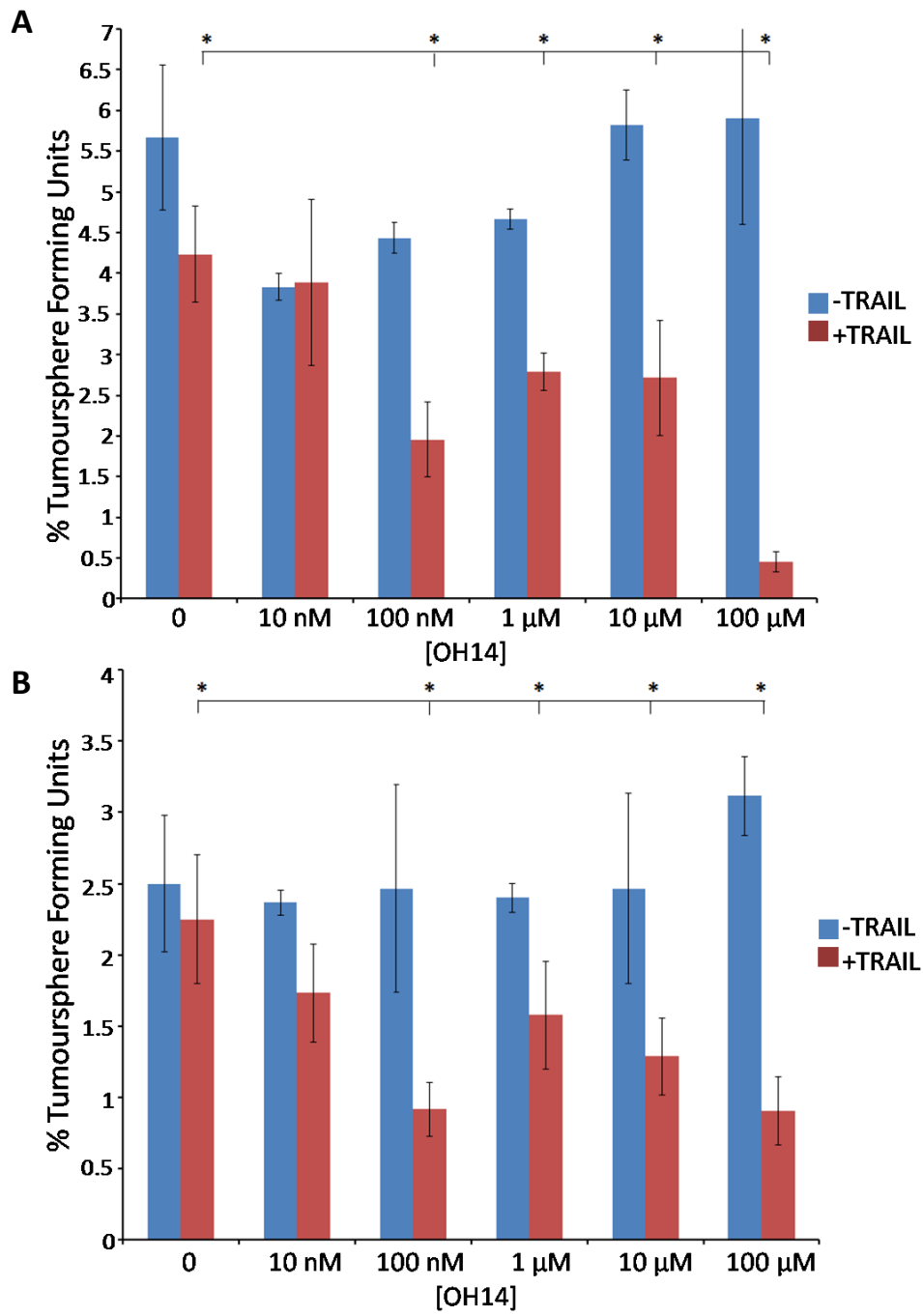
4.2.3.1 OH14 Sensitises Tumoursphere-Forming Cells to TRAIL in a Dose-Dependent Manner

The tumoursphere assay, in combination with the cell titre blue assay demonstrated that, of the three lead compounds, compound OH14 demonstrated the most significant and consistent ability to sensitise MCF-7 bulk cells and tumoursphere forming cells to TRAIL whilst having little effect when administered alone.

In order to fully establish the effect of this compound on increasing TRAIL sensitivity, a dose range was tested on the tumoursphere forming population of MCF-7 cells. Breast cancer cell lines contain a sub-population of around 3% of tumoursphere forming cells (Dontu *et al.*, 2003). The overall levels of spheres generated by the MCF-7 cells used in the previous experiments (Section 4.2.3), around 6% were slightly above the average obtained in many of our other investigations. Cell lines can vary between batches and laboratories, and repeating the experiment here with OH14, using a different batch of cells confirmed the initial result with OH14, but demonstrated a control tumoursphere potential more consistent with the norm.

OH14 significantly sensitised tumoursphere forming cells to TRAIL at a dose range of 100 μ M to 100 nM (Figure 4.6A) which was particularly evident following passage of the primary tumourspheres (Figure 4.6B). Confirming the initial OH14 test (Figure 4.5), tumoursphere forming cells were almost entirely eliminated by treatment with 100 μ M OH14 in combination 20 ng/ml (Figure 4.6C). In order to establish whether pre-treatment of adherent cells in bulk conditions was required for sensitising tumoursphere forming cells to TRAIL, we performed a treatment with OH14 after plating into anoikis conditions. Under these conditions, OH14 exhibited a similar dose-dependent ability to sensitise to TRAIL (Figure 4.6D).

Although the effects of the combination therapy on BT474 bulk cell viability were less significant than those observed in MCF-7 cells (Section 4.2.2.3), we have previously demonstrated siRNA mediated knockdown of c-FLIP acutely sensitised BT474 tumourspheres to TRAIL (Piggott *et al.*, 2011). Thus, the lead compound was assessed for its ability to affect tumoursphere formation in this cell line (Figure 4.7). OH14 significantly sensitised to TRAIL at a dose range of 100 μ M to 1 μ M in a dose-dependent manner in both primary tumourspheres (Figure 4.7A) and after passaging, without the addition of fresh compound (Figure 4.6B).



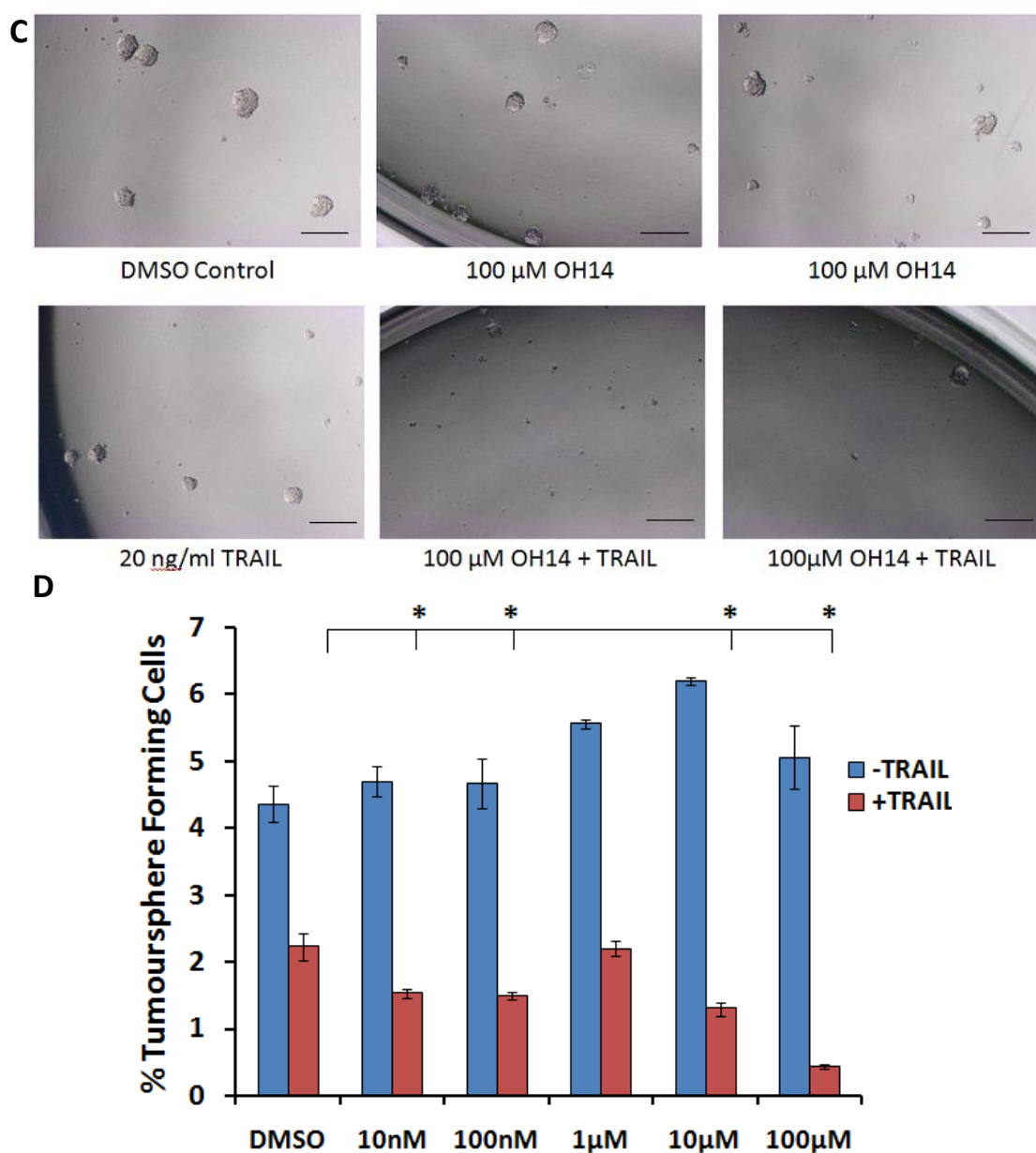


Figure 4.6: Compound OH14 significantly sensitises MCF-7 tumoursphere forming cells to TRAIL in a dose dependent manner.

MCF-7 cells were cultured for 24 hours before being treated with a dose range of compound OH14 (or vehicle control) for 1 hour, followed by TRAIL (or vehicle control) treatment at 20 ng/ml and 18 h incubation. Cells were then subjected to the tumoursphere assay, with no additional drug added. A) Passage 1: MCF-7 dose dependent decrease in the ability of cells to form tumourspheres when treated with OH14 in combination with TRAIL. B) Passage 2: MCF-7 dose dependent decrease in the ability of cells to form tumourspheres when treated with OH14 in combination with TRAIL. C) Representative images of MCF-7 tumourspheres under different treatment conditions. Scale bars = 100 μ m. D) Passage 2 of MCF-7 tumourspheres treated after plating Passage 1 (in anoikis conditions) with vehicle control (DMSO) or a dose range of OH14 alone or in combination with 20 ng/ml TRAIL. Error bars represent 3 internal replicates. *=p-value<0.05, t-test - TRAIL vs OH14 plus TRAIL.

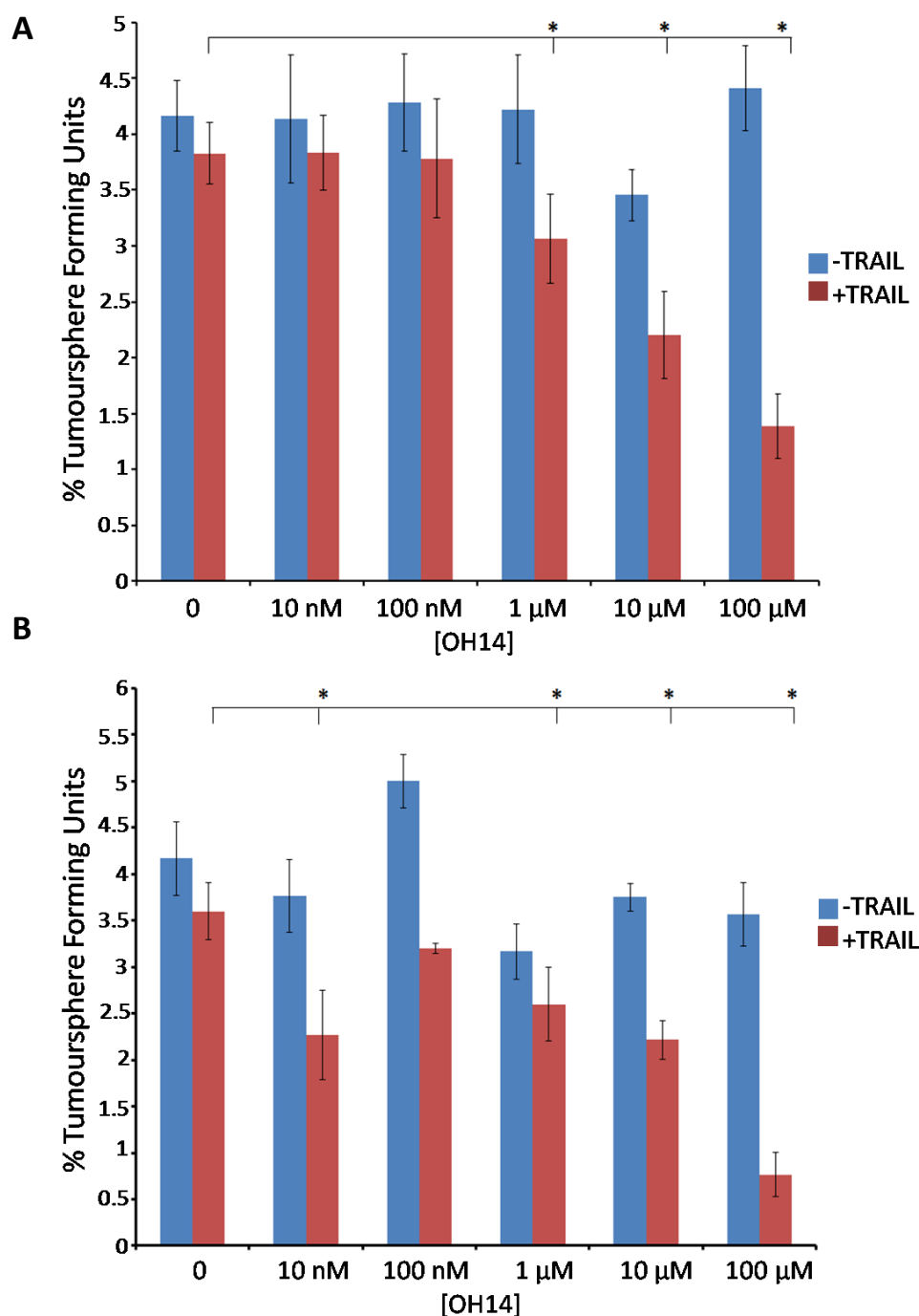


Figure 4.7: Compound OH14 sensitises BT474 tumoursphere forming cells to TRAIL in a dose dependent manner.

BT474 cells were cultured in adherent conditions for 24 hours before being treated with a dose range of OH14 (or vehicle control) for 1 hour, followed by TRAIL (or vehicle control) treatment at 20 ng/ml and 18 h incubation. Cells were then subjected to the tumoursphere assay, with no additional drug added. A) Tumoursphere Assay Passage One: Treatment with 20 ng/ml TRAIL in combination with OH14 reduced significantly the number of primary tumourspheres formed in BT474 cells in a dose dependent manner (*=p-value < 0.05, t-test TRAIL vs OH14 + TRAIL) B) Tumoursphere Assay Passage 2: Treatment of primary spheres with 20 ng/ml TRAIL in combination with OH14 significantly reduced the number of secondary tumourspheres formed in BT474 cells in a dose dependent manner (*=p-value < 0.05, t-test TRAIL vs OH14 plus TRAIL).

4.2.4 TRAIL Sensitivity in Clonogenic Colony Forming Assay

The clonogenic assay, an assay established for over 50 years, is an additional *in vitro* assay which tests one of the functional characteristics of stem cells, that is, the ability to propagate colonies from single cells through an enhanced proliferative potential. The assay is not as selective for CSCs as the tumoursphere assay, as demonstrated by the fact that between 10% and 70% of any given cell line population are able to form colonies, however, the assay is an informative accompaniment to the tumoursphere assay, which itself is partially restricted in that it only selects for stem-like cells which exhibit the property of anoikis resistance, a property which is not an absolute requirement for all breast CSCs (Liu *et al.*, 2013). Essentially, the assay evaluates the ability of single cells plated at low density to form colonies of greater than 32 cells (Grenman *et al.*, 1989), thus having undergone five or more divisions, over a period of 10 days in adherent culture conditions (Harrison *et al.*, 2013; Locke *et al.*, 2005) (Section 1.1.7.3). The assay is often thought of as a progenitor or proliferation assay rather than a stem cell assay *per se* as it enables evaluation of the variabilities in replicative viability between cells treated in different conditions.

The overall TRAIL sensitivity of four relevant breast cancer cell lines, which represent different subtypes of the disease, was analysed using the CFA. Cells were plated at a low density of 50 cells per square centimetre, allowed to attach, before being treated with TRAIL at 20 ng/ml. Colonies were left to form for 10 days, after which, colonies of over 32 cells were counted. TRAIL was able to significantly reduce colony formation in the four breast cancer cell lines tested (Figure 4.8A and B), although it did not completely prevent the formation of colonies in any of these lines.

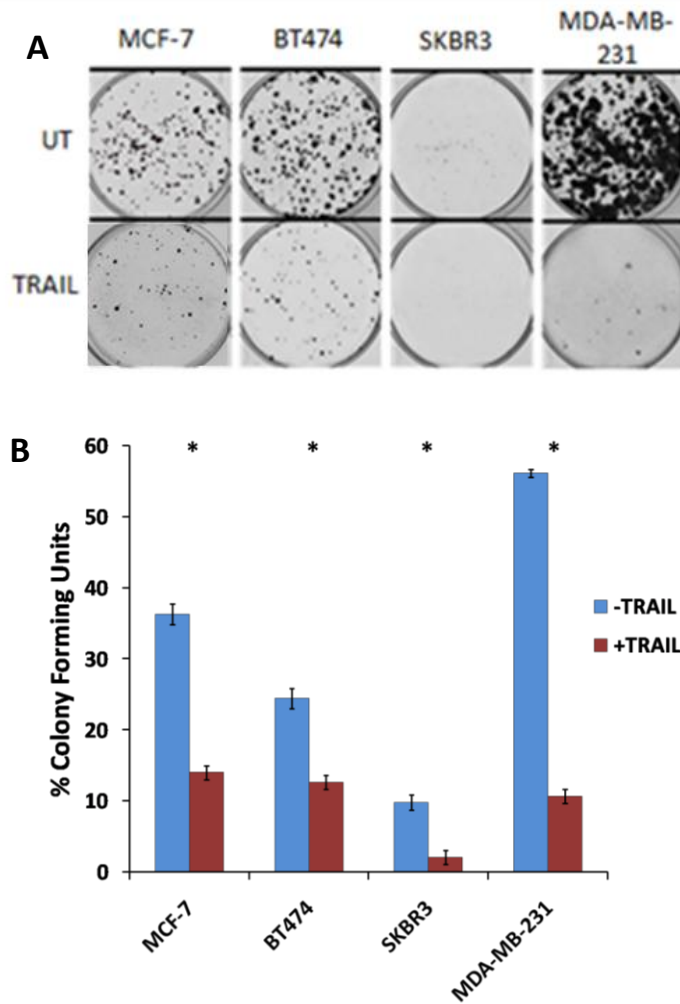


Figure 4.8: Colony Forming Cells are Sensitive to TRAIL

Cells were seeded at 50 cells/ cm² and treated with TRAIL at 20 ng/ml before being left for 10 days to grow. A) Representative images of colonies from 4 breast cancer cell lines. B) % Colony forming units in 4 cell lines. * = p<0.05, t-test between control and 20 ng/ml TRAIL treated colonies. Error bars represent standard error of the mean.

4.2.4.1 Compound OH14 Increases TRAIL Sensitivity of Colony Forming Cells

Although we have demonstrated, in section 4.2.3.1, that our main TRAIL-resistant cell line models are significantly TRAIL sensitive in the clonogenic assay, there was still a remaining population of cells, thus, we wished to establish whether we could further sensitise these cells to the effects of TRAIL.

To assay the ability of OH14 to target colony forming cells, we cultured MCF-7 and BT474 at low density as in Section 4.2.4 and treated as before, with the addition of OH14 1 hour before treatment with TRAIL. Our lead compound did indeed show an ability to significantly increase sensitivity to TRAIL and thus reduce ability of colony forming units to form in both MCF-7 and BT474 cell lines, to a similar level as that observed using the tumoursphere assay (Figure 4.9). TRAIL significantly reduced colony formation in both MCF-7 (A) and BT474 (C) cell lines ($p < 0.05$), however, TRAIL sensitivity was significantly increased ($p < 0.05$) by pre-treatment with OH14 at 100 μM , whilst the compound alone was found to be non-toxic.

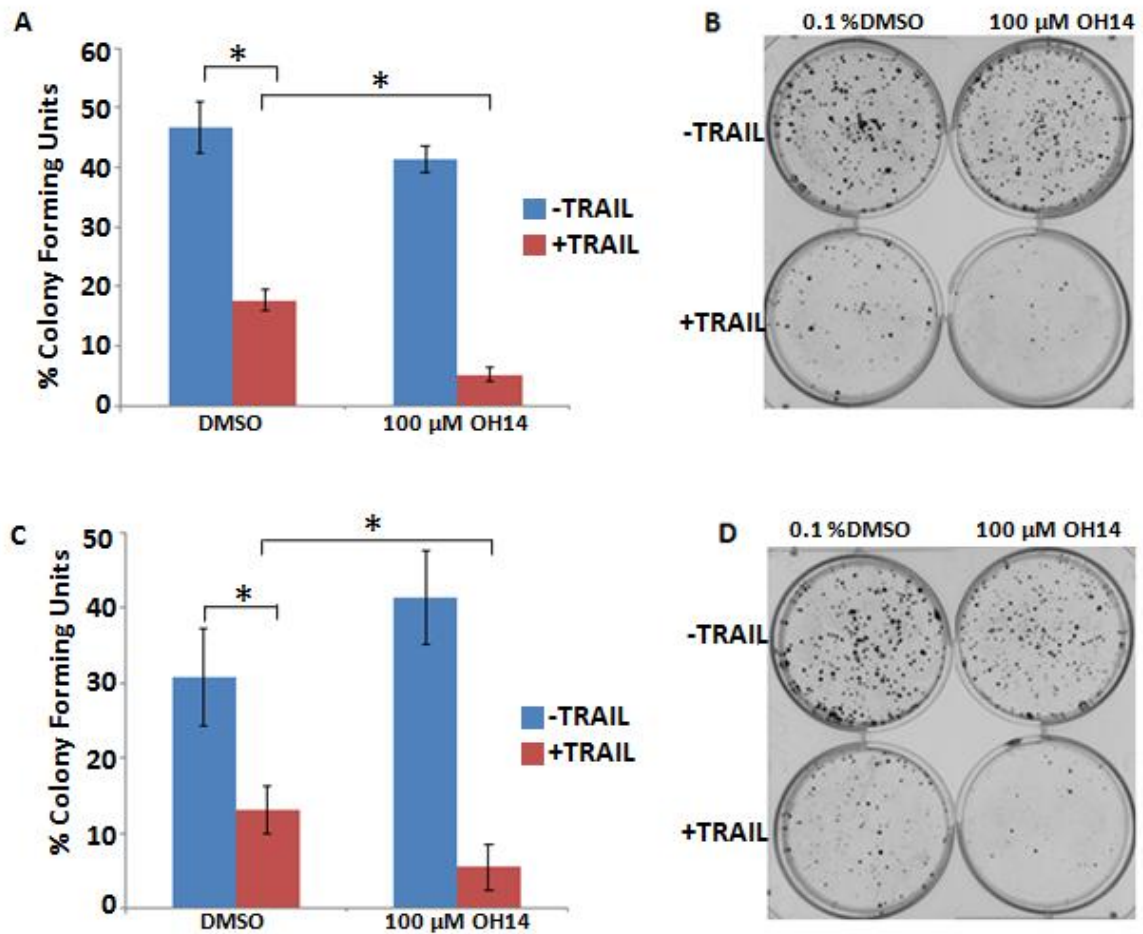


Figure 4.9: Colony forming cells are TRAIL sensitive and can be further sensitised by treatment with OH14.

A-B) MCF-7 and C-D) BT474 cell were plated at a low density of 50 cells per cm^2 for the CFA assay. After cells had attached, 100 μ M OH14 (or 0.1% DMSO vehicle control) was added for 1 h before the addition of 20 ng/ml TRAIL. Results represent at least 3 independent experiments, with errors calculated as standard error of the mean. $*$ =p-value<0.05, t-test.

4.2.5 Compounds Appear Less effective in Triple Negative and HER2+ve Breast Cancer Cell Lines

Our initial assays were performed on the two luminal-like, TRAIL-resistant, ER+ve cell lines, MCF-7 and BT474. Previous studies have demonstrated that breast cancer cells of a mesenchymal-like phenotype, such as MDA-MB-231 cells, are TRAIL-sensitive (Rahman *et al.*, 2009). Indeed, our lab have previously demonstrated the triple negative cell line, MDA-MB-231 to be around 60% sensitive to TRAIL when assayed for cell viability in the bulk population (Piggott *et al.*, 2011), while MDA-MB-231 tumoursphere populations were similarly sensitive (French *et al.*, 2015 in press). We wished to evaluate whether these already TRAIL-sensitive bulk- and tumoursphere- forming cells could be further sensitised by treatment with OH14.

Although we have previously observed that MDA-MB-231 tumoursphere forming cells are partially TRAIL sensitive, to around 60% (French *et al.*, 2015 in press), here, only in passage 2 was a modest TRAIL sensitivity evident (Figure 4.10B). Passage 1 shows contradictory results to our previous observations, with OH14 in fact increasing tumoursphere number when combined with TRAIL (Figure 4.10A). Upon passaging, however, which ultimately tests the key feature of CSCs; self-renewal, we did observe a modest TRAIL-sensitivity of MDA-MB-231 tumoursphere-forming cells, and observed that OH14 exhibited a modest yet significant ($p < 0.05$) ability to further sensitise to TRAIL at 100 μM (Figure 4.10B).

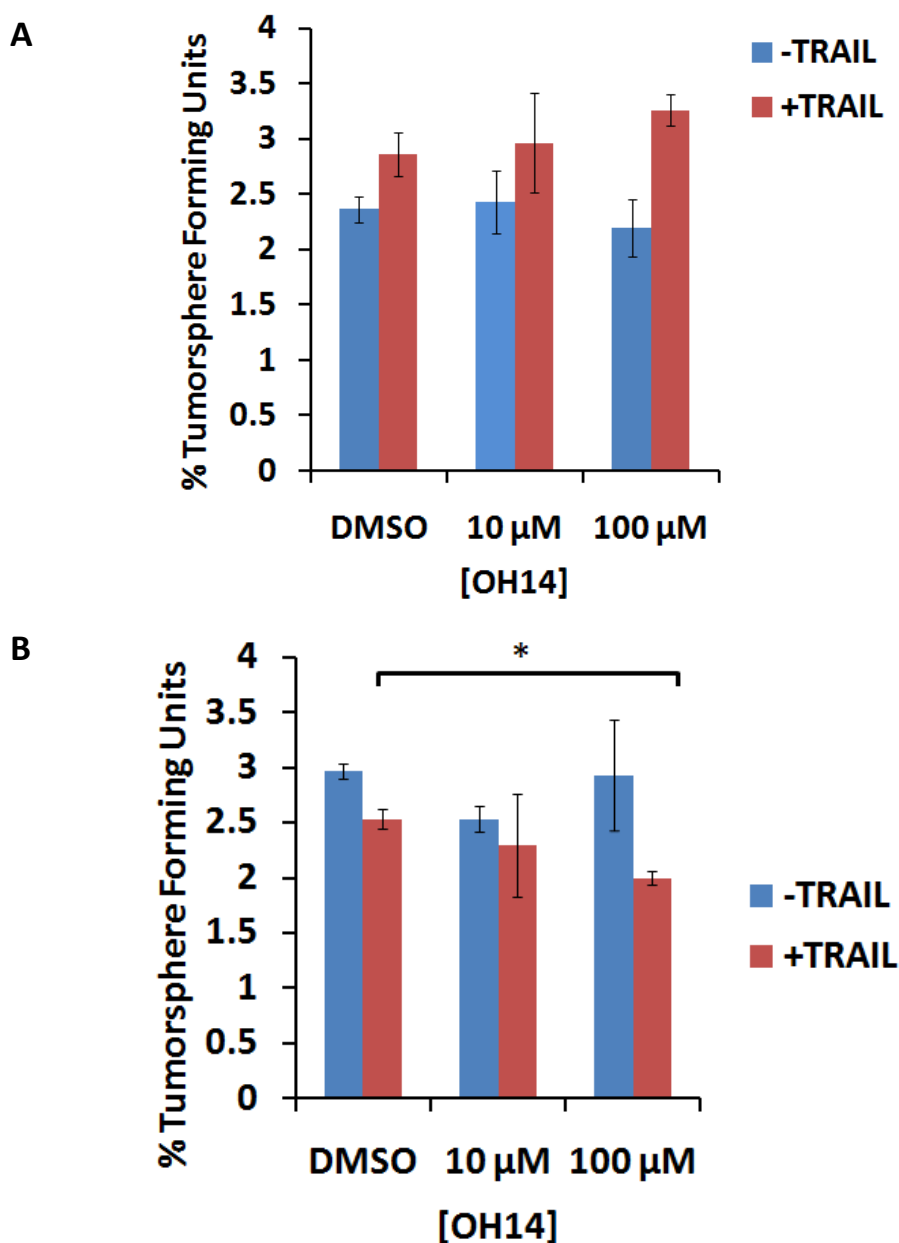


Figure 4.10: OH14 has a modest ability to sensitise MDA-MB-231 Tumoursphere Forming Cells to TRAIL only after Passaging

MDA-MB-231 Cells were treated in adherent conditions with vehicle control, OH14 at two concentrations and cells were left or treated with 20 ng/ml TRAIL after 1 h. 18 h later, cells were transferred to tumoursphere forming conditions. A) Passage 1: Treatment with 20 ng/ml TRAIL in this case did not significantly reduce primary tumoursphere forming ability alone or combined with OH14. B) Passage 2: After passaging, a significant effect of TRAIL alone, and in combination with 100 μ M OH14 could be observed (*= p <0.05, t-test). Results represent three technical replicates with errors calculated as standard error of the mean.

The HER2 positive, SKBR3 cell line has been previously observed to be TRAIL resistant in both bulk cell and tumoursphere forming conditions (Piggott *et al.*, 2011). Given that these cells are TRAIL resistant, we wished to evaluate whether OH14 could sensitise the tumoursphere forming and bulk cells to TRAIL.

Cells were treated in adherent conditions before being plated into the tumoursphere assay. Passage 1 (Figure 4.11A) and 2 (Figure 4.11B) data demonstrated that indeed SKBR3 tumoursphere forming cells do not respond to TRAIL. Initially, it appeared that OH14, at all concentrations tested, slightly increased the formation of primary tumourspheres (Figure 4.11 A), however, upon passaging and thus, when evaluating self-renewal, this was not the case. Passage 2 tumoursphere forming cells had a modest response to OH14, with OH14 sensitising to TRAIL at the two highest concentrations, 100 μ M and 10 μ M, although this was only significant ($p < 0.05$) at 10 μ M, where OH14 alone reduced sphere number, thus deeming the effect likely to be additive rather than synergistic. At lower concentrations, the combination of OH14 and TRAIL resulted in a slight increase in spheres, as previously observed in passage 1, although this effect was not observed at 100 nM, where sphere number was reduced (although not significantly) in the combination-treated tumourspheres.

An additive TRAIL sensitising effect was observed when OH14 was evaluated using Cell Titre blue to measure cell viability of SKBR3 cells (Figure 4.11C).

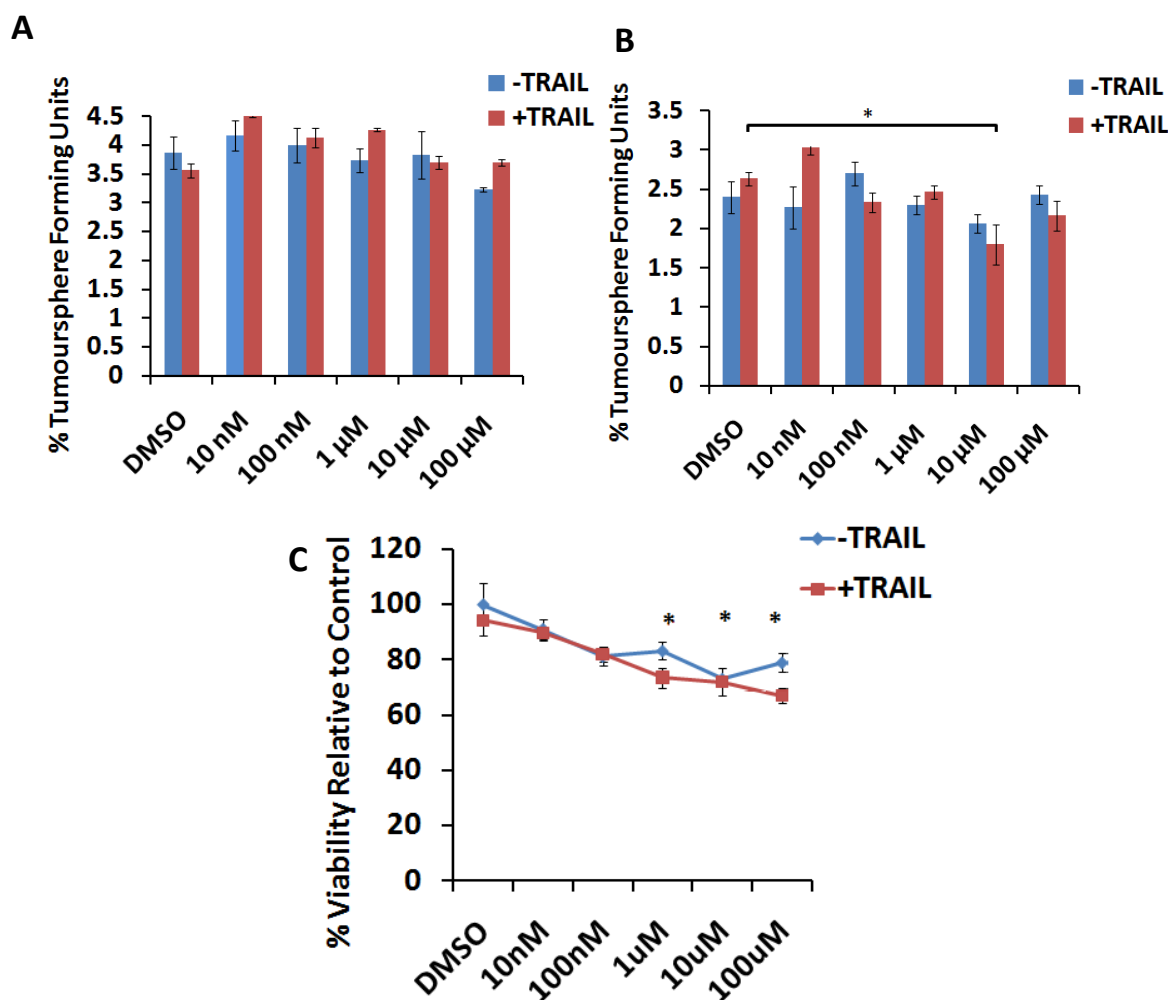


Figure 4.11: OH14 does not Sensitise SKBR3 Bulk or Tumoursphere Forming Cells to TRAIL

SKBR3 cells were treated with OH14 at several concentrations, with or without TRAIL at 20ng/ml and left for 18 h before being transferred to tumoursphere condition (A & B) or assayed for cell viability (C). Tumourspheres were counted after 7 days (A) or passaged and cultured for a further 7 days (B) to determine self-renewal capacity. Viability of the initial treated adherent cell population was measured using Cell Titre blue viability assay (C). Data represent three technical replicates, with error presented as the standard error of the mean. $*=p<0.05$, t-test TRAIL vs OH14 plus TRAIL.

4.2.6 Repeated Treatment with OH14 Slows Proliferation but does not Significantly Reduce Viability

The data above lead us to conclude that OH14 was the most efficacious c-FLIP inhibitor, which exhibited the least non-specific toxicity. It was therefore considered our primary pre-clinical lead compound.

In order to determine the long-term effects of OH14 on cell viability, we set up a 7 day daily treatment experiment with OH14 at 100 μ M, with two different cell confluences of MCF-7 cells, in order to ensure full cell confluence was not reached at too early a stage in the experiment. After 3 days of treatment, no significant difference was observed between OH14 and vehicle control (DMSO) treated cells at either cell density, this suggested that the cells proliferated at the same rate (Figure 4.12A, Day 1). By day 4, however, the proliferation rate of cells treated with OH14 appeared lower than those treated with control at both cell densities (Figure 4.12A, Day 4). At 7 days, a significant visual difference was observed, where untreated cells had formed a fully confluent monolayer, in contrast with OH14 treated cells which appeared to be around 70 and 80% confluent for 25000 and 50000 cells respectively (Figure 4.12A, Day 7). No significant decrease in viability was detected using the Cell Titre Blue assay (Figure 4.12B), although, this may have been due to the fact that the untreated cell population had reached 100% confluence and had become partially quiescent.

Cells from Day 7 of this experiment were plated into tumoursphere assay conditions to evaluate the effect of repeated treatment on stem and progenitor like cells. Prolonged treatment of MCF-7 cells in adherent culture conditions with OH14 at 100 μ M slightly, but significantly, reduced tumoursphere forming ability (Figure 4.13A). In contrast, however, when untreated cells (*i.e.* those which had received daily treatment with DMSO vehicle control) were plated into the same conditions, and 100 μ M OH14 was added when cells were plated out, no significant effect on tumoursphere forming ability was observed (Figure 4.13 B). OH14 appeared only to impare tumoursphere formation when a long term treatment had been performed on the bulk population, thus, this observation, in combination with the fact that overall cell viability was not significantly reduced, suggested that OH14 alone either affected cell viability more gradually than the rapid TRAIL mediated activation of apoptosis, or that cells underwent a delayed stochastic apoptosis in response to the single agent.

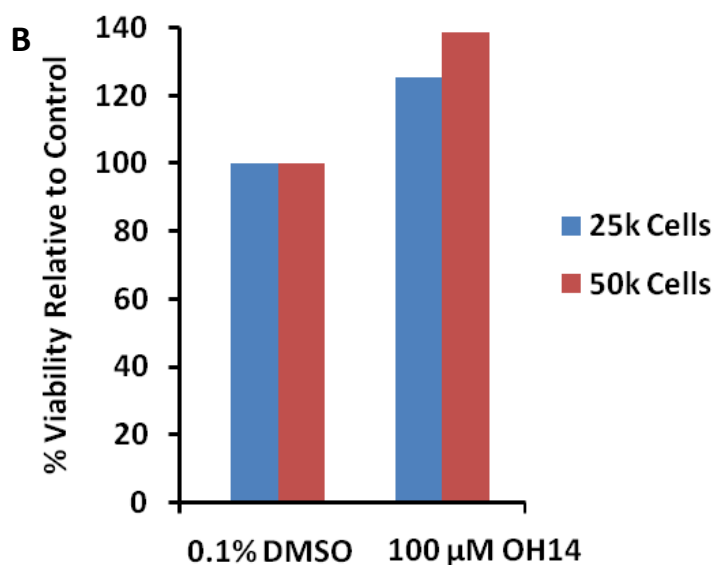
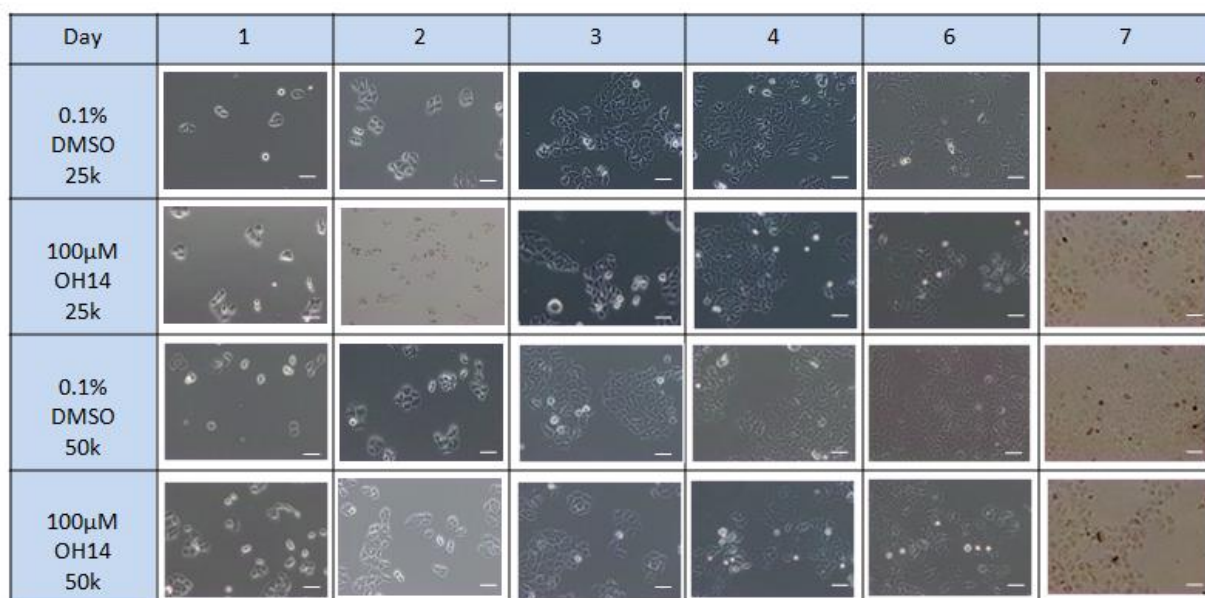
A

Figure 4.12: Daily Treatment with OH14 Slows Proliferation but does not Significantly Reduce Viability

MCF-7 cells were plated at two different cell densities (25000 cells per well and 50000 cells per well) in a 6 well plate. Media was refreshed daily with either 0.1% DMSO (vehicle control) or 100 µM OH14. A) Cells were assessed daily under microscope. Scale bar = 100 µM. B) Cell titre blue viability assay was performed after the 7 day daily treatment regime (assay was performed on one well of a 6 well plate per condition).

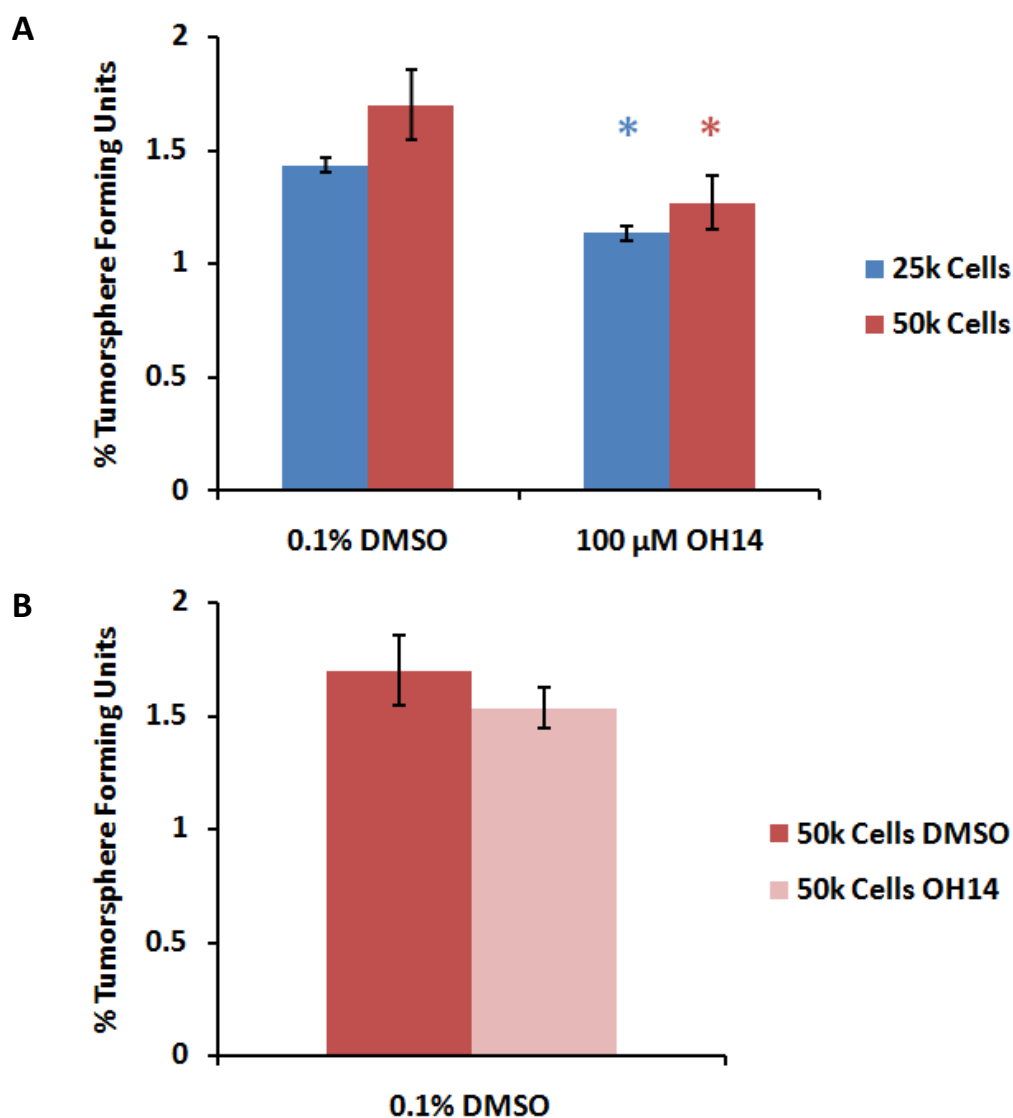


Figure 4.13: 7 Day Daily Treatment with OH14 Partially Reduces Tumoursphere Forming Ability

A) Two cell densities of MCF-7 cells which had been subjected to 7 days daily treatment with OH14 at 100 μ M or 0.1% DMSO vehicle control were plated into tumoursphere conditions and left for 7 days before tumourspheres were counted. 7 day treatment with OH14 significantly reduced tumoursphere-forming cells at both cell densities (*= p -value<0.05, t-test between untreated and OH14 (blue) or TRAIL and OH14 + TRAIL (red)). B) Cell density 50000 cells which had not previously been subjected to the 7 day OH14 treatment were subjected to tumoursphere conditions and either 0.1% DMSO or 100 μ M OH14 was added at the beginning of the assay, before being left for 7 days and tumourspheres counted. Errors calculated as standard error of the mean

4.2.7 Lead Compound OH14 is Non-Toxic to Non-Tumourgenic Cells

Part of the interest in TRAIL as a therapeutic is its ability to target cancer cells specifically, leaving non-cancerous cells viable. This is a desirable attribute for any novel cancer therapeutic and we wished to determine if this was also true for OH14.

To determine the cytotoxicity of OH14 on non-tumourgenic cells, we evaluated the compound using the Cell Titre Blue viability assay on MCF-10A cells. MCF-10A cells were derived from mammary tissue of a 36 year old healthy woman and have been cultured as immortalised but non-tumourgenic mammary epithelial cell line, and exhibits a stable karyotype (Soule *et al.*, 1990). These cells have few genetic alterations which are common in cultured breast epithelial cells, express normal p53 (Merlo *et al.*, 1995) and are ultimately used to represent non-tumourgenic mammary epithelial cells.

The lead compound, OH14, was assessed at a range of concentrations for its toxicity on the bulk population of MCF-10A cells, which show modest TRAIL-sensitivity (Piggott *et al.*, 2011), using the Cell Titre Blue viability assay over a 24 h period. The combined effect of OH14 and TRAIL was also analysed, since the treatment regime would consist of both TRAIL and OH14, thus it is important to fully establish the effect of the combination treatment in this cell line. Although a small, and non-significant, reduction in cell viability was seen, very little toxicity was observed in MCF-10A cells over this time period, with the IC_{50} value clearly not being reached even at the highest concentration of OH14 tested, 100 μ M (Figure 4.16). There was a modest, yet significant reduction in viability when cells were treated with TRAIL in combination with OH14, however, viability did not fall below 80% at all concentrations tested, thus, although significant, this decrease does not suggest a high level of toxicity.

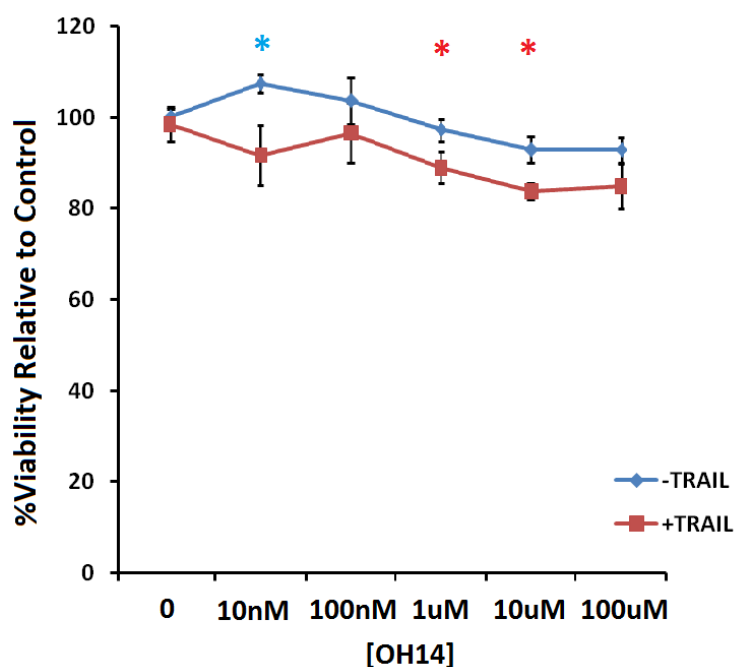


Figure 4.14: Lead Compound OH 14 is Non-Toxic to Non-Tumourgenic MCF-10A Cells Alone but partially decrease viability in combination with TRAIL

Nontransformed TRAIL resistant (Piggott *et al.*, 2011) human breast cell line MCF-10A cells cultured in adherent conditions and were treated at 70% confluence with vehicle control or OH14 at several concentrations for 1 h, before either adding 20 ng/ml or leaving with OH14 alone for 18 h. Cell viability was measured the next day using the CellTiter blue MTS assay of cell metabolism. *= p -value<0.05 between control and OH14 alone (blue) and TRAIL and OH14 + TRAIL (red). Results represent three individual experiments performed with four internal technical replicates with errors calculated as standard error of the mean.

4.3 Discussion

In this chapter, we have used multiple *in vitro* assays to evaluate 19 small molecules, identified in Chapter 3, for their ability to sensitise TRAIL-resistant breast cancer cells and stem-like cells, to TRAIL. Here, we identify several small molecules which demonstrate an ability to significantly sensitise the adherent, bulk population of TRAIL-resistant MCF-7 and BT474 cells to TRAIL. The compounds analysed had varied effects, from no effect on TRAIL sensitivity; increasing sensitivity; or even decreasing sensitivity and increasing viability in some cases. Several compounds, although able to sensitise to TRAIL at low concentrations, also significantly increased viability at high concentrations which may simply have been due to the fact that several of the compounds were not in solution and so particles were physically preventing cell proliferation. Alternatively, however, it may be that the compounds were binding to the site of FADD interaction on procaspase-8, due to the homology between c-FLIP and procaspase-8, and thus causing the effect of caspase-8 inhibition, and therefore potentiating an anti-apoptotic effect. Of the 19 small molecule inhibitors evaluated on MCF-7 and BT474 bulk cell viability, we selected 3 lead compounds OH14, OH16 and OH19, which demonstrated an ability to significantly sensitise TRAIL-resistant MCF-7 and BT474 cells to TRAIL to a similar level as that obtained using siRNA targeted to c-FLIP, whilst exhibiting little viability effects alone and demonstrating good solubility properties, to evaluate in the tumoursphere assay.

The most profound result obtained from our previous work on c-FLIP siRNA and TRAIL treatment was observed in the tumoursphere assay, where 100% of tumourspheres from 4 breast cancer cell lines tested were eliminated (Piggott *et al*, 2011). Here, we show that one of the three lead compounds, OH14, significantly reduced the tumorsphere-forming ability of cells from two TRAIL-resistant breast cancer cell lines at multiple concentrations, when administered in combination with TRAIL, whereas the other two initial lead inhibitors did not show such efficacy. Almost a total elimination of tumoursphere-forming cells generated from both MCF-7 and BT474 cells was observed when treated with 100 μ M OH14 in combination with TRAIL.

In addition, we have evaluated our compounds in the colony-forming assay - a proliferation or progenitor like assay. Initially, we noted that MCF-7 and BT474 colonies, which are TRAIL resistant in bulk and tumoursphere assays, were more

sensitive to TRAIL in these assay conditions. Colonies are varied in size and morphology, thus, this increased sensitivity may be due to the specificity of TRAIL for more mesenchymal-like cells (Rahman *et al.*, 2009). Regardless of this, however, TRAIL-sensitivity of BT474 and MCF-7 colonies was still significantly increased by treatment with our lead compound, OH14. Since 50% of cells plated form colonies, the assay is not representative of the minority stem cell population in the same way as the tumoursphere assay. However, this assay did provide further support to the cell viability and tumoursphere assays as the drug efficacy data follows a similar overall trend in each case.

The initial compound screens performed here were on two TRAIL-resistant ER+ve cell lines, as these were hypothesised to have the greatest response to our combination therapy, based on previous data, however, we explored the effects of our lead compound on two additional cell lines, which represent different subtypes of breast cancer. c-FLIP has been associated with TRAIL resistance in HER2 +ve breast cancer (Zang *et al.*, 2011) and we have previously shown the bulk and tumoursphere forming population of SKBR3 cells to be sensitive to siRNA c-FLIP suppression and TRAIL treatment (Piggott *et al.*, 2011). SKBR3 cells were not selected for high-throughput compound screening primarily due to the integrity of their tumoursphere-forming cells being sub-optimal, in addition to their reduced ability to form colonies in the CFA. When treated with OH14, primary SKBR3 tumourspheres were not sensitised to TRAIL, however, a modest, yet significant sensitisation was observed at 10 μ M upon passaging. This sensitisation, however, was likely to be additive rather than synergistic since OH14 itself reduced sphere number at this concentration. Similarly, OH14 did sensitise SKBR3 bulk cells, assessed using the viability assay, to TRAIL, although impacting on viability alone. Previously, knocking out c-FLIP using siRNA reduced SKBR3 viability by around 15%, whilst the combination led to a 45% increase in cell death (Piggott *et al.*, 2011), thus, OH14 was unable to phenocopy siRNA to such an extent on these cells.

The bulk population of triple-negative breast cancers are mostly TRAIL sensitive (Rahman *et al.*, 2009), thus, using a TN cell line in order to study our inhibitors would not have been optimal for the initial viability assay. However, as we have observed here using the CFA, our inhibitors can further increase the sensitivity of TRAIL-sensitive cells and so it may be possible to further sensitise these cells, although our previous work

using c-FLIP siRNA did not further sensitise the bulk population of the TN cell line, MDA-MB-231 to TRAIL (Piggott *et al.*, 2011). Previous work has, however, demonstrated the tumoursphere-forming population of this cell line to be highly sensitive to the combination of siRNA c-FLIP and TRAIL treatment (Piggott *et al.*, 2011) and so it was hypothesised that we may obtain a similar result with our lead compound. We did not observe a significant effect of OH14 on MDA-MB-231 primary tumoursphere forming cells, although, similar to SKBR3 tumoursphere-forming cells, a modest, yet significant effect was observed at 100 μ M upon passaging. Although we, and others, have shown that genetic suppression of c-FLIP can sensitise MDA-MB-231 and SKBR3 cells to TRAIL (Piggott *et al.*, 2011; Zang *et al.*, 2014), it may be that inhibition of the FADD-c-FLIP interaction using our inhibitors is not potent enough to exert this same effect.

One of the primary reasons that TRAIL is such a desirable therapeutic agent is the specificity it exhibits for targeting cancerous cells, whilst sparing non-cancerous cells, thus, retaining this lack of general cytotoxicity is an important feature of a TRAIL-sensitising agent. Since TRAIL resistance in these cells is thought to be largely due to the expression of decoy receptors, with anti-apoptotic proteins such as c-FLIP only playing a part when activated in combination with each other (Gura, 1997; Ashkenazi *et al.*, 1999; Lemke *et al.*, 2014; Griffith and Lynch, 1998) we hypothesised that our small molecule c-FLIP inhibitors would be non-toxic to these cells when administered alone, in accordance with published data using siRNA to c-FLIP on these cells (Piggott *et al.*, 2011). In accordance with this, we hypothesised that a partial induction of apoptosis may be observed when administered in combination with TRAIL, due to the potential role of anti-apoptotic proteins in normal cell TRAIL resistance, in addition to our published observations of 20% increase in cell death using c-FLIP siRNA and TRAIL in MCF-10A cells (Piggott *et al.*, 2011). Here, we have demonstrated, using the non-cancerous MCF-10A mammary cell line, that our lead compound was indeed not significantly toxic to this non-transformed cell line when administered alone. We observed a modest increase in cell death when treated in combination with TRAIL, similar to the level we have previously observed using siRNA (Piggott *et al.*, 2011). To ascertain further information regarding the long-term cytotoxicity of OH14, we performed daily treatment on the bulk population of MCF-7 cells at 100 μ M which demonstrated OH14 to be non-cytotoxic. Treatment with OH14 did, however, slow

proliferation after 4 days which may be due to the role c-FLIP has on stem-like cells, that is, inhibiting c-FLIP may be preventing growth of progenitor or stem-like cells, which help maintain the cell population. This data is preliminary and these experiments will be repeated with the use of stable c-FLIP deficient cell line (using shRNA or TALEN, for example) as well as a more efficacious analogue of OH14 in the future.

In conclusion, we have confirmed using several *in vitro* assays, that, of the 19 compounds initially selected using *in silico* protein modelling in Chapter 3, we have successfully identified one lead c-FLIP small molecule inhibitor, OH14, which shows an ability to significantly increase sensitivity of previously resistant breast cancer cells to TRAIL induced apoptosis in a number of different assays. The following chapters explore the mechanism of action of our lead compound, OH14 (Chapter 5), in addition to analysing analogues of OH14 to provide initial structural activity information for future compound generation (Chapter 6).

Chapter 5

Exploring the Mechanism of Action of OH14

Chapter 5: Exploring the Mechanism of Action of OH14

5.1 Introduction

The design of our inhibitors, using molecular modelling, aimed to generate small molecules which enter and bind within a pocket on the surface of c-FLIP L DED1 in order to block its interaction with the FL motif of FADD. Data presented in Chapter 4 demonstrated that a proportion of the candidate inhibitors do indeed function as intended, by sensitising previously resistant or partially resistant breast cancer cells to TRAIL, in several different cell-based assays. These cellular outcomes are consistent with the proposed mechanism of action of our inhibitors, however, it is important that this is confirmed *in vitro* by demonstrating that the interaction between FADD and c-FLIP is indeed impaired.

Many important cellular processes are reliant on protein:protein interactions (PPIs) and thus pharmacological inhibition of these interactions are an attractive target of small molecule drug design. Developing efficient pharmacological PPIs and indeed studying protein interactions *in vitro* can be quite a challenge, due to the dynamic nature of such processes, and despite the many potential techniques available, there are many drawbacks to each. A full understanding of the mechanism of such inhibitors, *i.e.* proving their ability to interfere with their target interactions is vital in order to progress such therapeutics. Through a collaboration with the Institute of Molecular Genetics, Prague, we had the opportunity to utilise FRET as a technique to study these interactions, through advice provided by Dr David Stanek. Additionally, Dr Ladislav Andera provided expertise for us to attempt to use the technique of TALEN in order to attempt to generate a stable c-FLIP negative cell line which would be used for performing mutational studies on c-FLIP key residues.

In addition to exploring the mechanism of action of OH14, we wished to evaluate its effects on additional cell lines, as well as evaluating its potential effect in CSC plasticity, *i.e.* the ability for non-cancer-stem cells to reacquire stem-like properties. Clinically, CSC-plasticity is a process of high importance since it implies that, even if all CSCs were eliminated from a tumour, any remaining bulk cells would be able to de-differentiate to a CSC-like state and thus, re-seed resulting in new tumour growth. A clinical strategy involving a combination treatment which eliminates CSCs and prevents

plasticity is therefore a highly desirable way of eliminating a tumour and preventing relapse. Studying plasticity *in vitro* is a complex task since observing an increase in CSCs alone does not demonstrate the process as it may be occurring by increased CSC self-renewal. It is necessary to eliminate all CSCs from a cell population before plasticity can be observed with some confidence. Our recent demonstrations that TRAIL in combination with siRNA c-FLIP can eliminate tumoursphere-forming cells from a panel of breast cancer cell lines *in vitro* has provided us with a tool for studying plasticity (Piggott *et al.*, 2011). We have recently optimised an *in vitro* assay, using our previous findings, which can be used as an *in vitro* model of plasticity (French, R., PhD Thesis 2014). This assay relies on the fact that, although all tumoursphere-forming ability is eliminated after treatment with TRAIL in c-FLIP suppressed cells, some viable cells remain which are able to re-acquire tumoursphere-forming ability (Piggott *et al.*, 2011). Using this optimised assay, we wished to analyse whether OH14 could impair CSC plasticity, which would enhance the clinical potential of this small molecule c-FLIP inhibitor.

5.1.1 FRET Acceptor Photobleaching

Fluorescence or Förster, after the scientist who originally discovered FRET, Resonance Energy Transfer (FRET) is a distance-dependent transfer of energy between an electronically excited fluorophore to a second, non-excited fluorophore. FRET efficiency depends on the donor and acceptor molecules being within 1-10 nm of one another and for the absorption spectrum of the acceptor to overlap with the emission spectrum of the donor (Jares-Erijman and Jovin, 2003).

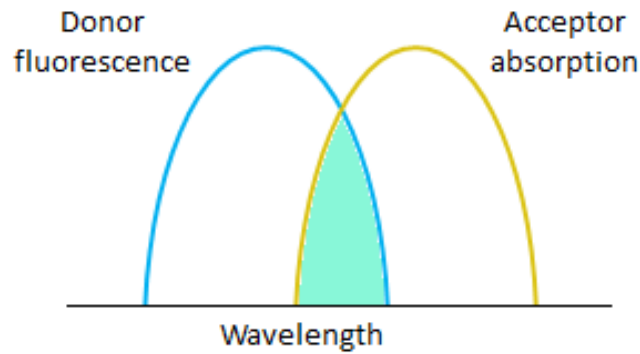


Figure 5.1: Representation of the FRET spectral overlap requirement of donor and acceptor.

Donor and acceptor emission and absorption spectra, respectively, must overlap in order to achieve successful FRET. Acceptor photobleaching FRET involves loss of the acceptor (e.g. in this case, YFP) signal, and an increase in the donor (e.g. in this case, CFP) signal.

FRET can be measured using a variety of methodologies; sensitized emission (SE-FRET); acceptor photobleach (AP-FRET); or fluorescence lifetime imaging (FLIM-FRET). AP-FRET, which is used in this study, is a method of measuring protein interactions using the exchange of energy between a donor and acceptor. The intensity of the donor will be measured before and after irreversible eradication of the acceptor by ‘bleaching’ using a high intensity light source. (Figure 5.2) Successful FRET interactions will prevent full emission of the donor, thus, the increase in donor intensity after acceptor bleaching demonstrates the presence or absence of FRET.

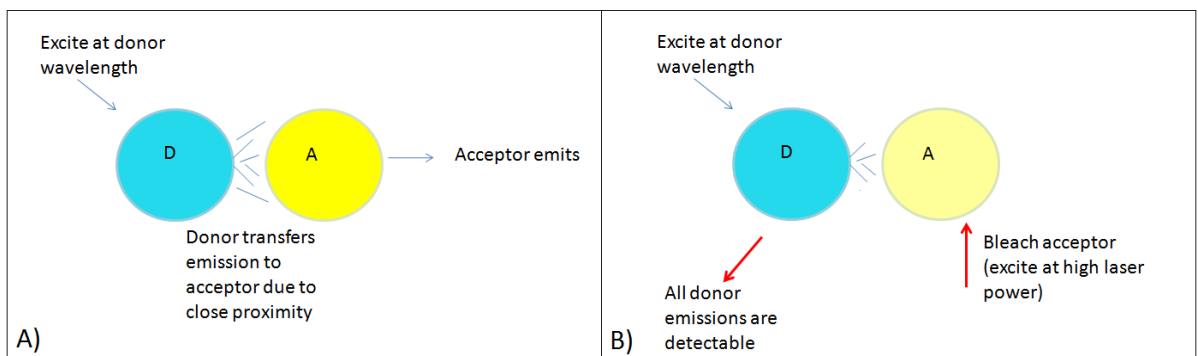


Figure 5.2: Schematic of FRET Acceptor Photobleaching using CFP Donor and YFP Acceptor

A) When donor is excited at its wavelength, in a case where donor and acceptor fluorophores are in close proximity, energy will be transferred from donor to acceptor which will cause the acceptor to emit. B) In this same case, if the acceptor is bleached by exciting at a very high laser power, the donor emissions will not be transferred and instead will be emitted as light. In both cases, if acceptor and donor are not in close proximity, then no transfer of energy will occur between the two fluorophores and so all donor emissions will be detectable, regardless of whether the acceptor is bleached or not.

5.1.2 TALEN Gene Manipulation

In February 2011, *Nature Biotechnology* released two articles on targeted genomic modification using Transcription activator-like effector nucleases (TALENs) (Miller *et al*, 2011; Zhang *et al.*, 2011). TALENs have since been used to modify the endogenous genes present in a variety of species from viruses, plants and yeast to insects, frogs and mammals, including mice (Kim and Kim, 2014).

TALEN technology was utilised in this chapter in order to attempt to eliminate c-FLIP from MCF-7 cells, and, ultimately generate a stable c-FLIP knock-out cell line, which we have not been able to successfully achieve using shRNA. If generated, this cell line could then be utilised for overexpression studies using SDM to analyse the importance of residues on c-FLIP we have identified in Chapter 3.

In this chapter, we explore the mechanism of action of our lead compound, OH14. We analyse the interactions between c-FLIP, procaspase-8 and FADD in TRAIL-sensitive and -resistant lines and demonstrate the ability of OH14 to interfere with the c-FLIP:FADD interaction. TALEN technology was utilised in order to attempt to generate a c-FLIP knock-out cell line, however, this was not successful and requires further work. Therefore additional mutagenesis studies c-FLIP:FADD interactions were not achievable at this time. We also explored the effect of our lead inhibitor on additional cell lines and on the CSC theory of plasticity, and demonstrated it to have potential therapeutic efficacy in targeting this important process.

5.2 Results

5.2.1 Procaspase-8 Cleavage Increases Over Time after TRAIL Treatment

Co-immunoprecipitation (co-IP) and Western blot were optimised in order to evaluate the relevant protein:protein interactions and caspase-8 activity, represented by procaspase-8 cleavage in TRAIL resistant and sensitive cells. In brief, optimisation involved evaluating differing pairs of antibodies against FADD and caspase-8 in order to achieve the best combination for use in co-IP.

Several groups have reported the presence of interactions between caspase-8 and FADD in TRAIL sensitive cell lines, and the lack of this interaction in TRAIL resistant lines (Day *et al.*, 2008; Dickens *et al.*, 2012; Safa and Pollok, 2011). We therefore wanted to establish whether this was the case in our cell lines. The levels of cleaved caspase-8 (p43 and p18 C8) was initially evaluated upon treatment with TRAIL after varying treatment times. Initial Western blot on TRAIL-sensitive MDA-MB-231s demonstrated an increase in the cleaved and therefore, active, forms of caspase-8 as the duration of TRAIL treatment increased up to 2 hours (Figure 5.3A). In contrast, TRAIL-resistant MCF-7 cells exhibited a barely detectable level of cleaved caspase-8 at 2 hours (Figure 5.3A). This Western should ideally be repeated with replicate samples and higher concentrations of protein to confirm these findings, particularly, since GAPDH confirms that the gel was not equally loaded. Comparing band intensity, by normalisation to GAPDH, confirmed however the increase in cleaved caspase-8 in MDA-MB-231 cells, while no marked differences were observed in total protein levels of c-FLIP or FADD between the MDA-MB-231 and MCF-7 cells.

After TRAIL-sensitive MDA-MB-231 cells were treated at time intervals with 100 ng/ml TRAIL no interaction between FADD and c-FLIP was evident, as no c-FLIP band was present (Figure 5.3B). Western blot confirmed an increase in the cleaved, p43/41 and p18 forms of caspase-8 over the duration of 2 hours. Additionally, FADD levels were confirmed to stay constant throughout the treatment duration. An interaction between FADD and caspase-8 was observed, although the band was faint, whilst an increasing interaction with FADD and the p43/41 was observed over time demonstrating cleavage of the pro-form of caspase-8 (procaspase-8) to its active cleaved form, whilst in complex with FADD (Figure 5.3B). Stable total levels of FADD

confirmed that this increase did not simply correlate with increasing protein levels of FADD.

In the future, this data needs to be compared in the TRAIL resistant MCF-7 cell line to establish if the immunoprecipitation of FADD and c-FLIP is achievable in resistant cells.

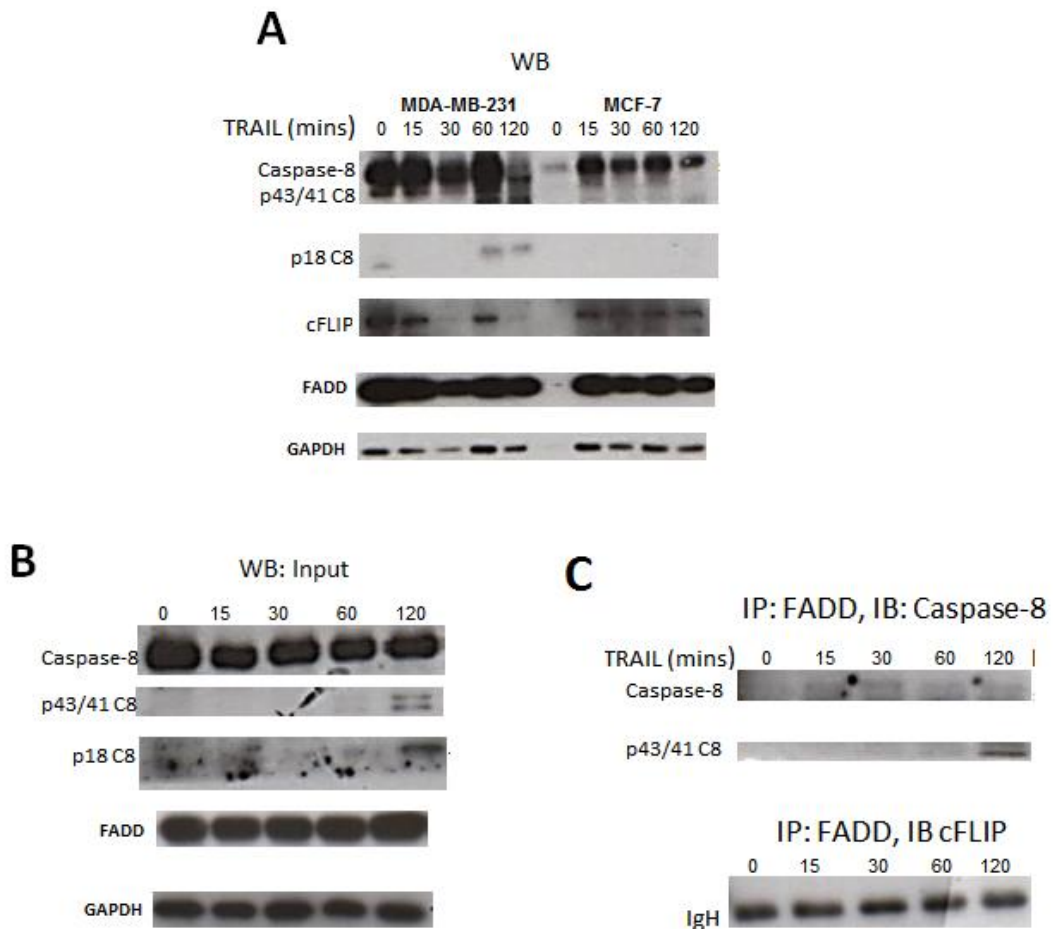


Figure 5.3: Caspase-8 Cleavage and Interaction with FADD Increases over Time in TRAIL Sensitive Cells.

A) Total protein extracts from MCF-7 and MDA-MB-231 cells, treated with 100 ng/ml TRAIL for the indicated timepoints, were probed for Caspase-8, FADD and c-FLIP protein levels. GAPDH is provided as loading control. B) Total protein input prior to co-IP (C) was probed for caspase-8 and FADD protein levels, with GAPDH as loading control. C) Total protein extracts from MDA-MB-231 cells, treated with TRAIL, were immunoprecipitated with anti-FADD antibodies. Immunoprecipitates were blotted with antibodies to FADD, Caspase- 8 and c-FLIP.

5.2.3 TRAIL Increases Caspase-8 Activity in Sensitive Cell Lines

TRAIL acts by inducing apoptosis mediated by the extrinsic, caspase-8 pathway. In the bulk population of TRAIL resistant MCF-7 cells, this pathway is blocked by the action of c-FLIP (Safa and Pollok, 2011; Day *et al.*, 2009; Piggott *et al.*, 2011), and thus, little caspase-8 activity will be observed when cells are treated with TRAIL. We therefore expected our lead compounds, which have demonstrable ability to sensitise to TRAIL, to cause an increase in caspase-8 activity when treated with TRAIL in these cells. In addition, we have previously observed that TRAIL does exert an effect on the colony forming activity of TRAIL resistant MCF-7 cells (Section 4.2.4), which is consistent with a recent study from our laboratory (French *et al.*, 2015 in press) thus, we wished to elucidate whether this occurred through the normal pathway of TRAIL activity.

To determine caspase-8 activity in this assay, the enzymatic Caspase-Glo 8 assay (Promega) was used. An initial evaluation of this assay was performed on the TRAIL sensitive MDA-MB-231 cells compared with TRAIL resistant MCF-7 cells (Figure 5.4 A-D) in order to confirm that this would indeed be a suitable assay for compound evaluation. Bulk cells from a TRAIL-resistant (MCF-7) and TRAIL-sensitive (MDA-MB-231) cell line were treated with either 20 ng/ml or 100 ng/ml TRAIL and left for around 2 hours, allowing for a significant induction of caspase-8 activity as observed in previous studies (MacFarlane *et al.*, 2000; Sharp *et al.*, 2005). Overall caspase-8 activity was higher in the TRAIL sensitive line, regardless of whether TRAIL had been added. Upon treatment with TRAIL at 20 ng/ml, caspase-8 activity was not altered in the TRAIL-resistant MCF-7 cells, however, a slight, although non-significant in this case, increase was observed in the TRAIL-sensitive line. When the concentration of TRAIL was raised to 100 ng/ml, an increase was detected in MDA-MB-231 cells, although this was not significant, however, no increase in caspase-8 activity was observed in MCF-7 cells (Figure 5.4E).

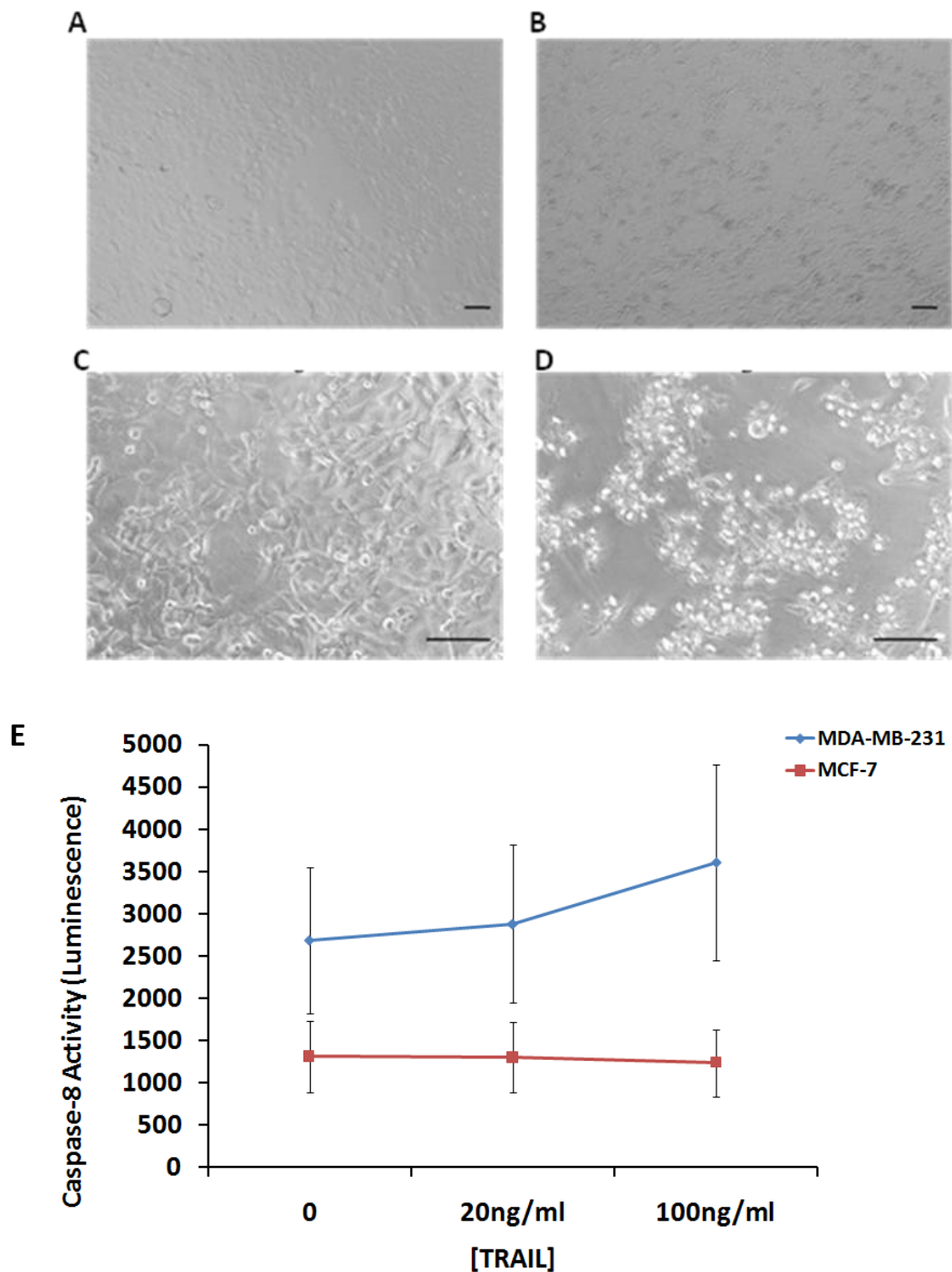


Figure 5.4: Caspase-8 Activity Increases upon TRAIL addition in TRAIL sensitive Cell Lines

Representative images of untreated A) TRAIL-resistant MCF-7 and C) TRAIL-sensitive MDA-MB-231. Representative images of 20 ng/ml TRAIL treatment for 18 h on B) MCF-7 and D) MDA-MB-231. Scale bars = 100 μm. E) TRAIL-sensitive MDA-MB-231 and TRAIL-resistant MCF-7 cells were plated in adherent conditions and left to attach overnight. After 24 h, vehicle control, 20 ng/ml or 100 ng/ml TRAIL was added and cells were left for around 2 h to allow the induction of caspase-8. Caspase-Glo 8 was performed according to manufacturers instructions and luminescence was read using a plate reader. Results represent 3 replicates.

5.2.3 c-FLIP Inhibitors Increase Caspase-8 Activity upon TRAIL Treatment

To evaluate the effect of our 3 initial compounds, OH14, 16 and 19 on caspase-8 activity in the bulk population of TRAIL resistant MCF-7 cells, we used caspase-glo 8 luminescence assay. The compounds alone did not significantly effect caspase-8 activity, when treated in combination with TRAIL, however, a significant increase in caspase-8 activity was observed (Figure 5.5A). This suggested our compounds are indeed specific in their ability to sensitise to TRAIL via the extrinsic, caspase-mediated pathway of apoptosis. One other compound was selected (OH12) which we previously observed to exhibit a modest TRAIL sensitising effect at some concentrations, but increased viability at several higher concentrations in the initial viability evaluation (Section 4.2.2). OH12 did not significantly increase caspase-8 activity, as hypothesised by its lack of efficacy in initial assays. OH14, 16 and 19 did show a modest, although non-significant, reduction in caspase-8 activity when treated alone which may be due to a suppression of baseline caspase-8 activation in the system, or alternatively an off-target effect of caspase-8 inhibition when the TRAIL pathway is not stimulated.

In addition to the caspase-glo assay, the idea that CFA cells are TRAIL sensitive due to the induction of caspase-mediated apoptosis was tested using a commercially available pan-caspase inhibitor (Z-Vad-FMK). This was performed in BT474 cells which are TRAIL resistant, however, like MCF-7 cells, their CFA cells are partially TRAIL sensitive (Section 4.2.4). The sensitivity of BT474 colony forming cells to TRAIL was rescued to 78%, by the addition of a pan-caspase inhibitor (Figure 5.5 B). When combined with OH14, BT474 CFA TRAIL-sensitivity was increased, as previously observed which was restored to a similar level as TRAIL alone by pre-treatment with the pan-caspase inhibitor, with a rescue to an average of 73%. Furthermore, we show here that the caspase inhibitor was able to rescue the MCF-7 CFA TRAIL-sensitivity significantly (p -value <0.001) (Figure 5.5 C) and demonstrated therefore that TRAIL is acting through the extrinsic pathway of apoptosis in the partially-sensitive MCF-7 colony forming cells. Evaluation of OH14 in combination with a caspase-inhibitor has not yet been performed on MCF-7 colony forming cells.

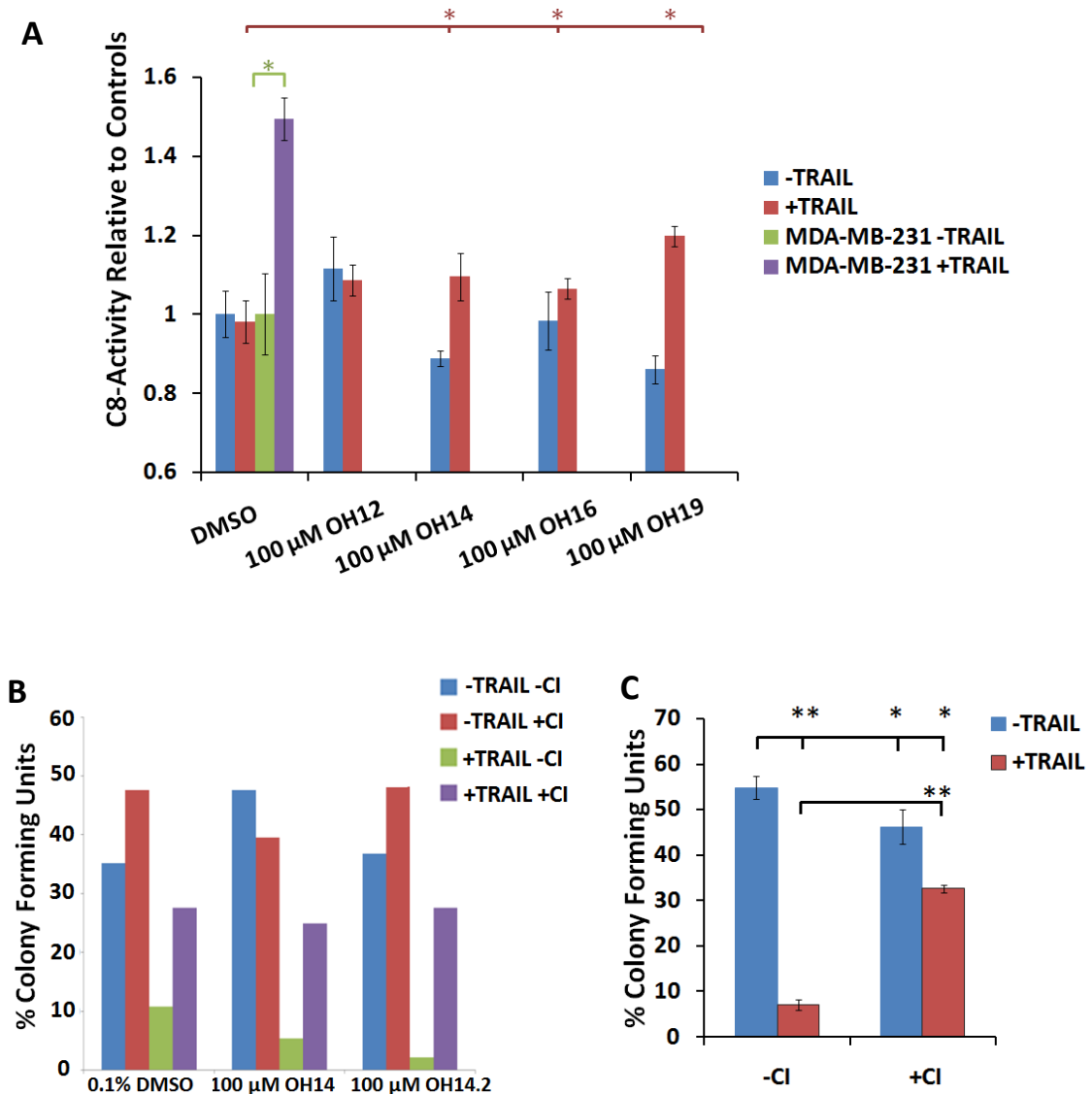


Figure 5.5: Small Molecule c-FLIP Inhibitors Sensitise to TRAIL via Caspase-mediated Pathway.

A) Caspase-8 (C8) Activity Assay (Caspase-Glo 8) performed on 70% confluent adherent MCF-7 cells after treatment with the 3 initial lead compounds (OH14, 16 and 19) and another, less active, compound (OH12) at 100 μ M alone or in combination with 20 ng/ml TRAIL. *=p-value<0.05, t-test TRAIL vs compound plus TRAIL (red) and untreated 231 vs TRAIL treated (green). B) CFA: BT474 cells plated at 50 cells per cm^2 , treated after attachment with OH14 (both 14.2 and 14 represent OH14) at 100 μ M alone or in the presence of a pan-caspase inhibitor (CI) at 10 μ M with or without 20 ng/ml TRAIL and left for 10 days to form colonies. C) CFA: MCF-7 cells were plated at 50 cells per cm^2 and left to attach before treatment with 20 ng/ml TRAIL in the presence or absence of the pan-caspase inhibitor at 0.1 μ M (CI) and left to form colonies. Results represent averages of 4 technical replicates over 2 experiments, error bars presented represent standard error of the mean. *=p-value<0.05, **=p-value<0.001, t-test.

5.2.2 FRET Acceptor Photobleaching

In our experiments, eCFP and eYFP serve as the donor-acceptor pair for AP-FRET.

5.2.2.1 FRET Optimisation: Plasmid Ratios

FRET constructs e-CFP-C1 and e-YFP-C1 were used to generate fusion constructs of FADD, c-FLIP and procaspase-8. We have successfully generated e-CFP-C1-FADD and e-YFP-c1-c-FLIP plasmids, however, cloning is ongoing for the procaspase-8 FRET constructs. Ultimately we wish to be able to use FRET to study the interactions of c-FLIP:FADD, c-FLIP:caspase-8 and caspase-8:FADD in the presence of our lead compound and ultimately in order to evaluate our c-FLIP mutants via mutagenesis of the FRET constructs.

In order for AP-FRET to be successful, it is optimal for both donor and acceptor to be expressed to relatively similar levels, thus, a considerable amount of optimisation was required. MCF-7 cells were initially chosen since these are the key TRAIL resistant model used in the previous inhibitor evaluations, however, HeLa cells, which are also TRAIL resistant are reported to be an easier cell line to transfect (Crowder and El-Deiry, 2012), thus we decided to use these cells for the initial FRET optimisation and inhibitor testing. We initially observed that it was difficult to obtain a strong fluorescent signal for CFP transfected cells in comparison to YFP expression, thus, we tested the expression obtained using several different ratios of CFP and YFP plasmid DNA to each other in order to achieve the optimum ratios for our system (Methods, Table 2.1). Fluorescence was observed using a confocal microscope to further confirm whether successful transfection of cells had taken place.

5.2.2.2 FRET Optimisation: Overexpression of FADD and c-FLIP FRET Constructs Induces Caspase-Mediated Apoptosis

In the process of plasmid optimisation we observed that when cells were transfected with either c-FLIP or FADD FRET constructs, a significant amount of cell death was present in comparison to when empty CFP and YFP constructs were transfected. We hypothesised that transfection with FADD-CFP is an overexpression of one of the key signalling components of the apoptotic pathway, therefore, this may cause cells to undergo apoptosis, due simply to the abundance of a key apoptotic protein. Although, it is not clear why c-FLIP:YFP expression induced cell death.

To determine whether the cell death was simply due to the overexpression of apoptotic proteins, and, in an attempt to optimise conditions for FRET experiments to take place, we pre-treated cells to be transfected with a pan-caspase inhibitor. The pan-caspase inhibitor, Z-VAD-FMK, blocks the active form of caspases and thus would not block the uncleaved form of procaspase-8 (or -10), which would still be able to compete with c-FLIP for FADD if no c-FLIP inhibitor was present.

HeLa cells were treated with the pan-caspase inhibitor Z-VAD-FMK at 10 μ M 1 hour before transfection with c-FLIP-YFP or FADD-CFP FRET constructs. After transfection, cells were left for 24 h before being visualised using a confocal microscope to check both viability and uptake of the plasmids. Transfection with both c-FLIP and FADD FRET constructs (either tagged to YFP or CFP) induced death in HeLa cells (Figure 5.6 A and C) and in MCF-7 cells (data not shown). Treatment of the cells with the pan-caspase inhibitor Z-VAD-FMK prior to transfection prevented this cell death, as cells appeared more viable, and showed increased expression of FRET constructs (Figure 5.6 B and D). This rescue was also observed in MCF-7 cells (data not shown).

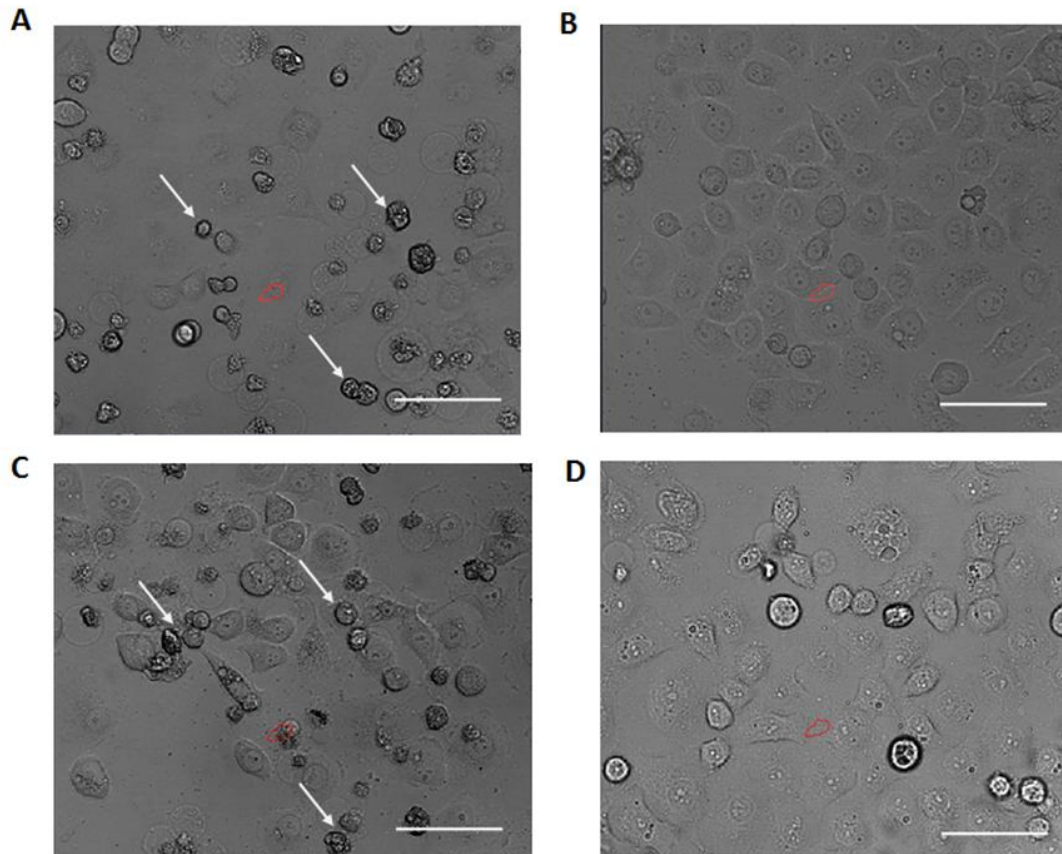


Figure 5.6: Pan-caspase Inhibitor Z-VAD-FMK Prevents Cell Death Induced by Overexpression of c-FLIP and FADD FRET Constructs

Hela cells were plated on 24 well glass bottom plates (Mattek), left to attach overnight and treated with vehicle control or pan-caspase inhibitor at 10 μ M Z-VAD-FMK for 1 hour before being transfected with either FADD-CFP or c-FLIP-YFP FRET constructs. Phase contrast microscopy was performed 24h after transfection. A) FADD-CFP treated with vehicle control B) FADD-CFP with caspase-inhibitor C) c-FLIP-YFP treated with vehicle control D) c-FLIP-YFP treated with with caspase-inhibitor. White arrows highlight cells which have rounded up and detached. Scale bars = 100 μ m.

5.2.2.2 CFP-YFP Construct Demonstrates FRET in HeLa Cells

To test the validity of FRET in our biological system, and ensure that successful FRET could be measured in our cells, we obtained a CFP-YFP fusion protein, to be used as a positive control. Since CFP and YFP are fused together, when transfected with the construct, cells should show an interaction between the proteins, *i.e.* an increase in CFP when YFP is bleached. Due to the fact that the proteins are fused, the level of FRET obtained is likely to be maximal, compared to when testing the FRET between two unfused proteins.

HeLa cells transfected with the fusion protein were analysed. A region of interest (ROI) was selected based on the ratio of CFP to YFP fluorescence, that is, the fluorescence intensity of CFP and YFP was relatively similar and was adjusted using the digital gain to ensure this was the case (Figure 5.7A). The average intensity within the ROI was plotted as a function of time (Figure 5.7B). The positive control showed a significant increase in donor (CFP) fluorescence intensity after the acceptor (YFP) was bleached and bleaching was continued, thus confirming the ability of FRET to be recorded using our system.

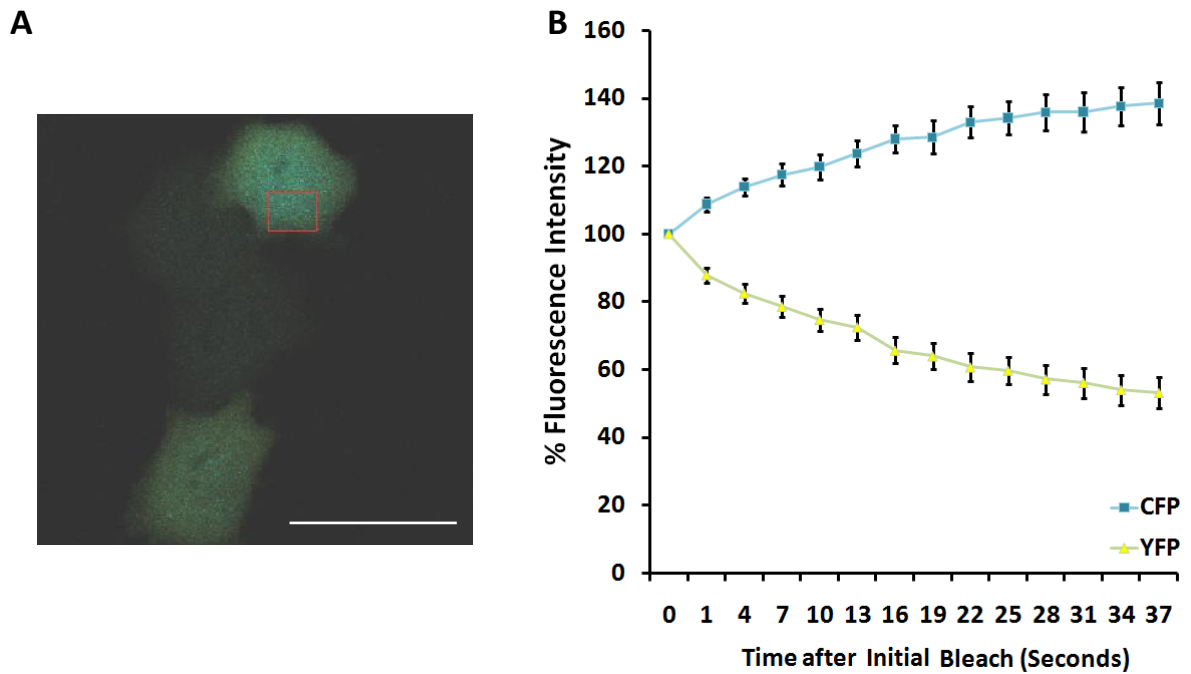


Figure 5.7: Fluorescence image of HeLa cells expressing CFP-YFP fusion construct.

A) Representative image of HeLa cells transfected with CFP-YFP fusion protein, before bleaching took place. Scale bar = 50 μm . B) Fluorescence of donor (CFP) and acceptor (YFP) were measured as a function of time during acceptor photobleaching (bleaching occurred at each time point). Intensities within the region of interest (red square (A)) from an average of 4 cells over 3 experiments were analysed and plotted.

5.2.2.3 OH14 Reduces the Number of Detectable FADD:c-FLIP Interactions in TRAIL Treated Cells

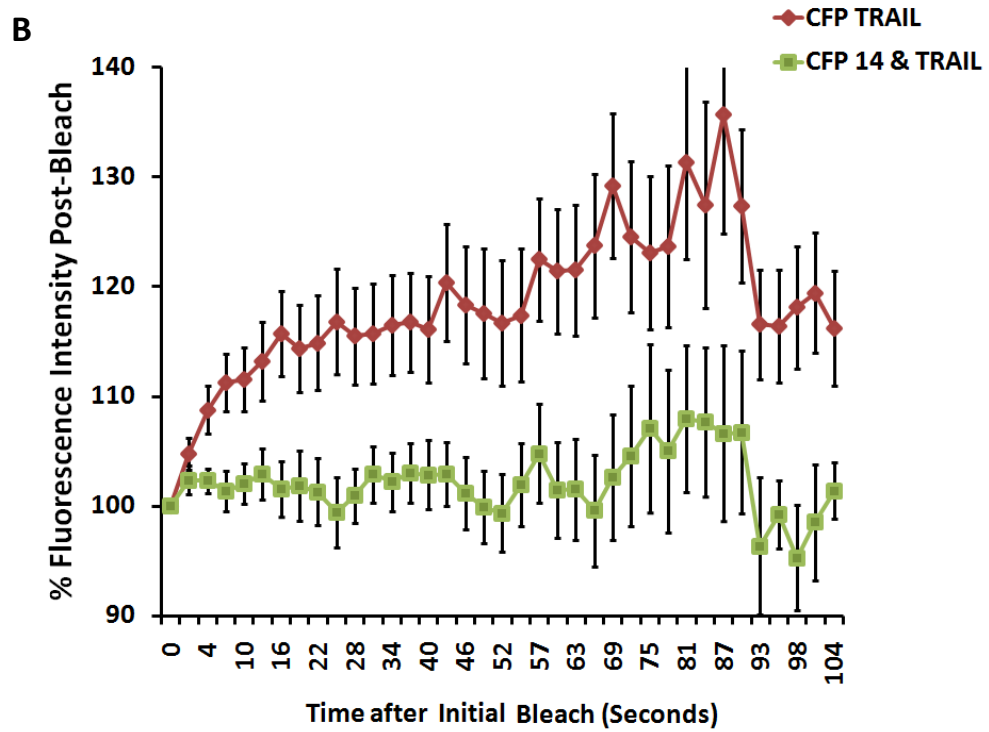
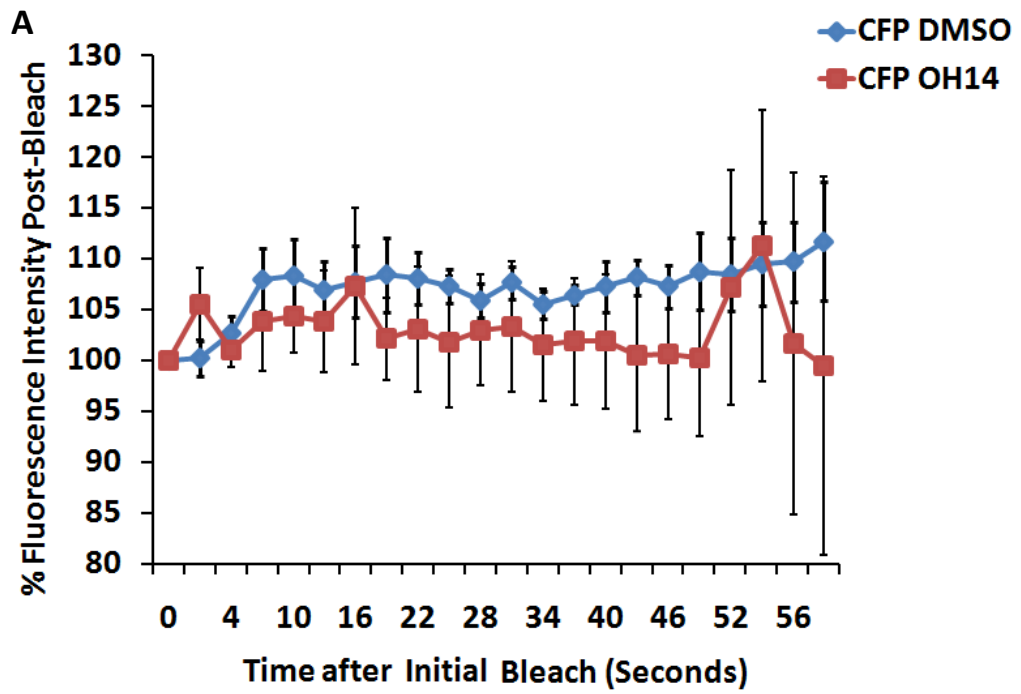
Our observation that the pan-caspase inhibitor prevented apoptosis induced by expression of our c-FLIP and FADD FRET constructs was such that in subsequent FRET experiments, cells were always treated with caspase-inhibitor before transfection, in order to ensure that they remained viable for FRET measurements to take place 24 hours later. Pan-caspase inhibitors act by binding to the active site on caspases (R and D systems), and therefore do not interfere directly with FADD complexes.

To determine whether our lead compound, OH14, could indeed inhibit the interaction between c-FLIP and FADD, HeLa cells were left untreated (vehicle control), treated with TRAIL alone, treated with 100 μ M OH14 alone or pre-treated with 100 μ M OH14 before TRAIL addition at 20 ng/ml. Untreated cells showed an increase of up to approximately 7% in CFP intensity upon YFP bleaching (Figure 5.8A, blue), suggesting that FRET was occurring to a small degree, that is, in unstimulated cells, c-FLIP and FADD do interact, but not to a great extent. When cells were first treated with OH14 at 100 μ M, FRET appeared to be slightly, although not significantly, reduced, compared with untreated cells (Figure 5.8A). Upon treatment with TRAIL, a significant increase in CFP intensity, of up to an average of approximately 35%, was observed at every time point after bleaching (Figure 5.8B, red), which suggested that stimulation of the apoptotic pathway in these TRAIL resistant cells has occurred, and that c-FLIP and FADD are indeed interacting. When the cells were pre-treated with OH14, however, the CFP intensity increased to only 5% compared with unstimulated cells (before bleaching) (Figure 5.8B, green), and overall was significantly lower than TRAIL alone, which suggested that OH14 successfully inhibited the interaction between c-FLIP and FADD.

The same FRET experiments were performed in MCF-7 cells, which initially showed a great deal of cytotoxicity when cells were transfected with the constructs, and so were not selected as our primary line for performing FRET experiments. When treated with TRAIL alone, we did, however observe an increase in FRET, which was reduced when TRAIL was treated in combination with OH14, although this experiment needs to be repeated in order to demonstrate the significance of this reduction (Figure 5.8C).

In any live cell, protein interactions will be dynamic, with the kinetics varying with protein expression and affinity between the proteins involved. By using a box-

scatter plot we have explored this variability in greater detail by looking at the responses at certain time points after bleaching: at the beginning; a third of the way in; and two thirds into reading. The mean bars demonstrate the overall trend, however, individual points clearly demonstrate that whilst there were many detectable interactions in one cell, there were few in another (Figure 5.8D).



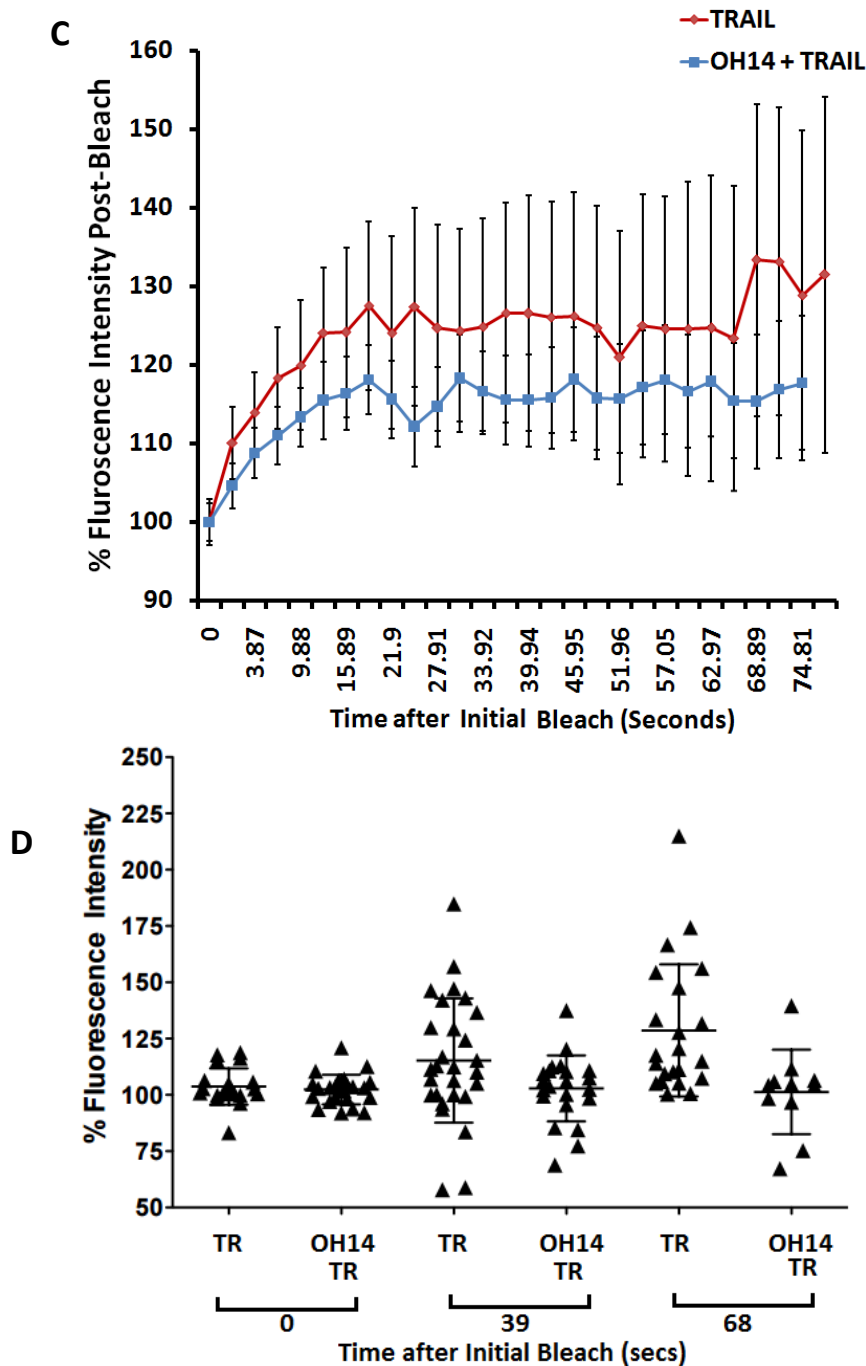


Figure 5.8: OH14 Reduces FADD:c-FLIP Interactions in TRAIL Treated TRAIL-resistant HeLa and MCF-7 Cells

HeLa cells were transfected with c-FLIP and FADD FRET plasmids, treated with caspase-inhibitor at the time of transfection were left for 24 h before treatments. Cells were then treated with A) vehicle control (0.1% DMSO, blue), 100 μ M OH14 alone or B) 100 μ M OH14 for 1 hour before 20 ng/ml TRAIL for 2 hours (Green), or 20 ng/ml TRAIL alone for 2 hours (Red). Multiple cells were recorded, results displayed are CFP fluorescence from the average of at least 7 cells on 3 independent experiments. There is a significant difference 4 seconds after bleaching between TRAIL and OH14 plus TRAIL (t-test for each time point). C) MCF-7 cells transfected and treated in same way as HeLa cells with either 20 ng/ml TRAIL alone for 2 h (Red) or 100 μ M OH14 for 1 h followed by 20 ng/ml TRAIL for 2 h (blue). Results represent the average of 10 cells on 1 experiment. Error bars in A-C represent standard error of the mean. D) Each data point represents a recording made on an individual HeLa cell. Bleaching occurred at each time point.

5.2.2.4 OH14 does not act by Reducing Overall c-FLIP Levels

To further confirm that our inhibitors act by interfering with protein interactions rather than overall protein levels, we wished to assess the levels of c-FLIP protein present during different treatment conditions. MCF-7 cells were cultured with vehicle control or OH14 at 100 μ M for 1 h before the addition of 20 ng/ml TRAIL or vehicle control for a further 2 h. Protein was extracted from MCF-7 cells post-treatment before being subjected to Western blotting (Figure 5.9A). No significant differences were observed between c-FLIP protein levels between treatments when normalised to GAPDH (Figure 5.9 B). Thus OH14 does not appear to alter c-FLIP expression or stabilisation of the protein.

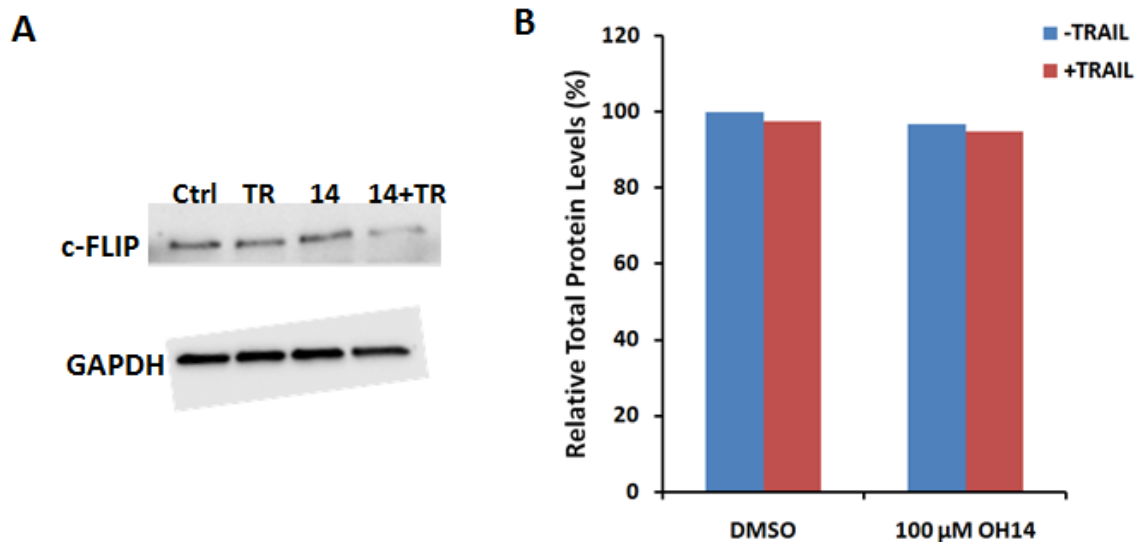


Figure 5.9: OH14 does not decrease c-FLIP protein levels

A) Western Blot: Total proteins were extracted from MCF-7 cells which had been subjected to various treatment conditions: Ctrl - 0.1% DMSO, TR - 20 ng/ml TRAIL for 2 h, 14 - 100 μ M OH14 for 3 h, 14+TR - 100 μ M OH14 for 1 h before the addition of 20 ng/ml TRAIL for a further 2 h. B) Densitometry analysis of total c-FLIP protein expression between MCF-7 cells treated conditions in A).

5.2.3 Generation of a c-FLIP TALEN Cell Line

In order to generate a stable c-FLIP knockout cell line, we transfected MCF-7 cells with TALEN constructs targeted to c-FLIP. Transfected cells were grown as single cell clones until enough cells were obtained for DNA extraction and PCR analysis. Following PCR evaluation, we used restriction digestion to analyse the potential clones (Figure 5.10A). We determined that the initial round of TALEN transfection successfully generated 4 potential c-FLIP heterozygote MCF-7 cell lines (Figure 5.10B) which required a second round of transfection with the TALEN constructs in order to attempt to generate a fully c-FLIP eliminated stable cell line.

Western blotting was performed on 4 of the potential heterozygotes as an additional confirmation of their reduced levels of c-FLIP (Figure 5.11A and B). Densitometry analysis of Western blots showed that clone 41 had the most reduced expression of c-FLIP and was therefore the clone of choice to undergo further evaluation and, subsequently, a second round of transfection (Figure 5.11C and D).

We have previously observed that overall c-FLIP levels within cells are not the reason for differences in sensitivity to TRAIL, rather it is possible that the subcellular localisation determines susceptibility (French *et al.*, 2015 in press) and thus, although our heterozygotes are likely to express a lower level of c-FLIP than wildtype cells, we did not expect to see a significant increase in TRAIL sensitivity in these cells until an elimination of c-FLIP was obtained. TRAIL sensitivity was tested using the Cell Titre Blue assay in the bulk population of untransfected MCF-7 and our TALEN cell clone 41. As hypothesised, no significant increase in TRAIL sensitivity was observed between the two cell lines using Cell Titre blue to measure cell viability (Figure 5.12).

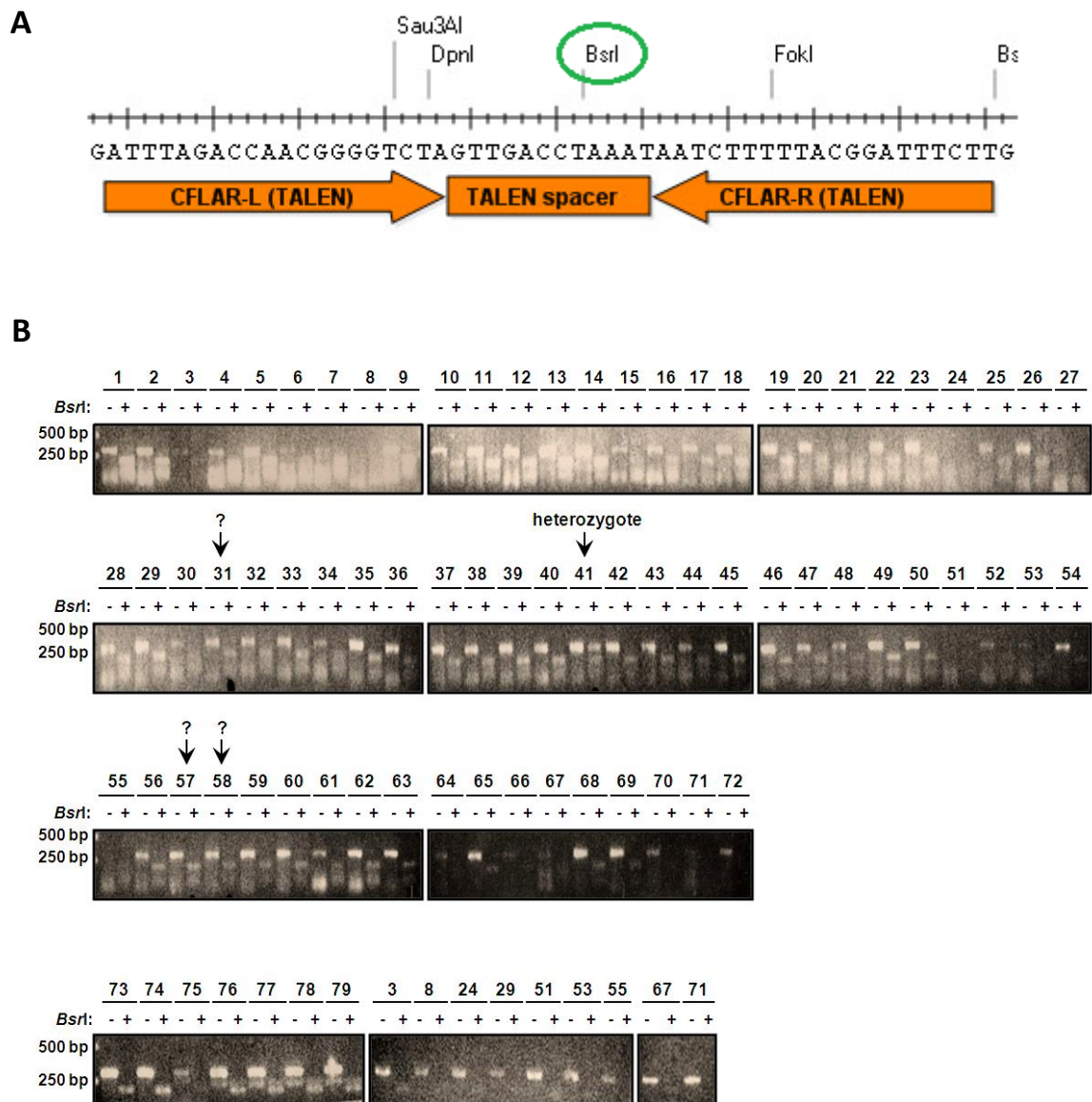


Figure 5.10: Analysis of clones from Initial round of MCF-7 TALEN transfection revealed potential c-FLIP heterozygotes.

A) TALENs were targeted to flanking sequences surrounding a unique restriction enzyme site to aid screening via *BsrI* restriction enzyme digest. Genomic DNA was extracted from transfected cells grown up from single cell clones. cFLIP was amplified (Methods 2.8.3.2) and the resulting DNA was amplified using *BsrI* restriction digestion. Samples successful for TALEN showed only 1 band, around 300 bp due to a lack of restriction digestion cleavage by *BsrI* within the TALEN spacer. Unsuccessful TALEN samples showed 2 bands, around 200 and 100 bp in size, due to cleavage by *BsrI* within the TALEN spacer site. Should TALEN be successful, two products will form, but if unsuccessful, DNA will be cut only at one site. B) Following genomic DNA extraction, 71 clones of MCF-7 cells transfected once with TALEN constructs were analysed by 2% agarose gel electrophoresis by *BsrI* cleavage. Arrows point to potential heterozygote clones.

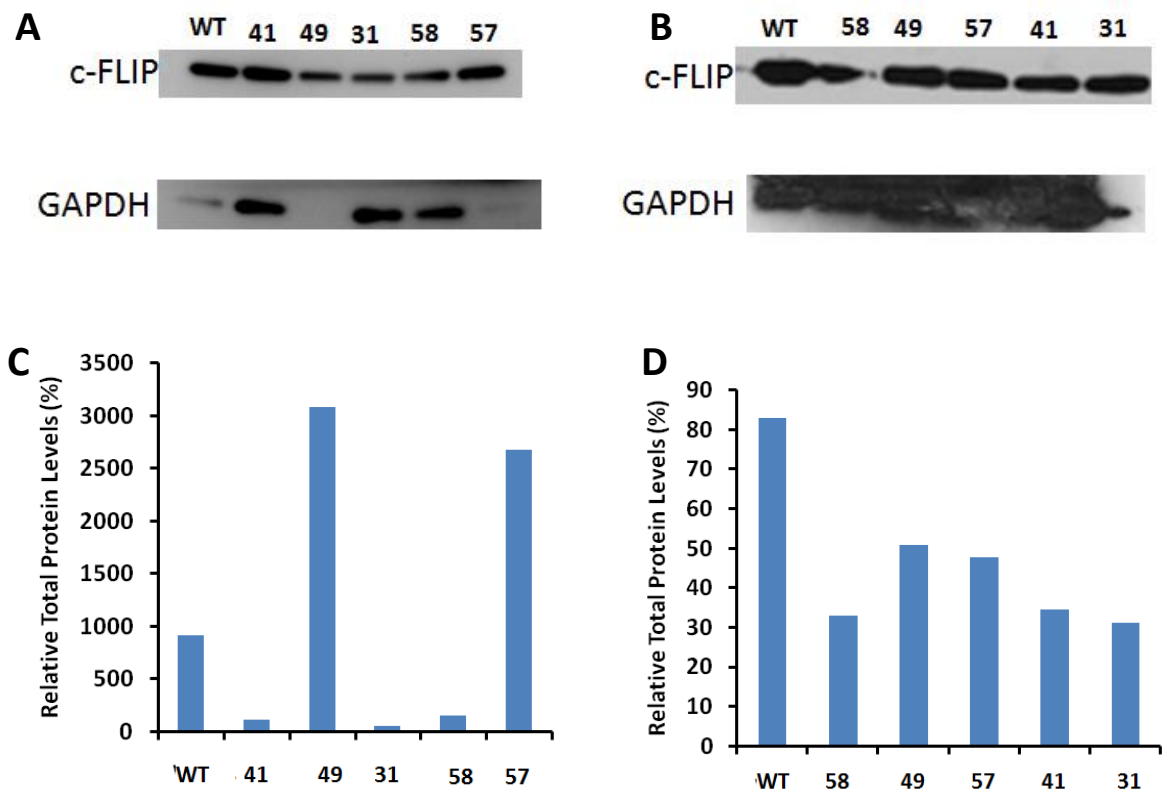


Figure 5.11: Western Blotting Confirms Reduced c-FLIP Protein in TALEN Transfected Cells

Western Blot: Total proteins were extracted from WT MCF-7 cells and our 4 TALEN heterozygote clones, and one non-heterozygote (49) as an additional negative control. A and B are repeats of the same cell samples. C & D) Densitometry was performed on the blots from A) and B) respectively, protein levels are relative to GAPDH.

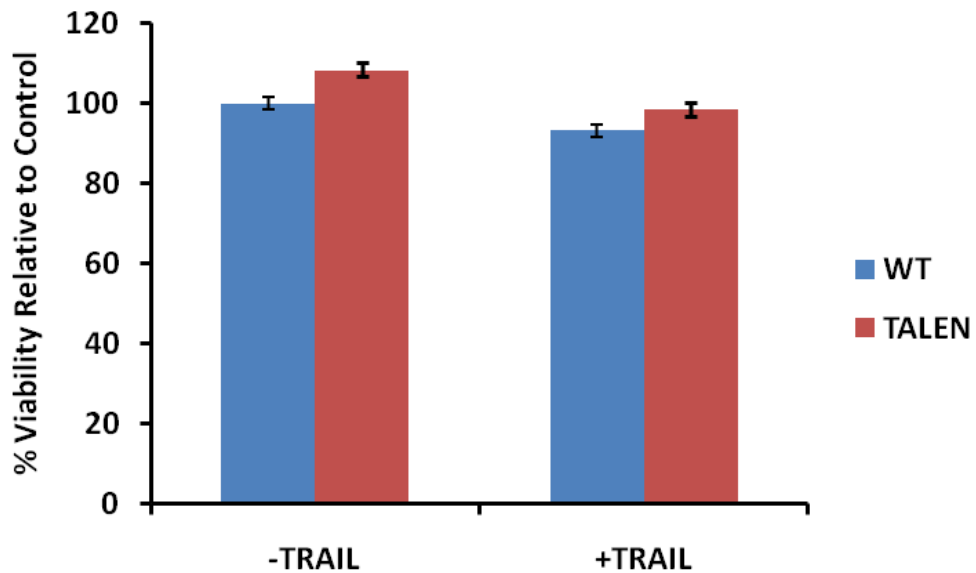


Figure 5.12: TRAIL sensitivity is not significantly increased after initial round of TALEN transfection in MCF-7 cells.

Untransfected MCF-7 cells (WT) and those subjected to one round of transfection with our TALEN c-FLIP constructs, and demonstrated to be the most well knocked down (TALEN - clone 41) were grown in adherent conditions to 70% confluence before being treated with 20 ng/ml TRAIL or vehicle control. Results represent a single experiment performed with 6 internal technical replicates. Error bars represent standard error of the mean.

5.2.3.1 Evaluation of Second Round of TALEN Transfected Cells

We performed a second round of transfection with the TALEN constructs on the clone identified to have the lowest c-FLIP levels in Section 5.2.3, clone 41. Transfection of TALEN constructs was performed in combination with mRFP for use in FACS sorting of transfected cells, in order to attempt to generate cells, and ultimately, a stable cell line, which were homozygous for the deletion of c-FLIP gene.

Clones from this second round were monitored during their growth and many were noted to have morphologies different to that of untransfected MCF-7 cells (Figure 5.13A and B). In addition, many of the clones had different proliferation rates to that of untransfected cells, with a few of the clones growing predominantly in colonies (Figure 5.13C and D). This may be due to the impact of removing c-FLIP from the cells, it may be as a by-product of the TALEN process overall, or may be as a result of using subclones of MCF-7 cells .

We analysed expression of successfully expanded clones using qPCR. qPCR analysis identified several clones with lower expression levels of c-FLIP relative to control, although none were identified with complete removal of the gene (Figure 5.14A). We then treated adherent cells of clone 40, which appeared to have the greatest c-FLIP reduction, with TRAIL, TALEN, however, no increase in TRAIL sensitivity was observed using the Cell Titre blue to assay cell viability (Figure 5.14B).

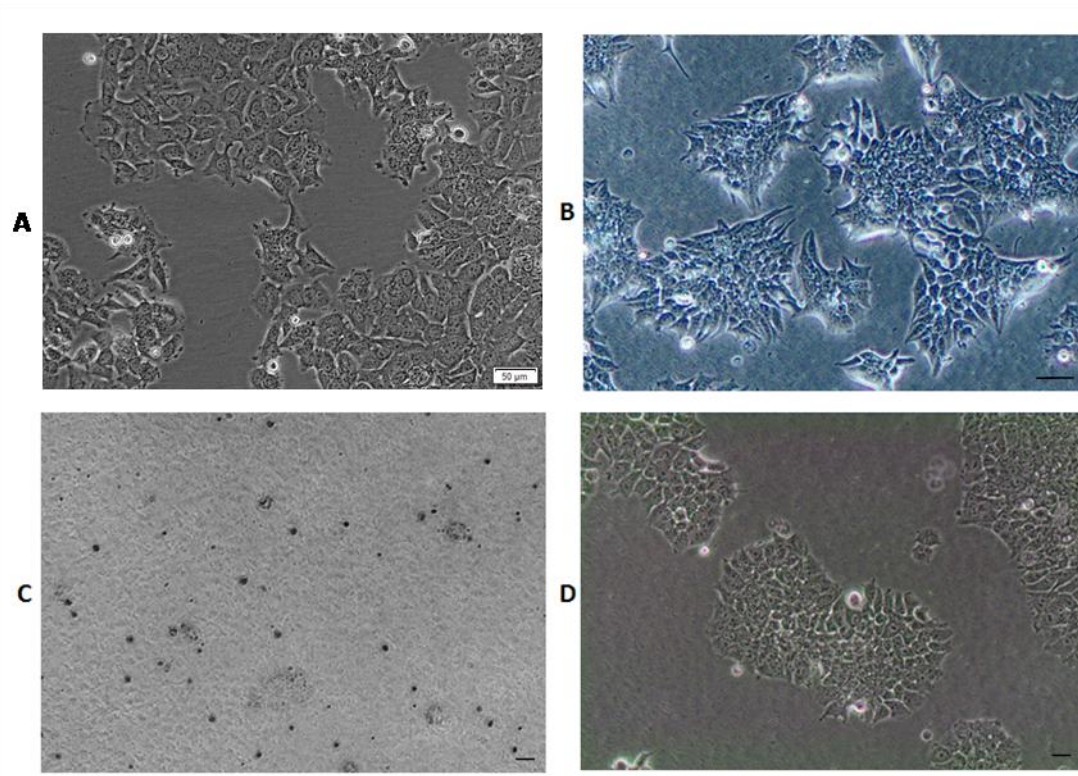


Figure 5.13: MCF-7 TALEN Double Transfected Cell Morphology and Growth Assessments.

The morphologies and growth rates of the TALEN clones varied considerably. A) Untransfected MCF-7 cells B) TALEN Clone 20 - mesenchymal-like morphology. C) TALEN Clone 13 - slow growth rate: small colonies with large amounts of cell death and resulting debris. D) TALEN clone 10 - cells grew in colonies with morphology similar to that of untransfected MCF-7s. Scale bar = 50 μm .

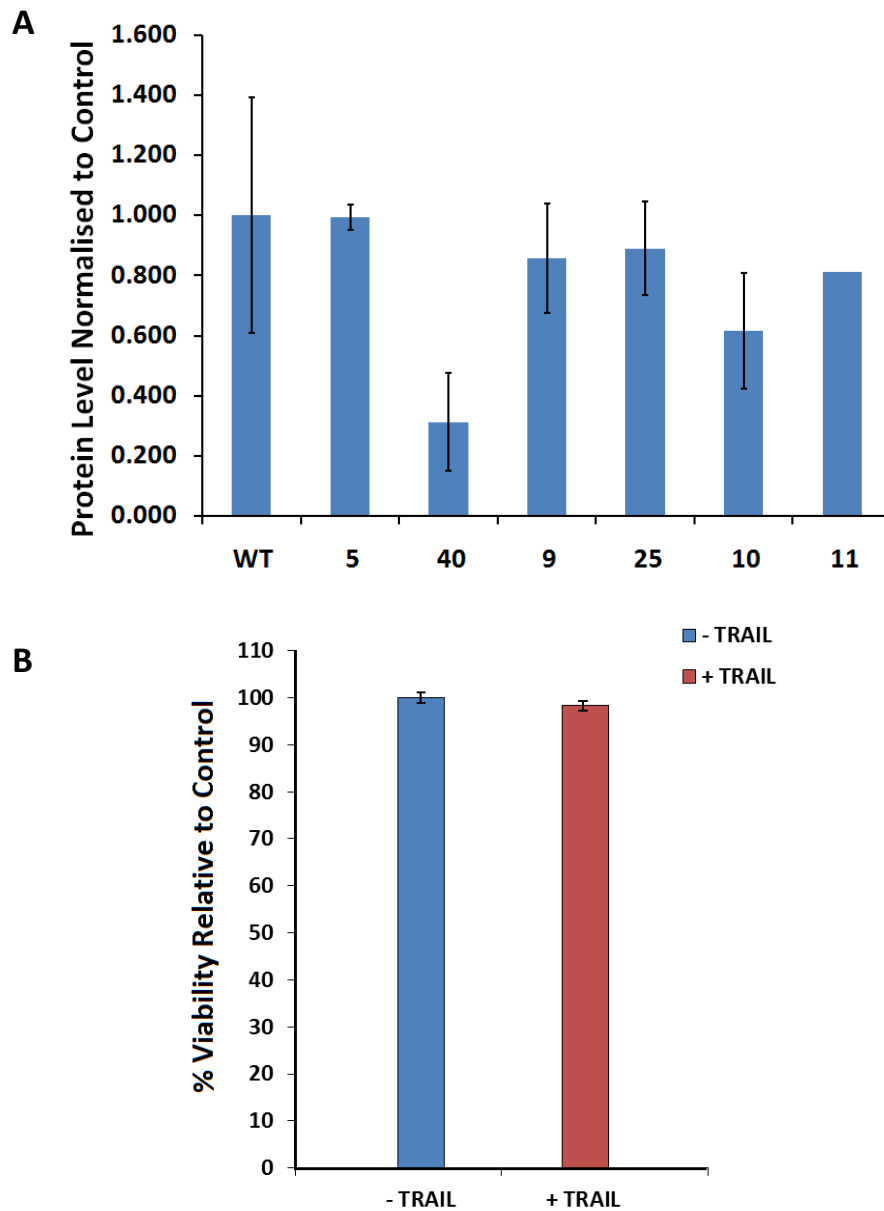


Figure 5.14: qPCR and Cell Viability Analysis of MCF-7 TALEN transfected cells from second round of transfection.

A) qPCR analysis of second round of transfection TALEN MCF-7 cells. B): TRAIL sensitivity of cells which had undergone the complete two rounds of TALEN transfection and selection. Clone 40 cells were cultured in a 96 wp for 24 h before the addition of 20 ng/ml TRAIL for 18 h. Cell Titre Blue was performed to measure cell viability. Results represent 3 technical replicates, error is presented as standard error of the mean.

5.2.4 Selection of Mutations for c-FLIP Mutational Studies

Currently, there are only two mutational studies performed on the DEDs of c-FLIP, which were published after the majority of the work in this project had been carried out (Hwang *et al.*, 2014; Majkut *et al.*, 2014), with studies involving mutations carried out on the structure of FADD being far more abundant (Section 1.3.7). We wished to further confirm the importance of the site on c-FLIPs DED1, which our inhibitors were designed to target. Analysis of this binding site identified several residues which play a key role in the interaction with FADD, based on our model (Chapter 3), these include; Methionine (Met) 1, Alanine (Ala) 3, Isoleucine (Ile) 6, Histidine (His) 7, Glutamic Acid (Glu) 10, Arginine (Arg) 38 and Arg 45 (Figure 5.15A).

We designed primers to target Ile 6, His 7, Arg 38 and Arg 45, initially, as these residues were identified to be important on our *in silico* model. Successful generation of constructs using these SDM primers has taken place (Figure 5.15B). We hypothesise that overexpression of wildtype c-FLIP in a c-FLIP knockout, and thus, TRAIL-sensitive cell line would confer a significant amount of protection to TRAIL induced apoptosis and, in contrast, overexpression of our mutants would not protect in the same way since they are designed to impede the c-FLIP:FADD anti-apoptotic interaction.

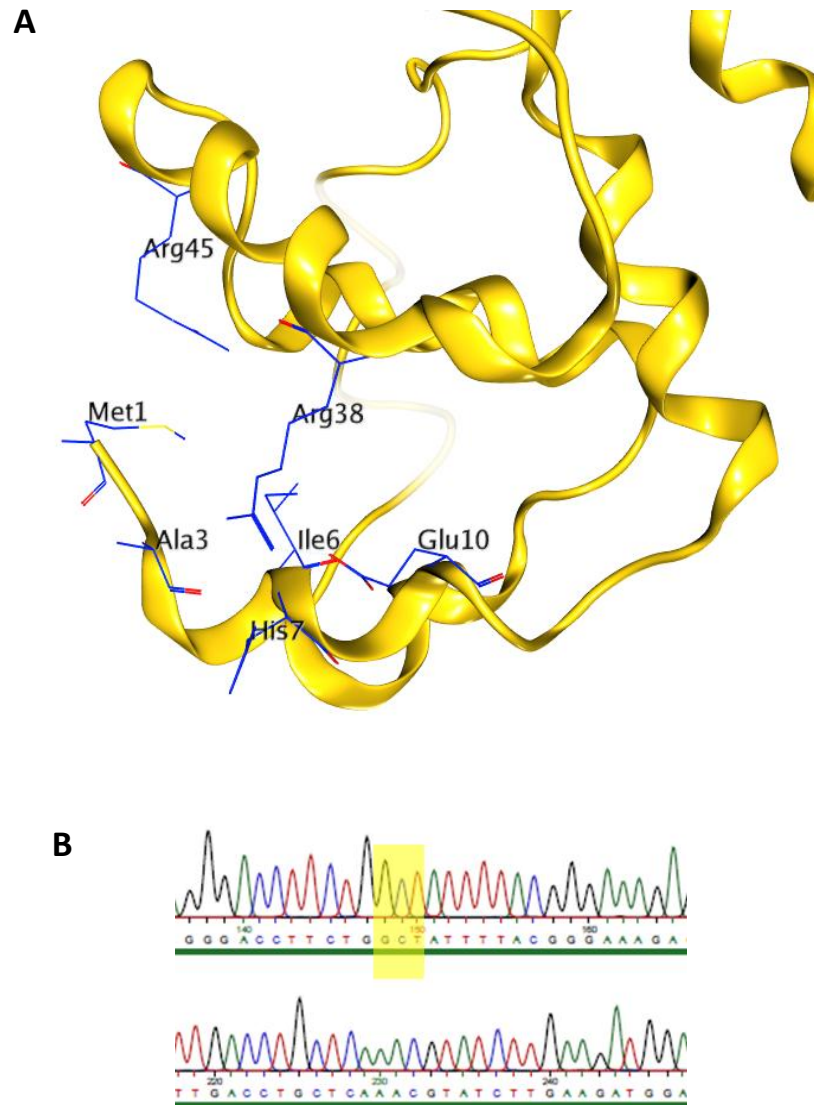


Figure 5.15: Interacting Residues in the c-FLIP DED1 Pocket and Generation of SDM Constructs.

A) Analysis of the interactive surface between c-FLIP and FADD, based on our interaction model, identify 7 residues which appear to have an integral role (Met 1, Ala 3, Ile 6, His 7, Glu 10, Arg 38 and Arg 45). B) Successful generation of c-FLIP mutants (representative sequencing result).

5.2.5 *In Vitro* Assay of CSC Plasticity

Studies have demonstrated the ability of non-stem cancer cells to de-differentiate into a stem cell-like state in what we and others have referred to as CSC plasticity (Section 1.1.7) (Gupta *et al.*, 2011; Chaffer *et al.*, 2011; French and Clarkson, 2012). Plasticity describes a state of flux between stem-like and non-stem-like sub-populations within a cancer cell field. Clinically, plasticity means that, even if all CSCs were eliminated from a cancerous population, any remaining bulk cells may have the ability to de-differentiate and therefore to become CSCs, thus enabling new tumour growth to occur. Therapeutic strategies should therefore take into account the need to either eliminate both stem-like and non-stem-like pools simultaneously, or to prevent the ability of cells to transition between these states.

The data from our lab, demonstrates that when combined with TRAIL, siRNA inhibition of c-FLIP, can *completely* eliminate tumoursphere-forming cells from breast cancer cell lines and that under these conditions, between 5% and 20% of the total cell population remains viable (Piggott *et al.*, 2011). This gives us the ability to study plasticity, since we have a viable population of non-CSCs with which to study the reacquisition of CSC-like activity.

We have previously reported that BT474 breast cancer cells treated with TRAIL and siRNA targeted to c-FLIP to eliminate tumoursphere forming cells, if allowed to recover in the absence of TRAIL in adherent conditions for 7 days regain the ability to form tumourspheres (Piggott *et al.*, 2011). We have re-capitulated this in MCF-7 cells, showing the kinetics of tumoursphere recovery over 7 days (Figure 5.16).

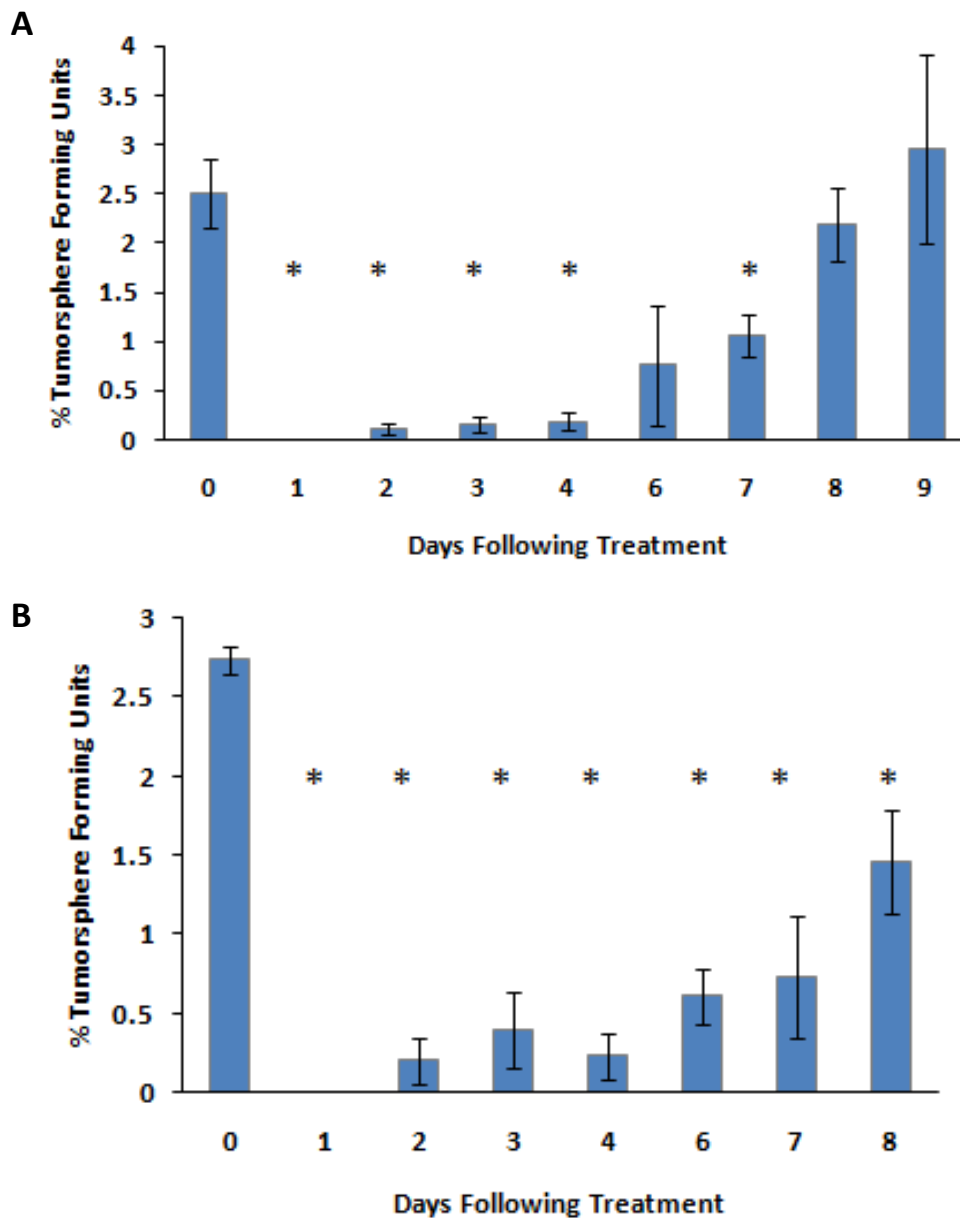


Figure 5.16: *In Vitro* Model of breast CSC Plasticity

MCF-7 cells were subjected to siRNA to c-FLIP for 48 h, after which TRAIL was administered at 20 ng/ml and cells were left for 18 h. Subsequently, cells were subjected to the tumoursphere assay to confirm complete elimination of tumourspheres (day 1). Remaining cells were seeded in adherent culture conditions and left to recover over 9 days, with tumoursphere forming ability being assayed each day by plating in tumoursphere conditions and counting after 7 days. A) Passage 1: siRNA c-FLIP successfully eliminated all tumourspheres initially, however, surviving cells regained the ability to form tumourspheres by day 2, with full tumoursphere forming ability restored after 9 days. B) Passage 2: Tumourspheres from passage 1 could be successfully passaged, however, formation did not reach the level of untreated spheres by day 9. Results are averages of three independent experiments, performed with three internal technical replicates (*= $p < 0.05$, t-test).

5.2.5 OH14 Impacts on MCF-7 Cell Plasticity after siRNA c-FLIP Treatment

The previous data (Figure 5.16) was generated using siRNA to c-FLIP thus, during the reacquisition of tumoursphere activity, c-FLIP mRNA levels would be no longer repressed due to the transient nature of siRNA knockdown. We wished to determine whether long term suppression of c-FLIP may impede the ability of cells to reacquire tumoursphere-forming ability in our assay of plasticity.

To test this we used our lead compound to retain the suppression of c-FLIP. Although the compound itself targets the c-FLIP:FADD interactive surface, it is possible that this inhibition is relevant to the role of c-FLIP in plasticity, in addition to the fact that binding of the compound itself may impact on the other functions of c-FLIP.

Following the elimination of tumourspheres using FLIPi and TRAIL, the surviving cells were plated in adherent conditions and treated with OH14 at 10 μ M for 7 days; replacing culture media and drug daily. Treatment of the surviving population with OH14 prevented the formation of tumourspheres after the 7 day 'recovery' period in comparison with cells which were left untreated, which recovered to around 50% on passage 1 (Figure 5.17). OH14 profoundly inhibited the clonal expansion of these residual viable cells in adherent culture (Figure 5.16). It is possible therefore that the lack of tumoursphere formation could be due to the inability of the cells to proliferate to form floating colonies.

In parallel work carried out by Luke Piggott, c-FLIP has been suppressed permanently by shRNA, which demonstrated the same inhibition of tumoursphere reacquisition (Piggott, L, personal communication). This confirms the c-FLIP specificity of this effect on plasticity.

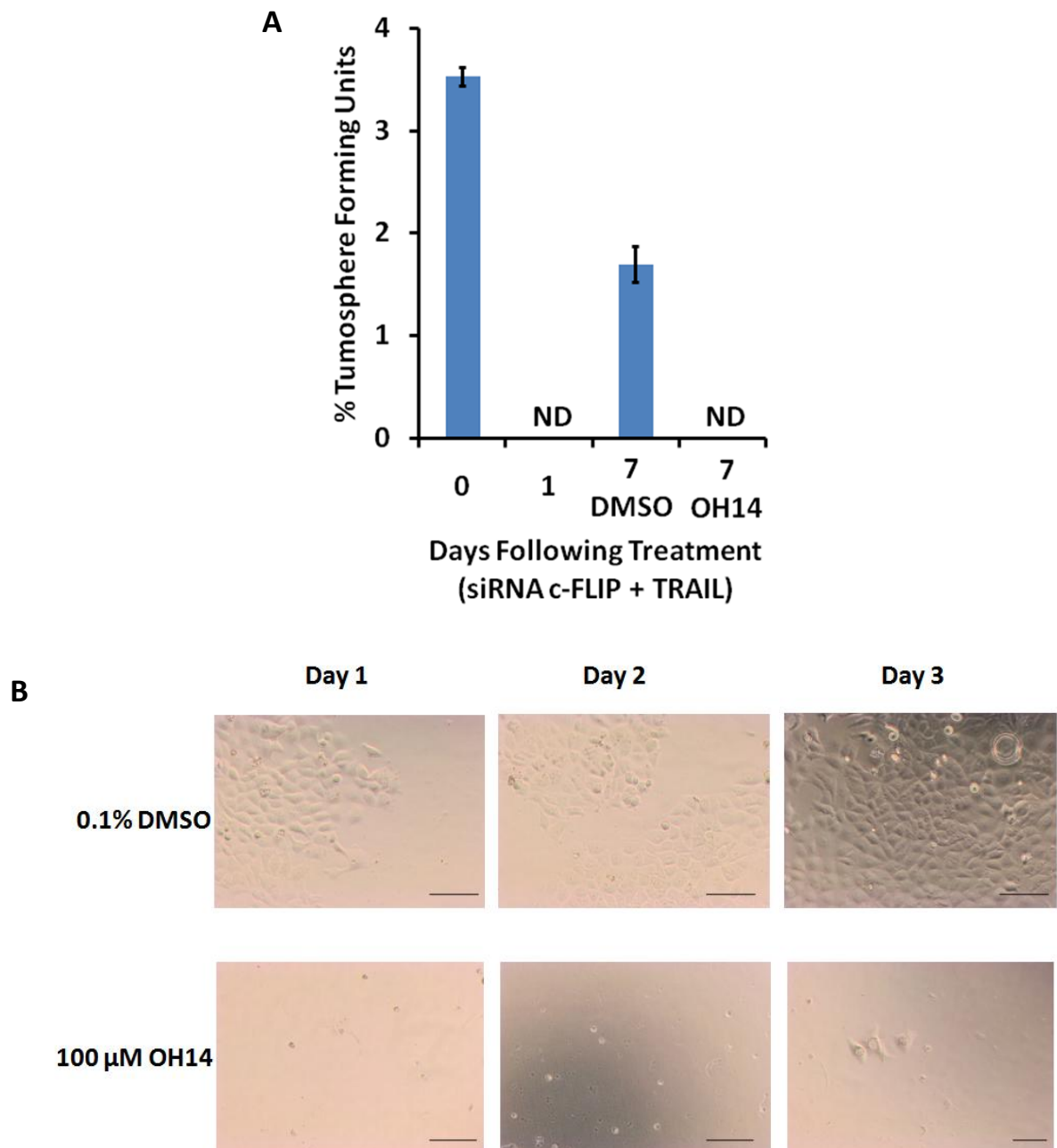


Figure 5.17: Treatment with Lead Compound OH14 Impairs Ability of Cells to reacquire Tumoursphere Forming Ability following FLIPi + TRAIL

MCF-7 cells which had been treated with c-FLIP siRNA for 48 h were treated with TRAIL for 18 h and then subjected to tumoursphere conditions to demonstrate complete loss of tumoursphere forming ability (A - Day 1). B) The remaining cell population were re-seeded in adherent conditions and left to recover for around 7 days with daily 0.1% DMSO or 100 μM OH14 treatment, after which tumoursphere forming potential was reassessed. C) Daily visual inspection of the cells in adherent culture prior to re-plating into the tumoursphere assay demonstrated that OH14 appeared to prevent the re-expansion of the cell population. Scale bars = 50 μm.

5.3 Discussion

Many studies have demonstrated the interaction between c-FLIP and FADD, in addition to the interaction between c-FLIP and procaspase-8, to play an integral role in TRAIL resistance (Irmeler *et al.*, 1997; Safa and Pollok, 2011; Safa *et al.*, 2012; Dickens *et al.*, 2012). In the previous chapters, we identified one lead small molecule, OH14, which can sensitise previously resistant breast cancer bulk; progenitor-like or colony-forming; and stem-like or tumoursphere-forming cells to TRAIL induced apoptosis. OH14 was initially selected *in silico* based on its ability to specifically bind to c-FLIP and prevent interaction with FADD. In this chapter, we performed evaluation of the biological interactions of c-FLIP and validated the mechanism of action of OH14 *in vitro*. In addition, we explored the effects of the lead inhibitor on another important process of cancer biology that c-FLIP may have a role in: cancer stem cell plasticity (Piggott *et al.*, 2011; French, 2014 unpublished).

Previous data has shown the presence of an interaction between c-FLIP and FADD, and of procaspase-8 and FADD in TRAIL-resistant and TRAIL-sensitive lines respectively (Safa and Pollok, 2011; Zhang and Fang, 2005; Sprick *et al.*, 2000; Medema *et al.*, 1997). Here, we confirm the presence of the latter interaction, in our biological system using co-immunoprecipitation in TRAIL-sensitive MDA-MB-231 cells and the lack of an interaction between c-FLIP and FADD, suggesting that this interaction is indeed important for TRAIL sensitivity, although these results will need to be compared with a TRAIL-resistant line, in addition to utilising our lead inhibitor within the experiment. Treatment with TRAIL over a four point timecourse on TRAIL sensitive MDA-MB-231 demonstrated an increase in cleaved (p43 and p18), and therefore active, caspase-8 over time, up to 2 h, after treatment with 100 ng/ml TRAIL. This is in accordance with previous studies which have demonstrated a similar increase caspase-8 cleavage upon treatment with TRAIL over time (Suliman *et al.*, 2001; Wang *et al.*, 2008). In contrast, no increase in p43 caspase-8 was observed in the TRAIL-resistant MCF-7s, suggesting TRAIL induced caspase-8 activation was indeed prevented. Previous studies have demonstrated similar findings in TRAIL-resistant cell lines, including in colon cancer, whereby TRAIL treatment in a TRAIL-resistant line showed significantly less caspase-8 cleavage than in a TRAIL-sensitive line (Zhang *et al.*, 2005). FADD and c-FLIP protein levels were confirmed to be similar between the two lines, despite their differing TRAIL

sensitivities, thus, sensitivity may instead be due to differential localisation of c-FLIP in sensitive versus resistant cells. Our lab has recently demonstrated the importance of subcellular localisation, rather than overall protein levels, of c-FLIP to be most important for its anti-apoptotic role. These recent results demonstrated that TRAIL-resistant cell lines express c-FLIP predominantly in the cytoplasm, whereas c-FLIP is confined to the nucleus in those which are TRAIL-sensitive. Furthermore, when c-FLIP localisation was assessed in the tumoursphere forming cells of these same cell lines, the partially sensitive tumoursphere-forming cells of the MCF-7 cell line expressed c-FLIP in the nucleus, in contrast to the bulk cells, which showed nuclear expression of c-FLIP (French *et al.*, 2015 in press).

Our hypothesised mechanism of action, based on *in silico* drug design, was that OH14 directly inhibited the interaction between c-FLIP and FADD. Here we have shown, using acceptor-photobleaching FRET-based confocal microscopy, that our lead inhibitor, OH14 did indeed significantly reduce interactions between c-FLIP and FADD in TRAIL stimulated TRAIL-resistant HeLa and MCF-7 cells. The constructs themselves induced cell death, which was prevented by use of a caspase-inhibitor. Indeed, several studies have shown similar results, demonstrating that transient expression with FADD leads to increased activation of apoptotic pathways, even in the absence of TRAIL, which can be blocked by a pan-caspase inhibitor (Siegel *et al.*, 1998; Grunert *et al.*, 2012; Matsumura *et al.*, 2000; Gomez-Angelats and Cidlowski, 2003), although the reason that expression of c-FLIP:YFP induced caspase-dependent cell death is unclear. As our FRET experiments were based on live cells, we did obtain a large degree of variation in responses which is in accordance with the fact that interactions in a biological system are dynamic: they may be transient and frequently altering with fluctuations in protein interaction kinetics (Li *et al.*, 2011). Despite this, we have been able to observe an overall trend in our data, although it is unlikely to be true for 100% of the cells in a population. In future, our FRET constructs may be used to perform mutational studies in order to elucidate the importance of our identified interacting residues using FRET.

Since TRAIL acts via the extrinsic caspase-mediated pathway of apoptosis, leading to the activation of caspase-8 (Section 1.2), we hypothesised that a specific inhibitor which sensitises to TRAIL would therefore, increase caspase-8 activity, and, thus blocking caspase activity would inhibit this effect. Our data suggest that our

inhibitors are indeed specifically acting in this manner, as we have shown that pre-treatment with a pan-caspase inhibitor significantly impaired the ability of our compounds to sensitise to TRAIL. In addition, we have observed a modest, yet significant, increase in caspase-8 activity upon treatment of our lead compound in combination with TRAIL, further confirming this mechanism of action.

We have identified, using our *in silico* interaction models, several residues on the interactive pocket of c-FLIP which appear important for the anti-apoptotic interaction with FADD, and, as such, were targeted with our small molecule inhibitors. Here, we have attempted to generate a stable c-FLIP knock-out cell line, using TALEN technology, to analyse our identified residues. Cell clones which had reduced c-FLIP levels and survived the second transfection had significantly altered morphology and proliferation rate, and many did not survive passaging. Those clones which did survive the second transfection did indeed exhibit reduced c-FLIP levels, as measured by qPCR, but did not show an increased sensitivity to TRAIL using an assay of cell viability. It may be that despite the reduction in c-FLIP levels induced by this double transfection, the phenotype of the cells was further altered, either by inhibition of c-FLIP or subclonal expansion, which prevented any significant change in TRAIL sensitivity being observed. Furthermore, as c-FLIP was not completely eliminated from these cells, the remaining c-FLIP may have been sufficient to retain their TRAIL resistance, as we have recently demonstrated that c-FLIP mediated TRAIL-sensitivity may be due to c-FLIP localisation rather than expression levels (French *et al.*, 2015 in press), thus, only a total elimination of c-FLIP would be likely to cause a significant sensitisation to TRAIL. Additionally, it is possible that use of TALEN to modify the genes itself has compromised cell viability, since TALEN does not release the ends it has bound to immediately after cleavage, DNA repair may be interfered with thus potentially inducing cell death (Beumer *et al.*, 2013; Mali *et al.*, 2013). Furthermore, our TALEN constructs targetted an area within exon 4 of c-FLIP (nucleotides 935-946, approximately amino acids 148-151), toward the middle of DED2 on c-FLIP (Methods, Figure 2.9). It is possible that targetting this site, around 30% into the sequence of c-FLIP, may not be sufficient to knock down the whole protein, especially since it is DED1 and 2 that are important for TRAIL resistance, thus, it may be that these domains remain intact and available to retain the anti-apoptotic role of c-FLIP. Since c-FLIP was not completely eliminated, it would have been more relevant

to assess the clones using FRET to evaluate whether there was a reduction in interactions, however, since the proliferation of the transfected cells was altered, the majority of cells did not survive additional transfection and plating on FRET assay plates, and would not have survived laser bleaching. Further work is required to ascertain an appropriate assay or optimum clone for performing mutagenesis studies.

The ability of a cancer therapy to prevent CSC plasticity is clinically desirable, as, when combined with a treatment to eliminate bulk tumour cells, a CSC and chemotherapy combination therapeutic regime may have the potential to destroy the original tumour whilst also preventing relapse (Vinogradov and Wei, 2012; Han *et al.*, 2013; Frank *et al.*, 2010). Although OH14 was designed to target the c-FLIP:FADD interaction, long-term treatment with the compound may abrogate additional functions of c-FLIP, perhaps due to compound binding at one site inducing conformational changes at other protein domains. We have observed here, that OH14 may have potential efficacy for targeting CSC plasticity in our *in vitro* model of the process. After elimination of tumoursphere-forming cells using siRNA c-FLIP, we observed that daily OH14 treatment of the remaining viable cells, replated in adherent conditions prevented growth compared with vehicle control treated cells. Prolonged treatment of OH14 does not affect overall cell viability (Chapter 4), however, it does result in a modest, yet significant reduction in tumoursphere forming ability, in contrast to a single overnight treatment, which did not significantly alter tumourspheres (Chapter 4). Section 4.2.6 explored the effect of long-term treatment with OH14, which demonstrated a lack of overall cytotoxicity, although a slowing of proliferation was observed, it is possible, therefore, that treatment with OH14 effects a more gradual process, such as plasticity, and prevents reacquisition of breast CSCs or progenitor cells, thus leading to the ultimate death of the surviving population, which require breast CSCs to propagate and proliferate. A repeat of our plasticity study using stable c-FLIP inhibition, for example, using shRNA is required as an appropriate control to make more definite conclusions about the actions of OH14 in plasticity. Since c-FLIP in combination with TRAIL induces the extrinsic pathway of apoptosis, it is likely that bCSCs are lost by cell death. We will address this in future using the pan-caspase inhibitor Z-VAD-FMK, to determine whether treatment with the caspase-inhibitor can rescue tumoursphere

ablation. Alternatively, it is possible that cells which survive FLIPi/TRAIL are quiescent, which may be assessed using flow cytometry of pyronin γ and hoescht (Shapiro 1981).

In conclusion, we have demonstrated that our lead compound OH14 was able to sensitise to TRAIL through direct interference with the c-FLIP:FADD interaction and therefore, facilitated TRAIL-induced apoptosis through a caspase-mediated pathway, leading to activation of caspase-8. We have observed that the effects of our inhibitor may be even more clinically important than initially evaluated, as the inhibitor appeared to prevent CSC plasticity, in our *in vitro* model.

Chapter 6

Biological Evaluation of OH14 Analogues

Chapter 6: Biological Evaluation of OH14 Analogues

6.1 Introduction

Agents which have been demonstrated to have an ability to sensitise to TRAIL, via effects, albeit non-specific, on c-FLIP are often seen to be working at relatively high, micromolar, concentrations (Chen *et al.*, 2010, Rao-Bindal *et al.*, 2014; Li *et al.*, 2013) (Section 1.3.6), and exhibiting a high IC₅₀, *i.e.* the concentration required to achieve 50% inhibition of a specific target. Reducing the dose of c-FLIP inhibitor required to achieve such effects is beneficial in terms of improving any potential safety and tolerability issues that may result from treatment.

We selected compound OH14 as our lead compound after thorough biological evaluation using assays of cell viability, proliferation, and stem cell functionality performed in Chapter 4 and evaluation of the mechanism of action in Chapter 5. Subsequently, in this Chapter, we both obtained (from SPECS database) and generated (in house at Cardiff School of Pharmacy) analogues of OH14 to be tested in relevant, high-throughput assays, with the aim of identifying compounds which have similar efficacy to OH14 but exhibited lower effective working concentrations, as we have previously observed OH14 to function best at >10 micromolar concentrations. Due to the fact we will evaluate multiple compounds, we wanted to select an assay that was both relatively high-throughput and representative of the TRAIL-sensitising ability of our compounds. The clonogenic or colony forming assay was selected for this purpose, as it was demonstrated, in Chapter 4, to produce results which correlated well with both bulk cell viability and tumoursphere forming ability in both MCF-7 and BT474 cell line models. This fits in with the output of the assay being a progenitor-like proliferation assay, thus encompassing two of the features of cell viability and tumoursphere forming assays. Analogues of OH14 will help us to establish an initial structure-activity relationship for our compounds which will help us to further refine analogue generation in the future.

Here, we have tested a series of 39 analogues of OH14 for their ability to increase the sensitivity of breast cancer colony forming cells to TRAIL. We have successfully identified around 7 analogues which exhibit a similar or improved efficacy as OH14.

6.2 Results

We obtained 8 analogues of OH14 from Specs database and 29 analogues of OH14 were synthesised in house at Cardiff School of Pharmacy, by Gilda Giancotti, in order to identify potential analogues with similar or improved efficacy than OH14.

6.2.1 SPECS Based Analogues

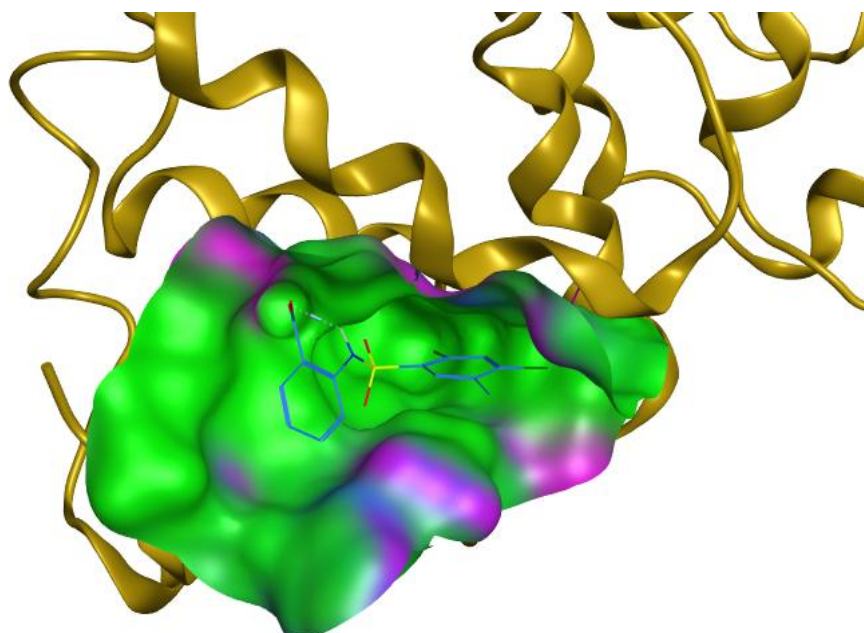
Initially, 8 analogues of OH14 (Termed 14.1-14.9, 14.2 is the same as compound OH14) were identified and obtained from Specs (Table A6.1, appendix). These compounds were selected as they were 90% identical to OH14 and retained the important sulphonamide group but had alterations in the aromatic rings and side groups.

6.2.2 OH14 Synthesis and Analogue Design

After identifying OH14 as our lead compound, in-house synthesis of the compound was begun at Cardiff School of Pharmacy (performed primarily by Gilda Giancotti). The method of synthesis (appendix section A6.1) followed a previously described method of synthesis for similar chemical structural compounds (Peifer *et al.*, 2007).

The lead compound, OH14, was predicted to form hydrogen bonds with several key amino acid residues on c-FLIP, including Glu 10, Lys 18, Arg 38 and Arg 45, amongst others (Figure 6.1). Analogues of OH14 were therefore selected and designed to so that these or similar bonds were formed, as evaluated by entering in the structure of analogues on the *in silico* structure of c-FLIP and assessing the compounds affinity to these residues.

A



B

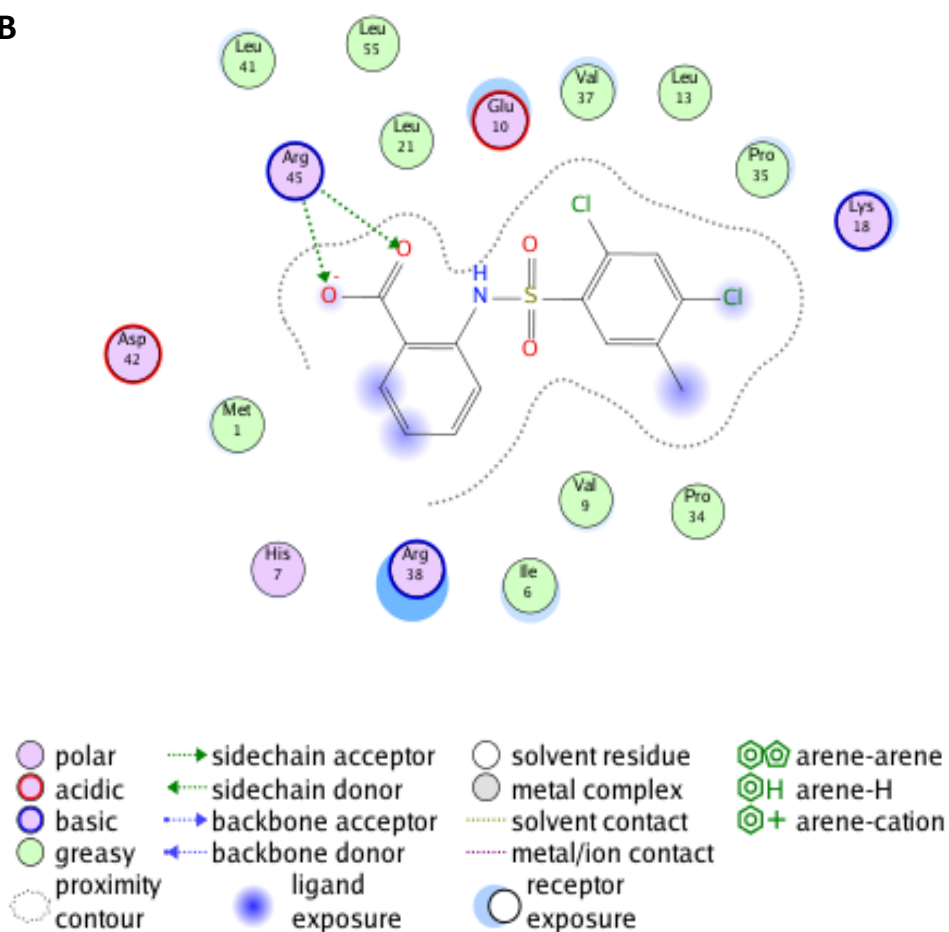


Figure 6.1: Ligand interaction of Compound OH14 in the predicted binding pocket on c-FLIP

A) Predicted binding pocket on surface of c-FLIP DED1 with lead compound OH14 docked. Part of c-FLIP is shown in yellow ribbon format. Compound OH14 is presented in ball and stick format. B) Ligand interaction diagram of OH14 in c-FLIP pocket, with relevant key.

6.2.3 Analogue Modifications and Synthesis

The sulphonamide group on OH14 was identified as a highly important component of the compound for binding with the pocket on c-FLIP, and thus, this group was to be retained on all analogues. Alterations to the aromatic rings were therefore the most logical first points of modification. A range of hydrophobic groups were chosen to replace the two chlorine and methyl groups present on OH14 (R), in order to elucidate whether alternative hydrophobic groups at different positions on the aromatic ring could increase fit within the pocket and overall stability of the compound within solution and within the pocket. Additionally, replacing the carboxylic acid with a methyl ester group on the other aromatic ring (R¹) was considered (Figure 6.2). A methyl ester group was considered due to its hydrophobicity, which could facilitate cell permeation through the lipid cell membrane in addition to the fact that, once through the membrane, in a more hydrophilic environment, ester hydrolysis to carboxylic acid would occur, thus re-enabling interactions with amino acid residues on c-FLIP. This methyl ester would be synthesised to occupy varying positions on the aromatic ring to fully explore whether alternative reactions with other amino acids on c-FLIP may occur and subsequently improve the affect of the compound.

Twelve analogues of OH14 were initially designed which conserve the central sulphonamide group which connects the two aromatic rings (Previous Figure 6.3) but have a variety of substitutions on the aromatic rings (Table 6.2). Synthesis of the analogues was similar to OH14 synthesis (appendix A6.2).

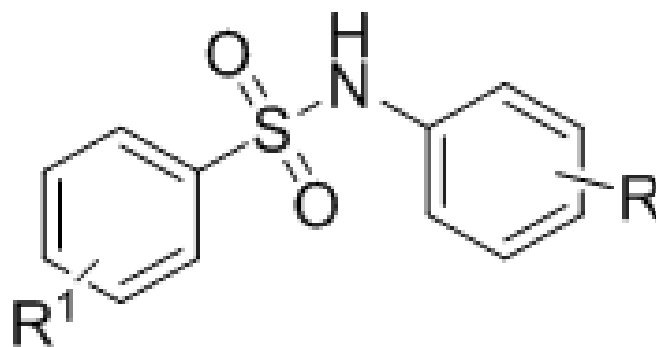


Figure 6.2: Central Scaffold for Pharmacy Synthesised Analogues of OH14

R and R¹ represent the two groups to be modified by the addition of either a range of hydrophobic groups (on R) or a methyl ester (on R¹).

Table 6.1: Aromatic Ring Substitutions for Pharmacy Synthesised Analogues of OH14

Compound	R	R ¹
GG1	2-methyl ester	2,4-dichloro-5-methyl
GG2	3-methyl ester	2,4-dichloro-5-methyl
GG3	4-methyl ester	2,4-dichloro-5-methyl
GG4	2-methyl ester	4-trifluoromethyl
GG5	2-methyl ester	3,4-dimethyl
GG6	2-methyl ester	3,4-dichloro
GG7	2-methyl ester	2,4-dichloro
GG8	2-methyl ester	2,4-dimethyl
GG9	2-methyl ester	2,5-dimethyl
GG10	2-methyl ester	2,5-dichloro
GG11	2-methyl ester	4-tert-butyl
GG12	2-methyl ester	4-methyl-3-chloro

6.2.3.1 Cardiff School of Pharmacy Synthesised Analogues

Two sets of analogues were synthesised by Gilda Giaccotti at Cardiff School of Pharmacy. Pharmacy synthesised compounds, GG 1-12 featured modifications discussed in section 6.2.3 (Table A6.2, appendix). The additional 17 Pharmacy Synthesised analogues, termed N1-17 in the results section (Table A6.3, appendix) followed similar structural substitutions to those explained previously, for compounds GG1-12 and were produced by Mahmoud El-Hiti.

6.3 Analogue Analysis

6.3.1 Compound Solubility

The solubility of all the compounds in cell culture media was assessed as in Section 4.2.1 in order fully understand the properties and thus, the effects, of these compounds. Ideally, compounds would all be soluble when dissolved at 100 mM in DMSO and subsequently in aqueous cell media to aid biological evaluation. At this point, we also wished to establish whether OH14 was soluble directly in sterile water, as this would eliminate the need for DMSO and would thus allow higher concentrations to be tested without risking toxicity to cells due to high percentage of DMSO. OH14, however, did not dissolve in water and required a minimum of 10 μ l DMSO to 1 ml water/media in order to dissolve.

All of the SPECS analogues of OH14, 14.1-14.9, dissolved at 100 mM in DMSO and remained in solution when further diluted in cell culture media (Table 6.2). Analogues N1-17, synthesised by Cardiff School of Pharmacy, did not all remain in solution (Table 6.3). All but one of the GG1-12 analogues, synthesised by Cardiff School of Pharmacy, all dissolved at 100 mM in DMSO and in subsequent aqueous media dilutions to make up working stock (Table 6.4).

Table 6.2: Solubility of SPECS Analogues of OH14

Visual assessment of compound solubility in DMSO or after overnight incubation in media (100 μ M, 10 μ M, 1 μ M, 100 nM, 10 nM). '✓' indicates no detected problems with solubility.

Compound	100 mM in DMSO	100 μ M in Aqueous Media
14.1	✓	✓
(14.2 = OH14)	✓	✓
14.3	✓	✓
14.4	✓	✓
14.5	✓	✓
14.6	✓	✓
14.7	✓	✓
14.8	✓	✓
14.9	✓	✓

Table 6.3: Solubility of Pharmacy Synthesised Compounds N1-17

Visual assessment of compound solubility in DMSO or after overnight incubation in media (100 μ M, 10 μ M, 1 μ M, 100 nM, 10 nM). '✓' indicates no detected problems with solubility.

Compound	100 mM in DMSO	100 μ M in Aqueous Media
N1	✓	Soluble at ≤ 10 μ M
N2	✓	Soluble at ≤ 10 μ M
N3	50 mM	Soluble at ≤ 10 μ M
N4	✓	Soluble at ≤ 10 μ M
N5	✓	Soluble at ≤ 1 μ M
N6	✓	Soluble at ≤ 1 μ M
N7	✓	✓
N8	✓	✓
N9	✓	Soluble at ≤ 10 μ M
N10	✓	Soluble at ≤ 10 μ M
N11	✓	✓
N12	10 mM	Soluble at ≤ 10 μ M
N13	✓	Soluble at ≤ 10 μ M
N14	✓	Soluble at ≤ 10 μ M
N15	✓	Soluble at ≤ 1 μ M
N16	✓	Soluble at ≤ 0 μ M
N17	10 mM	Soluble at ≤ 10 μ M

Table 6.4: Solubility of Pharmacy Synthesised Compounds GG1-12

Visual assessment of compound solubility in DMSO or after overnight incubation in media (100 μ M, 10 μ M, 1 μ M, 100 nM, 10 nM). '✓' indicates no detected problems with solubility.

Compound	100 mM in DMSO	100 μ M in Aqueous Media
GG1	✓	Soluble at ≤ 10 μ M
GG2	✓	✓
GG3	✓	✓
GG4	✓	✓
GG5	✓	✓
GG6	✓	✓
GG7	✓	✓
GG8	✓	✓
GG9	✓	✓
GG10	✓	✓
GG11	50 mM	✓
GG12	✓	✓

6.3.2 Testing the Efficacy of Novel Compounds

Chapter 4 utilised several assays for the evaluation of inhibitor efficacy however, the clonogenic or colony forming assay (CFA) was chosen to evaluate the new inhibitors initially as it provides the most representative combined result for the compounds when compared with the cell viability and tumoursphere assays. Additionally, it is easily replicated for testing multiple compounds and requires relatively little resources in comparison. The tumoursphere assay was utilised after initial clonogenic testing, as it provides the most representative result for stem cell survival *in vitro* and was the assay in which the most profound effects have been previously observed for both siRNA c-FLIP and for our compounds. Analogues, like OH14, were considered to be efficacious if they significantly increased sensitivity to TRAIL, without being significantly toxic when administered alone.

6.2.1.1 SPECS Analogues of OH14: Colony Forming Assay

The 8 SPECS analogues of OH14 were tested in MCF-7 and BT474 cells using the colony forming assay at 100 μ M initially, as this was the dose of OH14 which we established to be the most affective in several assays (Chapter 4).

Overall, the analogues exhibited similar effects on MCF-7 (Figure 6.3A) and BT474 (Figure 6.3B) colony forming cells, with 6 compounds demonstrating similar efficacy to OH14 (compounds 14.3, 14.4, 14.6, 14.7 and 14.8) and compound 14.9 demonstrating a modest improvement on the activity of OH14 in both cell lines. Compounds 14.3, 14.4, 14.7 were less active in BT474 cells, with only 14.8 and 14.6 demonstrating a significant ability to sensitise to TRAIL. In both cell lines, compounds 14.1 and 14.5 showed no significant difference from TRAIL alone. 14.7 in both cell lines reduced colony-formation ability when administered alone, and yet did not significantly improve on the effect of TRAIL.

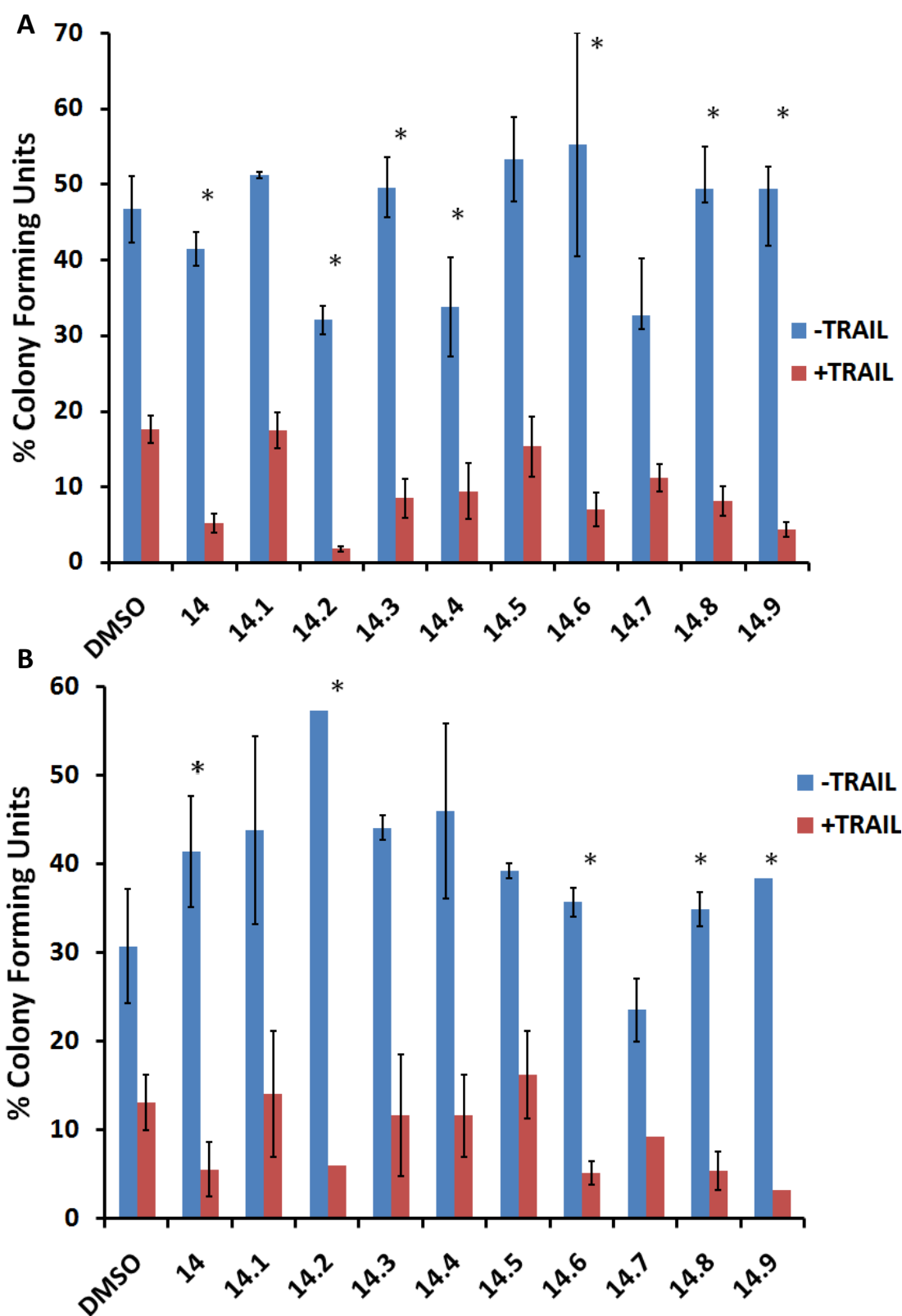


Figure 6.3: Specs Analogues 14.1-14.9 in combination with TRAIL have similar effects on colony growth of MCF-7 and BT474 cells.

Specs Analogues 14.1-14.9 (14.2 = newer preparation of OH14) at 100 μ M on A) MCF-7 and B) BT474 cells plated at 50 cells per cm^2 and left to grow for 10 days before colonies were counted. Results represent at least 3 individual biological repeats. *=p-value<0.05, t-test between TRAIL and compound + TRAIL.

6.2.2.2 SPECS Analogues of OH14: Tumoursphere Assay

The stem cell compartment of a tumour is the ultimate target of a c-FLIP inhibitor and TRAIL combination therapy, thus, the analogues were also analysed using the tumoursphere assay.

When plated in tumoursphere conditions, cells treated with 4 of the 8 new analogues did not significantly improve on the TRAIL-sensitising effect of OH14 on MCF-7 tumoursphere forming cells. Compounds 14.6, 14.7 and 14.8 significantly increased MCF-7 tumoursphere forming cell TRAIL sensitivity, although to a smaller degree than OH14 (Figure 6.4A). Compound 14.9 showed a modest improvement on the TRAIL-sensitising ability of OH14, similar to that observed in the colony forming assay (Section 6.2.2.1).

The compounds were slightly more effective on BT474 tumoursphere-forming cells, with 6 of the 8 compounds showing an ability to sensitise to TRAIL (Figure 6.4B). Compounds 14.3 and 14.4, which were not efficacious in MCF-7 cells did show an ability to sensitise to TRAIL, although the effect with 14.4 appeared additive due to the effect of the compound when administered alone. Compound 14.9 again was the most effective analogue, sensitising to TRAIL by approximately 50%, similar to OH14. Interestingly, 14.7, which previously reduced colony-forming number alone on both MCF-7 and BT474 cells did not exhibit this same effect but did exert a small yet significant ability to sensitise BT474 tumoursphere forming cells to TRAIL.

A modest alteration in tumoursphere forming ability was observed for some compounds when administered alone, particularly on BT474 tumoursphere-forming cells, however, the effect of the effective most effective compounds (14.6, 14.7, 14.9) in combination with TRAIL did appear synergistic rather than additive across both cell lines. Overall, the effect of our analogues when analysed in the tumoursphere assay appeared to follow a similar trend to the colony-forming assay, further demonstrating the assay to be a good surrogate test to give an initial idea about the efficacy of analogues. Across both the tumoursphere and the colony forming assays, in both cell lines tested, 14.9 showed consistent efficacy, with a modest improvement on the activity OH14.

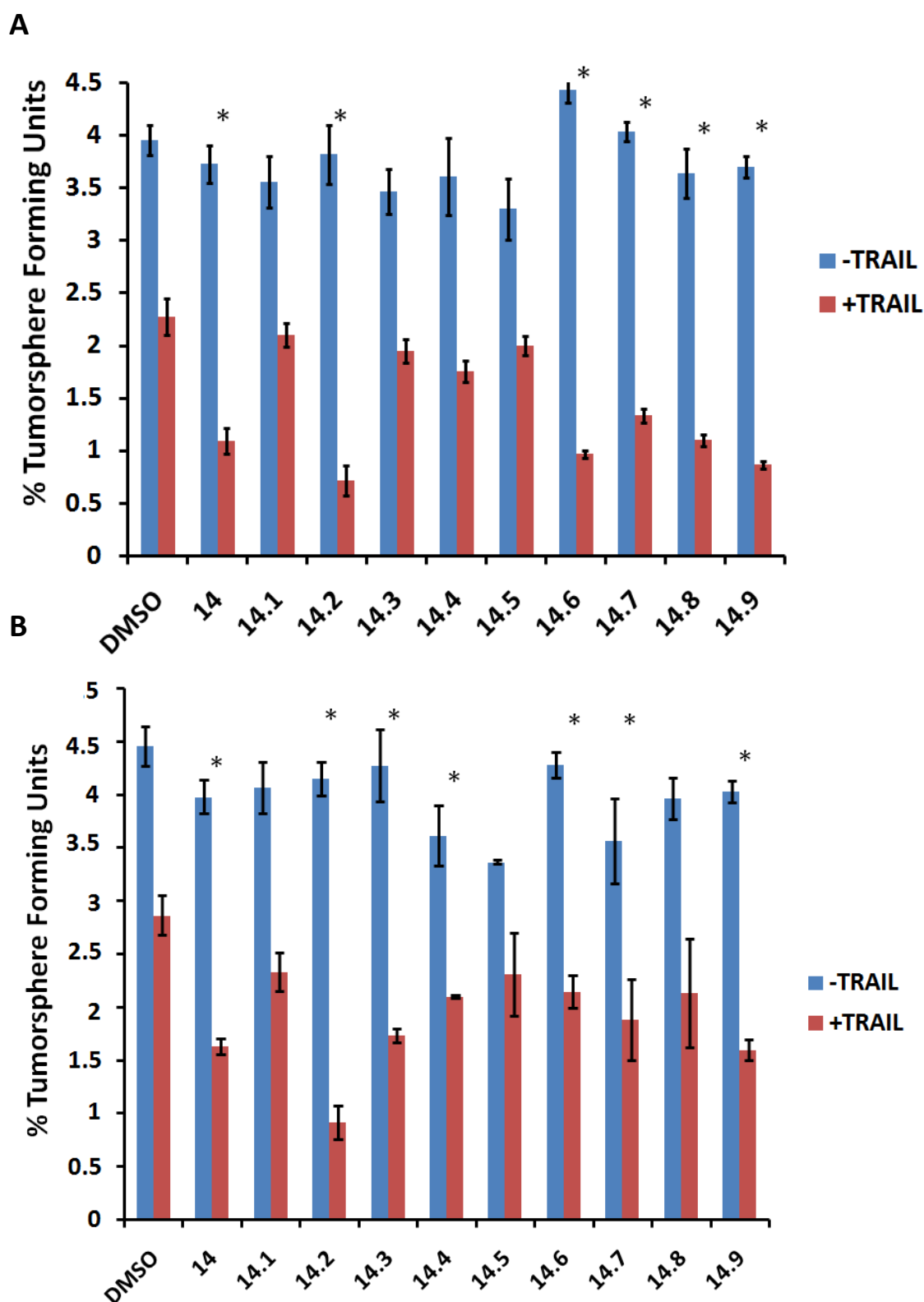


Figure 6.4: Several SPECS Analogues Sensitise MCF-7 and BT474 Tumoursphere Forming Cells to TRAIL to a similar level as OH14.

A) MCF-7 and B) BT474 cells were cultured for 24 h in a 96 wp, before being treated with vehicle control or compound at 10 μ M for 1 h. 20 ng/ml TRAIL (or control) was added after 1 h and the cells were left for 18 h. The following day, cells were subjected to the tumoursphere assay, with no additional drug added. A) Passage 1: MCF-7 B) Passage 1: BT474. Results represent passage 3 replicates, with error bars displaying standard error of the mean. *= p -value<0.05, t-test between TRAIL and compound + TRAIL. Compound 14.2 = newer preparation of OH14.

6.2.2 Pharmacy Synthesised Analogues

6.2.2.1 Pharmacy Synthesised Analogues N1-17: Colony Forming Assay

To analyse the effect of OH14 analogues on MCF-7 progenitor-like cells, we performed the colony-forming assay, as described previously. This assay gave an initial idea as to the efficacy of the compounds, as we have previously demonstrated that the effects observed in the CFA are representative of effects which can be obtained from the tumoursphere assay.

Initially, compounds were treated at 100 μM as this was the concentration at which we had previously observed the best effect with OH14. At 100 μM , in addition to the previously observed solubility issues (Table 6.5), however, several of the compounds were highly toxic to MCF-7 colony forming cells at this concentration (Figure 6.5A). We therefore decided to commence with evaluation at 10 μM in order to retain compounds in solution and thus not induce toxicity simply due to physical barriers to growth, as well as observing whether compounds which initially appeared toxic could be titrated down in order to uncover their actual efficacy as TRAIL sensitising agents.

Overall, the first series of compounds had similar efficacy to OH14, when treated at 10 μM (Figure 6.5B). Compounds N10, N13 and N17 showed a modest increase in efficacy compared with OH14, increasing sensitivity to TRAIL by an average of 60% as opposed to 55%. Five of the analogues did not improve on the efficacy of OH14 but did retain the ability of OH14 to significantly sensitise to TRAIL by on average 50%, whereas six compounds had a slightly reduced efficacy, and did not significantly enhance TRAIL-sensitivity. Many of the compounds, although demonstrating a consistent trend, did show a large variability in their ability to sensitise to TRAIL, thus producing a wide error range which may be due to issues with solubility, as we previously observed several of these compounds to be partially soluble in aqueous media or indeed, in DMSO (Table 6.5 previously).

Three of this first set of pharmacy-synthesised compounds, N15, N5 and N6, appeared toxic to the cells at both 100 and 10 μM , even when administered without TRAIL. These compounds, however, had been observed to be partially out of solution at 100-10 μM (Table 6.5 previously), which may explain their toxicity *i.e.* cells were physically prevented from growing due to compound particles blocking their ability to

do so. In order to elucidate the potential reasons for the toxicity of the two most significantly toxic compounds, N5 and N15, a cell viability experiment was performed using a dose-range of the compounds on the bulk population of MCF-7 cells. Cell viability was not significantly affected by N15 at 4 of 5 concentrations tested, with a significant decrease in viability only observed with both analogues at 100 μ M (Figure 6.6 A and B).

N10, N13 and N17 were selected as compounds of interest for future evaluation, due to their ability to reproduce the effects of OH14, with a modest improvement observed in some cases.

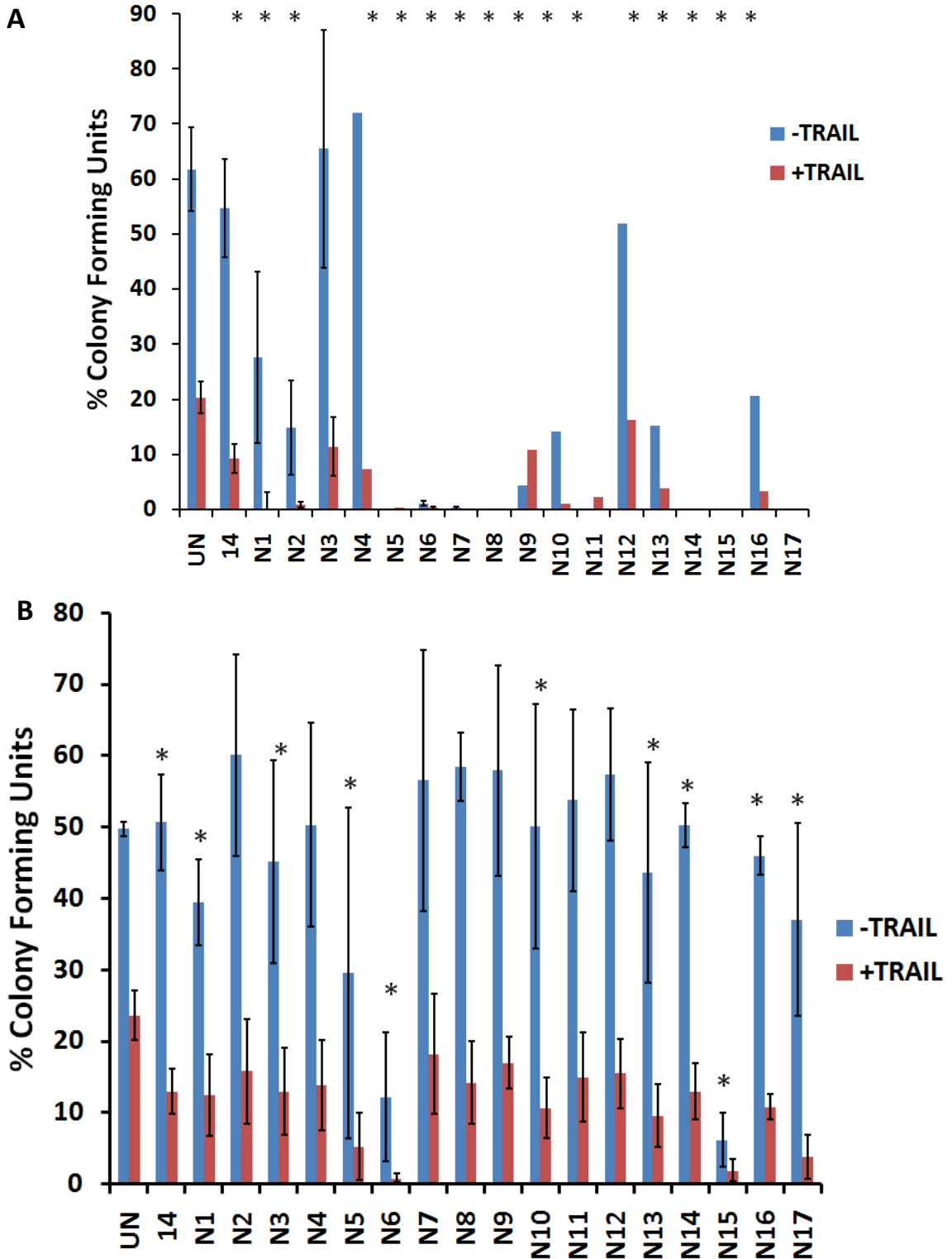


Figure 6.5: Several Series 1 Analogues Sensitise MCF-7 colonies to TRAIL in a similar manner to OH14.

MCF-7 cells were plated at 50 cells per cm² and treated with vehicle control, OH14 (14) or analogues at A) 100 μM or B) 10 μM alone or in combination with 20 ng/ml TRAIL and left to grow for 10 days before colonies were counted. Results represent 1 to 3 individual experiments for A and at least 3 individual biological repeats for B. * = p-value < 0.05 t-test between TRAIL and compound + TRAIL.

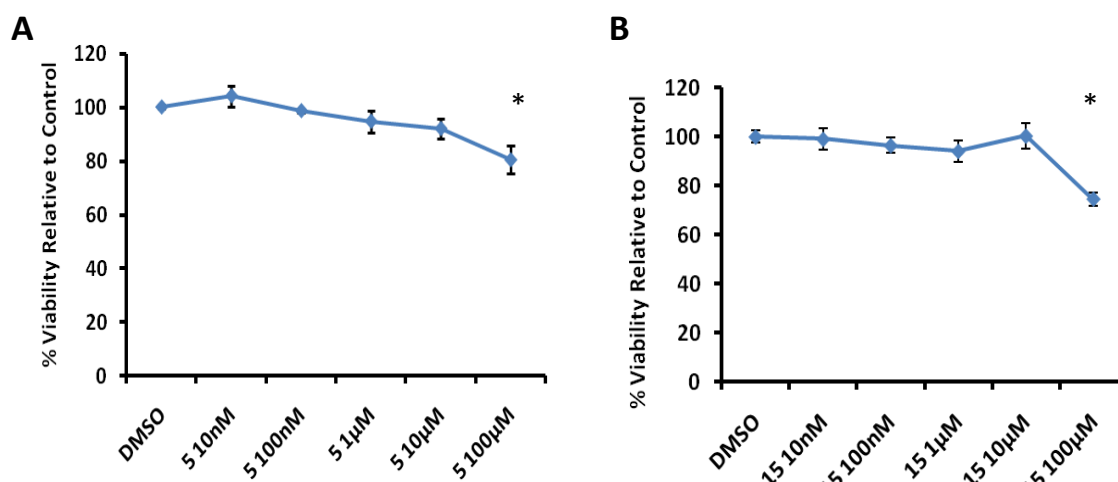


Figure 6.6: Analogues are less toxic to the bulk population of MCF-7 cells than colony forming cells

MCF-7 cells were plated to achieve a confluence of 70% before treatment with a dose range of analogues A) N5 and B) N15. After 24 h Cell Titre Blue was performed to evaluate cell viability. Results represent averages from 4 technical replicates. Error bars are presented as standard error of the mean. *= p -value <0.05 , t-test between vehicle control (DMSO) and compound.

6.2.2.2 Pharmacy Synthesised Analogues GG1-12: Colony Forming Assay

The second series of Pharmacy compounds, GG1-12 had more variation in their ability to increase the sensitivity of MCF-7 colony forming cells to TRAIL. The majority of the compounds, including GG1, 2, 5, 6, 7, 9 and 11, were not as active as OH14, showing no significant decrease in CFU number compared with TRAIL alone. Four of the compounds, GG2, 6, 8 and 10 appeared to increase the number colony forming cells when treated alone, whilst some, including GG3 and GG11, reduced colony forming cells.

Compounds GG4 and 12 demonstrated the most similar ability to increase MCF-7 colony forming cell sensitivity to TRAIL, as OH14, improving on TRAIL alone by up to 80%. GG3, 8 and 10 showed a significant TRAIL-sensitisation, although this was more modest than the effect of OH14 (Figure 6.7), increasing sensitivity to TRAIL by approximately 70%.

Subsequently, GG4, GG8 and GG12 were selected as compounds of interest for future evaluation.

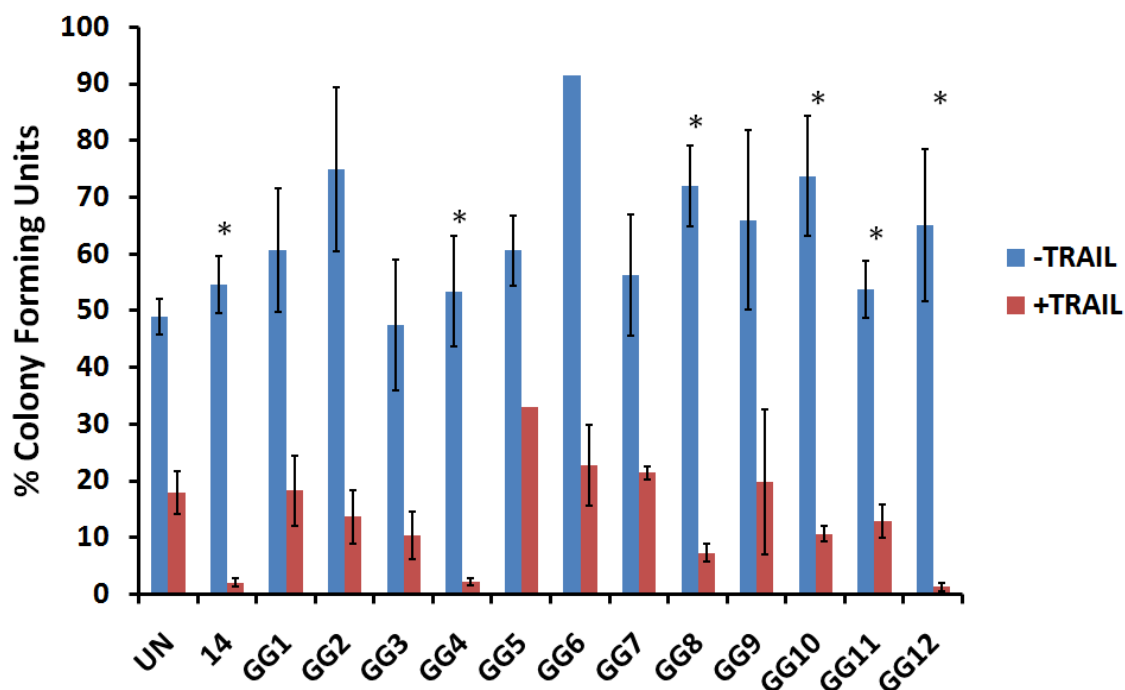


Figure 6.7: Several Series 2 Analogues Sensitise MCF-7 colonies to TRAIL in a similar manner to OH14.

MCF-7 cells were plated at 50 cells per cm^2 , allowed to attach and treated with vehicle control, OH14 (14) or Pharmacy Synthesised analogues of OH14: compounds GG1-12 at 10 μM , before being left to form colonies which were counted after 10 days. All results are averages of three or more independent experiments. *= p -value <0.05 , t-test between TRAIL and compound + TRAIL. Error bars represent standard error of the mean.

6.3 Discussion

In chapter 4 we used several *in vitro* assays to screen our 19 commercially available compounds and identified OH14 as our initial lead compound. The aim of this chapter was to select and design novel analogues of OH14 which may improve on the efficacy of OH14 and provide an initial structure-activity relationship.

Although molecular modelling is a very useful tool for distinguishing between active and non-active compounds, it cannot accurately predict activity at μM concentration of compounds with highly similar structures. Consequently, we obtained 8 commercially available analogues from Specs database, which showed 90% structural similarity with OH14, and 29 compounds were synthesised in-house, by Gilda Giancotti and Mahmoud El-Hiti, at Cardiff School of Pharmacy for *in vitro* evaluation. Three primary structural modifications on the structure of OH14 were implemented when designing analogues.

Only compounds which dissolved in the common solvent, DMSO and were soluble in aqueous solution were potential lead analogues. The majority of the analogues we analysed here fit these criteria. Alterations to the structure of OH14 appeared to impact on the solubility of the compounds, with many being partially insoluble in DMSO, or coming out of solution when further diluted in cell media. Solubility of a compound is an important feature when selecting potential drug candidates, thus, those candidates with impaired solubility will not be carried through for further testing. The presence of a carboxylic acid group on a compound aids in solubility due to the ability to form hydrogen bonds, thus, this feature will be retained on analogues in the future.

We selected the colony-forming assay as our initial screen for the compounds as it provides a repeatable result which is representative of both viability and tumoursphere-forming ability (as observed in Chapter 4). Here we have evaluated a total of 37 analogues of OH14. The 8 commercially available analogues were assessed on MCF-7 and BT474 cells in both colony-forming and tumoursphere assays. These compounds, 14.1-14.9, as predicted, showed similar efficacy data when analysed in the CFA and tumoursphere assays. Compound 14.9 performed with the greatest efficacy of all SPECS analogues tested, showing consistent and significant ability to sensitise to

TRAIL across both MCF-7 and BT474 tumoursphere- and colony-forming cells, in a seemingly synergistic manner, to the same or better level as OH14.

The remaining 29 Pharmacy-synthesised analogues were assayed only in MCF-7 cells, thus, their effects in BT474, as well as other cell lines, is yet to be evaluated. We observed the analogues to have varied activities, with many compounds unable to improve on the effect of TRAIL alone and others some showing toxicity to colony forming cells when administered alone (Figures 6.6-6.8). N5 and N15, observed to be the most toxic analogues to colony forming cells did not demonstrate significant toxicity on the bulk population of MCF-7 cells until the highest concentration of 100 μ M was administered, thus suggesting this toxicity is restricted to progenitor-like colony-forming cells.

Ultimately, we identified six pharmacy synthesised analogues: GG4, GG8, GG12, N10, N13, N17 and one SPECS analogues, 14.9, which increased sensitivity of MCF-7 colony forming cells to TRAIL, by at least 80%; a similar sensitisation to that achieved with OH14. Comparison of the chemical structures of compound OH14 and the structures of these analogues suggest that perhaps removal of one or both of the chlorine atoms on the aromatic ring of OH14 plays a key role in increasing efficacy of the compound (Figure 6.8). The absence of these chlorine groups 6 of the 7 lead analogues may have increased solubility in aqueous solution, thus, perhaps the increased efficacy of due to the fact that a higher concentration of drug in media is achieved and therefore more can enter the cells. The ability of N13 and N17 to increase colony-forming sensitivity to TRAIL may, however, be an additive rather than synergistic effect since a decrease in colony forming ability was observed when these compounds were treated alone. This decrease was not seen for the other lead analogues, and so it is likely that their efficacy was indeed due to a synergistic effect with TRAIL.

These analogues will be analysed in the future on additional relevant assays to ascertain a lead analogue. Further structural modifications may be able to lower the working concentrations of the drugs, although, if their toxicity to untransformed cells remains non-significant, identifying a promising drug candidate with a relatively high working concentration is feasible.

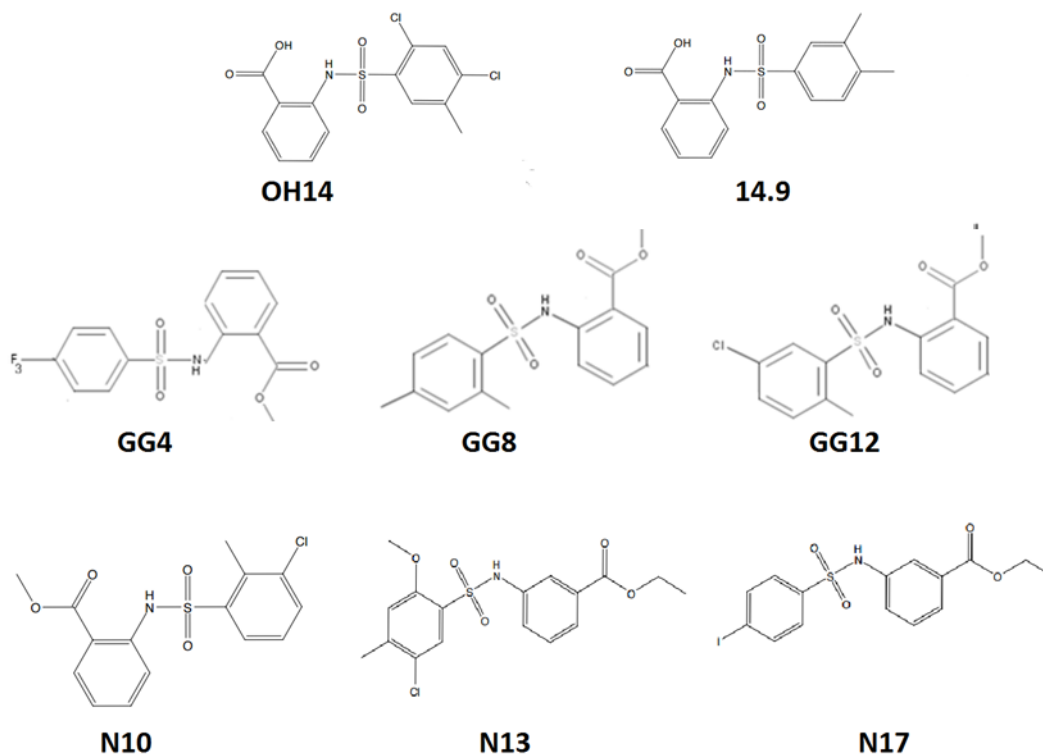


Figure 6.8: Structures of Most Efficacious Pharmacy Synthesised Analogues

Chemical structures of OH14 and most efficacious analogues of OH14: 14.9, GG4, GG8, GG12, N10, N13, N17.

In conclusion, we have identified and synthesised several chemical analogues of OH14, which were designed to retain the important features of the compound. Using primarily the colony-forming assay, we have identified 7 potential lead analogues of OH14 which will be evaluated in additional assays in order to attempt to identify more efficacious lead compound.

Chapter 7

General Discussion

Chapter 7: General Discussion

TRAIL is an endogenous death ligand which exhibits cancer cell-specific cytotoxicity (Gura, 1997; Lempke *et al.*, 2014) (Section 1.2). There is a large body of evidence for TRAIL as a therapeutic in multiple cancer types due to its cancer-specific ability to induced apoptosis. Research is growing into specific apoptosis inducing agents, with the strive to find more cancer cell-targeted treatment options.

Studies have demonstrated TRAIL to be most efficacious in mesenchymal-like breast cancer lines (Rahman *et al.*, 2009), with many cell lines from other subtypes of the disease exhibiting TRAIL resistance. We, and others, have demonstrated c-FLIP to have a key role in TRAIL resistance (Piggott *et al.*, 2011; Safa and Pollok, 2011). c-FLIP directly competes with procaspase-8/-10 for interaction with FADD upon TRAIL pathway stimulation (Dickens *et al.*, 2012; Safa, 2012; Scaffidi *et al.*, 1999) (Section 1.3). It is this anti-apoptotic role that, if inhibited, could facilitate a route to TRAIL sensitisation.

Breast cancer stem-like cells, although contributing to only around 4% of a tumour, are thought to have a key role in resistance to treatment and disease relapse (Vinogradov and Wei, 2012). We have recently been able to successfully eliminate tumoursphere-forming cells, which are an *in vitro* model of CSC-like cells (Dontu *et al.*, 2003), in a panel of breast cancer cell lines using the combination of c-FLIP suppression, using siRNA, and treatment with TRAIL (Piggott *et al.*, 2011). There is therefore much evidence to support the therapeutic potential for TRAIL sensitising agents, and, in particular, agents which prevent the anti-apoptotic role of c-FLIP, however, there are currently no c-FLIP specific inhibitors of which we are aware.

7.1 Targeting c-FLIP with Small Molecule Inhibitors

Several studies have identified agents which decrease c-FLIP expression, and sensitise cells to TRAIL or other chemotherapeutics (Trivedi and Mishra, 2015). These agents function by interfering with c-FLIP transcription, degradation or translation (Safa *et al.*, 2008; Safa and Pollok, 2011). Furthermore, many of these agents act via inducing DNA damage, and will usually affect other proteins, thus reducing their target-specificity (Safa, 2012). The combination of TRAIL with a c-FLIP-specific small molecule inhibitor that retains a cancer-specific mechanism of action is therefore highly desirable. The high homology between c-FLIP and procaspase-8 (Goltsev *et al.*, 1997) means that a

small molecule targeted to c-FLIP could potentially also inhibit this pro-apoptotic protein, however, therefore any method of c-FLIP suppression must be highly specific.

We have used *in silico* modelling to model the structure of c-FLIP and associated proteins and develop interaction models. We have confirmed that the structures of the DEDs of procaspase-8 and c-FLIP are indeed very similar and show a great amount of structural homology (Goltsev *et al.*, 1997). Our models demonstrated, however, that the potential interactive surface between DED1 of procaspase-8 or c-FLIP and the DED of FADD shows some variation in physical and electrostatic properties. We identified a site on DED1 of c-FLIP which provides a specific target for small molecule inhibitors to bind and interfere with the interaction with FADD and potentially also affect any interaction between c-FLIP and procaspase-8, whilst sparing the site of FADD interaction on procaspase-8 itself. A recent publication by Dickens *et al.* have shown a similar *in silico* model for the structure of caspase-8, modelled using different software but a similar homology model, based on v-FLIP, MC159 (Dickens *et al.*, 2012) which supports the accuracy of our model. Additionally, after the completion of our *in silico* modelling and initial compound testing, two publications emerged which performed similar *in silico* analyses of c-FLIP and FADD (Hwang *et al.*, 2014; Majkut *et al.*, 2014). In particular, Majkut *et al.* constructed a very similar model to ours of the c-FLIP DED1:FADD interaction, providing further support for our own model.

A structure-based virtual screen was performed on c-FLIP and procaspase-8 in parallel. After a multi-step *in silico* selection process, 19 small molecules were selected for their potential ability to prevent the interaction between c-FLIP and FADD, whilst sparing the interaction between procaspase-8 and FADD.

7.2 Biological Evaluation of c-FLIP Small Molecule Inhibitors

We performed biological evaluation of the 19 compounds primarily on the two previously described TRAIL-resistant breast cancer cell lines MCF-7 and BT474 which demonstrated several of our 19 c-FLIP inhibitors to have an ability to partially sensitise these cells to TRAIL induced apoptosis. The ability of the compounds to sensitise to TRAIL, with little viability alterations when administered alone was similar to that observed previously on MCF-7 and BT474 cells using siRNA to remove c-FLIP followed by treatment with TRAIL (Piggott *et al.*, 2011), thus in effect, our lead compounds were

able to phenocopy c-FLIP siRNA. Treatment with one of our lead compounds, OH14, at a range of concentrations, in assays which are used to represent stem-like and progenitor cells respectively, demonstrated a dose-dependent ability of the compound to significantly sensitise both MCF-7 and BT474 tumoursphere- and colony-forming cells to TRAIL, whilst remaining non-toxic when administered alone. In order to fully differentiate between additive and synergistic effects of the compounds, ideally, the IC50 of the drugs would need to be reached, using a combination of cell and interaction assays.

Our initial data demonstrated OH14 in a TN breast cancer and PR -ve cell line to only modestly increase sensitivity to TRAIL at one concentration. Studies have demonstrated HER2 status to be associated with TRAIL resistance, in that HER2 +ve cancers are more TRAIL resistant (Zang *et al.*, 2014), thus, perhaps HER2 receptor status impacts on sensitivity to the combination therapy, with HER2 cells expressing a different variant of c-FLIP. Both SKBR3 and MDA-MB-231 cells, unlike BT474 and MCF-7 cells, are PR -ve cell lines, thus, it may be that lack of expression of this hormone receptor impacts on the ability of these cells to be sensitised to TRAIL by our inhibitors, although this hypothesis has not yet been explored.

An additional explanation for the differences in sensitivity to OH14 is that both the MDA-MB-231 and SKBR3 cell lines may express a modified variant of c-FLIP. Even a one amino acid alteration in the sequence of c-FLIP around the pocket of DED1, which we have selected OH14 to target, could lead to the compounds being ineffective. Protein sequence variation is common in cell lines, as demonstrated by around 15 million, of reported single nucleotide polymorphisms (SNPs) present in the human genome. These have been identified in a large-scale project 'The 1000 Genomes Project' which characterised human genome sequence variation and correlate results with genotype and phenotype information (1000 Genomes Project Consortium, 2010). In order to explore the idea that the c-FLIP sequence variation plays a role in the lack of OH14 sensitivity to some cell lines, sequencing of the c-FLIP gene is required in order to determine its primary structure in these cell lines. In addition, further evaluation into the effects of OH14 or lead analogues in other breast cancer cell lines, including triple negative, PR -ve and HER-2 positive cell lines is required.

Our results thus far suggested that our lead compound was most efficacious in the micromolar range, with the concentrations at which our lead compound was most efficacious in multiple assays from 10 to 100 μM , deeming OH14 to have a low potency. Although this is a relatively high concentration, many non-specific c-FLIP-inhibiting agents, for example the Akt Inhibitor API-1 (Li *et al.*, 2012); the HDAC agent MS-275 (entinostat) (Rao-Bindal *et al.*, 2013); also act at micromolar levels. Furthermore, pan-caspase inhibitors, such as Z-VAD-FMK (Promega) are recommended for use at micromolar concentrations, up to 100 μM (Promega, Datasheet). Testing of analogues of OH14 has begun and has provided us with an initial structure activity relationship for the compound, with the identifications of several compounds which exhibited different activity to OH14, with some showing improved efficacy. It is hoped that we will identify an analogue of OH14 with improved efficacy and a lower working concentration, thus a larger therapeutic range.

7.3 Mechanism of Action: c-FLIP:FADD Interactions

The pharmacological disruption of PPIs is an increasingly important tool in modern medicine. Compounds targeted to protein-protein interactions, involving crucial processes in both disease and normal states, such as apoptosis, must have their mechanism of action validated to demonstrate that it exerts its desired effect through the inhibition of the target protein interaction (Roszkik *et al.*, 2013). Several studies have reported on the presence of interactions between the DEDs of FADD and c-FLIP, FADD and procaspase-8, and c-FLIP and procaspase-8 (Day *et al.*, 2008; Dickens *et al.*, 2012; Safa and Pollok, 2011). One of the key reasons for TRAIL resistance is the competition between c-FLIP and procaspase-8 for interacting and binding with the DED present on FADD (Safa, 2012), thus, demonstrating that our inhibitors prevent this interaction is of great importance.

In Chapter 5, we utilised co-IP and Western blot in a TRAIL-resistant line to demonstrate an interaction between caspase-8 and FADD, however, further optimisation is required for compound analysis using co-IP. We have, however optimised FRET acceptor-photobleaching to evaluate the ability OH14 to interfere with the interaction between c-FLIP and FADD in TRAIL-resistant HeLa and MCF-7 cells. FRET provides a technique for studying protein:protein interactions which does not rely on

antibodies, which are often are not highly sensitive and can exhibit poor target selectivity. FRET has previously been utilised, in different formats, including flow cytometry FRET, to demonstrate FADD:caspase-8 and -10 interactions (Wang *et al.*, 2001; Muppidi *et al.*, 2006), TRAIL-receptor interactions (Neumann *et al.*, 2014) and FADD self-association (Muppidi *et al.*, 2006), however, FRET has not yet been performed to evidence c-FLIP:FADD interactions. Using FRET, we were able to show that our lead inhibitor, OH14, can prevent the interaction between c-FLIP and FADD in HeLa cells stimulated with TRAIL, and, although less profound, a similar effect was observed in MCF-7 cells. Furthermore, using several assays to evaluate caspase activity, we have demonstrated that our lead compound OH14 indeed facilitates TRAIL-induced apoptosis through the caspase-mediated pathway, and, as such, in combination with our FRET studies, have demonstrated the highly specific likely mechanism of action of OH14.

7.4 Residues Involved in c-FLIPs Anti-Apoptotic Role

Primers for site directed mutagenesis have been designed and plasmids have been generated to target residues I6, H7, R38 and R45 on DED1 of c-FLIP, although successful biological evaluation of these has not yet taken place.

At the time of the study, there were no mutational studies published on the DEDs of c-FLIP. Much more recently, however, two studies have emerged which look into mutations on the relevant domains of c-FLIP and both utilise *in silico* modelling. One study utilised *in silico* modelling and carried out mutations on DED2 of c-FLIP. This study, performed by Hwang *et al.*, evaluated mutations of E80A, L84A, K169A and Y171A, all present within DED2, and, using co-IP, showed a disturbed interaction with FADD, in addition to lowering the overall stability of the DEDs of c-FLIP (Hwang *et al.*, 2014).

Majkut and team evaluated mutations in both DED1 and DED2 of c-FLIP, and, in particular the residue, H7 in DED1: one of the residues which we had selected based on *in silico* modelling. They observed that an H7G FLIP mutant had a modest reduction in the ability to block apoptosis and bind to procaspase-8 when compared to wildtype FLIP, whilst F114A in DED2 impacted more significantly on FADD procaspase-8 binding

although this was not the expected outcome, since based on their own *in silico* model, they expected H7 to be of greater importance (Majkut *et al.*, 2014).

Interestingly, an equivalent amino acid residue on procaspase-8, Y8, was shown to be important for the interaction with FADD and activation of downstream executioner caspases upon TRAIL stimulation, whilst mutation of F122A in DED2 did not have any effect. A double mutant, F122A/Y8G however, reduced the ability of procaspase-8 and FADD to interact even more than Y8G alone, suggesting again, that both DED domains are important for these interactions, although processing of procaspase-8 may be impacted (Majkut *et al.*, 2014). Furthermore, they assessed mutations on FADD at F25A and H7G, demonstrating the H7G mutant to have more important role in FADD:c-FLIP interactions. The group demonstrated, however, that, unlike murine c-FLIP R (Ueffing *et al.*, 2008) both DED1 and DED2 are required for the anti-apoptotic activity of c-FLIP S (Majkut *et al.*, 2014). These results provide interesting, although non-conclusive information about some of the DED residues of importance in c-FLIP, FADD and procaspase-8 interactions.

In the future, we aim to use our mutagenesis plasmids to demonstrate residues on c-FLIP which are important for its ability to interact with FADD. Confirming the importance of these residues will be used by using mutant c-FLIP overexpression versus wildtype c-FLIP overexpression in c-FLIP knock-out cell lines, such as those generated using TALEN. Unfortunately, we were unable to successfully generate a c-FLIP null cell line using TALEN technology (Chapter 5) and our siRNA cells do not have enough of a long term and stable reduction of c-FLIP to perform these studies. We hope to generate an shRNA c-FLIP cell line, or continue to work on generating a TALEN c-FLIP cell line in order to perform our own mutational studies. In addition, we may utilise our c-FLIP:YFP FRET constructs as our cloning template in order to generate mutant c-FLIP FRET constructs which will be analysed using FRET.

7.5 Future Directions

There are many additional avenues of evaluation into the potential effects and efficacy of our inhibitors, and indeed, targeting c-FLIP as a therapeutic strategy that we wish to explore in the future.

Synthesis and testing of new analogues is ongoing in order to improve efficacy and divulge structure-activity-relationship information about the compounds. Further testing of these analogues, in particular, the analogues which have demonstrated the greatest effects so far: GG4, GG8, GG12, N10, N13, N17 and 14.9, in additional relevant assays, primarily the tumoursphere assay and assays to demonstrate mechanism of action, will be performed in the future in order to attempt to establish a novel and more efficacious lead compound. Our optimised FRET acceptor-photobleaching will be utilised for this, alongside additional interaction assays, such as the proximity ligation assay, which is a highly selective and sensitive method for detecting protein interactions (Leuchowius *et al.*, 2010).

All work carried out in this study was performed on immortalised cell lines, as opposed to primary tumours. In order to increase the clinical relevance of our findings, it would be of interest in future to analyse our compounds in, for example, clinical human breast tumour biopsy samples. Preliminary data from our lab, analysing OH14 plus TRAIL in such samples has shown promise for the combination therapy in this material (Andreia Silva, personal communications). In addition, evaluation of our c-FLIP inhibitors in other cancer types would certainly be of interest. High expression levels of c-FLIP occurs in many cancers, including: liver, bladder, ovarian, colon, colorectal, prostate and breast cancers (Safa *et al.*, 2008) and, as such, c-FLIP has been associated with TRAIL resistance, and indeed to play a role in chemotherapy resistance, in many of these cancer types (Okano *et al.*, 2003; Kim *et al.*, 2002; Safa, 2012; Lee *et al.*, 2013; Lempke *et al.*, 2014, Zang *et al.*, 2014). It would be of great interest, therefore, to test OH14 and lead analogues of OH14 in alternative cancer types which show potential to be sensitised to TRAIL in a similar way as our breast cancer cell lines. Through use of HeLa cells in our FRET studies, we have demonstrated that our inhibitors do indeed inhibit the c-FLIP:FADD interaction in this cervical cancer line, which supports the hypothesis that our inhibitors may work in other cancer types.

Work in this study focussed on a dual combination of our c-FLIP inhibitors and TRAIL, the ultimate therapy would likely include a chemotherapeutic regime. A triple therapeutic action, such as this, could allow for the targeting of both cancer stem cells, and the bulk tumour cells, enabling a complete coverage of the cancerous cells present within a tumour, and the surrounding environment. Preliminary studies from our lab have shown promise for such a triple-combination therapy with OH14, TRAIL and chemotherapy *in vitro* (Timothy Robinson, Personal communications). In addition, c-FLIP has been demonstrated to impact on chemotherapy resistance (Safa, 2012), thus, future work will be carried out to establish an optimum drug combination, dose and treatment schedule with OH14 or a lead analogue.

The existence of cancer stem-like cells, in combination with CSC plasticity, the ability of a cancer cell to de-differentiate and become a CSC, are recently proposed theories often used to explain cancer relapse (Section 1.1.7) (Wicha *et al.*, 2006; Flemming, 2015). A cancer therapeutic which could eliminate CSCs and prevent plasticity, in combination with a treatment which can eliminate bulk cells, is highly clinically desirable. Although OH14 was designed to inhibit the interaction between c-FLIP and FADD, it may be that blocking this site on c-FLIP alters other functions of c-FLIP. Preliminary data using OH14 on our *in vitro* model of plasticity is promising. However, much further investigation is required in order to elucidate whether, and how, OH14 prevents plasticity in our model.

One of the primary criterion of our *in vitro* compound assessment was the ability of the compound to dissolve in the common lab reagent DMSO, in order to achieve a millimolar stock solution. DMSO is a widely used solvent for dissolving hydrophobic drug molecules, since it is amphipathic in nature and is used in both *in vitro* and *in vivo* studies. In general, DMSO is only used at low concentrations, since at higher concentrations undesirable side effects have been observed (Galvao *et al.*, 2014). Although only low concentrations of DMSO were utilised here, at latter stages of drug development, we may attempt to modify the chemical structure in order to increase the water solubility of the drug and, thus, eliminate the reliance on DMSO for preparing initial stock drug solutions. This would benefit both *in vitro* and *in vivo* studies as it would likely allow a higher concentration of drug to be administered, which would have been previously restricted due to the potential toxicity of the vehicle.

Ultimately, in order to progress this potential combination therapy further, *in vivo* studies would be required to provide toxicity, pharmacodynamics and side effect profiles for OH14 or its analogues, in addition to evaluating the *in vivo* efficacy of combination therapy overall.

Table 7.1: Summary of all compounds tested.

Compound obtained from: OM = original modelling SPECS (Chapter 3), SPECS analogue of 14 = S14, Pharmacy analogue Mahmoud = PM, Pharmacy analogue Gilda = PG.
Efficacy: - = lack of solubility, observed toxicity or no observed efficacy, + = some efficacy but potential toxicity, ++ = efficacy but below OH14, +++ = efficacy equal or great than OH14.

Compound	Obtained	Efficacy
OH1	OM	+
OH2	OM	-
OH3	OM	+
OH4	OM	-
OH5	OM	-
OH6	OM	+
OH7	OM	-
OH8	OM	-
OH9	OM	-
OH10	OM	-
OH11	OM	-
OH12	OM	-
OH13	OM	-
OH14	OM	+++
OH15	OM	-
OH16	OM	++
OH17	OM	-
OH18	OM	-
OH19	OM	++
14.1	S14	-
14.3	S14	+
14.4	S14	+
14.5	S14	-
14.6	S14	+
14.7	S14	+
14.8	S14	+
14.9	S14	+++
N1	PM	+
N2	PM	+
N3	PM	+
N4	PM	+
N5	PM	+
N6	PM	-

N7	PM	-
N8	PM	+
N9	PM	+
N10	PM	+++
N11	PM	+
N12	PM	+
N13	PM	+++
N14	PM	+
N15	PM	-
N16	PM	+
N17	PM	+++
GG1	PG	-
GG2	PG	-
GG3	PG	+
GG4	PG	+++
GG5	PG	-
GG6	PG	-
GG7	PG	-
GG8	PG	++
GG9	PG	-
GG10	PG	+
GG11	PG	+
GG12	PG	+++

Bibliography

- 1000 Genomes Project Consortium, A map of human genome variation from population-scale sequencing. *Nature* 2010, **467**:1061-73
- Al-Hajj, M., Wichas, M.S., Benito-Hernandez, A., Morrison, S.J. and Clarke, M.F., Prospective identification of tumorigenic breast cancer cells. *Proc Natl Acad Sci USA* 2003, **100**:3983-3988
- Aj-Hajj, M. and Clarke, M.F., Self-renewal and solid tumor stem cells. *Oncogene* 2004, **23**:7274-7282
- Almendro, V. and Fuster, G., Heterogeneity of breast cancer: etiology and clinical relevance. *Clin Transl Oncol* 2011, **13**(11):767-73
- Althius, M.D., Fergenbaum, J.H., Garcia-Closas, M., *et al.*, Etiology of hormone receptor-defined breast cancer: a systematic review of the literature. *Cancer Epidemiol Biomarkers Prev* 2004, **13**(10):1558-68
- Anders, C.K. and Carey, L.A., Biology, metastatic patterns, and treatment of patients with triple-negative breast cancer. *Clin Breast Cancer* 2009, **9**(Suppl 2):S73-81
- Ashkenazi, A., Targeting death and decoy receptors of the tumour-necrosis factor superfamily. *Nat Rev Cancer* 2002, **2**(6):420-30
- Ashkenazi, A. and Dixit, V.M., Death Receptors: signaling and modulation. *Science* 1998, **281**:(5381):1305-8
- Ashkenazi, A., Pai, R.C., Fong, S., Leung, S., Lawrence, D.A. *et al.*, Safety and antitumor activity of recombinant soluble Apo2 ligand. *J Clin Invest* 1999, **104**(2):155-62
- Barrandon, Y. and Green, H., Three clonal types of keratinocyte with different capacities for multiplication. *Proc Natl Acad Sci* 1987, **84**:2302-2306
- Belada, D., Mayer, J., Czuczman, M.S., Flinn, I.W., Durbin-Johnson, B. and Bray, G.L., Phase II study of dulanermin plus rituximab in patients with relapsed follicular non-Hodgkin's lymphoma (NHL). *J Clin Oncol* 2010, **28**(15s):8104
- Bertucci, F. and Birnbaum, D., Reasons for breast cancer heterogeneity. *J Biol* 2008, **7**(2):6
- Beumer, K.J., Trautman, J.K., Christian, M., Dahlem, T.J., Lake, C.M. *et al.*, Comparing Zinc Finger Nucleases and Transcription Activator-Like Effector Nucleases for Gene Targeting in *Drosophila*. *G3* 2013, **3**(10):1717-1725

- Bijangi-Vishehsaraei, K., Saadatazdeh, M.R., Huang, S., Murphy, M.P. and Safa, A.R., 4-(4-Cholor-2-methylphenoxy)-N-hydroxybutanamide (CMH) targets mRNA of the c-FLIP variants and induces apoptosis in MCF-7 human breast cancer cells. *Mol Cell Biochem* 2010, **342**:133-142
- Binkley, J.M., Harris, S.R., Levangie, P.K., Pearl, M., Guglielmino, J. *et al.*, Patient Perspectives on Breast Cancer Treatment Side Effects and the Prospective Surveillance Model for Physical Rehabilitation for Women with Breast Cancer. *Cancer* 2012, **118**(8):2207-2216
- Blanpain, C., Van Keymeulen, A., Rocha, A.S., Ousset, M., Beck, B., Bouvencourt, G., *et al.*, Distinct stem cells contribute to mammary gland development and maintenance. *Nature*, **479**:183-193
- Bombonati, A. and Sgroi, D.C., The molecular pathology of breast cancer progression. *J Pathol* 2011, **223**(2):307-317
- Bray, F., Ren, J.S., Masuyer, E. and Ferlay, J., Estimates of global cancer prevalence for 27 sites in the adult population in 2008. *Int J Cancer* 2013, **132**(5):1133-45
- Brenton, J.D., Carey, L.A., Ahmed, A.A. *et al.*, Molecular classification and molecular forecasting of breast cancer: ready for clinical application? *J Clin Oncol* 2005, **23**:7350-7360
- Brooks, S.C., Locke, E.R. and Soule, H.D., Estrogen receptor in a human cell line (MCF-7) from breast carcinoma. *J Biol Chem* 1973, **248**(17):6251-3
- Brown, J.M., Vessella, R.L., Kostenuik, P.J., Dunstan, C.R., Lange, P.H. and Corey, E., Serum osteoprotegerin levels are increased in patients with advanced prostate cancer. *Clin Cancer Res* 2001, **7**(10):2977-83
- Bucur, O., Gaidos, G., Yatawara, A., Pennarun, B., Rupasinghe, C. *et al.*, A novel caspase-8 selective small molecule potentiates TRAIL-induced cell death. *Sci Rep* **5**(9893)
- Buzdar, A.U., Powell, K.C., Legha, S.S. and Blumenschein, G.R., Treatment of advanced breast cancer with aminoglutethimide after therapy with tamoxifen. *Cancer* 1982, **50**(9):1708-1712
- Buzdar, A.U., Role of biologic therapy and chemotherapy in hormone receptor- and HER2-positive breast cancer. *Ann Oncol* 2009, **20**(6):993-9
- Cardoso, F., Costa, A., Norton, L., Senkus, E., Aapro, M. *et al.*, ESO-ESMO 2nd international consensus guidelines for advanced breast cancer (ABC2). *Ann Oncol* 2014, **25**:1871-1888
- Carrington, P.E., Sandu, C., Wei, Y., Hill, J.M., Morisawa, G. *et al.*, The structure of FADD and its mode of interaction with procaspase-8. *Mol Cell* 2006, **22**(5):599-610

- Cavasotto, C.N. and Phatak, S.S., Homology modelling in drug discovery: current trends and applications. *Drug Discov Today* 2009, **14**(13/14): 676-683
- Cermak, T., Doyle, E.L., Christian, M., Wang, Li, Zhang, Y. *et al.*, Efficient design and assembly of custom TALEN and other TAL effector-based constructs for DNA targeting. *Nucleic Acids Res* 2011, **39**(12):e82
- Chaffer, C.L., Brueckman, I., Scheel, C., Kaestli, A.J., Wiggins, P.A. *et al.*, Normal and neoplastic nonstem cells can spontaneously convert to a stem-like state. *PNAS* 2011, **108**(19):7950-7955
- Chang, L., Kamata, H., Solinas, G., Luo, J.L., Maeda, S. *et al.*, The E3 ubiquitin ligase itch couples JNK activation to TNF α -induced cell death by inducing c-FLIPL turnover. *Cell* 2006, **124**:601-613
- Chari, R.V., Targeted cancer therapy: conferring specificity to cytotoxic drugs. *Acc Chem Res* 2008, **41**(1):98-107
- Chen, S., Fu, L., Raja, S.M., Yue, P., Khuri, F.R. and Sun S-Y., Dissecting the roles of DR4, DR5 and c-FLIP in the regulation of Geranylgeranyltransferase I inhibition-mediated augmentation of TRAIL-induced apoptosis. *Mol Cancer* 2010, **9**:23
- Chen, S., Cao, W., Yue, P., Hao, C., Khuri, F.R. *et al.*, Celecoxib promotes c-FLIP degradation through Akt-independent inhibition of GSK3. *Cancer Res* 2011, **71**(19):6270-81
- Cheng, J., Hylander, B.L., Baer, M.R., Chen, X. and Repasky, E.A., Multiple mechanisms underlie resistance of leukemia cells to Apo2 Ligand/TRAIL. *Mol Cancer Ther* 2006, **5**:1844
- Chinnaiyan, A.M., O'Rourke, K., Tewari, M. and Dixit, V.M., FADD, a novel death domain-containing protein, interacts with the death domain of Fas and initiates apoptosis. *Cell* 1995, **81**:505-512
- Cheung, H.H., Mahoney, D.J., LaCasse, E.C. and Korneluk, R.G., Down-regulation of c-FLIP enhances death of cancer cells by Smac mimetic compound. *Cancer Res* 2009, **69**:7729
- Clarkson, R.W.E., Wayland, T., Lee, J., Freeman, T. and Watson, C.J., Gene expression profiling of mammary gland development reveals putative roles for death receptors and immune mediators in post-lactational regression. *Breast Cancer Res* 2004, **6**(2):R92-R109
- Claudinot, S., Nicolas, M., Oshima, H., Rochat, A. and Barrandon, Y., Long-term renewal of hair follicles from clonogenic multipotent stem cells. *Proc Nat Acad Sci* 2005, **102**:14677-14682

Clarke, G.M., Osborne, C.K. and McGuire, W.L., Correlations between estrogen receptor, progesterone receptor, and patient characteristics in human breast cancer. *JCO* 1984, **2**(10):1102-1109

Clarke, M.F., Dick, J.E., Dirks, P.B., Eaves, C.J., Jamieson, C.H.M. *et al.*, Cancer stem cells – perspectives on current status and future directions: AACR workshop on cancer stem cells. *Cancer Res* 2006, **66**(19):9339-44

Cleator, S., Heller, W., Coombes, R.C., Triple-negative breast cancer: therapeutic options. *Lancet Oncol* 2007, **8**(3):235-44

Congreve, M., Murray, C.W. and Blundell, T.L., Keynote review: Structural biology and drug discovery. *Drug Discov Today*, **10**(13):895-907

Crowder, R.N. and El-Deiry, W.S., Caspase-8 regulation of TRAIL-mediated cell death. *Exp Oncol* 2012, **34**(3):160-4

CRUK Cancer Research UK, cancerresearchuk.org/health-professional/cancer-statistics/statistics-by-cancer-type/breast-cancer, Accessed October 2014

CRUK Cancer Research UK, cancerresearchuk.org/health-professional/cancer-statistics/survival, Accessed October 2014

Dal Ben, D., Buccioni, M., Lambertucci, C., Thomas, A. and Volpini, R., Simulation and comparative analysis of binding modes of nucleoside and non-nucleoside agonists at the A_{2B} adenosine receptor. *In Silico Pharm* 2013, **1**:24

Daniels, R.A., Turley, H., Kimberley, F.C., Liu, X.S., Ch'EN, P. *et al.*, Expression of TRAIL and TRAIL receptors in normal and malignant tissue. *Cell Res* 2005, **15**(6):430-8

Day, T.W. and Safa, A.R., RNA interference in cancer: targeting the anti-apoptotic protein c-FLIP for drug discovery. *Mini Rev Med Chem* 2009, **9**(6):174-8

Day, T.W., Huang, S. and Safa, A.R., c-FLIP knockdown induces ligand-independent DR5-, FADD-, caspase-8, and caspase-9-dependent apoptosis in breast cancer cells. *Biochem Pharmacol* 2008, **76**:1694-704

Day, T.W., Sinn, A.L., Huang, S., Pollok, K.E., Sandusky, G.E. and Safa, A.R., c-FLIP Gene Silencing Eliminates Tumor Cells in Breast cancer Xenografts without Affecting stromal cells. *Anticancer Res* 2009, **29**:3383-3886

Dean, M., Fojo, T. and Bates, S., Tumour stem cells and drug resistance. *Nat Rev Cancer* 2005, **5**:275-284

Dickens, L.S., Boyd, R.S., Jukes-Jones, R., Hughes, M.A., Robinson, G.L. *et al.*, A death effector domain chain DISC model reveals a crucial role for caspase-8 chain assembly in mediating apoptotic cell death. *Mol Cell* 2012, **47**(2):291-305

- Dimri, G., Band, H. and Band, V., Mammary epithelial cell transformation: insights from cell culture and mouse models. *Breast Cancer Res* 2005, **7**:171-179
- Ding, S.L., Sheu, L.F., Tu, J.C., Yang, T.L., Chen, B.F. *et al.*, Abnormality of the DNA double-strand-break checkpoint/repair genes, ATM, BRCA1 and TP53, in breast cancer is related to tumour grade.
- Ding, Q., Lee, Y.K., Shaefer, E.A., Peters, D.T., Veres, A. *et al.*, A TALEN genome-editing system for generating human stem cell-based disease models. *Cell Stem Cell* **12**(2):238-51
- Dohrman, A., Russell, J.Q., Cuenin, S., Fortner, K., Tschopp, J. and Budd, R.C., Cellular FLIP Long Form Augments Caspase Activity and Death of T Cells through Heterodimerization with and Activation of Caspase-8. *J Immunol* 2005, **175**(1):311-318
- Dontu, G., Abdullah, W.M., Foley, J.M., Jackson, K.W., Clarke, M.F. *et al.*, In vitro propagation and transcription profiling of human mammary stem/progenitor cells. *Genes & Devel* 2003, **17**:1253-1270
- Drasin, D.J., Robin, T.P. and Ford, H.L., Breast cancer epithelial-to-mesenchymal transition: examining the functional consequences of plasticity. *Breast Cancer Res* 2011, **13**(6):226
- Eberstadt, M., Huang, B., Chen, Z., Meadows, R.P., Ng, S.C. *et al.*, NMR structure and mutagenesis of the FADD (Mort1) death-effector domain. *Nature* 1998, **392**(6679):941-5
- Eckhardt, B.L., Francis, P.A., Parker, B.S. and Anderson, R.L, Strategies for the discovery and development of therapies for metastatic breast cancer. *Nat Rev Drug Discov* 2012, **11**:479-497
- Elmore, S., Apoptosis: A review of programmed cell death. *Toxicol Pathol* 2007, **35**(4):495-516
- Elnemr, A., Ohta, T., Yachie, A., Kayahara, M., Kitagawa, H., Fujimura, T. *et al.*, Human pancreatic cancer cells disable function of Fas receptors at several levels in Fas signal transduction pathway. *Int J Oncol* 2001, **18**(2):311-6
- Emery, J.G., McDonnell, P., Burke, M.B., Deen, K.C., Lyn, S. *et al.*, Osteoprotegerin is a receptor for the cytotoxic ligand TRAIL. *J Biol Chem* 1998, **273**(23):14363-7
- Fabian, C.J., The what, why and how of aromatase inhibitors: hormonal agents for treatment and prevention of breast cancer. *Int J Clin Pract* 2007, **61**(12):2051-2063
- Ferlay, J., Soerjomataram, I., Ervik, M., Dikshit, R., Eser, S. *et al.*, Cancer Incidence and Mortality Worldwide: IARC Cancer Base No 11., GLOBOCAN 2012 v1.0. Accessed 30.07.14

Flemming, A., Targeting the root of cancer relapse. *Nat Rev Drug Discov* 2015, **14**:165

Forero-Torres, A., Varley, K.E., Abramson, V.G., Li, Y., Vaklavas, C. *et al.*, TBCRC 019: A Phase II Trial of Nanoparticle Albumin-Bound Paclitaxel with or without the Anti-Death Receptor 5 Monoclonal Antibody Tigatuzumab in Patients with Triple-Negative Breast Cancer. *Clin Cancer Res* 2015, **12**:2722

Frank, N.Y., Schatton, T. and Frank, M.H., The therapeutic promise of the cancer stem cell concept. *J Clin Invest* 2010, **120**(1):41-50

French, R., The Role of cFLIP in Breast Cancer Stem Cells. PhD Thesis September 2014

French, R. and Clarkson, R., The complex nature of breast cancer stem-like cells: heterogeneity and plasticity. *J Stem Cell Res Ther* 2012, **S7**:009

French, R., Hayward, O., Jones, S., Yang, W. and Clarkson, R., Cytoplasmic levels of cFLIP determine a selective susceptibility of breast cancer stem/progenitor-like cells to TRAIL. *Mol Cancer* 2015 in press

Galvao, J., Davis, B., Tilley, M., Normando, E., Duchon, M.R. and Cordeiro, M.F., Unexpected low-dose toxicity of the universal solvent DMSO. *FASEB J* 2014, **28**(3):1317-30

Gao, S., Lee, P., Wang, H., Gerald, W., Alder, M., Zhang, L. *et al.*, The androgen receptor directly targets the cellular Fas/FaL-associated death domain protein-like inhibitory protein gene to promote the androgen-independent growth of prostate cancer cells. *Mol Endocrinol* 2005, **19**:1792-802

Garvey, T., Bertin, J., Siegel, R., Lendardo, M. and Cohen, J., The death effector domains (DEDs) of the molluscum contagiosum virus MC159 v-FLIP protein are not functionally interchangeable with each other or with the DEDs of caspase-8. *Virology* 2002, **300**(2):217-25

Garvey, T.L., Bertin, J., Siegel, R.M., Wang, G.H., Lenardo, M.J. and Cohen, J.I., Binding of FADD and caspase-8 to molluscum contagiosum virus MC159 v-FLIP is not sufficient for its antiapoptotic function. *J Virol* 2006, **76**(2):697-706

Goltsev, Y.V., Kovalenko, A.V., Arnold, E., Varfolomeev, E.E., Brodianskii, V.M. and Wallach, D., CASH, a novel caspase homologue with death effector domains. *J Biol Chem* 1997, **272**:19641-19644

Gomez-Angelats, M. and Cidlowski, J.A., Molecular evidence for the nuclear localization of FADD, *Cell Death and Differentiation* 2003, **10**:791-797

Green, D.R. and Kroemer, G., The pathophysiology of mitochondrial cell death. *Science* 2004, **305**(5684):626-9

- Grenman, R., Burk, D., Virolainen, E., Buick, R.N., Church, J. *et al.*, Clonogenic cell assay for anchorage-dependent squamous carcinoma cell lines using limiting dilution. *Int J Cancer* 1989, **44**(1):131-6
- Griffith, T.S. and Lynch, D.H., TRAIL: a molecule with multiple receptors and control mechanisms. *Curr Opin Immunol* 1998, **10**(5):559-63
- Griffith, T.S., Chin, W.A., Jackson, G.C., Lynch, D.H. and Kubin, M.Z., Intracellular regulation of TRAIL-induced apoptosis in human melanoma cells. *J Immunol* 1998, **161**:2833-2840
- Grunert, M., Gottschalk, K., Kapahnke, J., Gundisch, S., Kieser, A. and Jeremias, I., The adaptor protein FADD and the initiator caspase-8 mediate activation of NF- κ B by TRAIL. *Cell Death and Disease* 2012, **3**:e414
- Gupta, P.B., Fillmore, C.M., Jiang, G., Shapira, S.D., Tao, K. *et al.*, Stochastic state transitions give rise to phenotypic equilibrium in populations of cancer cells. *Cell* 2011, **146**(4):633-644
- Gura, T., How TRAIL kills cancer cells, but not normal cells. *Science* 1997, **277**(5327):768
- Haag, C., Stadel, D., Zhou, S., Bachem, M.G., Moller, P. *et al.*, Identification of c-FLIP(L) and c-FLIP(S) as critical regulators of death receptor-induced apoptosis in pancreatic cancer cells. *Gut* 2011, **60**(2):225-37
- Han, L., Shi, S., Gong, T., Zhang, Z. and Sun, X., Cancer stem cells: therapeutic implications and perspectives in cancer therapy. *Acta Pharmaceutica Sinica B* 2013, **3**(2):65-75
- Hanahan, D. and Weinberg, R.A., The hallmarks of cancer. *Cell* 2000, **100**:57-70
- Hanahan, D. and Weinberg, R.A., Hallmarks of cancer: the next generation. *Cell* 2011, **144**(5):646-74
- Harrison, H., Rogerson, L., Gregson, H.J., Brenna, K.R., Clarke, R.B. and Landberg, G., Contrasting Hypoxic Effects on Breast Cancer Stem Cell Hierachy Is Dependent on ER- α Status. *Cancer Res* 2013, **73**:1420
- Hassan, M.S.U., Ansari, J., Spooner, D. and Hussain, S.A., Chemotherapy for breast cancer (review). *Oncol Rep* 2010, **24**:1121-1131
- He, L., Olson, D.P., Wu, X., Karpova, T.S., McNally, J.G. and Lipsky, P.E., A flow cytometric method to detect protein-protein interaction in living cells by directly visualizing donor fluorophore quenching during CFP-->YFP fluorecence resonance energy transfer (FRET). *Cytometry* 2003, **55**(2):71-85

- Herbst, R.S., Eckhardt, S.G., Kurzrock, R., Ebbinghaus, S., O'Dwyer, P.J. *et al.*, Phase I dose-escalation study of recombinant human Apo2L/TRAIL, a dual proapoptotic receptor agonist, in patients with advanced cancer. *J Clin Oncol* 2010, **28**(17):2839-46
- Hess, B., Kutzner, C., Spoel, D.V.d. and Lindahl, E., Algorithms for highly efficient, load-balanced and scalable molecular simulation. *J Chem Theory Comput* 2008, **4**:435-447
- Hoelder, S., Clarke, P.A. and Workman, P., Discovery of small molecule cancer drugs: successes, challenges and opportunities. *Mol Oncol* 2012, **6**(2):255-178
- Holliday, D.L. and Speirs, V., Choosing the right cell line for breast cancer research. *Breast Cancer Res* 2011, **13**:215
- Howard, J.H. and Bland, K.I., Current management and treatment strategies for breast cancer. *Curr Opin Obstet Gynecol* 2012, **24**(1):44-8
- Hu, Y. and Fu, L., Targeting cancer stem cells: a new therapy to cure cancer patients. *Am J Cancer Res* 2012, **2**(3):340-356
- Hutchinson, L., Breast cancer: challenges, controversies, breakthroughs. *Nat Rev Clin Oncol* 2010, **7**:669-670
- Hwang, E.Y., Jeong, M.S., Park, S.Y. and Jang, S.B., Evidence of complex formation between FADD and c-FLIP death effector domains for the death inducing signaling complex. *BMB Rep* 2014, **47**(9):488-493
- Iglesias, J.M., Beloqui, I., Garcia-Garcia, F., Leis, O., Vazquez-Martin, A. *et al.*, Mammosphere formation in breast carcinoma cell lines depends upon expression of E-cadherin. *PLoS ONE* 2013, **8**(10):e77281
- Irmeler, M., Thome, M., Hahne, M., Schneider, P., Hofmann, K. *et al.*, Inhibition of death receptor signals by cellular FLIP. *Nature* 1997, **388**:190-195
- Jares-Erijman, E.A. and Jovin, T.M., FRET imaging, *Nat Biotech* 2003, **21**(11):1387
- Johnstone, R.W., Frew, A.J. and Smyth, M.J., The TRAIL apoptotic pathway in cancer onset, progression and therapy. *Nat Rev Cancer* 2008, **8**:782-798
- Jordan, V.C. and Murphy, C.S., Endocrine pharmacology of antiestrogens as antitumor agents. *Endocrine Reviews* 1990, **11**:578-610
- Kaiser, J., The cancer stem cell gamble. *Science* 2015, **347**(6219):226-229
- Kalluri, R. and Neilson, E.G., Epithelial-mesenchymal transition and its implications for fibrosis. *J Clin Invest* 2003, **112**(12):1776-1784

Kao, J., Salari, K., Bocanegra, M., Choi, Y-L., Girard, L. *et al.*, Molecular Profiling of Breast Cancer Cell Lines Defines Relevant Tumor Models and Provides a Resource for Cancer Gene Discovery. *PLoSone* 2009, **4**(7):e6146

Kasubhai, S.M., Bendell, J.C., Kozloff, M., Kapp, A.M., Ashkenazi, A. and Royer-Joo, S., Phase 1b study of dulanermin combined with FOLFIRI (with or without bevacizumab [BV]) in previously treated patients (Pts) with metastatic colorectal cancer (mCRC). *J Clin Oncol* 2012, **30**:3543

Kaufmann, M., Bozic, D., Briand, C., Bodmer, J.L., Zerbe, O. *et al.*, Identification of a basic surface area of the FADD death effector domain critical for apoptotic signalling. *FEBS Lett* 2002, **527**(1-3):250-4

Kim, D., Sun, M., He, L., Zhou, Q.H., Chen, J., Sun X.M. *et al.*, A small molecule inhibits Akt through direct binding to Akt and preventing Akt membrane translocation. *J Biol Chem* 2010, **285**:8383-94

Kim, H. and Kim, J-S., A guide to genome engineering with programmable nucleases. *Nat Rev Gen* 2014, **15**:321-334

Kim, J., Fisher, M.J., Xu, S.Q. and el-Deiry, W.S., Molecular determinants of response to TRAIL in killing of normal and cancer cells. *Clin Cancer Res* 2000, **6**(2):335-46

Kim, M.J., Kim, H.B., Bae, J.H., Lee, J-W., Park, S-J. *et al.*, Sensitisation of human K562 leukemic cells to TRAIL-induced apoptosis by inhibiting the DNA-PKcs/Akt-mediated cell survival pathway. *Biochem Pharmacol* 2009, **78**(6):573-82

Kim, Y., Suh, N., Sporn, M. and Reed, J.C., An inducible pathway for degradation of FLIP protein sensitizes tumor cells to TRAIL-induced apoptosis. *J Biol Chem* 2002, **277**(25):22320-9

Kitchen, D.B., Decornez, H., Furr, J.R. and Bajorath, Docking and scoring in virtual screening for drug discovery methods and applications. *Nat Rev Drug Discov* 2004, **3**:935-949

Kreike, B., van Kouwenhove, M., Horlings, H., Gene expression profiling and histopathological characterization of triple-negative/basal-like breast carcinomas. *Breast Cancer Res* 2007, **9**:R65

Lasfargues, E.Y., Coutinho, W.G. and Redfield, E.S., Isolation of two human tumor epithelial cell lines from solid breast carcinomas. *J Natl Cancer Inst* 1978, **61**(4):967-78

Lawson, J.C., Blatch, G.L. and Edkins, A.L., Cancer stem cells in breast cancer and metastasis. *Breast Cancer Res Treat* 2009, **118**(2):241-54

LeBlanc, H.N. and Ashkenazi, A., Apo2L/TRAIL and its death and decoy receptors. *Cell Death Differ* 2003, **10**(1):66-75

- Leary, A.F., Sirohi, B. and Johnston, S.R.D., Clinical trials update: endocrine and biological therapy combinations in the treatment of breast cancer. *Breast Cancer Res* 2007, **9**(5):112
- Lee, S., Yoon, C.Y., Byun, S.S., Lee, E. and Lee, S.E., The role of c-FLIP in cisplatin resistance of human bladder cancer cells. *J Urol* 2013, **189**(6):2327-34
- Leeson, P., Drug discovery: chemical beauty contest. *Nature* 2012, **481**:455-456
- Lemke, J., von Karstedt, S., Zinngrebe, J. and Walczak, H., Getting TRAIL back on track for cancer therapy. *Cell Death Differ* 2014, **21**(9):1350-1364
- Lens, S.M.A., Kataoka, T., Fornter, K.A., Tinel, A., Ferrero, I. *et al.*, The Caspase 8 Inhibitor c-FLIPL Modulates T-Cell Receptor-Induced Proliferation but Not Activation-Induced Cell Death of Lymphocytes. *Mol Cell Biol* 2002, **22**(15):5419-5433
- Lesk, A.M. and Chothia, C.H., The response of protein structures to amino-acid sequence changes. *Phil Trans R Soc Lond A* 1986, **317**(1540):345-356
- Leuchowius, K-J., Jarvius, M., Wickstrom, M., Rickardson, L., Landergren, U. *et al.*, High content screening for inhibitors of protein interactions and post-translational modifications in primary cells by proximity ligation. *Mol Cell Proteomics* 2010, **9**(1):178-183
- Li, B., Ren, H., Yue, P., Chen, M., Khuri, F.R. and Sun, S.Y., The novel Akt inhibitor API-1 induces c-FLIP degradation and synergizes with TRAIL to augment apoptosis independent of Akt inhibition. *Cancer Prev Res (Phila)* 2012, **5**(4):612-20
- Li, F-Y, Jeffrey, P.D., Yu, J.W. and Shi, Y., Crystal structure of a viral FLIP. *J Biol Chem* 2006, **281**:2960-2968
- Li, Y-C., Rodewald, L.W., Hoppman, C., Wong, E.T., Lebreton, S. *et al.* A versatile platform to analyze low affinity and transient protein-protein interactions in living cells in real time. *Cell Rep* 2014, **9**(5):1946-1958
- Ling, J., Herbst, R.S., Mendelson, D.S., Eckhardt, S.G., O'Dwyer, P. *et al.*, Apo2L/TRAIL pharmacokinetics in a phase 1a trial in advanced cancer and lymphoma. *J Clin Oncol* 2006, **24**(18S):3047
- Liu, S., Cong, Y., Wang, D. *et al.*, Breast cancer stem cells transition between epithelial and mesenchymal states reflective of their normal counterparts. *Stem Cell Reports* 2013, **2**(1):78-91
- Locke, M., Heywood, M., Fawell, S. and Mackenzie, I.C., Retention of intrinsic stem cell hierarchies in carcinoma-derived cell lines. *Cancer Res* 2005, **65**(19):8944-50

- Lopez-Garcia, M.A., Geyer, F.C., Lacroix-Triki, M., Marchio, C. and Reis-Filho, J.S., Breast cancer precursors revisited: molecular features and progression pathways. *Histopathology* (2010), **57**:171-192
- Luo, M., Brooks, M. and Wicha, M.S., Epithelial-mesenchymal plasticity of breast cancer stem cells: implications for metastasis and therapeutic resistance. *Curr Pharm Des* 2015, **21**(10):1301-10
- MacFarlane, M., Merrison, W., Dinsdale, D. and Cohen, G.M., Active Caspases and Cleaved Cytokeratins Are Sequestered into Cytoplasmic Inclusions in Trail-Induced Apoptosis. *J Cell Biol* 2000, **148**(6):1239-1254
- Macias, H. and Hinck, L., Mammary Gland Development. *Rev Dev Biol* 2012, **1**(4):533-557
- Majkut, J., Sgobba, M., Holohan, C., Crawford, N., Logan, A.E. *et al.*, Differential affinity of FLIP and procaspase 8 for FADD's DED binding surfaces regulates DISC assembly. *Nat Commun* **28**(5):3350
- Malhotra, G.K., Zhao, X., Band, H. and Band, V., Histological, molecular and functional subtypes of breast cancers. *Cancer Biol Ther* 2010, **10**(10):955-60
- Mali, P., Aach, J., Stranges, P.B., Esvelt, K.M., Moosburner, M. *et al.*, CAS9 transcriptional activators for target specificity screening and paired nickases for cooperative genome engineering. *Nat Biotechnol* 2013, **31**(9):1038
- Mariani, S.M. and Krammer, P.H., Surface expression of TRAIL/Apo-2 ligand in activated mouse T and B cells. *Eur J Immunol* 1998, **28**(5):1492-8
- Matsumura, H., Shimizu, Y., Ohsawa, Y., Kawahara, A., Uchiyama, Y. and Nagata, S., Necrotic death pathway in Fas receptor signaling. *J Cell Biol* 2000, **151**:1247-1256
- Mawji, I.A., Simpson, C.D., Hurren, R., Gronda, M., Williams, M.A. *et al.*, Critical role for Fas-associated death domain-like interleukin-1-converting enzyme-like inhibitory protein in anoikis resistance and distant tumor formation. *J Natl Cancer Inst* 2007, **99**:811-822
- McDonnell, D.P. and Wardell, S.E., The molecular mechanisms underlying the pharmacological actions of ER modulators: Implications for new drug discovery in breast cancer. *Curr Opin Pharmacol* 2010, **10**(6):620-628
- McPherson, K., Steel, C.M. and Dixon, J.M., Breast cancer - epidemiology, risk factors and genetics. *BMJ* 2000, **321**(7261):624-628
- Medema, J.P., Scaffidi, C., Kischkel, F.C. *et al.*, FLICE is activated by associated with the CD95 death-inducing signalling complex (DISC). *EMBO* 1997, **16**(10):2794-2804

- Merlo, G.R., Basolo, F., Fiore, L., Duboc, L. and Hynes, N.E., p53-dependent and p53-independent activation of apoptosis in mammary epithelial cells reveals a survival function of EGF and insulin. *JCB* 1995, **128**(6):1185
- Micheau, O., Cellular FLICE-inhibitory protein: An attractive therapeutic target? *Expert Opin Ther Targets* 2003, **7**:559-73
- Micheau, O., Thome, M., Schneider, P., Holler, N., Tschopp, J. *et al.*, The long form of FLIP is an activator of caspase-8 at the Fas death-inducing signaling complex. *J Biol Chem* 2002, **277**:45162-71
- Miller, J.C., Tan, S., Qiao, G., Barlow, K.A., Wang, J. *et al.*, A TALE nuclease architecture for efficient genome editing. *Nat Biotechnol* 2011, **29**(2):143-8
- Milne, R.L. and Antoniou, A.C., Genetic modifiers of cancer risk for *BRCA1* and *BRCA2* mutation carriers. *Ann Oncol* 2011, **22**(1):11-17
- Mincey, B.C., Genetics and the management of women at high risk for breast cancer. *Oncologist* 2003, **8**(5):466-473
- Mishra, J.K. and Panda, G., Diversity-Oriented Synthetic Approach to Naturally Abundant S-Amino Acid Based Benzannulated Enantiomerically Pure Medium Ring Heterocyclic Scaffolds Employing Inter- and Intramolecular Mitsunobu Reactions. *J Comb Chem* 2007, **9**(2):321-338
- Moreno-Bueno, G., Portillo, F. and Cano, A., Transcriptional regulation of cell polarity in EMT and cancer. *Oncogene* 2008, **27**:6958-6969
- Morony, S., Capparelli, C., Sarosi, I., Lacey, D.L., Dunstan, C.R. and Kostenuik, P.J., Osteoprotegerin inhibits osteolysis and decreases skeletal tumor burden in syngeneic and nude mouse models of experimental bone metastasis. *Cancer Res* 2001, **61**(11):4432-6
- Naito, M., Katayama, R., Ishioka, T., Suga, A., Takubo, K. *et al.*, Cellular FLIP inhibits β -catenin ubiquitylation and enhances Wnt signaling. *Mol Cell Biol* 2004, **24**(19):8414-8427
- Nam, S.Y., Jung, G.A., Hur, G.C., Chung, H.Y., Kim, W.H., Seol, D.W. and Lee, B.L., Upregulation of FLIP(S) by Akt, a possible inhibition mechanism of apoptosis in human gastric cancers. *Cancer Sci* 2003, **94**:1066-1073
- Nayeem, A., Sitkoff, D. and Krystek, S., Jr., A comparative study of available software for high-accuracy homology modelling: From sequence alignments to structural models. *Protein Sci*, **15**(4):808-824
- Neumann, S., Hasenauer, J., Pollak, N. and Scheurich, P., Dominant negative effects of TNF-related apoptosis-inducing ligand (TRAIL) receptor 4 on TRAIL receptor 1 signaling by formation of heteromeric complexes. *J Biol Chem* 2014, **289**(23):16576-87

- Neve, R.M., Chin, K., Fridlyand, J. *et al.*, A collection of breast cancer cell lines for the study of functionally distinct cancer subtypes. *Cancer Cell* 2006, **10**(6):515-27
- Norbury, C.J. and Hickson, I.D., Cellular responses to DNA damage. *Annu Rev Pharmacol Toxicol* 2001, **41**:367-401
- NCIN: National Cancer Intelligence Network. *The second all breast cancer report.*, Birmingham NCIN 2011
- O'Donovan, P.J. and Livingston, D.M., BRCA1 and BRCA2: breast/ovarian cancer susceptibility gene products and participants in DNA double-strand break repair. *Carcinogenesis* 2010, **31**(6):961-967
- Okano, H., Shiraki, K., Inoue, H., Kawakita, T., Yamanaka, T. *et al.*, Cellular FLICE/caspase-8-inhibitory protein as a principal regulator of cell death and survival in human hepatocellular carcinoma. *Lab Invest* 2003, **83**(7):1033-43
- Olsson, A., Diaz, T., Aguilar-Santelises, M., Osterborg, A., Celsing, F. and Jondal, M., Sensitisation to TRAIL-induced apoptosis and modulation of FLICE-inhibitory protein in B chronic lymphocytic leukemia by actinomycin D. *Leukemia* 2001, **15**(12):1868-77
- Pan, G., Ni, J., Wei, G. *et al.*, An antagonist decoy receptor and a death-domain containing receptor for TRAIL. *Science* 1997, **277**(5327):815-818
- Pan, Y., Xu, R., Peach, M., Huang, C., Branstetter, D. *et al.*, Application of pharmacodynamics assays in a phase Ia trial of Apo2L/TRAIL in patients with advanced tumors. *J Clin Oncol* 2007, **25**:3535
- Panka, D.J., Mano, T., Suhara, T., Walsh, K. and Mier, J.W., Phosphatidylinositol 3-kinase/Akt activity regulates c-FLIP expression in tumor cells. *J Biol Chem* 2001, **276**:6893-6
- Parker, J.S., Mullins, M., Cheang, M.C.U., Leung, S., Voduc, D. *et al.*, Supervised risk predictor of breast cancer based on intrinsic subtypes. *J Clin Oncol* 2008, **27**(8):1160-1167
- Peifer, C., Kinkel, K., Abadleh, M., Schollmeyer, D. And Laufer, S., From Five- to Six-Membered Rings: 3,4-Diarylquinolinone as Lead for Novel p38MAP Kinase Inhibitors. *J Med Chem* 2007, **50**(6):1213-1221
- Pellegrini, G., Dellambra, E., Golisano, O., Martinelli, E., Fantozzi, I. *et al.*, p63 identifies keratinocyte stem cells. *Proc Nat Acad Sci* 2001, **98**:3156-3161
- Peter, M.E., The flip side of FLIP, *Biochem J* 2004, **382**(2):E1
- Polyak, K., Breast cancer: origins and evolution. *J Clin Invest* 2007, **117**(11):3155-3163

- Polyak, K., Is Breast Tumor Progression Really Linear? *Clin Cancer Res* 2008, **14**:339
- Polyak, K., Heterogeneity in breast cancer. *J Clin Invest* 2011, **121**(10):3786-3788
- Pietras, A., Cancer stem cells in tumor heterogeneity. *Adv Cancer Res* 2011, **112**:255-281
- Piggott, L., Omidvar, N., Pérez, S.M., Eberl, M. and Clarkson, R.W.E., Suppression of apoptosis inhibitor c-FLIP selectively eliminates breast cancer stem cell activity in response to the anti-cancer agent, TRAIL. *Breast Cancer Res* 2011, **13**(5):R88
- Prat, A., Parker, J.S., Karginova, O., Fan, C., Livasy, C. *et al.*, Phenotypic and molecular characterization of the claudin-low intrinsic subtype of breast cancer. *Breast Cancer Res* 2010, **12**:R68
- Qiu, Y., Liu, X., Zou, W., Yue, P., Lonial, S. *et al.*, The farnesyltransferase inhibitor R115777 up-regulates the expression of death receptor 5 and enhances TRAIL-induced apoptosis in human lung cancer cells. *Cancer Res* 2007, **67**:4973-4980
- Quintaville, C., Incoronato, M., Puca, L., Acunzo, M., Zanca, C. *et al.*, c-FLIPL enhances anti-apoptotic Akt functions by modulation of Gsk3 β activity. *Cell Death Differ* 2010, **17**(12):1908-16
- Rachet, B., Maringe, C., Nur, U., Quaresma, M., Shah, A. *et al.*, Population based cancer survival trends in England and Wales up to 2007: an assessment of the NHS cancer plan for England. *Lancet Oncol* 2009, **10**:351-69
- Rahman, M., Pumphrey, J.G. and Lipkowitz, S., The TRAIL to targeted therapy of breast cancer. *Adv Cancer Res* 2009, **103**:43-73
- Rahman, M., Davis, S.R., Pumphrey, J.G., Bao, J., Nau, M.M. *et al.*, TRAIL induces apoptosis in triple-negative breast cancer cells with a mesenchymal phenotype. *Breast Cancer Res Treat* 2009, **113**:217-230
- Rao-Bindal, K., Koshkina, N.V., Stewart, J. and Kleinerman, E.S., The histone deacetylase inhibitor, MS-275 (entinostat), downregulates c-FLIP sensitizes osteosarcoma cells to FasL, and induces the regression of osteosarcoma lung metastases. *Curr Cancer Drug Targets* 2013, **13**(4):411-22
- Reynolds, B.A. and Weiss, S., Generation of neurons and astrocytes from isolated cells of the adult mammalian central nervous system. *Science* 1992, **255**:1707-1710
- Ricci, M.S., Jin, Z., Dews, M., Yu, D., Thomas-Tikhonenko, A. *et al.*, Direct repression of FLIP expression by c-myc is a major determinant of TRAIL sensitivity. *Mol Cell Biol* 2004, **24**(19):8541-55

- Ricci, M.S., Kim, S.H., Ogi, K., Plastaras, J.P., Ling, J. *et al.*, Reduction of TRAIL-induced Mcl-1 and cIAP2 by c-Myc or sorafenib sensitizes resistant human cancer cells to TRAIL-induced death. *Cancer Cell* 2007, **12**(1):66-80
- Ring, C.S., Sun, E., McKerrow, J.H., Lee, G.K., Rosenthal, P.J. *et al.*, Structure-based inhibitor design by using protein models for the development of antiparasitic agents. *Proc Natl Acad Sci USA* 1993, **90**(8):3583-7
- Ripperger, T., Gadzicki, D., Meindl, A. and Schlegelberger, B., Breast cancer susceptibility: current knowledge and implications for genetic counselling. *Eur J Hum Genet* 2009, **17**(6):722-731
- Rossin, A., Derouet, M., Abdel-Sater, F. and Hueber, A.O., Palmitoylation of the TRAIL receptor DR4 confers an efficient TRAIL-induced cell death signalling. *Biochem J* 2009, **419**(1):185-92
- Roszik, J., Toth, G., Szollosi, J. and Vereb, G., Validating pharmacological disruption of protein-protein interactions by acceptor photobleaching FRET imaging. *Methods Mol Biol* 2013, **986**:165-78
- Ryu, B.K., Lee, M.G., Chi, S.G., Kim, Y.W. and Park, J.H., Increased expression of c-FLIP(L) in colonic adenocarcinoma. *J Pathol* 2001, **194**:15-19
- Safa, A.R., c-FLIP, A master anti-apoptotic regulator. *Exp Oncol* 2012, **34**(3):176-184
- Safa, A.R., Roles of c-FLIP in Apoptosis, Necroptosis, and Autophagy. *J Carcinog Mutagen* 2013, **6**:003
- Safa, A.R., Day, T.W. and Wu, C.H., Cellular FLICE-like inhibitory protein (C-FLIP): a novel target for cancer therapy. *Curr Cancer Drug Targets* 2008, **8**(1):37-46
- Safa, A.R. and Pollok, K.E., Targeting the anti-apoptotic protein c-FLIP for cancer therapy. *Cancers (Basel)* 2011, **3**:1639-71
- Samanta, D., Gilkes, D.M., Chaturvedi, P., Xiang, L. and Semenza, G.L., Hypoxia-inducible factors are required for chemotherapy resistance of breast cancer stem cells. *PNAS* 2014, **111**(50):E5429-E5438
- Sandhiya, S., Melvin, G., Kumar, S.S. and Dkhar, S.A., The dawn of hedgehog inhibitors: Vismodegib. *J Pharmacol Pharmacother* 2013, **4**(1):4-7
- Savjani, K.T., Gajjar, A.K. and Savjani, J.K., Drug Solubility: Importance and Enhancement Techniques. *ISRN Pharm* 2012, 195727
- Scaffidi, C., Schmitz, I., Krammer, P.H. and Peter, M.E., The role of c-FLIP in modulation of CD95-induced apoptosis. *J Biol Chem* 1999, **274**(3):1541-8

- Schimmer, A.D., Thomas, M.P., Hurren, R., Gronda, M., Pellecchia, M. *et al.*, Identification of small molecules that sensitize resistant tumor cells to tumor necrosis factor-family death receptors. *Cancer Res* 2006, **66**(4):2367-2375
- Schonthal, A.H., Antitumor properties of dimethyl-celecoxib, a derivative of celecoxib that does not inhibit cyclooxygenase-2: implications for glioma therapy. *Neurosurg Focus* 2006, **20**:E21
- Schlotter, C.M., Vogt, U., Allgayer, H. And Brandt, B., Molecular targeted therapies for breast cancer treatment. *Breast Cancer Res*, **10**:211
- Schuchmann, M., Schulze-Bergkamen, H., Fleischer, B., Schattenberg, J.M. *et al.*, Histone deacetylase inhibition by valproic acid down-regulates c-FLIP/CASH and sensitizes hepatoma cells towards CD95- and TRAIL receptor mediated apoptosis and chemotherapy. *Oncol Rep* 2006, **15**(1):227-30
- Senkus, E., Kyriakides, S., Penault-Llorca, F., Poortmans, P., Thompson, A. *et al.*, Primary breast cancer: ESMO Clinical Practice Guidelines for diagnosis, treatment and follow-up. *Ann Oncol* 2013, **0**:1-17
- Siegal, G.P., Barsky, S.H., Terranova, V.P. and Liotta, L.A., Stages of neoplastic transformation of human breast tissue as monitored by dissolution of basement membrane components. An immunoperoxidase study. *Invasion Metastasis* 1981, **1**(1):54-70
- Shanakar, S., Singh, T.R., Fandy, T.E., Luetrakul, T., Ross, D.D. *et al.*, Interactive effects of histone deacetylase inhibitors and TRAIL on apoptosis in human leukemia cells: involvement of both death receptor and mitochondrial pathways. *Int J Mol Med* 2005, **16**(6):1125-38
- Shapiro, H.M., Flow cytometric estimation of DNA and RNA content in intact cells stained with hoechst 33342 and pyronin γ . *Cytometry* 1981, **2**(3):143-150
- Sharp, D.A., Lawrence, D.A. and Ashkenazi, A., Selective Knockdown of the Long Variant of Cellular FLICE Inhibitory Protein Augments Death Receptor-mediated Caspase-8 Activation and Apoptosis. *J Biol Chem* 2005, **280**:19401-19409
- Sheridan, J.P., Marsters, S.A., Pitti, R.M. *et al.*, Control of TRAIL-induced apoptosis by a family of signaling and decoy receptors. *Science* 1997, **277**:818-821
- Shi, B., Tran, T., Sobkoviak, R. and Pope, R.M., Activation-induced degradation of FLIP(L) is mediated via the phosphatidylinositol 3-kinase/Akt signaling pathway in macrophages. *J Biol Chem* 2009, **284**:14513-23
- Shin, M.S., Kim, H.S., Lee, S.H., Park, W.S., Kim, S.Y. *et al.*, Mutations of tumor necrosis factor-related apoptosis-inducing ligand receptor 1 (TRAIL-R1) and receptor 2 (TRAIL-R2) genes in metastatic breast cancers. *Cancer Res* 2001, **61**:4942-4946

- Shirely, S. and Micheau, O., Targeting c-FLIP in cancer. *Cancer Lett* 2013, **332**(2):141-150
- Siegel, R.M., Martin, D.A., Zheng, L., Ng, S.Y., Bertin, J. *et al.*, Death-effector Filaments: Novel Cytoplasmic Structures that Recruit Caspases and Trigger Apoptosis. *JCB* 1998, **141**(5):1243-1253
- Simpson, P.T., Gale, T., Fulford, L.G., Reis-Filho, J.S. and Lakhani, S.R., The diagnosis and management of pre-invasive breast disease: Pathology of atypical lobular hyperplasia and lobular carcinoma *in situ*. *Breast Cancer Res* 2003, **5**(5):258-62
- Soria, J-C., Smit, E., Khayat, D., Besse, B., Yang, X. *et al.*, Phase 1b Study of Dulanermin (recombinant human Apo2L/TRAIL) in Combination With Paclitaxel, Carboplatin, and Bevacizumab in Patients With Advanced Non-Squamous Non-Small-Cell Lung Cancer. *JCO* 2010, **28**(9):1527-1533
- Sorlie, T., Perou, C.M., Tibshirani, R. *et al.*, Gene expression patterns of breast carcinomas distinguish tumor subbreast cancerclasses with clinical implications. *Proc Natl Acad Sci USA* 2001, **98**:10869-10874
- Soria, J.C., Smit, E., Khayat, D., Besse, B., Yang, X. *et al.*, Phase 1b study of dulanermin (recombinant human Apo2L/TRAIL) in combination with paclitaxel, carboplatin and bevacizumab in patients with advanced non-squamous non-small-cell lung cancer. *J Clin Oncol* 2010, **28**:1527-1533
- Soria, J.C., Mark, Z., Zatloukal, P., Szyma, B., Albert, I. *et al.*, Randomised phase II study of dulanermin in combination with paclitaxel, carboplatin, and bevacizumab in advanced non-small-cell lung cancer. *J Clin Oncol* 2011, **29**(33):4442-51
- Sotiriou, C., Wirapati, P., Loi, S. *et al.*, Gene expression profiling in breast cancer: understanding the molecular basis of histologic grade to improve prognosis. *J Natl Cancer Inst* 2006, **98**(4):262-72
- Soule, H.D., Maloney, T.M., Wolman, S.R., Peterson, W.D., Brenz, R. *et al.*, Isolation and characterisation of a spontaneously immortalized human breast epithelial cell line, MCF-10. *Cancer Res* 1990, **50**(18):6075-86
- Sprick, M.R., Weigand, M.A., Rieser, E., Racuch, C.T., Juo, P. *et al.*, FADD/MORT1 and Caspase-8 are recruited to TRAIL receptors 1 and 2 and are essential for apoptosis mediated by TRAIL receptor 2. *Immunity* 2000, **12**(6):599-609
- Stingl, J. and Caldas, C., Molecular heterogeneity of breast carcinomas and the cancer stem cell hypothesis. *Nat Rev Cancer* 2007, **7**:791-799
- Stuckey, D.W. and Shah, K., TRAIL on trial: preclinical advances in cancer therapy. *Trends Mol Med* 2013, **19**(11):685-694
- Subramaniam, D.S. and Isaacs, C., Utilizing prognostic and predictive factors in breast cancer. *Curr Treat Options Oncol* 2005, **6**(2):147-59

- Suliman, A., Lam, A., Datta, R. and Srivastava, R.K., Intracellular mechanisms of TRAIL: apoptosis through mitochondrial-dependent and -independent pathways. *Oncogene* 2001, **20**(17):2122-33
- Szegezdi, E., O'Reilly, A., Davy, Y. *et al.*, Stem cells are resistant to TRAIL receptor-mediated apoptosis. *J Cell Mol Med* 2009, **13**(11-12):4409-14
- Takeda, K., Hayakawa, Y., Smyth, M.J., Kayagaki, N., Yamaguchi, N. *et al.*, Involvement of tumor necrosis factor-related apoptosis inducing ligand in surveillance of tumor metastasis by liver natural killer cells. *Nat Med* 2001, **7**:94-100
- Taylor-Papadimitriou, J., Berdichevsky, F., D'Souza, B. and Burchell, J., Human models of breast cancer. *Cancer Surv* 1993, **16**:59-78
- Tazzari, P.L., Tabellini, G., Ricci, F., Papa, V., Bortul, R. *et al.*, Synergistic proapoptotic activity of recombinant TRAIL plus the Akt inhibitor Perifosine in acute myelogenous leukemia cells. *Cancer Res* 2008, **68**(22):9394-403
- Terry, P.D. and Rohan, T.E., Cigarette Smoking and the Risk of Breast Cancer in Women: A Review of the Literature. *Cancer Epidemiol BioMarkers Prev* 2002, **11**:953
- Thiery, J.P., Acloque, H., Huang, R.Y. and Nieto, M.A., Epithelial-mesenchymal transitions in development and disease. *Cell* 2009, **139**:871-890
- Thiery, J.P., Epithelial-mesenchymal transitions in tumour progression. *Nat Rev Cancer* 2002, **2**:442-454
- Thiery, J.P., Epithelial-mesenchymal transitions in development and pathologies. *Curr Opin Cell Biol* 2006, **15**:740-746
- Thome, M. and Tschopp, J., Regulation of lymphocyte proliferation and death by FLIP. *Nat Rev Immunol* 2001, **1**(1):50-8
- Thompson, E.W. and Haviv, I., The social aspects of EMT-MET plasticity. *Nat Med* 2011, **17**:1048-1049
- Thun, M.J., Henley, S.J. and Patrono, C., Nonsteroidal anti-inflammatory drugs as anticancer agents: mechanistic, pharmacologic, and clinical issues. *J Natl Cancer Inst* 2002, **94**:252-266
- Tinoco, G., Warsch, S., Glück, S., Avancha, K. And Montero, A.J., Treating breast cancer in the 21st Century: Emerging biological therapies. *J Cancer* 2013, **4**(2):117-132
- Trivedi, R. and Mishra, D.P., Trailing TRAIL resistance: novel targets for sensitization in cancer cells. *FONC* 2015, **5**(69):1-20

Ueffing, N., Keli, E., Freund, C., Kuhne, R., Schulze-Osthoff, K. and Schmitz, I., Mutational analyses of c-FLIPR, the only murine short FLIP isoform, reveal requirements for DISC recruitment. *Cell Death Differ* 2008, **15**(4):733-82

Valmiki, M.G. and Ramos, J.W., Death effector domain-containing proteins. *Cell Mol Life Sci* 2009, **66**(5):814-30

van Dijk, M., Halpin-McCormick, A., Sessler, T., Samali, A. and Szegezdi, E., Resistance to TRAIL in non-transformed cells is due to multiple redundant pathways. *Cell Death and Disease* 2013, **4**:e702

Verastem.com, Novel Drugs Targeting Cancer Stem cells verastem.com/research, Accessed 28.04.15

Vinogradov, S. and Wei, X., Cancer stem cells and drug resistance: the potential of nanomedicine. *Nanomedicine* 2013, **7**(4):597-615

Vogel, V.G., Breast cancer prevention: a review of current evidence. *CA Cancer J Clin* 2000, **50**(3):156-70

Wagner, K.W., Punnoose, E.A., Januario, T., Lawrence, D.A., Pitti, R.M. *et al.*, Death-receptor-O-glycosylation controls tumor-cell sensitivity to the proapoptotic ligand Apo2L/TRAIL. *Nat Med* 2007, **13**:1070-1077

Wainberg, Z.A., Messersmith, W.A., Peddi, P.F., Kapp, A.V., Ashkenazi, A. *et al.*, A phase 1B study of dulanermin in combination with modified FOLFOX6 plus bevacizumab in patients with metastatic colorectal cancer. *Clin Colorectal Cancer* 2013, **12**:248-254

Walczak, H., Miller, R.E., Ariail, K., Gliniak, B., Griffith, T.S. *et al.*, Tumoricidal activity of tumor necrosis factor-related apoptosis-inducing ligand in vivo. *Nat Med* 1999, **5**(2):157-63

Walker, R.A., Immunohistochemical markers as predictive tools for breast cancer. *J Clin Pathol*, **61**:689-696

Wang, J., Chun, H.J., Wong, W., Spencer, D.M. and Lenardo, M.J., Caspase-10 is an initiator caspase in death receptor signaling. *PNAS* 2001, **98**(24):13884-13888

Wang, P., Zhang, J., Bellail, A., Jiang, W., Hugh, J. *et al.*, Inhibition of RIP and c-FLIP enhances TRAIL-induced apoptosis in pancreatic cancer cells. *Cellular Signalling* 2008, **20**(1):268

Wang, S. and El-Deiry, W.S., TRAIL and apoptosis induction by TNF-family death receptors. *Oncogene* 2003, **22**:8628-8633

Wang, Y., Engels, I.H., Knee, D.A., Nasoff, M., Deveraux, Q.L. and Quon, K.C., Synthetic lethal targeting of MYC by activation of the DR5 death receptor pathway. *Cancer Cell* 2004, **5**(5):501-12

- Wang, Z., Goulet, T., Stanton, K.J., Sadaria, M. and Nakshatri, H., Differential effect of anti-apoptotic genes Breast cancer1-xL and c-FLIP on sensitivity of MCF-7 breast cancer cells to paclitaxel and docetaxel. *Anticancer Res* 2005, **25**:2367-2380
- Waszkoqycz, B., Clark, D.E. and Gancia, E., Outstanding challenges in protein-ligand docking and structure-based virtual screening. *WIREs Comput Mol Sci* 2011, **1**:229-259
- Weber, C.H. and Vincenz, C., The death domain superfamily: a tale of two interfaces? *Trends Biochem Sci*, **26**:475-481
- Weigelt, B., Geyer, F.C. and Reis-Filho, J.S., Histological types of breast cancer: How special are they? *Mol Oncol* **4**(3):192-208
- Wicha, M.S., Liu, S. and Dontu, G., Cancer stem cells: an old idea – a paradigm shift. *Cancer Res* 2006, **66**(4):1883-90
- Wiezorek, J., Holland, P. and Graves, J., Death receptor agonists as a targeted therapy for cancer. *Clin Cancer Res* 2010, **16**(6):1701-8
- Williams, J.M. and Daniel, C.W., Mammary ductal elongation: differentiation and myoepithelium basal lamina during branching morphogenesis. *Dev Biol* 1983, **97**:274-290
- Wong, R.S.Y., Apoptosis in cancer: from pathogenesis to treatment. *J Exp & Clin Cancer Res* 2011, **30**:87
- Xiang, Z., Advances in Homology Protein Structure Modeling, *Curr Protein Pept Sci* 2007, **7**(3):217-227
- Xiao, C.W., Xiaojuan, Y., Li, Y., Reddy, S.A.G. and Tsang, B.K., Resistance of human ovarian cancer cells to tumour necrosis factor α is a consequence of nuclear factor κ B-mediated induction of fass-associated death domain-like interleukin-1 β -converting enzyme-like inhibitory protein. *Cancer* 2003, **144**(2):623
- Xu, Z., Tang, K., Wang, M., Rao, Q., Liu, B. and Wang, J., A new caspase-8 isoform caspase-8s increased sensitivity to apoptosis in Jurkat cells. *J Biomed Biotech* 2009, 930462
- Yang, J., Wang, L., Zheng, L., Wan, F., Ahmed, M. *et al.*, Crystal structure of MC159 reveals molecular mechanism of DISC assembly and FLIP inhibition. *Mol Cell* 2005, **20**:939-949
- Yang, X., Merchant, M.S., Romero, M.E., Tsokos, M., Wexler, L. *et al.*, Induction of caspase 8 by interferon gamma renders some neuroblastoma (NB) cells sensitive to tumor necrosis factor-related apoptosis-inducing ligand (TRAIL) but reveals that a lack of membrane TR1/TR2 also contributes to TRAIL resistance in NB. *Cancer Res* 2003, **63**:1122-1129

- Yee, L., Burris, H.A., Kozloff, M., Wainberg, Z., Pao, M. *et al.* Phase Ib study of recombinant human Apo2L/TRAIL plus irinotecan and cetuximab or FOLFIRI in metastatic colorectal cancer (mCRC) patients (pts). Preliminary results. *J Clin Oncol* 2009, **27**: 4129
- Yee, L., Fanale, M., Dimick, K., Calvert, S., Robins, C. *et al.*, A phase IB safety and pharmacokinetic (PK) study of recombinant human Apo2L/TRAIL in combination with rituximab in patients with low-grade non-Hodgkin lymphoma. *J Clin Oncol* 2007, **25**: 8078
- Yeh, W.C., Itie, A., Elia, A.J., Ng, M., Shu, H.B. *et al.*, Requirement for Casper (c-FLIP) in regulation of death receptor-induced apoptosis and embryonic development. *Immunity* 2000, **12**(6):633-42
- Yen, W-C., Fischer, M.M., Axelrod, F., Bond, C., Cain, J. *et al.*, Targeting Notch Signaling with a Notch2/Notch3 Antagonist (Tarextumab) Inhibits Tumor Growth and Decreases Tumor-Initiating Cell Frequency. *Clin Cancer Res* 2015, **21**:2084
- Yerbes, R. and Lopez-Rivas, A., Itch/AIP-4-independent proteasomal degradation of cFLIP induced by the histone deacetylase inhibitor SAHA sensitizes breast tumour cells to TRAIL. *Invest New Drugs* 2012, **30**(2):541-7
- Younes, A., Vose, J.M., Zelenetz, A.D., Smith, M.R., Burris, H.A. *et al.*, A Phase 1b/2 trial of mapatumumab in patients with relapsed/refractory non-Hodgkin's lymphoma. *Br J Cancer* 2010, **103**(12):1783-1787
- Zang, F., Wei, X., Leng, X., Yu, M. and Sun, B., C-FLIP(L) contributes to TRAIL resistance in HER-2-positive breast cancer. *Biochem and Biophys Res Comm* 2014, **450**(1):267-273
- Zerafa, N., Westwood, J.A., Cretney, E., Mitchell, S., Waring, P. *et al.*, Cutting edge: TRAIL deficiency accelerates haematological malignancies. *J Immunol* 2005, **175**(9):5586-90
- Zhang, F., Cong, L., Lodato, S., Kosuri, S., Church, G.M. and Arlotta, P., Efficient construction of sequence-specific TAL effectors for modulating mammalian transcription. *Nat Biotechnol* 2011, **29**(2):149-53
- Zhang, K. and Waxman, D.J., PC3 prostate tumor-initiating cells with molecular profile FAM65B^{high}/MFI12^{low}/LEF1^{low} increase tumor angiogenesis. *Mol Cancer* 2010, **9**:319
- Zhang, L. and Fang, B., Mechanisms of resistance to TRAIL-induced apoptosis in cancer. *Cancer Gene Ther* 2005, **12**:228-237
- Zhang, L., Zhu, H., Teraishi, F., Davis, J.J., Guo, W. *et al.*, Accelerated degradation of caspase-8 protein correlates with TRAIL resistance in a DLD1 human colon cancer cell line. *Neoplasia* 2005, **7**(6):594-602

Zhang, N., Hopkins, K. and He, Y.W., The long isoform of cellular FLIP is essential for T lymphocyte proliferation through an NF- κ B independent pathway. *J Immunol* 2008, **180**:5506-11

Zhang, X.D., Nguyen, T., Thomas, W.D., Sanders, J.E. and Hersey, P., Mechanisms of resistance of normal cells to TRAIL induced apoptosis vary between different cell types. *FEBS Letters* 2000, **482**(3):193-199

Zhang, Y. and Zhang, B., TRAIL resistance of breast cancer cells is associated with constitutive endocytosis of death receptors 4 and 5. *Mol Cancer Res* 2008, **6**(12):1861-71

Zong, H., Yin, B., Chen, J., Ma, B., Cai, D. and He, X., Over-expression of c-FLIP confers the resistance to TRAIL-induced apoptosis on gallbladder cancer. *Tohoku J Exp Med* 2009, **217**(3):203-8

Appendices

A6.1 OH14 Synthesis

Amounts equal to 2-anthranilic acid (5.78 mmol), 2,4-dichloro-5-methyl-phenyl sulfonyl chloride (5.78mmol) and NaOH were mixed into 50 ml of water and stirred at room temperature overnight. The product was filtered, washed with water, dried and recrystallized from EtOH.

A6.2: Analogue Synthesis

P-toluenesulfonyl chloride (7.95 mmol), under an atmosphere of nitrogen, was added to the stirred solution of methyl anthranilate (6.62 mmol) in anhydrous pyridine (20 ml). The reaction mixture was stirred at room temperature for 6 hours and was then quenched by the addition of water. The aqueous layer was extracted using ethylacetate (3 x 50 ml additions) and dried over anhydrous sodium sulphate. The solvent was removed under vacuum, and the crude product was then chromatographed over silica gel (eluen: hexane/ethylacetate 9/1), to produce a compound yield of 85%. This method followed a previously described method of synthesis for similar chemical structural compounds (Mishra and Panda, 2007).

Table A6.1: SPECS analogues of Compound OH14 (14 and 14.2 are the same compound).

H d = hydrogen donors, H a = hydrogen acceptors

Cpd.	MW (g/mol)	Formula	H d	H a	
OH14	360.22	C₁₄H₁₁Cl₂NO₄S	2	5	
14.1	360.22	C ₁₄ H ₁₁ Cl ₂ NO ₄ S	2	5	
14.2	360.22	C₁₄H₁₁Cl₂NO₄S	2	5	Same structure as 14
14.3	339.8	C ₁₅ H ₁₄ ClNO ₄ S	2	5	
14.4	360.22	C ₁₄ H ₁₁ Cl ₂ NO ₄ S	2	5	
14.5	332.21	C ₁₃ H ₁₁ Cl ₂ NO ₃ S	2	4	
14.6	325.77	C ₁₄ H ₁₂ ClNO ₄ S	2	5	
14.7	360.22	C ₁₄ H ₁₁ Cl ₂ NO ₄ S	2	5	
14.8	380.64	C ₁₃ H ₈ Cl ₃ NO ₄ S	2	5	
14.9	305.35	C ₁₅ H ₁₅ NO ₄ S	2	5	

Table A6.2: Pharmacy Synthesised Compounds – GG1-12

Compound	MW (g/mol)	Structure
GG1	374.239	
GG2	374.239	
GG3	374.239	
GG4	359.3	
GG5	319.37	
GG6	360.21	
GG7	360.21	
GG8	319.37	
GG9	319.37	
GG10	360.2	

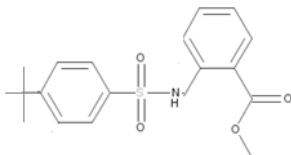
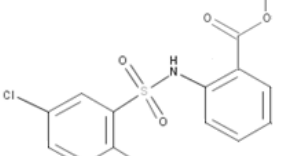
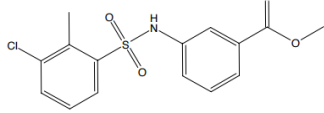
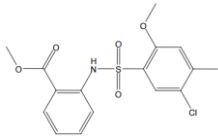
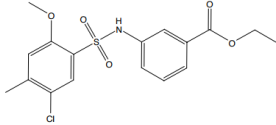
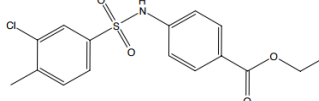
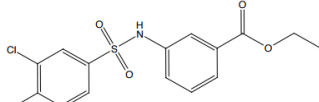
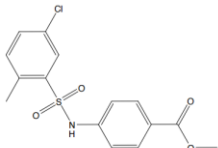
GG11	347.4	
GG12	339.8	

Table A6.3: Pharmacy Synthesised Analogues N1-17

Analogues were generated of OH14 in order to improve the efficacy of the compound and provide further information as to the most important structural features of the inhibitors.

Compound	MW (g/mol)	Formula	Structure
N1	407.79	$C_{16}H_{13}ClF_3NO_4S$	
N2	442.24	$C_{16}H_{12}Cl_2NO_4S$	
N3	393.77	$C_{15}H_{11}ClF_3NO_4S$	
N4	428.2	$C_{15}H_{14}ClNO_4S$	
N5	431.2	$C_{15}H_{14}INO_4S$	
N6	339.79	$C_{15}H_{14}ClNO_4S$	
N7	393.77	$C_{15}H_{11}ClF_3NO_4S$	
N8	338.79	$C_{15}H_{14}ClNO_4S$	
N9	339.75	$C_{15}H_{14}ClNO_4S$	
N10	339.8	$C_{15}H_{14}ClNO_4S$	

N11	339.8	$C_{15}H_{14}ClNO_4S$	
N12	369.8	$C_{16}H_{16}ClNO_5S$	
N13	383.85	$C_{17}H_{13}ClNO_5S$	
N14	353.82	$C_{16}H_{16}ClNO_4S$	
N15	353.82	$C_{16}H_{16}ClNO_4S$	
N16	339.8	$C_{15}H_{14}ClNO_4S$	
N17	431.25	$C_{15}H_{14}INO_4S$	